Phase III Report

GEOTECHNICAL ASSESSMENT OF THE NO.2 TUNNEL OF THE DONKIN MORIEN PROJECT, SYDNEY, NOVA SCOTIA

A MICROCOMPUTER FINITE ELEMENT SOFTWARE FOR THE DESIGN OF STEEL SUPPORT SYSTEMS WITH SPECIAL REFERENCE TO THE DONKIN MORIEN PROJECT

Submitted by:

Dr. F.P. Hassani

and

Dr. H.S. Mitri

Department of Mining and Metallurgical Engineering

McGill University, Montreal, Quebec, H3A 2A7

Submitted to:

Department of Energy, Mines and Resources

CANMET - CRL Division

Cape Breton Coal Research Laboratory

210 George St.

Sydney, Nova Scotia

B1P 1J3

DSS Contract No: 63 SS. 23440-7-9054 -01- 59

Date: September 1989

191 pp

MICROMEDIA

91-00303/

Contents

Abstract III

Résumé IV

Contents V

List of Figures IX

List of Tables XIII

1 Geology 1

1.1 Introduction 1
1.2 Scope of the Problem 2
1.3 Tunnel No. 2 3
1.4 Long Tunnel Section of the Tunnel 5
1.5 Regional Geology of Cape Breton Island and Sydney Coalfield 7
1.6 Lithology 8
1.6.1 Sandstones 8
1.6.2 Interbedded Siltstones and Sandstones 8
1.6.3 Siltstones 8
1.6.4 Interbedded Siltstones and Mudstones 8
1.6.5 Mudstones 9
1.6.6 Carbonaceous Mudstones 9
1.6.7 Coal 9
1.7 Mechanical Properties of Rocks 9

2 Parametric Studies **11**
2.1 Computer Program S4 11
2.2 Numerical Modelling by Program S4 15
2.3 Roof Load Formulae 18
2.4 Effect of Load Distribution 19
2.5 Geometric Parameters 19
2.6 Modes of Failure 20
2.7 Parametric Studies 22
2.7.1 Semi-Circular Arch under Sinusoidal Load 22
2.7.2 Circular Arch under Radial Pressure 27
2.7.3 Circular Arch under Sinusoidal Load 32
2.7.4 Straight Leg Arch under Sinusoidal Load 37
2.8 Splay Leg Arch under Sinusoidal Load 54

3 Stress Analysis **67**
3.1 Introduction 67
3.2 Computer Software MSAP2D 67
3.3 Pre- and Post- Processors 70
3.3.1 PRESAP 70
3.3.2 POSTSAP 70
3.4 Model Simulation 72
3.4.1 Input Stresses 72
3.4.2 Selection of Chainages 73
3.5 Results 74
3.5.1 Stress Analysis 74
3.5.2 Displacements 74
3.5.3 Material Safety Level 75

4 Geotechnical Assessment of the No.2 Tunnel **134**
4.1 Rock-Support Interaction 134
4.2 Rationale for Calculating Safety Margins 135
4.3 Discussions 138

5 Conclusions **144**
5.1 Summary 144
5.2 Further Research 145

References 147

Appendix A 149

Appendix B 152

List of Figures

1.1 Project Location Map 4
1.2 Details of Tunnel Alignment; Tunnels 2 and 3 5
1.3 Lovat Tunnel Boring Machine; Schematic showing Basic Configuration 6
1.4 Typical Details of the Rock Supports Installed in the Sections of the Tunnel No. 2 7
1.5 Hoek and Brown Failure Envelope 10

2.1 Beam-Column Element 12
2.2 Simulation of H or I - Section 12
2.3 Distribution of Numerical Integration Points 13
2.4 Material Model 13
2.5 Automatic Load Control Parameters 14
2.6 Types of Mine Roadway Steel Supports 16
2.7 Finite Element Model of Arches 17
2.8 Elastic Plastic Mechanism of Failure of Arch 21
2.9 Semi Circular Arch under Sinusoidal Load 23
2.10 Circular Arch under Pressure 28
2.11 Circular Arch under Sinusoidal Load 33
2.12 Straight Leg Arch under Sinusoidal Load with $\lambda = 0.2$ 38
2.13 Straight Leg Arch under Sinusoidal Load with $\lambda = 0.3$ 42
2.14 Straight Leg Arch under Sinusoidal Load with $\lambda = 0.4$ 46
2.15 Straight Leg Arch under Sinusoidal Load with $\lambda = 0.6$ 50
2.16 Splay Leg Arch under Sinusoidal Load with $\lambda = 0.2$ and $\phi = 5°$ 55
2.17 Splay Leg Arch under Sinusoidal Load with $\lambda = 0.2$ and $\phi = 10°$ 59
2.18 Splay Leg Arch under Sinusoidal Load with $\lambda = 0.2$ and $\phi = 15°$ 63

3.1 Flowchart of MSAP2D System 68
3.2 No.2 Tunnel, Model Diagram User-Specified Nodes 77
3.3 No.2 Tunnel, Model Diagram. Finite Element Mesh around the Tunnel Opening 78
3.4 No.2 Tunnel, Model Diagram. Zooming of Finite Element Mesh around the Opening 79
3.5 No.2 Tunnel, Model Diagram. Stress Pattern around the Opening 80
3.6 No.2 Tunnel, Model Diagram. Displacements of Nodal Points around the Opening 81
3.7 No.2 Tunnel, Model Diagram. Parameters of the Failure Criteria 82
3.8 No.2 Tunnel, Model Diagram. Zooming of Material Failure Pattern 83
3.9 No.2 Tunnel, CH925 User-Specified Finite Element Diagram . 84
3.10 No.2 Tunnel, CH925. Finite Element Mesh 85
3.11 No.2 Tunnel, CH925. Zooming of Mesh around the Opening . 86
3.12 No.2 Tunnel, CH925. Material Pattern around the Opening . 87
3.13 No.2 Tunnel, CH925. Zooming of Nodal Point Displacements around the Opening 88
3.14 No.2 Tunnel, CH925. Stress Pattern around the Opening . . . 89
3.15 No.2 Tunnel, CH925. Zooming of Stresses around the Opening 90
3.16 No.2 Tunnel, CH925. Parameters of the Material Failure Criteria 91
3.17 No.2 Tunnel, CH925. Failure Pattern around the Opening . . 92
3.18 No.2 Tunnel, CH925. Zooming of Failure Pattern 93
3.19 No.2 Tunnel, CH1831. User Specified Finite Element Diagram with Node Numbers 94
3.20 No.2 Tunnel, CH1831. User Specified Finite Element Diagram without Node Numbers 95
3.21 No.2 Tunnel, CH1831. Finite Element Mesh 96
3.22 No.2 Tunnel, CH1831. Zooming of Mesh around the Opening . 97
3.23 No.2 Tunnel, CH1831. Material Pattern around the Opening . 98
3.24 No.2 Tunnel, CH1831. Zooming of Material around the Opening 99
3.25 No.2 Tunnel, CH1831. Ground Displacement around the Opening 100
3.26 No.2 Tunnel, CH1831. Stress Pattern 101
3.27 No.2 Tunnel, CH1831. Zooming of Stress Pattern around the Opening 102

3.28 No.2 Tunnel, CH1831. Parameters of Material Failure Criteria 103
3.29 No.2 Tunnel, CH1831. Material Safety Level around the Opening 104
3.30 No.2 Tunnel, CH1831. Zooming of Material Safety Level . . . 105
3.31 No.2 Tunnel, CH2263. User Specified Finite Element Diagram with Node Numbers 106
3.32 No.2 Tunnel, CH2263. User Specified Finite Element Diagram without Node Numbers 107
3.33 No.2 Tunnel, CH2263. Finite Element Mesh 108
3.34 No.2 Tunnel, CH2263. Zooming of Mesh around the Opening . 109
3.35 No.2 Tunnel, CH2263. Material Pattern around the Opening . 110
3.36 No.2 Tunnel, CH2263. Zooming of Material around the Opening 111
3.37 No.2 Tunnel, CH2263. Ground Displacement around the Opening 112
3.38 No.2 Tunnel, CH2263. Zooming of Stress Pattern around the Opening 113
3.39 No.2 Tunnel, CH2263. Parameters of Material Failure Criteria 114
3.40 No.2 Tunnel, CH2263. Zooming of Material Safety Level . . . 115
3.41 No.2 Tunnel, CH2996. User Specified Finite Element Diagram with Node Numbers 116
3.42 No.2 Tunnel, CH2996. Finite Element Mesh 117
3.43 No.2 Tunnel, CH2996. Zooming of Mesh around the Opening . 118
3.44 No.2 Tunnel, CH2996. Material Pattern around the Opening . 119
3.45 No.2 Tunnel, CH2996. Ground Displacement around the Opening 120
3.46 No.2 Tunnel, CH2996. Zooming of Stress Pattern around the Opening 121
3.47 No.2 Tunnel, CH2996. Parameters of Material Failure Criteria 122
3.48 No.2 Tunnel, CH2996. Zooming of Material Safety Level . . . 123
3.49 No.2 Tunnel, CH3522. User Specified Finite Element Diagram with Node Numbers 124
3.50 No.2 Tunnel, CH3522. User Specified Finite Element Diagram without Node Numbers 125
3.51 No.2 Tunnel, CH3522. Finite Element Mesh 126
3.52 No.2 Tunnel, CH3522. Zooming of Mesh around the Opening . 127
3.53 No.2 Tunnel, CH3522. Material Pattern around the Opening . 128
3.54 No.2 Tunnel, CH3522. Zooming of Material around the Opening 129

3.55 No.2 Tunnel, CH3522. Ground Displacement around the Opening 130
3.56 No.2 Tunnel, CH3522. Zooming of Stress Pattern around the Opening 131
3.57 No.2 Tunnel, CH3522. Parameters of Material Failure Criteria 132
3.58 No.2 Tunnel, CH3522. Zooming of Material Safety Level . . . 133

4.1 Rock-Support Interaction Diagram 136
4.2 Typical Layout of Instrumentation on Steel Set 137
4.3 Pressure Cell (to Measure Axial Stresses) 139
4.4 Pressure Cell (to Measure Radial Pressure) 140

List of Tables

1.1 Mechanical Properties of the Rocks 10

2.1 Geometric Properties of H-Section used as Steel Supports . . . 19
2.2 Effect of Sinusoidal Load Distribution on the Behaviour of Semi- circular Arch 24
2.3 Effect of Pressure Distribution on the Behaviour of circular Arch 29
2.4 Effect of Sinusoidal Load Distribution on the Behaviour of circular Arch 34
2.5 Effect of Sinusoidal Load Distribution on the Behaviour of Straight Leg Arch (D-Type) 39
2.6 Effect of Sinusoidal Load Distribution on the Behaviour of Straight Leg Arch (D-Type) 43
2.7 Effect of Sinusoidal Load Distribution on the Behaviour of Straight Leg Arch (D-Type) 47
2.8 Effect of Sinusoidal Load Distribution on the Behaviour of Straight Leg Arch (D-Type) 51
2.9 Effect of Sinusoidal Load Distribution on the Behaviour of Splay Leg Arch (A-Type) 56
2.10 Effect of Sinusoidal Load Distribution on the Behaviour of Splay Leg Arch (A-Type) 60
2.11 Effect of Sinusoidal Load Distribution on the Behaviour of Splay Leg Arch (A-Type) 64

4.1 Comparison of Measured and Computed Axial Stresses 141
4.2 Comparison of Measured and Computed Radial Pressure . . . 142

Chapter 1

Geology

1.1 Introduction

In order to access the Harbour Coal Seam located under the Atlantic Ocean, approximately 3.5 kilometers offshore in Cape Breton, Nova Scotia, two parallel tunnels were driven in 1984-86. This project is known as Donkin-Morien Project. The geological strata encountered in these tunnels comprise a sedimentary sequence of sandstones, siltstones and mudstones. The tunnels were driven by different methods, in the identical strata and hence provided an excellent opportunity to compare the results. Tunnel No. 2 was driven by using an advanced mechanical method i.e by using a 7.6 m-diameter full face shielded Lovat Tunnel Boring Machine (TBM) and was supported by ring beams (steel sets) to a distance of 3579 meters. Tunnel No. 3 was initially driven by the traditional method of Drill and Blast to a distance of 1027 m with dimension of 7.6 m wide and 5.3 m high and supported by rock bolts and shotcrete. The remaining length of the tunnel was completed by using TBM, to a distance of 3573 meters.

In this study, the emphasis is placed upon Tunnel No. 2. The following are the project objectives.

1. Detailed parametric study using the finite element nonlinear model S4 (steel set support systems) to generate design charts for use to evaluate the structural performance of various support systems.

2. Simulation of the steel support system used in the Tunnel No.2.

3. Evaluation of ground response around the steel support by means of a variety of linear finite element models.

4. Combination of results from (2) and (3) with in-situ geological data in an effort to assess the reliability of the existing support system, n only to the present project, but also to the future mining conditions.

In the detailed parametric study of support system, steel arches from H-section of different dimensions are analyzed to examine the strength and stiffness characteristics. Other parameters like support shape, its diameter and splay leg angle are also examined. Features of parametric studies are the load- deformation response and ultimate load-diameter response.

Prediction of stress distribution around underground openings is a complex problem to solve especially without a numerical analysis technique like the finite element method. The displacement and stress distribution around Tunnel No. 2 of the Donkin Morien are examined. Hoek-Brown failure criterion is used at the stage of checking the material safety levels. Tensile and compressive forces around the opening are plotted to show their distribution. Finally the rock-support interaction is studied and the results are compiled. The supports are provided for two reasons:

1. to control the deformation (usually the deformation is very small) in the opening

2. to avoid any local failures of wall rock adjacent to the opening.

If there are cracks in the rocks near the opening due to either blasting, joints or faults, then these rocks can eventually fall.

1.2 Scope of the Problem

In the late 1970's the Cape Breton Development Corporation, the owner and the operator of coal mines in the Sydney Coalfield, discovered a significant undersea coal resource off Cape Perce on the east side of Cape Breton Island, Nova Scotia. After exploration of surveys and comprehensive project definition study, the work started in 1980 on the Donkin Morien Development Project. Initially it was decided to have four tunnels to intersect the Harbour Coal Seam, the desired coal seam. Tunnels were excavated from

Cape Perce, driven in a northerly direction under the Atlantic Ocean. Each of these tunnels was to be approximately $30m^2$ in cross-section area, 3.5 to 4.0 km in length, approximately 200 m below seabed. The location of the project is given in Figure 1.1 and detail showing the alignment of Tunnels No. 2 and No. 3 is given in Figure 1.2.

For the early extraction of the coal, initially two parallel tunnels 50 meters apart, center to center, were excavated. These tunnels were driven through a sedimentary sequence of sandstone, siltstone, mudstone and various coal seams to intersect the Harbour Coal Seam, approximately 3.5 kilometers offshore.

1.3 Tunnel No. 2

There were two purposes of Tunnel No. 2, the main purpose was to intersect the Harbour Coal Seam and the secondary purpose was to experiment the use of tunnel boring machine. The experimental Tunnel Boring Machine (TBM) drivage was carried out using a modified Lovat Tunnelling Equipment Inc. fully shielded soft ground machine fitted with a head capable of driving through rock and using a rock cutter head, with 4 m diameter. After the successful experimental boring, it was decided to build a 7.6 m diameter full-face tunnel boring machine to develop Tunnel No. 2. The machine was propelled by a series of 200 mm diameter hydraulic jacks pushing off the support system (steel sets) which was installed inside the tail of the machine. A schematic of the basic configuration of the tunnel boring machine is given in Figure 1.3.

The support system adopted for use with tunnel boring machine comprised a system of steel sets and thrust blocks. The steel sets were generally spaced at 1.5 m center to center along the tunnel except in isolated areas of weaker zone and close to the coal seams where the spacing was reduced to 1 m. Typical details of the rock supports installed in the sections of Tunnel No. 2 driven by tunnel boring machine are given in Figure 1.4. One complete steel ring is made up of six identical segments of a W-beam 150 × 23 kg/m (150 mm × 150 mm × 23 mm wide flange) which is rolled to fit the perimeter of tunnel. The steel sets were assembled inside the shield of the tunnel boring machine and subsequently expanded and blocked with spacers from square hollow steel sections, against the rock, when they were pushed out of

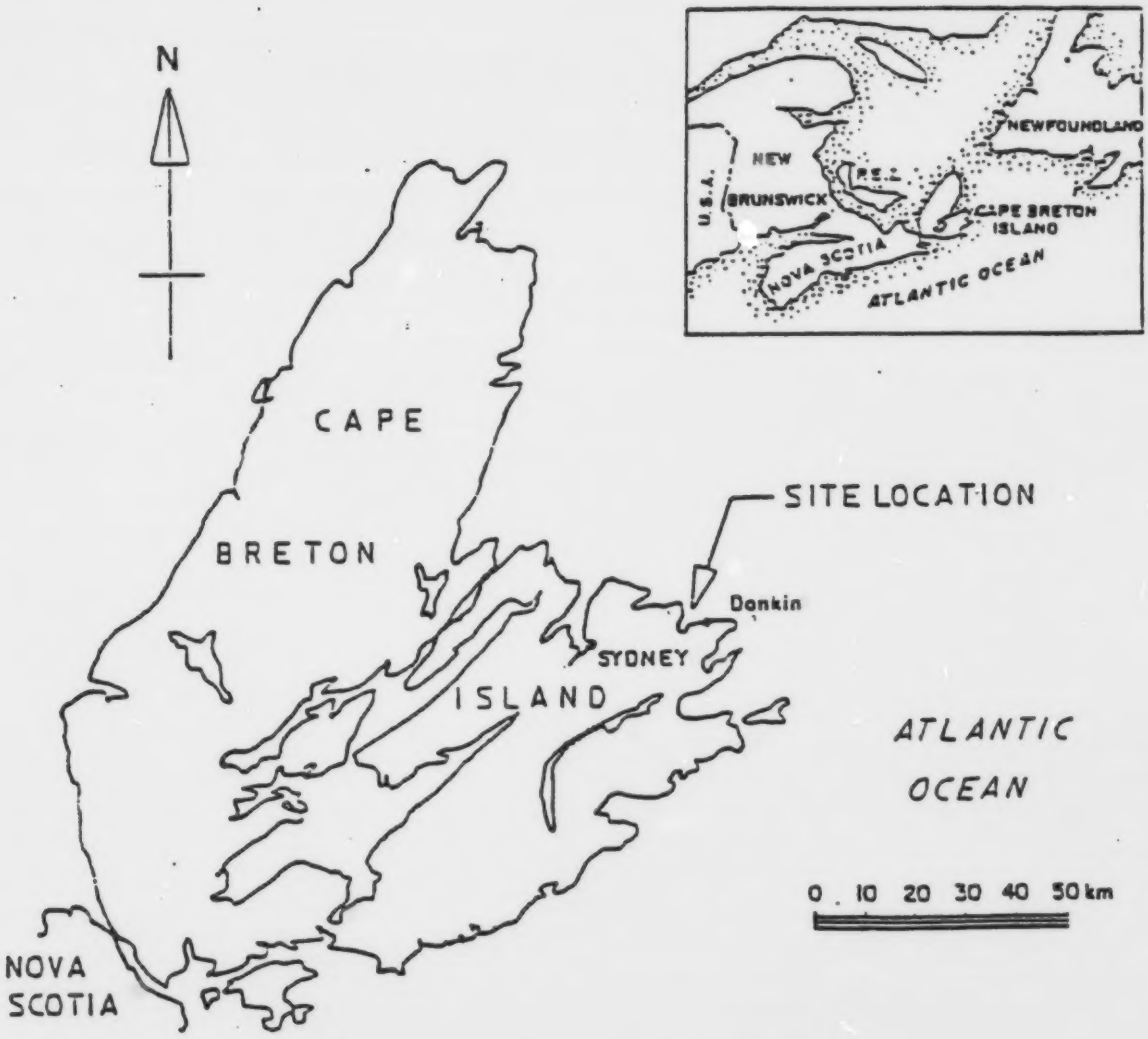

Figure 1.1: Project Location Map

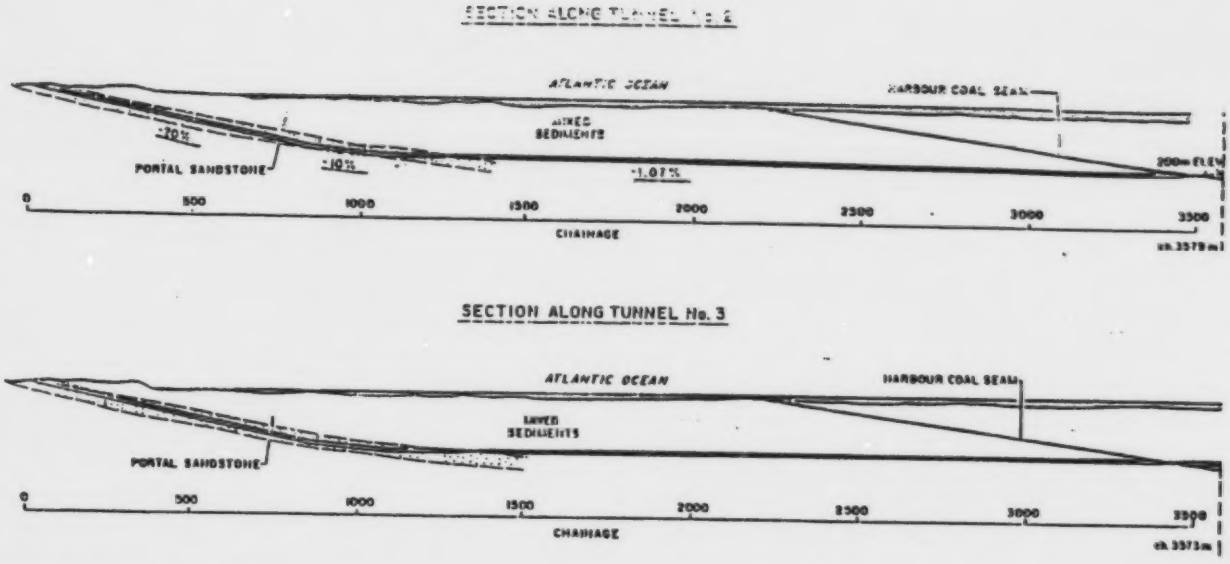

Figure 1.2: Details of Tunnel Alignment; Tunnels 2 and 3

the back of the tunnel boring machine to expand the steel sets against the tunnel. The spacers consisted of 24 thrust blocks made from 101 mm × 101 mm square hollow sections, which were installed to act as spacers between the steel sets. These were installed to transmit the load from the hydraulic jacks during drivage. Prefabricated wire mesh panels were installed across the crown to retain the small pieces of loose materials and occasionally they were supplemented with steel lagging.

1.4 Long Tunnel Section of the Tunnel

Both tunnels were driven at a decline of 20 % for the first 700 meters, in order to have sufficient protection when driving under the ocean, followed by a transition of 10 % to chainage 1027 m. The initial 500 meter of the tunnel was completely surrounded by portal sandstone. After chainage 1100 the tunnel passes through different geological strata, with a slight decline of 1.07 % to the end of drivage.

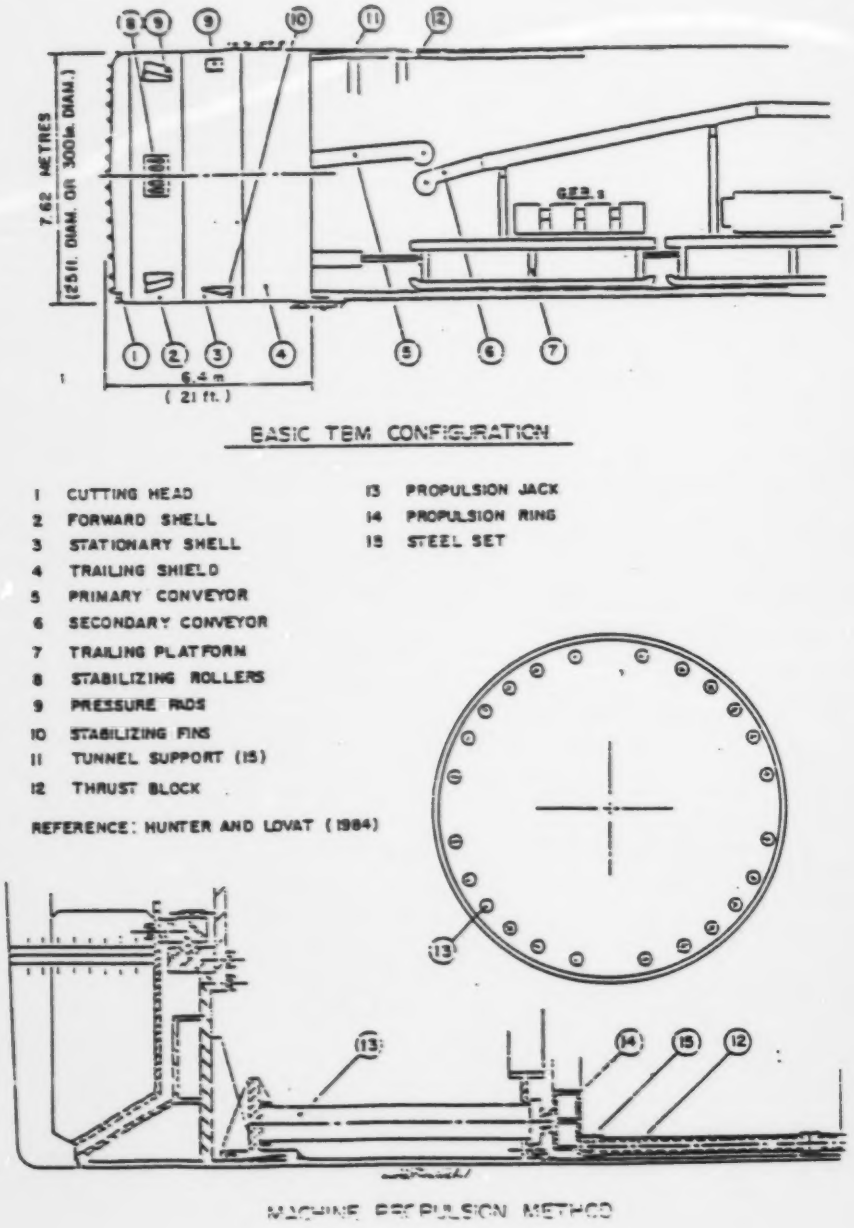

Figure 1.3: Lovat Tunnel Boring Machine; Schematic showing Basic Configuration

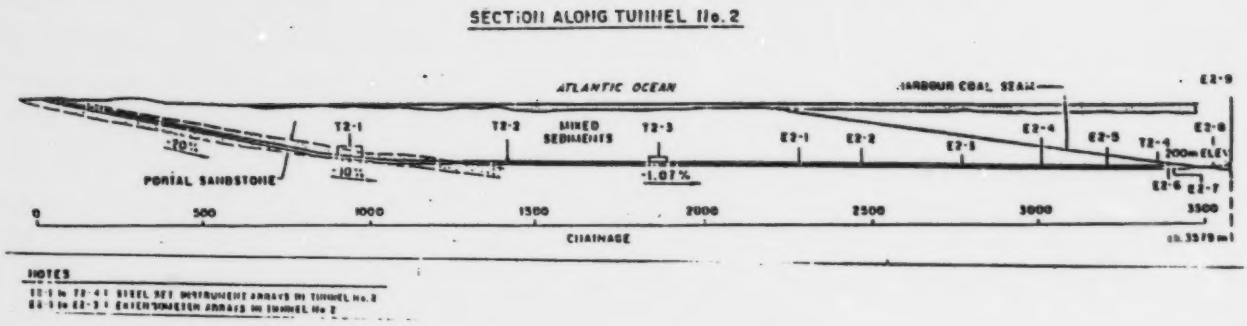

Figure 1.4: Typical Details of the Rock Supports Installed in the Sections of the Tunnel No. 2

1.5 Regional Geology of Cape Breton Island and Sydney Coalfield

The geology of Cape Breton Island consists of deformed and metamorphosed basement complex unconformaly overlain by gently deformed, weakly to unmetamorphosed sedimentary rocks. This basement complex has metaedimentary, metavolanic and plutonic rocks, while the overlying sedimentary rocks of the Carboniferous Period are predominantly composed of clastic rocks including conglomerates, sandstones, siltstones, shales and mudstone. The entire Cape Breton Island was glaciated during the Pleistocene Period. The duration of ice movement was from the west, fanning out both northeastward and south eastward, towards the Atlantic Ocean.

The Sydney Coalfield forms part of an extensive offshore sedimentary basin that outcrops along the northeast shore of the Cape Breton Island. The coalfield rocks are situated stratigraphically with the Morien Group of the late Carboniferous Period.

The Morien Group consists of a 1500 to 2000 meter thickness of coal measures rock comprised of sandstone, siltstone, mudstone, and coal horizons.

1.6 Lithology

The individual horizons within the stratigraphic sequence in the Donkin area alter laterally and vertically because of facies changes. The detailed examination of the core recovered from the borehole indicates that the following major lithological types may be recognized

1.6.1 Sandstones

The sandstones are predominantly light grey and are fine to coarse grained. Some homogeneity occurs although laminated or coarse bedded sections are more frequently encountered. Occasionally 400 to 800 mm thick layers of lenticular siltstone and/or mudstone inclusions have also been noted within the sandstone sequence. Quartz and Feldspar with grain size ranging from 0.06 mm to 2.0 mm are main constituents of sandstone. There is intergranular carbonate cement (calcite or dolomite) present locally.

1.6.2 Interbedded Siltstones and Sandstones

Tunnels also passed through the interbedded siltstones and sandstones. Sandstones are either interbedded or interlaminated with siltstones. The transition between the rock types is generally gradational but is abrupt in some places.

1.6.3 Siltstones

After the sandstones, siltstones are significantly in large amounts. Siltstones are grey in color and mostly laminated to cross-laminated with finer lamine of mudstones and fine sandstones. Sometimes ironstone nodules occur within the siltstones. These types of siltstones form transitional zones between sandstone and mudstone units.

1.6.4 Interbedded Siltstones and Mudstones

The mechanical properties of both siltstones and mudstones change when they are found in interbedded shape. The siltstone frequently grade into

mudstone and vice versa. Mostly this change is gradual but abrupt sometimes. The interbedded siltstone and mudstone units are frequently fissile and described as shaley.

1.6.5 Mudstones

The mudstones are predominantly light to dark grey and contains a high percentage of clay minerals, with some silt sized grains. Mudstones appear as massive or laminated in both the sedimentary and engineering sense. They tend to break along bedding and on other irregular conchoidal surface and to disintegrate on exposure to atmospheric conditions such as melting and drying or freezing or thawing.

1.6.6 Carbonaceous Mudstones

The mechanical properties of carbonaceous mudstones and coal seam are identical. Carbonaceous mudstone is dark grey in color, exhibits bedding and other sedimentary structures which vary from massive to laminated within individual beds.

1.6.7 Coal

The coal seam of Donkin Morien vary from thin dull to bright black cleated coal, which is commonly pyrite and contains minor mudstone and kaolinite clay partings to seams in excess of 2 m thick, consisting of bright thinly bedded coal with few mudstone interbeds.

1.7 Mechanical Properties of Rocks

The mechanical properties of above mentioned rocks are reported here, are extracted from the Donkin Morien Project report. The reported Hoek-Brown parameters (m and s values (Fig. 1.5)) of Carbonaceous Mudstones and Coal were very low. When these values were applied to check the material safety level around the tunnel (explain later on), the results gave a material failure around the tunnel. This is seldom possible. Parametric study has been done

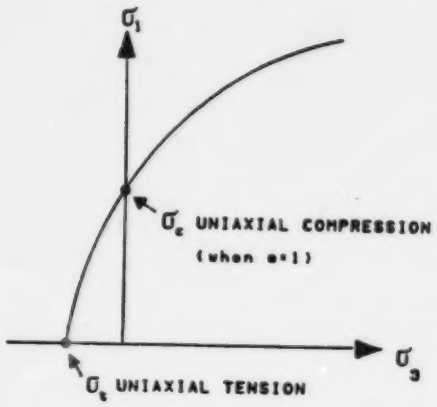

Figure 1.5: Hoek and Brown Failure Envelope

on a model of the tunnel to obtain proper m and s values. The mechanical properties are as follows :-

ROCK TYPE	MODULUS ELASTICITY (MPa)	POISSON'S RATIO	UNIT WEIGHT (MN/m^3)	HOEK-BROWN PARAMETERS		
				UNIAXIAL COMPRESSIVE STRESS (MPa)	m	s
SANDSTONES	34000	0.25	0.022	93	5	0.1
INTERBEDDED SILTSTONES & SANDSTONES	17600	0.25	0.022	131	5	0.1
SILTSTONES	11000	0.25	0.0261	83	5	0.1
INTERBEDDED SILTSTONES & MUDSTONES	9000	0.25	0.0261	36	5	0.1
MUDSTONES	5400	0.25	0.0216	36	5	0.1
CARBONACEOUS MUDSTONES	3450	0.1	0.015	16.6	5	0.65
COAL	3450	0.1	0.015	16.6	5	0.65

Table 1.1: Mechanical Properties of the Rocks

Chapter 2

Parametric Studies

2.1 Computer Program S4

Steel arches are considered as one of the best support types in underground tunnels. The basic objective of the support is to mobilise and conserve the inherent strength of the rock mass so that it becomes self-supporting. A number of attempts have been made to assess the behaviour of various types of steel arches (12-16) . A computer program called S4 (steel set support systems) based on the finite element method has been recently developed by Mitri and Hassani (1) to examine the strength and stiffness characteristics of H-section steel arches.

Program S4 is non-linear ; this is necessary because the applied (roof) load may induce material yielding and may cause significant deformation before the collapse of arch takes place. Therefore program S4 was developed to incorporate both material and geometric non- linearities.

In program S4, a beam-column (cubic linear) element with six degree-of-freedom is used as shown in Fig. 2.1. The cross-section of an arch is simulated to the section like H or I with two different widths b and w and two different thickness t and d an shown in Fig. 2.2 . A total Lagrangian approach is employed with the numerical integration point an shown in the Fig. 2.3 to include the large deformation effects of the supports. A trilinear material model is also included to account for material non-linearities due to yielding and strain hardening (Fig. 2.4) . The Newton-Raphson method is used for non-linear analysis and is automated to the point of peak load with

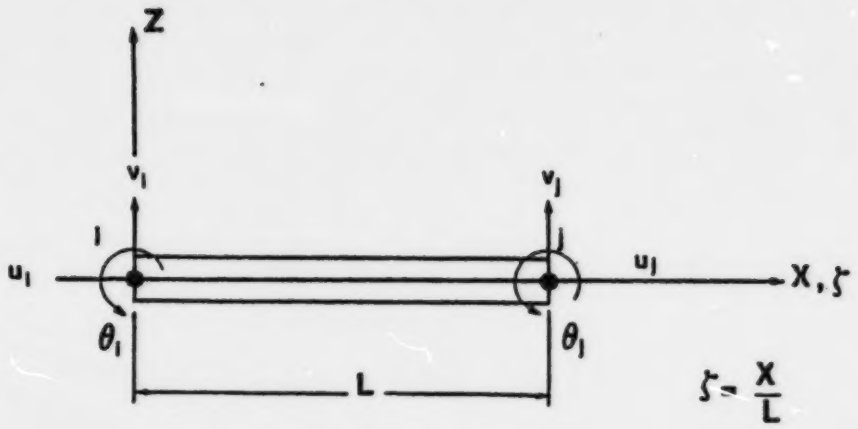

Figure 2.1: Beam-Column Element

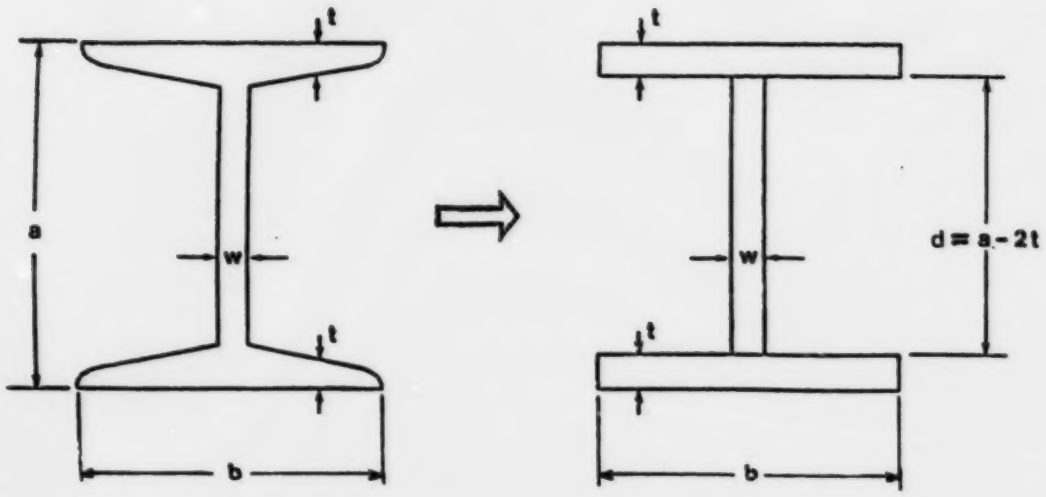

Figure 2.2: Simulation of H or I - Section

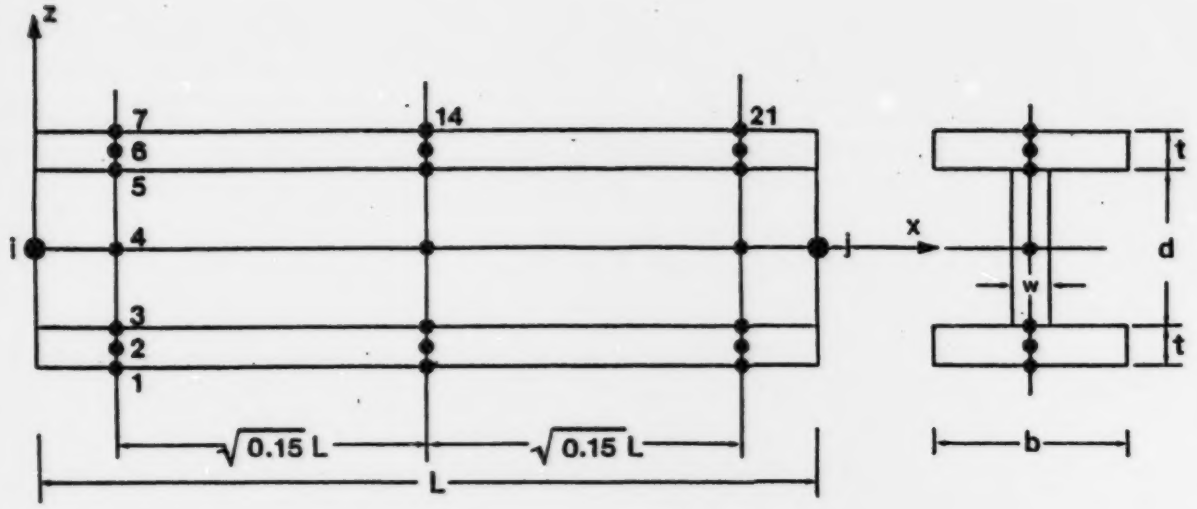

Figure 2.3: Distribution of Numerical Integration Points

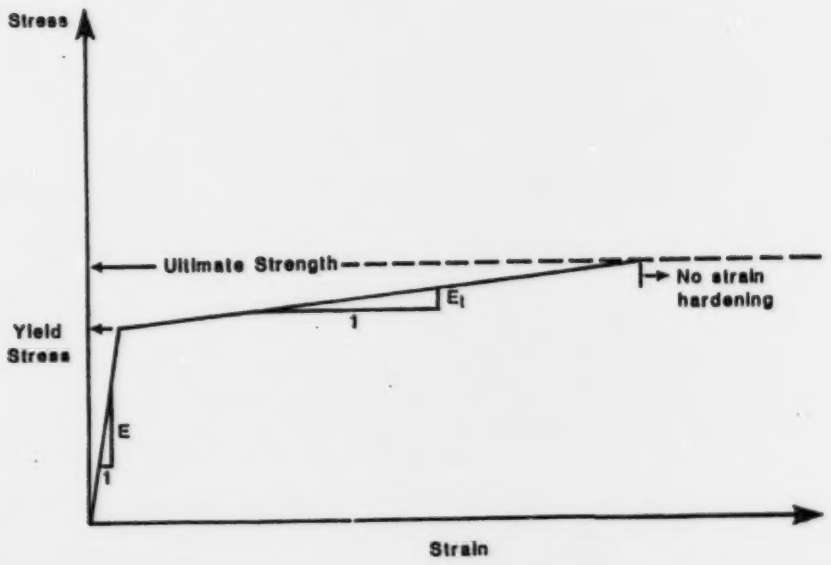

Figure 2.4: Material Model

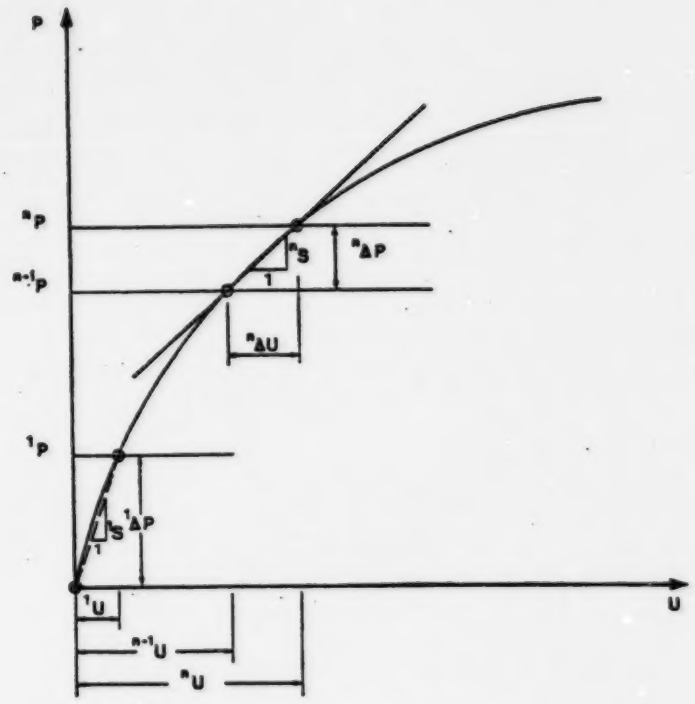

Figure 2.5: Automatic Load Control Parameters

the help of a load-control Parameters (Fig 2.5).

It should be noted that program S4 does not account for the rock-support interaction effects. In view of the fact that the host rock should provide additional constraint to the support deformation, one should anticipate conservative load bearing estimates from program S4 in the absence of such constraints. Nevertheless, contrary to Civil Engineering type of tunnels, complete rock-support contact is seldom achieved due to the common surface irregularities of coal mine roadways particularly in weak rock zones. The problem thus becomes overly complex to model if one has to consider the "true" frictional forces at the rock-support interface.

2.2 Numerical Modelling by Program S4

The basic support geometry is defined by the following three fundamental parameters, shown in Fig. 2.6

1. The diameter of the arch, D
2. The leg-to-overall height ratio, λ i.e $\lambda = h/H$
3. The splay leg angle, ϕ

The program computes the ultimate load at which the support collapses and also the maximum corresponding deflection. The deformational response δ, is expressed in terms of percentage of the crown vertical deflection Δ, to the support diameter D, i.e

$$\delta = \frac{\Delta}{D} \times 100$$

Because of the symmetry, only a quarter of the circular support is enough to analyze. The rest of the support geometries i.e. semi-circular arch, straight-leg arch and splay-leg arch can be analyzed using half of the support. In order to find the minimum number of elements required for a specific case,the program was run with different number of elements to study the convergence of results. It is finally found that 18 elements are good enough for circular and semi-circular arches. 24 elements are proven to be adequate for straight leg and splay leg arches with 6 elements for the leg as shown in Fig. 2.7. All models are fixed at the base and a guided roller is provided at the crown, to reflect the condition of symmetry. The Program S4 is capable of analyzing most of the types of the load cases which are possible in reality i.e. in the field. These are :

1. radial pressure
2. concentrated load
3. sinusoidal gravity load, and
4. uniformly distributed gravity load.

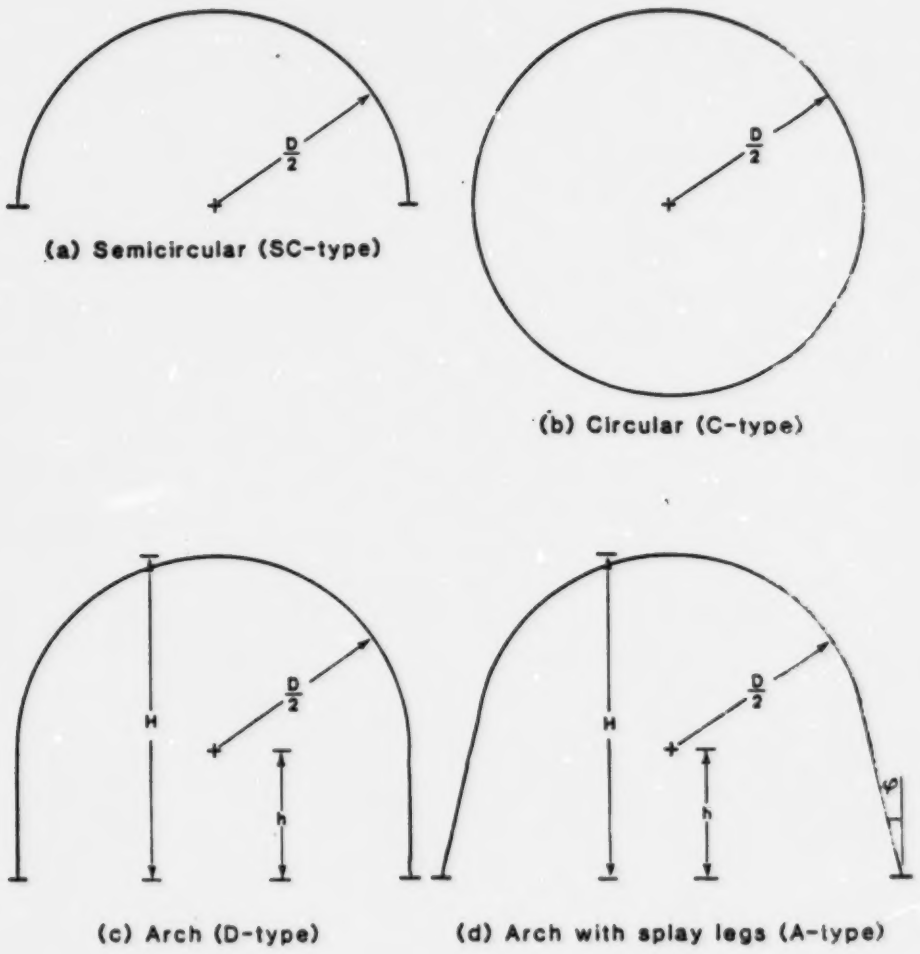

Figure 2.6: Types of Mine Roadway Steel Supports

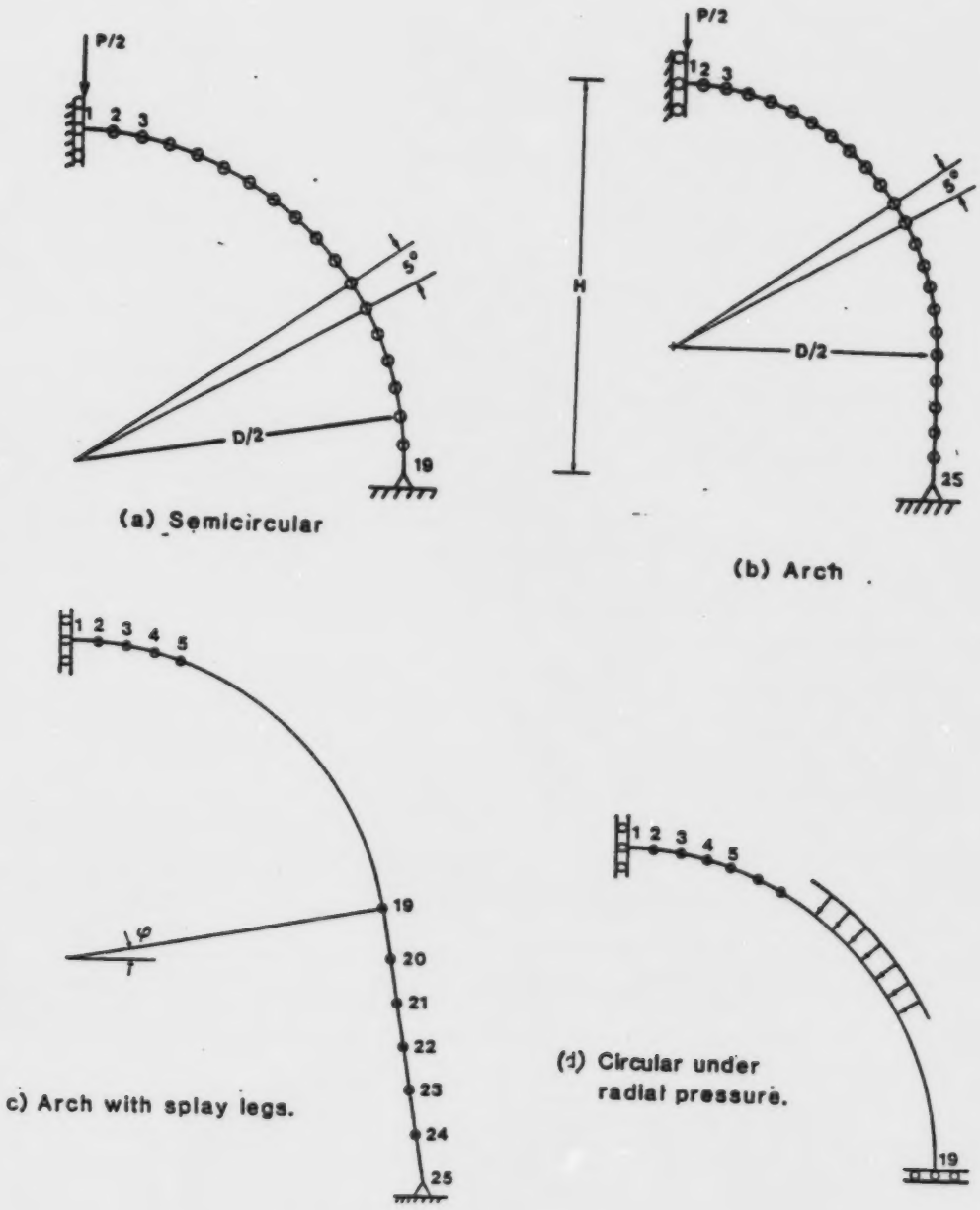

Figure 2.7: Finite Element Model of Arches

Furthermore, it is possible to apply load on the full length of crown or only a fraction of it by prescribing the percentage loaded length of crown in the program S4. If an arch has elements with sections of different dimensions, S4 can handle such features. The material of all models is assumed linear elastic-perfectly plastic to allow yielding and hence inelastic deformations are accounted for.

2.3 Roof Load Formulae

As mentioned before, the main objective of a support is to offer sufficient resistance to carry the envelope of fractured strata formed above the roadway as a result of excavation. In order to find the non-uniform gravity-type loading pattern above the steel support, which develops due to fracturing of the rock around the roadway opening, a number of instrumentation techniques have been employed. Previous studies [1] show that the concentrated load assumption underestimated the load-bearing capacity while uniformly distributed load gives overestimates the response. The sinusoidal load appears to give an acceptable load-deformation response, in accordance with in-situ observations. The load per unit length of gravity-type sinusoidal load is given by

$$\mathrm{P} = \mu \sin\theta \qquad \text{(a)}$$

Which after integration over the crown length gives

$$P_u = \mu D \qquad \text{(b)}$$

Where μ = non-dimensional load factor, its value is obtained from the results of the numerical models.

In case of splay-leg-type support, it is assumed that the splay leg are also subjected to gravity load which is uniform and equal to

$$\mathrm{P} = \mu \sin\theta \qquad \text{(c)}$$

Which ultimately, gives

$$P_u = \mu D \cos\phi + 2\mu \tan\phi(\tfrac{D}{2}\sin\phi + h) \qquad \text{(d)}$$

Initially $\mu = 1$. The non-linear analysis is then carried out and μ is increased incrementally as further resistance is offered by the support until failure of the steel support is imminent, at this specific point $\mu = \mu_{ult.}$ μ_{ult} can be directly taken from the output of the S4 computer program.

SECTION	FLANGE b x t (mm)	WEB a x w (mm)
H1	76 X 8.4	76 X 8.9
H2	89 X 9.9	89 X 9.5
H3	102 X 10.3	102 X 9.5
H4	114 X 11.5	114 X 9.5
H5	114 X 11.5	127 X 10.2
H6	127 X 13.2	152 X 10.4

Table 2.1: Geometric Properties of H-Section used as Steel Supports

2.4 Effect of Load Distribution

It has been shown by Mitri and Hassani (3) that sinusoidal load gives the most acceptable results. Therefore in the present study, the sinusoidal load is kept and the effect of section size of the steel arches is studied in conjunction with the parameters λ (the leg-to- overall height ratio), ϕ (splay leg angle) and D (the diameter of the support).

The data used for the simulation of the models conforms with the specification of British Standards Institute for H-section steel arches [13] of Grade A with 430 MPa tensile strength. However, for modelling purposes, a yield stress value should be defined. A ratio of 1.6 of tensile strength to yield stress has been assumed which gives a yield stress of 268 MPa. Young's Modulus of elasticity is taken as 200 GPa. With these values, the slope of the second portion of the material model is found to be 0.815 GPa. In order to accommodate the design requirements, six standard H-sections are analyzed. Dimensions of H-sections used in arches are listed in table 2.1.(17)

2.5 Geometric Parameters

Geometric parameters of arches are :-

1. semi-circular under sinusoidal load
2. circular under sinusoidal load

3. circular under uniform radial pressure

4. straight leg (D-type) under sinusoidal load

5. splay leg (A-type) under sinusoidal load.

To differentiate between the data of the models, the designation of a model is taken according to its properties and loading conditions imposed. For instance D32S-0-H3 means straight leg arch (D-type), diameter = 3 m, leg-to- overall height ratio λ =0.2, S stands for sinusoidal load, splay leg angle, ϕ = 0 and H3 defines the section properties of the arch. Similarly A42S-5-H6 would mean splay-legged arch, 4 m diameter, λ = 0.2, sinusoidal load, ϕ (splay leg angle) =5° and section H6.

2.6 Modes of Failure

Failure of the steel arches can be ascribed to one of the following three modes of failure.

1. Plastic Instability. Failure of steel arches due to full development of plastic hinges at more than two places is termed as Plastic Instability. Because of these plastic hinges, a collapse mechanism develops and the arch fails. In Fig. 2.8 D1 (2 meter diameter) and D2 (3 meter diameter) are failed by plastic instability. D1 and D2 show that the behaviour of steel arches remain in the elastic zone as long as graph is straight line and then the plastic hinge starts developing with the curving of the graph and finally it failed.

2. Inelastic Buckling. Arches fail before they fully develop sufficient number of the plastic hinges. Plastic hinge at one place does not cause a plastic mechanism but due to the slenderness ratio of the steel set an inelastic buckling mode of failure takes place instead. In Fig. 2.8 D3, D4,... D8 all failed by inelastic buckling. This type of failure is not desirable in practice.

3. Elastic Buckling. Examples of elastic buckling are straight leg arches with λ more than 0.3 and diameter more than 5 meters i.e with high slenderness ratio. The ultimate load obtained in this case is about 7.0

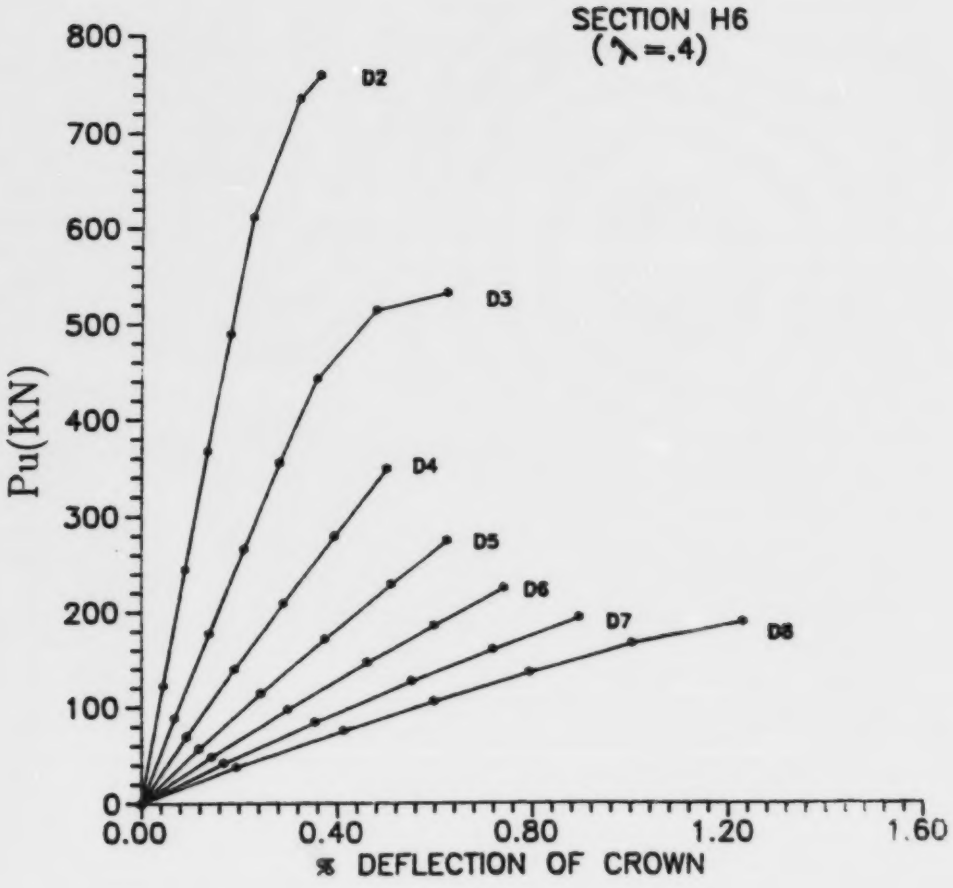

Figure 2.8: Elastic Plastic Mechanism of Failure of Arch

kN and the stresses at failure are well within the elastic range. This type of failure is highly undesirable as it does not give any sort of warning before failure, and hence can cause major damage.

2.7 Parametric Studies

2.7.1 Semi-Circular Arch under Sinusoidal Load

In underground mining, semi-circular arches have a significant role as ground support because of their high structural performance. In this study, semi-circular arches are analyzed under sinusoidal load and the ultimate loads are given in Table 2.5. and load-deformation curves are given in Fig. 2.9. These results show that there is definite improvement in performance as heavier sections are used. Typically, H6 model is 5.74 times stronger than H1 when the diameter is 5 m. In practice such a comparison may serve as a basis for setting alternative designs by varying the spacing between supports (i.e. altering the load per arch) and the selected sections accordingly.

From the graphs the effect of diameter change on the support behaviour is quite evident. The larger the diameter the less tendency of support to take the load. Economy of arches can also be considered using the design table. For example, with 5m diameter, H6 gives much higher resistance than steel section H5.

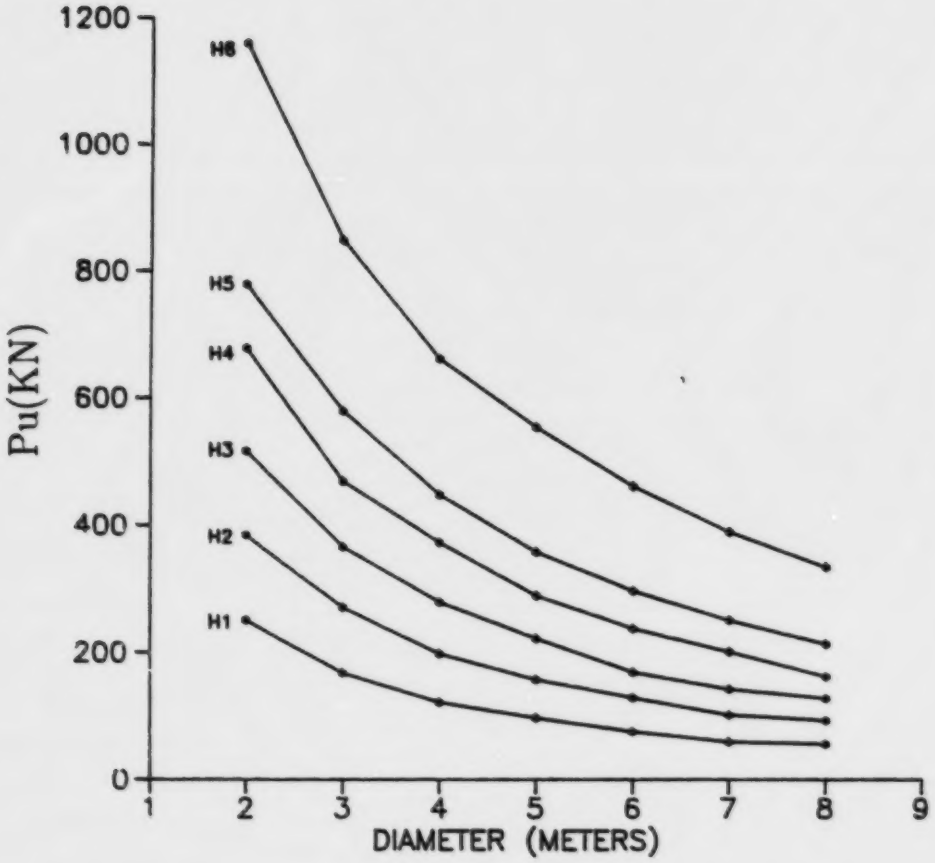

Figure 2.9: Semi Circular Arch under Sinusoidal Load

MODEL DESIGNATION.	DIA (mm)	ϕ (DEG)	Pu (Kn)	% δ
SC2S-H1	2000	0	250.48	0.398
SC3S-H1	3000	0	167.04	0.567
SC4S-H1	4000	0	120.96	0.697
SC5S-H1	5000	0	96.20	0.899
SC6S-H1	6000	0	74.88	0.932
SC7S-H1	7000	0	58.52	1.006
SC8S-H1	8000	0	55.2	1.359
SC2S-H2	2000	0	384.4	0.330
SC3S-H2	3000	0	270.0	0.510
SC4S-H2	4000	0	197.12	0.617
SC5S-H2	5000	0	156.6	0.784
SC6S-H2	6000	0	127.92	0.958
SC7S-H2	7000	0	100.8	0.926
SC8S-H2	8000	0	92.16	1.194
SC2S-H3	2000	0	515.84	0.286
SC3S-H3	3000	0	365.4	0.426
SC4S-H3	4000	0	278.4	0.578

Table 2.2: Effect of Sinusoidal Load Distribution on the Behaviour of Semi-circular Arch

MODEL DESIGNATION.	DIA (mm)	ϕ (DEG)	Pu (Kn)	% δ
SC5S-H3	5000	0	221.2	0.737
SC6S-H3	6000	0	168.0	0.664
SC7S-H3	7000	0	141.12	0.762
SC8S-H3	8000	0	126.72	0.932
SC2S-H4	2000	0	677.12	0.407
SC3S-H4	3000	0	468.0	0.373
SC4S-H4	4000	0	372.0	0.577
SC5S-H4	5000	0	288.4	0.614
SC6S-H4	6000	0	236.52	0.722
SC7S-H4	7000	0	200.2	0.820
SC8S-H4	8000	0	161.28	0.786
SC2S-H5	2000	0	777.48	0.227
SC3S-H5	3000	0	578.46	0.358
SC4S-H5	4000	0	446.4	0.473
SC5S-H5	5000	0	356.7	0.586
SC6S-H5	6000	0	295.68	0.691
SC7S-H5	7000	0	249.48	0.789
SC8S-H5	8000	0	212.16	0.860
SC2S-H6	2000	0	1158.4	0.292
SC3S-H6	3000	0	846.3	0.291

MODEL DESIGNATION.	DIA (mm)	ϕ (DEG)	Pu (Kn)	% δ
SC4S-H6	4000	0	660.0	0.373
SC5S-H6	5000	0	552.0	0.515
SC6S-H6	6000	0	459.36	0.596
SC7S-H6	7000	0	388.08	0.668
SC8S-H6	8000	0	332.64	0.727

2.7.2 Circular Arch under Radial Pressure

Table 2.10 and Fig. 2.10 show the ultimate load values and load-deformation curves respectively for the case of circular arch under radial pressure. The effect of section properties and diameter are very obvious. These results can be used when excavation is done in hard rock (hard rocks apply a radial pressure on the supports). Spacing of arches (supports), in this case depends largely on the diameter and the section properties of an arch.

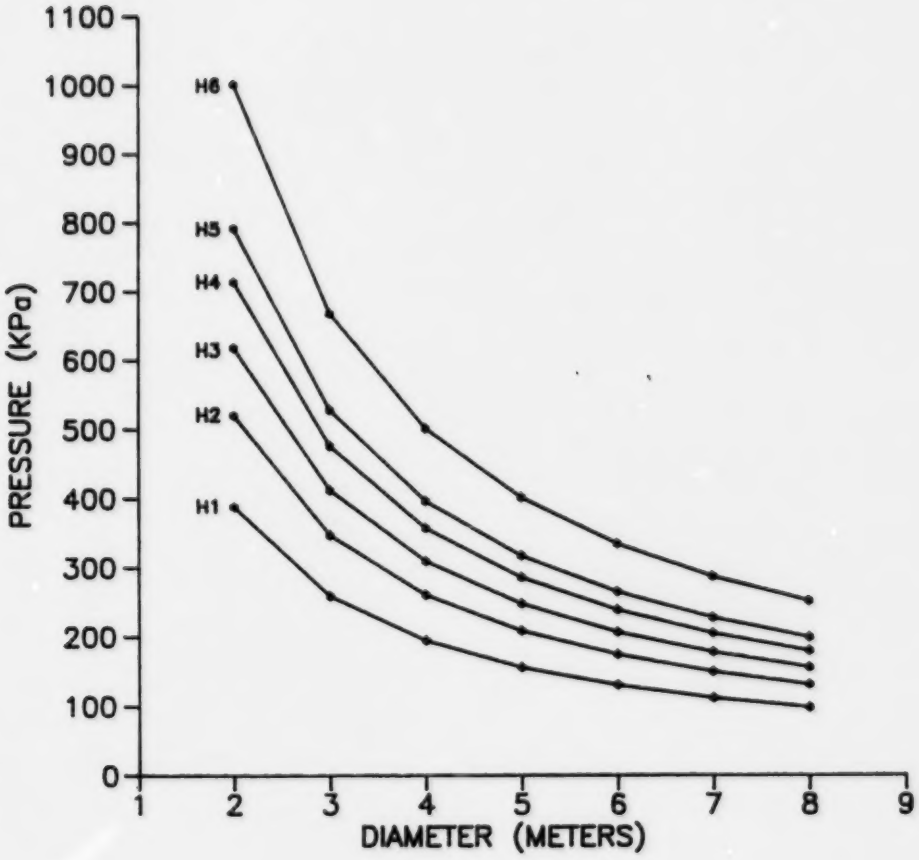

Figure 2.10: Circular Arch under Pressure

MODEL DESIGNATION.	DIA (mm)	ϕ (DEG)	PRESSURE (KPa)	% δ
C2P-H1	2000	0	387.2	0.053
C3P-H1	3000	0	258.0	0.0537
C4P-H1	4000	0	193.6	0.0537
C5P-H1	5000	0	154.8	0.0536
C6P-H1	6000	0	129.2	0.0533
C7P-H1	7000	0	110.4	0.0517
C8P-H1	8000	0	96.8	0.0462
C2P-H2	2000	0	519.2	0.0537
C3P-H2	3000	0	346.0	0.0537
C4P-H2	4000	0	259.6	0.0537
C5P-H2	5000	0	207.6	0.0537
C6P-H2	6000	0	173.2	0.0536
C7P-H2	7000	0	148.4	0.0533
C8P-H2	8000	0	129.6	0.0523
C2P-H3	2000	0	616.8	0.0537
C3P-H3	3000	0	411.2	0.0537
C4P-H3	4000	0	308.4	0.0537
C5P-H3	5000	0	246.8	0.0537

Table 2.3: Effect of Pressure Distribution on the Behaviour of circular Arch

MODEL DESIGNATION.	DIA (mm)	ϕ (DEG)	PRESSURE (KPa)	% δ
C6P-H3	6000	0	205.6	0.0537
C7P-H3	7000	0	176.4	0.0537
C8P-H3	8000	0	154.4	0.0537
C2P-H4	2000	0	712.4	0.0537
C3P-H4	3000	0	474.8	0.0537
C4P-H4	4000	0	356.0	0.0537
C5P-H4	5000	0	284.8	0.0537
C6P-H4	6000	0	237.6	0.0537
C7P-H4	7000	0	203.6	0.0537
C8P-H4	8000	0	178.0	0.0537
C2P-H5	2000	0	790.4	0.0537
C3P-H5	3000	0	526.8	0.0537
C4P-H5	4000	0	395.2	0.0537
C5P-H5	5000	0	316.0	0.0537
C6P-H5	6000	0	263.6	0.0537
C7P-H5	7000	0	226.0	0.0537
C8P-H5	8000	0	197.6	0.0537
C2P-H6	2000	0	1000.0	0.0537
C3P-H6	3000	0	666.4	0.0537

MODEL DESIGNATION.	DIA (mm)	ϕ (DEG)	PRESSURE (KPa)	% δ
C4P-H6	4000	0	500.0	0.0537
C5P-H6	5000	0	400.0	0.0537
C6P-H6	6000	0	333.2	0.0537
C7P-H6	7000	0	285.6	0.0537
C8P-H6	8000	0	250.0	0.0537

2.7.3 Circular Arch under Sinusoidal Load

Performance of circular arches under sinusoidal load is very different from circular arches under radial pressure. Table 2.9 and Fig. 2.11 are for circular arch. It is clear from these data that circular arch offer less resistance to sinusoidal load as compared to semi-circular arch. For example section H5 with 5 m diameter of semi- circular arch can resist 3.29 times more load than the circular arch with same section properties.

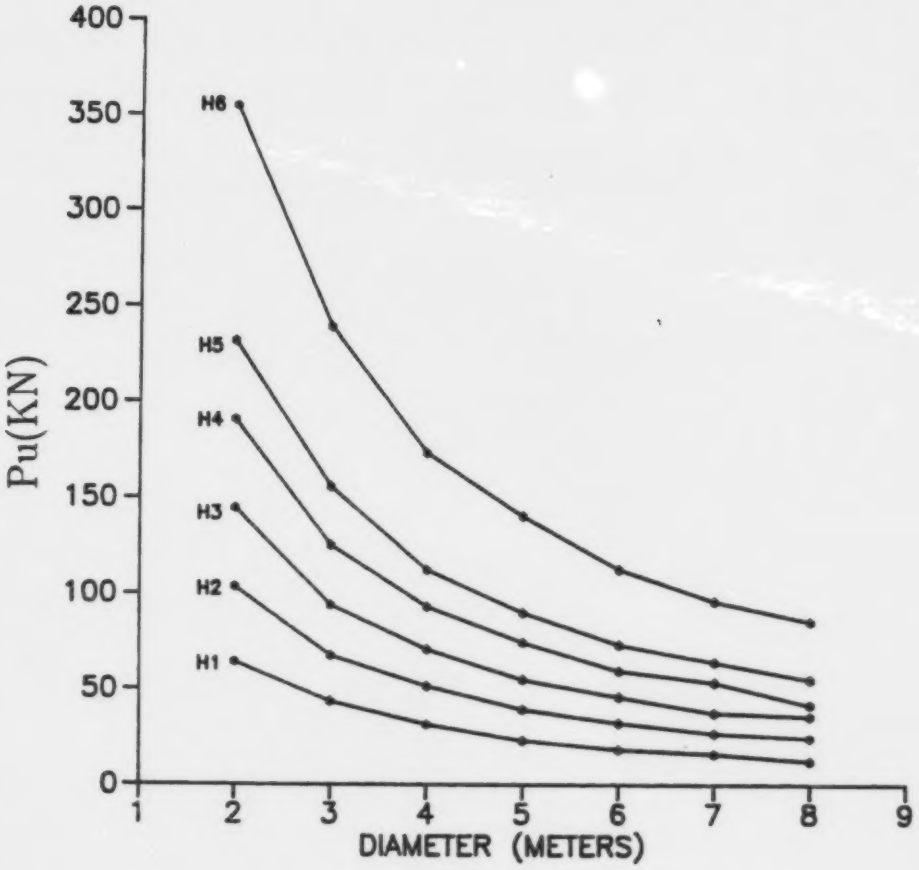

Figure 2.11: Circular Arch under Sinusoidal Load

MODEL DESIGNATION	DIA (mm)	ϕ (DEG)	Pu (kn)	% δ
C2S-H1	2000	0	63.96	1.504
C3S-H1	3000	0	43.2	2.746
C4S-H1	4000	0	31.2	3.524
C5S-H1	5000	0	22.8	4.261
C6S-H1	6000	0	18.24	5.333
C7S-H1	7000	0	15.96	5.878
C8S-H1	8000	0	12.16	7.196
C2S-H2	2000	0	103.32	1.600
C3S-H2	3000	0	67.2	2.283
C4S-H2	4000	0	51.2	3.271
C5S-H2	5000	0	39.0	3.677
C6S-H2	6000	0	31.92	4.391
C7S-H2	7000	0	26.6	5.174
C8S-H2	8000	0	24.32	5.928
C2S-H3	2000	0	144.32	1.436
C3S-H3	3000	0	93.6	2.003

Table 2.4: Effect of Sinusoidal Load Distribution on the Behaviour of circular Arch

MODEL DESIGNATION	DIA (mm)	ϕ (DEG)	Pu (kn)	% δ
C4S-H3	4000	0	70.4	2.992
C5S-H3	5000	0	54.6	3.340
C6S-H3	6000	0	45.6	3.7256
C7S-H3	7000	0	37.24	4.662
C8S-H3	8000	0	35.52	4.955
C2S-H4	2000	0	190.24	1.328
C3S-H4	3000	0	124.8	1.826
C4S-H4	4000	0	92.8	2.674
C5S-H4	5000	0	74.1	2.983
C6S-H4	6000	0	59.28	3.38
C7S-H4	7000	0	53.2	3.985
C8S-H4	8000	0	41.44	4.407
C2S-H5	2000	0	231.24	1.187
C3S-H5	3000	0	154.98	1.985
C4S-H5	4000	0	112.0	2.262
C5S-H5	5000	0	89.7	2.624
C6S-H5	6000	0	72.96	2.991
C7S-H5	7000	0	63.84	3.575
C8S-H5	8000	0	54.72	4.22

MODEL DESIGNATION	DIA (mm)	ϕ (DEG)	Pu (kn)	% δ
C2S-H6	2000	0	354.24	1.020
C3S-H6	3000	0	238.62	1.535
C4S-H6	4000	0	172.8	1.862
C5S-H6	5000	0	140.0	2.599
C6S-H6	6000	0	112.32	2.674
C7S-H6	7000	0	95.76	2.922
C8S-H6	8000	0	85.12	3.412

2.7.4 Straight Leg Arch under Sinusoidal Load

Apart from the effect of diameter and section properties, the leg to overall height ratio λ , is studied in this section. Table 2.1, 2.2, 2.3, 2.4 gives the ultimate Pu and percentage crown deflection Δ . Whereas Figs. 2.12, 2.13, 2.14 and 2.15 show the relationship between ultimate Pu and diameter D. Analyses prove that more the value of λ less stronger will be the structure.

The important point to be notice here is the buckling failure of sections H1, H2 and H3 when λ is more than 0.2 and the diameter is more than 5 meters. This type of failure is not desirable in practice. So in designing, arches as the supports in the underground tunnels, one should avoid λ more than 0.2, specially when the diameter is more than 5 meters.

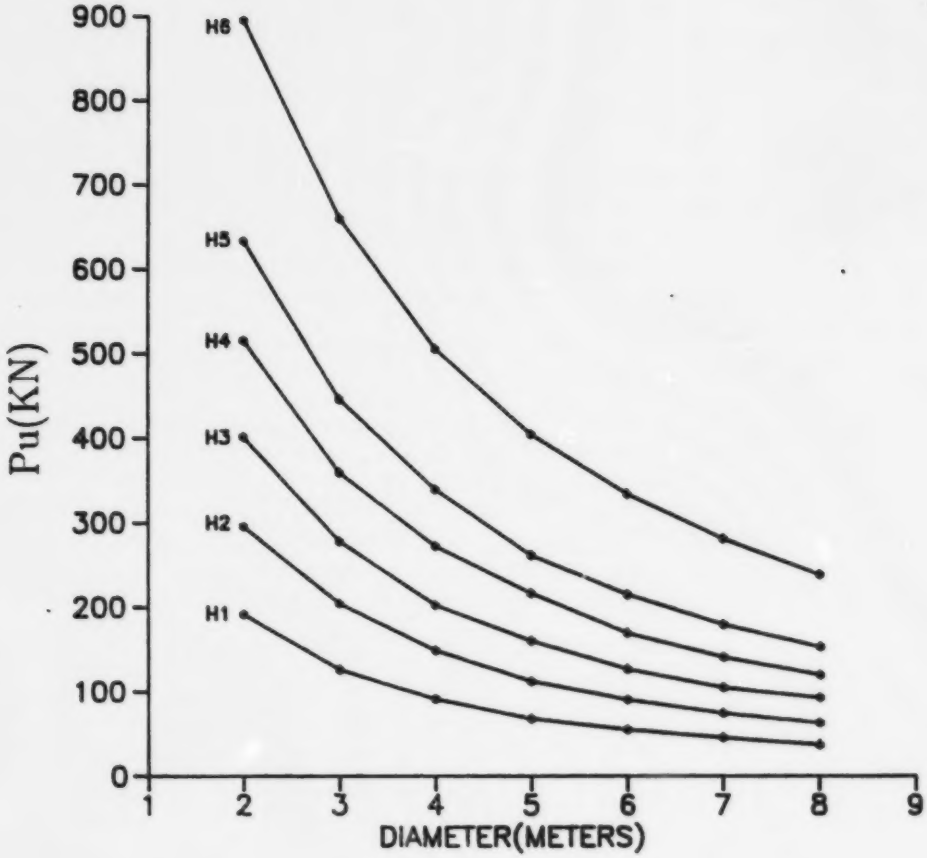

Figure 2.12: Straight Leg Arch under Sinusoidal Load with $\lambda = 0.2$

MODEL DESIGNATION.	DIA (mm)	λ	ϕ (DEG)	Pu (Kn)	$\%\delta$
D2.2S-0-H1	2000	0.2	0	190.96	0.567
D3.2S-0-H1	3000	0.2	0	125.28	0.812
D4.2S-0-H1	4000	0.2	0	90.72	0.987
D5.2S-0-H1	5000	0.2	0	67.5	1.082
D6.2S-0-H1	6000	0.2	0	54.72	1.286
D7.2S-0-H1	7000	0.2	0	45.08	1.476
D8.2S-0-H1	8000	0.2	0	36.8	1.829
D2.2S-0-H2	2000	0.2	0	295.12	0.456
D3.2S-0-H2	3000	0.2	0	203.4	0.757
D4.2S-0-H2	4000	0.2	0	147.84	0.875
D5.2S-0-H2	5000	0.2	0	111.84	0.955
D6.2S-0-H2	6000	0.2	0	90.0	1.123
D7.2S-0-H2	7000	0.2	0	73.92	1.278
D8.2S-0-H2	8000	0.2	0	62.56	1.422
D2.2S-0-H3	2000	0.2	0	400.52	0.391
D3.2S-0-H3	3000	0.2	0	277.40	0.599

Table 2.5: Effect of Sinusoidal Load Distribution on the Behaviour of Straight Leg Arch (D-Type)

MODEL DESIGNATION.	DIA (mm)	λ	ϕ (DEG)	Pu (Kn)	%δ
D4.2S-0-H3	4000	0.2	0	201.6	0.715
D5.2S-0-H3	5000	0.2	0	159.30	0.888
D6.2S-0-H3	6000	0.2	0	126.0	0.927
D7.2S-0-H3	7000	0.2	0	104.16	1.058
D8.2S-0-H3	8000	0.2	0	92.16	1.282
D2.2S-0-H4	2000	0.2	0	514.35	0.347
D3.2S-0-H4	3000	0.2	0	358.2	0.517
D4.2S-0-H4	4000	0.2	0	271.44	0.693
D5.2S-0-H4	5000	0.2	0	215.6	0.877
D6.2S-0-H4	6000	0.2	0	168.48	0.887
D7.2S-0-H4	7000	0.2	0	140.0	0.993
D8.2S-0-H4	8000	0.2	0	119.04	1.091
D2.2S-0-H5	2000	0.2	0	632.32	0.355
D3.2S-0-H5	3000	0.2	0	444.54	0.510
D4.2S-0-H5	4000	0.2	0	338.4	0.701
D5.2S-0-H5	5000	0.2	0	260.4	0.725
D6.2S-0-H5	6000	0.2	0	213.84	0.847
D7.2S-0-H5	7000	0.2	0	178.36	0.953
D8.2S-0-H5	8000	0.2	0	152.0	1.0369
D2.2S-0-H6	2000	0.2	0	894.04	0.255
D3.2S-0-H6	3000	0.2	0	658.44	0.401

MODEL DESIGNATION.	DIA (mm)	λ	ϕ (DEG)	Pu (Kn)	%δ
D4.2S-0-H6	4000	0.2	0	504.0	0.521
D5.2S-0-H6	5000	0.2	0	403.1	0.632
D6.2S-0-H6	6000	0.2	0	332.64	0.733
D7.2S-0-H6	7000	0.2	0	279.72	0.826
D8.2S-0-H6	8000	0.2	0	237.12	0.894

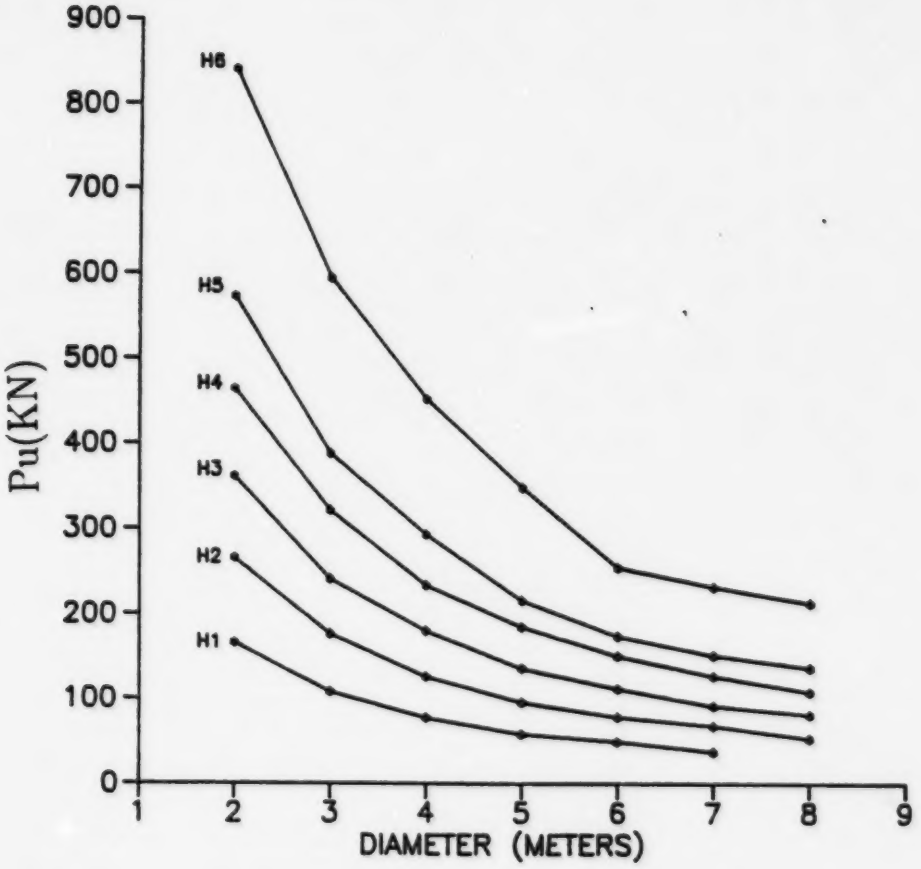

Figure 2.13: Straight Leg Arch under Sinusoidal Load with $\lambda = 0.3$

MODEL DESIGNATION.	DIA (mm)	λ	ϕ (DEG)	Pu (Kn)	%δ
D2.3S-0-H1	2000	0.3	0	165.6	0.611
D3.3S-0-H1	3000	0.3	0	107.6	0.863
D4.3S-0-H1	4000	0.3	0	76.96	1.055
D5.3S-0-H1	5000	0.3	0	57.6	1.212
D6.3S-0-H1	6000	0.3	0	48.96	1.583
D7.3S-0-H1	7000	0.3	0	36.96	1.678
D8.3S-0-H1	8000	0.3	0	8.0*	0.335*
D2.3S-0-H2	2000	0.3	0	265.36	0.574
D3.3S-0-H2	3000	0.3	0	175.74	0.789
D4.3S-0-H2	4000	0.3	0	125.28	0.934
D5.3S-0-H2	5000	0.3	0	95.0	1.047
D6.3S-0-H2	6000	0.3	0	77.76	1.25
D7.3S-0-H2	7000	0.3	0	67.2	1.574
D8.3S-0-H2	8000	0.3	0	52.8	1.623
D2.3S-0-H3	2000	0.3	0	360.84	0.479
D3.3S-0-H3	3000	0.3	0	240.12	0.647
D4.3S-0-H3	4000	0.3	0	179.2	0.877

* Arch failed by buckling.

Table 2.6: Effect of Sinusoidal Load Distribution on the Behaviour of Straight Leg Arch (D-Type)

MODEL DESIGNATION.	DIA (mm)	λ	ϕ (DEG)	Pu (Kn)	$\%\delta$
D5.3S-0-H3	5000	0.3	0	135.0	0.962
D6.3S-0-H3	6000	0.3	0	111.0	1.131
D7.3S-0-H3	7000	0.3	0	90.72	1.281
D8.3S-0-H3	8000	0.3	0	80.64	1.596
D2.3S-0-H4	2000	0.3	0	463.76	0.418
D3.3S-0-H4	3000	0.3	0	320.4	0.676
D4.3S-0-H4	4000	0.3	0	232.96	0.748
D5.3S-0-H4	5000	0.3	0	183.6	0.923
D6.3S-0-H4	6000	0.3	0	149.76	1.082
D7.3S-0-H4	7000	0.3	0	126.0	1.219
D8.4S-0-H4	8000	0.3	0	107.52	1.333
D2.3S-0-H5	2000	0.3	0	572.16	0.437
D3.3S-0-H5	3000	0.3	0	387.0	0.548
D4.3S-0-H5	4000	0.3	0	292.32	0.741
D5.3S-0-H5	5000	0.3	0	199.2	1.059
D6.3S-0-H5	6000	0.3	0	160.08	0.754
D7.3S-0-H5	7000	0.3	0	150.5	1.036
D8.3S-0-H5	8000	0.3	0	136.0	1.272
D2.3S-0-H6	2000	0.3	0	839.68	0.365
D3.3S-0-H6	3000	0.3	0	593.34	0.498
D4.3S-0-H6	4000	0.3	0	451.2	0.698

* Arch failed by buckling.

MODEL DESIGNATION.	DIA (mm)	λ	ϕ (DEG)	Pu (Kn)	%δ
D5.3S-0-H6	5000	0.3	0	347.2	0.684
D6.3S-0-H6	6000	0.3	0	253.44	0.636
D7.3S-0-H6	7000	0.3	0	249.48	1.022
D8.3S-0-H6	8000	0.3	0	212.16	1.095

* Arch failed by buckling.

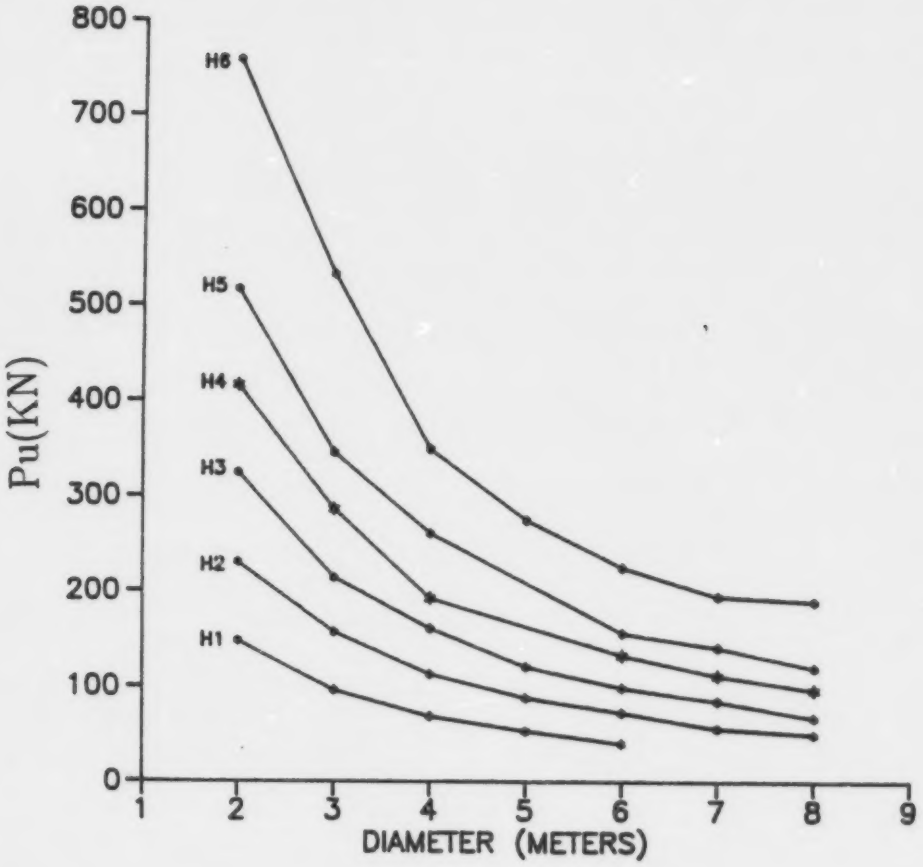

Figure 2.14: Straight Leg Arch under Sinusoidal Load with $\lambda = 0.4$

MODEL DESIGNATION.	DIA (mm)	λ	ϕ (DEG)	Pu (Kn)	$\%\delta$
D2.4S-0-H1	2000	0.4	0	147.32	0.733
D3.4S-0-H1	3000	0.4	0	95.58	0.987
D4.4S-0-H1	4000	0.4	0	68.0	1.199
D5.4S-0-H1	5000	0.4	0	52.8	1.514
D6.4S-0-H1	6000	0.4	0	39.4	1.689
D7.4S-0-H1	7000	0.4	0	7.7*	0.349*
D8.4S-0-H1	8000	0.4	0	7.2*	0.402*
D2.4S-0-H2	2000	0.4	0	229.68	0.553
D3.4S-0-H2	3000	0.4	0	156.24	1.016
D4.4S-0-H2	4000	0.4	0	112.32	1.056
D5.4S-0-H2	5000	0.4	0	87.5	1.325
D6.4S-0-H2	6000	0.4	0	72.0	1.567
D7.4S-0-H2	7000	0.4	0	55.44	1.680
D8.4S-0-H2	8000	0.4	0	49.28	2.007
D2.4S-0-H3	2000	0.4	0	324.0	0.563
D3.4S-0-H3	3000	0.4	0	213.36	0.741
D4.4S-0-H3	4000	0.4	0	159.84	1.084

Table 2.7: Effect of Sinusoidal Load Distribution on the Behaviour of Straight Leg Arch (D-Type)

MODEL DESIGNATION.	DIA (mm)	λ	ϕ (DEG)	Pu (Kn)	%δ
D5.4S-0-H3	5000	0.4	0	120.0	1.090
D6.4S-0-H3	6000	0.4	0	97.92	1.295
D7.4S-0-H3	7000	0.4	0	84.0	1.634
D8.4S-0-H3	8000	0.4	0	66.88	1.672
D2.4S-0-H4	2000	0.4	0	415.2	0.472
D3.4S-0-H4	3000	0.4	0	285.36	0.898
D4.4S-0-H4	4000	0.4	0	184.32	0.676
D5.4S-0-H4	5000	0.4	0	163.8	1.044
D6.4S-0-H4	6000	0.4	0	132.0	1.222
D7.4S-0-H4	7000	0.4	0	110.88	1.378
D8.4S-0-H4	8000	0.4	0	84.0	1.759
D2.4S-0-H5	2000	0.4	0	514.6	0.503
D3.4S-0-H5	3000	0.4	0	344.52	0.652
D4.4S-0-H5	4000	0.4	0	259.84	0.595
D5.4S-0-H5	5000	0.4	0	174.8	0.741
D6.4S-0-H5	6000	0.4	0	149.04	0.926
D7.4S-0-H5	7000	0.4	0	140.0	1.320
D8.4S-0-H5	8000	0.4	0	119.04	1.435

MODEL DESIGNATION.	DIA (mm)	λ	ϕ (DEG)	Pu (Kn)	%δ
D2.4S-0-H6	2000	0.4	0	757.64	0.368
D3.4S-0-H6	3000	0.4	0	531.0	0.483
D4.4S-0-H6	4000	0.4	0	348.0	0.503
D5.4S-0-H6	5000	0.4	0	273.6	0.626
D6.4S-0-H6	6000	0.4	0	223.58	0.742
D7.4S-0-H6	7000	0.4	0	193.2	0.896
D8.4S-0-H6	8000	0.4	0	188.0	1.23

* Arch failed by buckling.

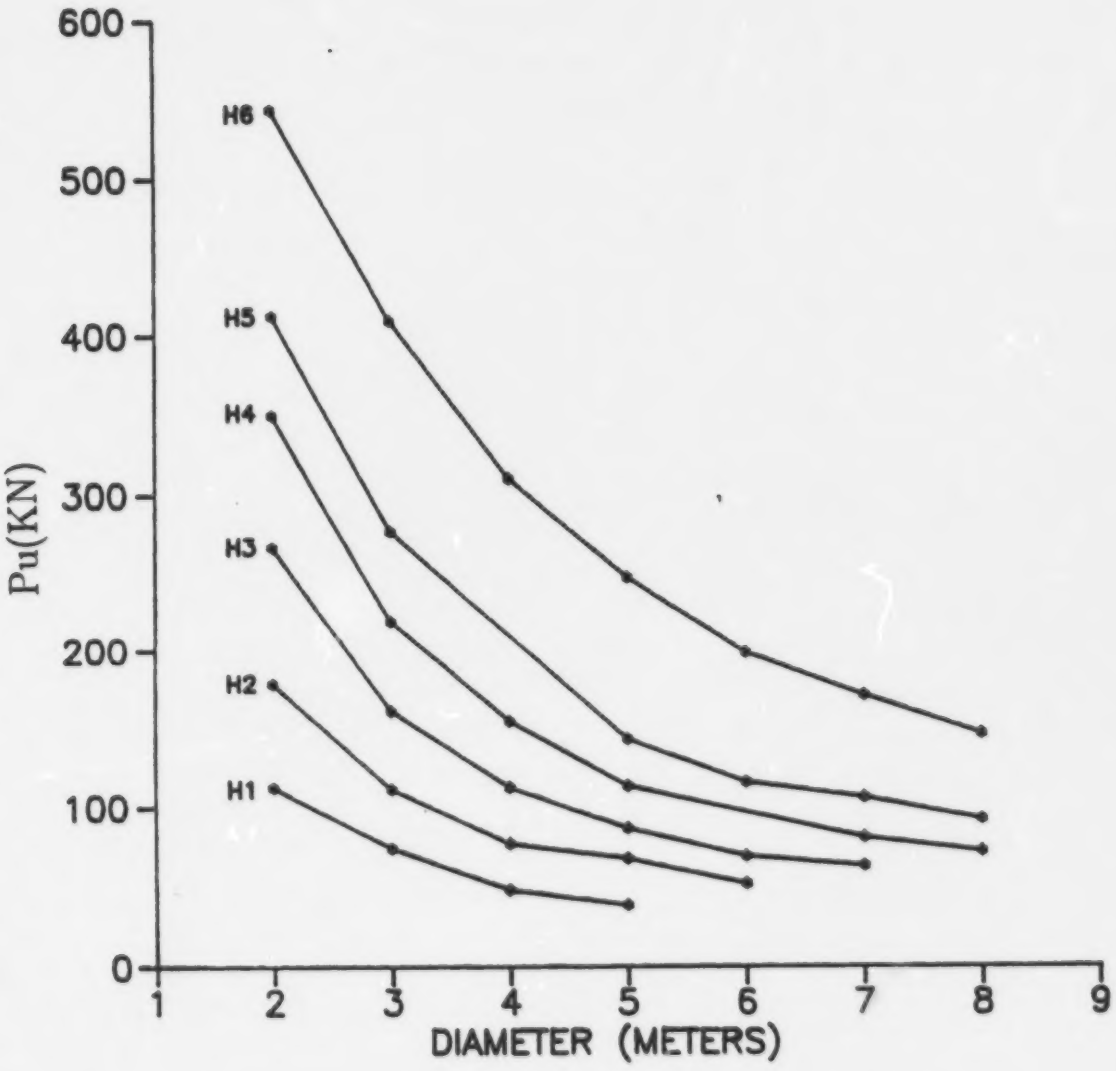

Figure 2.15: Straight Leg Arch under Sinusoidal Load with $\lambda = 0.6$

MODEL DESIGNATION.	DIA (mm)	λ	ϕ (DEG)	Pu (Kn)	$\%\delta$
D2.6S-0-H1	2000	0.6	0	112.0	0.922
D3.6S-0-H1	3000	0.6	0	73.92	1.612
D4.6S-0-H1	4000	0.6	0	48.0	1.477
D5.6S-0-H1	5000	0.6	0	38.4	1.984
D6.6S-0-H1	6000	0.6	0	6.6*	0.362*
D7.6S-0-H1	7000	0.6	0	5.6*	0.423*
D8.6S-0-H1	8000	0.6	0	4.8*	0.483*
D2.6S-0-H2	2000	0.6	0	178.08	0.716
D3.6S-0-H2	3000	0.6	0	110.76	0.965
D4.6S-0-H2	4000	0.6	0	76.8	1.217
D5.6S-0-H2	5000	0.6	0	67.6	2.083
D6.6S-0-H2	6000	0.6	0	51.84	2.053
D7.6S-0-H2	7000	0.6	0	9.1*	0.361*
D8.6S-0-H2	8000	0.6	0	8.0*	0.412*
D2.6S-0-H3	2000	0.6	0	266.4	0.994
D3.6S-0-H3	3000	0.6	0	160.38	0.917
D4.6S-0-H3	4000	0.6	0	112.0	1.090
D5.6S-0-H3	5000	0.6	0	86.4	1.351

* Arch failed by buckling.

Table 2.8: Effect of Sinusoidal Load Distribution on the Behaviour of Straight Leg Arch (D-Type)

MODEL DESIGNATION.	DIA (mm)	λ	ϕ (DEG)	Pu (Kn)	%δ
D6.6S-0-H3	6000	0.6	0	69.0	1.604
D7.6S-0-H3	7000	0.6	0	63.0	2.555
D8.6S-0-H3	8000	0.6	0	11.2*	0.359*
D2.6S-0-H4	2000	0.6	0	349.2	0.868
D3.6S-0-H4	3000	0.6	0	218.4	0.952
D4.6S-0-H4	4000	0.6	0	153.92	1.429
D5.6S-0-H4	5000	0.6	0	112.8	1.181
D6.6S-0-H4	6000	0.6	0	102.96	1.954
D7.6S-0-H4	7000	0.6	0	80.64	1.823
D8.6S-0-H4	8000	0.6	0	72.0	2.722
D2.6S-0-H5	2000	0.6	0	411.8	0.624
D3.6S-0-H5	3000	0.6	0	276.12	0.836
D4.6S-0-H5	4000	0.6	0	165.6	0.763
D5.6S-0-H5	5000	0.6	0	142.5	1.729
D6.6S-0-H5	6000	0.6	0	115.2	1.293
D7.6S-0-H5	7000	0.6	0	105.56	2.121
D8.6S-0-H5	8000	0.6	0	92.0	2.267
D2.6S-0-H6	2000	0.6	0	543.0	0.343
D3.6S-0-H6	3000	0.6	0	408.24	0.661
D4.6S-0-H6	4000	0.6	0	309.12	0.963

* Arch failed by buckling.

MODEL DESIGNATION.	DIA (mm)	λ	ϕ (DEG)	Pu (Kn)	%δ
D5.6S-0-H6	5000	0.6	0	246.4	1.289
D6.6S-0-H6	6000	0.6	0	197.64	1.467
D7.6S-0-H6	7000	0.6	0	170.10	1.945
D8.6S-0-H6	8000	0.6	0	145.6	1.981

* Arch failed by buckling.

2.8 Splay Leg Arch under Sinusoidal Load

This is a very useful type of an arch in underground tunnels. Not only that it provides high performance but also it gives more space by splaying the legs of the arch. The leg to overall height ratio (λ) and the splay leg angle (ϕ) are the parameters which are emphasized in this section. Sinusoidal load is applied and the behaviour of the arches is studied. Tables 2.6, 2.7, and 2.8 give the necessary information like ultimate load, percentage crown deflection, sections properties etc. Whereas Figures 2.16, 2.17 and 2.18 show graphically the effect of increasing diameter against ultimate load. In these graphs λ is taken as 0.2 constant while ϕ increases from 5° to 15°. Selection of λ as 0.2 is based on the parametric studies of straight leg arches.

Study shows an improvement in the performance of arches by increasing an angle ϕ . The ultimate load of section H6, when ϕ =0 and λ =0.2, is about 900 kN. With the same section and λ the ultimate load is increased to 1000 kN when $\phi = 5°$, ultimate load is further increased to 1100 kN when $\phi = 10°$ and with $\lambda = 15°$ the maximum ultimate load obtained is 1300 kN. Which certainly proved that splayed leg arches could be preferred on straight leg arches on the basis of high performance and more space is provided by splaying of the arches.

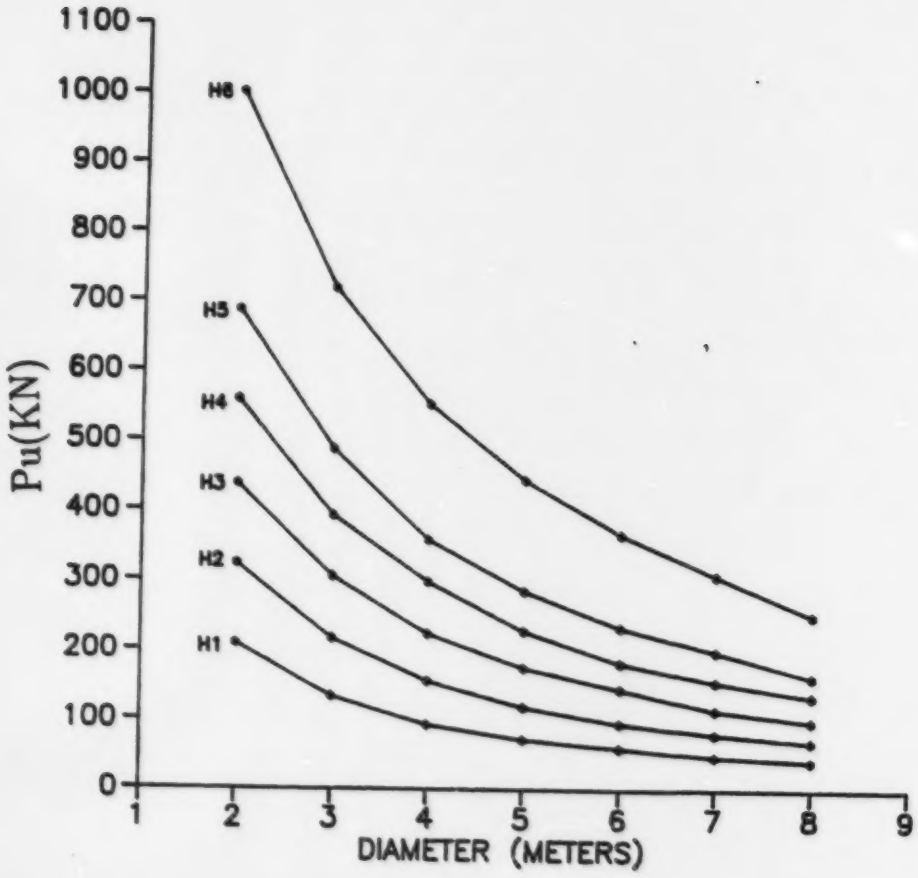

Figure 2.16: Splay Leg Arch under Sinusoidal Load with $\lambda = 0.2$ and $\phi = 5°$

MODEL DESIGNATION.	DIA (mm)	λ	ϕ (DEG)	Pu (Kn)	% δ
A2.2S-5-H1	2000	0.2	5	208.58	0.576
A3.2S-5-H1	3000	0.2	5	132.68	0.701
A4.2S-5-H1	4000	0.2	5	92.31	0.788
A5.2S-5-H1	5000	0.2	5	71.39	0.995
A6.2S-5-H1	6000	0.2	5	59.45	1.196
A7.2S-5-H1	7000	0.2	5	47.38	1.383
A8.2S-5-H1	8000	0.2	5	41.35	1.553
A2.2S-5-H2	2000	0.2	5	323.05	0.453
A3.2S-5-H2	3000	0.2	5	215.95	0.629
A4.2S-5-H2	4000	0.2	5	155.08	0.763
A5.2S-5-H2	5000	0.2	5	117.95	0.860
A6.2S-5-H2	6000	0.2	5	94.53	1.027
A7.2S-5-H2	7000	0.2	5	79.26	1.188
A8.2S-5-H2	8000	0.2	5	68.59	1.337
A2.2S-5-H3	2000	0.2	5	437.52	0.384
A3.2S-5-H3	3000	0.2	5	304.63	0.611
A4.2S-5-H3	4000	0.2	5	222.86	0.709

Table 2.9: Effect of Sinusoidal Load Distribution on the Behaviour of Splay Leg Arch (A-Type)

MODEL DESIGNATION.	DIA (mm)	λ	ϕ (DEG)	Pu (Kn)	% δ
A5.2S-5-H3	5000	0.2	5	174.47	0.901
A6.2S-5-H3	6000	0.2	5	144.01	1.081
A7.2S-5-H3	7000	0.2	5	113.73	1.057
A8.2S-5-H3	8000	0.2	5	98.138	1.183
A2.2S-5-H4	2000	0.2	5	558.35	0.338
A3.2S-5-H4	3000	0.2	5	391.41	0.520
A4.2S-5-H4	4000	0.2	5	297.45	0.718
A5.2S-5-H4	5000	0.2	5	227.09	0.754
A6.2S-5-H4	6000	0.2	5	181.54	0.787
A7.2S-5-H4	7000	0.2	5	154.36	1.004
A8.2S-5-H4	8000	0.2	5	133.91	1.102
A2.2S-5-H5	2000	0.2	5	686.64	0.379
A3.2S-5-H5	3000	0.2	5	486.49	0.512
A4.2S-5-H5	4000	0.2	5	356.94	0.548
A5.2S-5-H5	5000	0.2	5	284.32	0.721
A6.2S-5-H5	6000	0.2	5	232.63	0.850
A7.2S-5-H5	7000	0.2	5	197.88	0.963
A8.2S-5-H5	8000	0.2	5	161.48	0.939
A2.2S-5-H6	2000	0.2	5	1000.42	0.324
A3.2S-5-H6	3000	0.2	5	717.33	0.398

MODEL DESIGNATION.	DIA (mm)	λ	ϕ (DEG)	Pu (Kn)	% δ
A4.2S-5-H6	4000	0.2	5	551.41	0.523
A5.2S-5-H6	5000	0.2	5	443.20	0.640
A6.2S-5-H6	6000	0.2	5	365.31	0.733
A7.2S-5-H6	7000	0.2	5	306.29	0.818
A8.2S-5-H6	8000	0.2	5	250.27	0.797

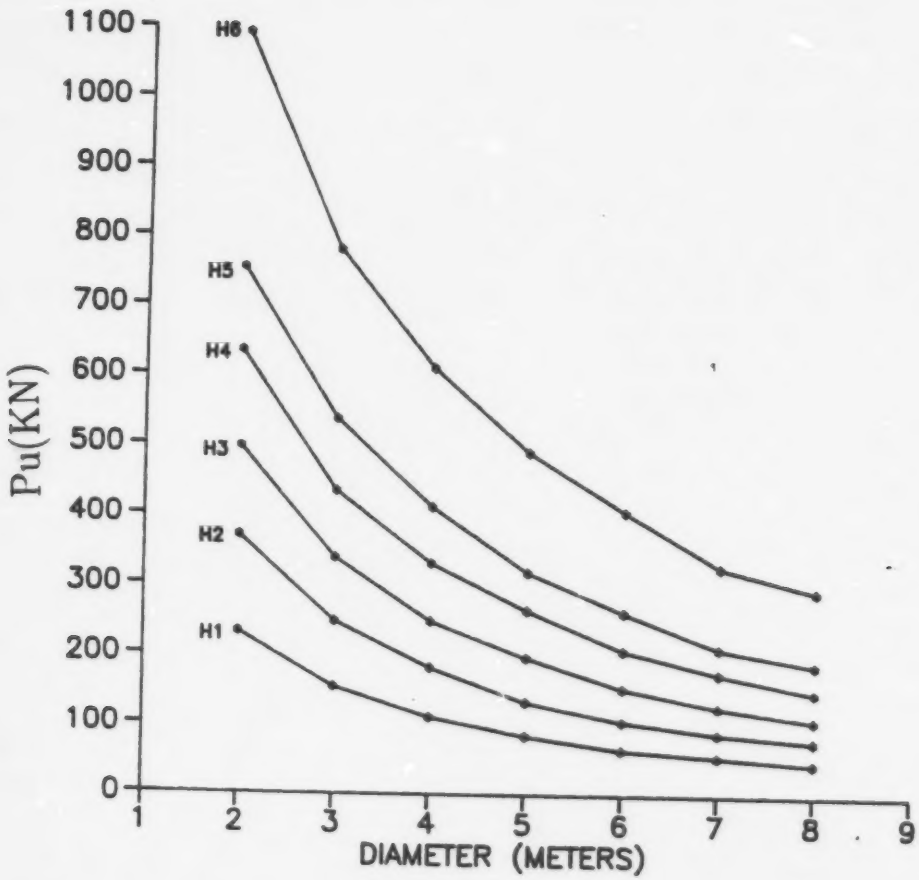

Figure 2.17: Splay Leg Arch under Sinusoidal Load with $\lambda = 0.2$ and $\phi = 10°$

MODEL DESIGNATION	DIA (mm)	λ	ϕ (DEG)	Pu (Kn)	% δ
A2.2S-10-H1	2000	0.2	10	231.39	0.523
A3.2S-10-H1	3000	0.2	10	153.08	0.783
A4.2S-10-H1	4000	0.2	10	110.19	0.920
A5.2S-10-H1	5000	0.2	10	83.91	1.029
A6.2S-10-H1	6000	0.2	10	64.33	1.144
A7.2S-10-H1	7000	0.2	10	55.476	1.444
A8.2S-10-H1	8000	0.2	10	46.28	1.626
A2.2A-10-H2	2000	0.2	10	369.17	0.495
A3.2S-10-H2	3000	0.2	10	247.03	0.727
A4.2S-10-H2	4000	0.2	10	180.79	0.817
A5.2S-10-H2	5000	0.2	10	132.23	0.811
A6.2S-10-H2	6000	0.2	10	105.27	0.978
A7.2S-10-H2	7000	0.2	10	88.11	1.137
A8.2S-10-H2	8000	0.2	10	78.32	1.388
A2.2S-10-H3	2000	0.2	10	496.61	0.409
A3.2S-10-H3	3000	0.2	10	337.37	0.555

Table 2.10: Effect of Sinusoidal Load Distribution on the Behaviour of Splay Leg Arch (A-Type)

MODEL DESIGNATION	DIA (mm)	λ	ϕ (DEG)	Pu (Kn)	% δ
A4.2S-10-H3	4000	0.2	10	247.16	0.648
A5.2S-10-H3	5000	0.2	10	195.58	0.824
A6.2S-10-H3	6000	0.2	10	152.57	0.867
A7.2S-10-H3	7000	0.2	10	126.23	1.004
A8.2S-10-H3	8000	0.2	10	108.15	1.130
A2.2S-10-H4	2000	0.2	10	633.25	0.371
A3.2S-10-H4	3000	0.2	10	433.23	0.469
A4.2S-10-H4	4000	0.2	10	329.89	0.647
A5.2S-10-H4	5000	0.2	10	263.18	0.850
A6.2S-10-H4	6000	0.2	10	206.60	0.818
A7.2S-10-H4	7000	0.2	10	174.44	0.934
A8.2S-10-H4	8000	0.2	10	148.16	1.033
A2.2S-10-H5	2000	0.2	10	752.80	0.300
A3.2S-10-H5	3000	0.2	10	535.90	0.462
A4.2S-10-H5	4000	0.2	10	410.49	0.525
A5.2S-10-H5	5000	0.2	10	317.53	0.659
A6.2S-10-H5	6000	0.2	10	261.15	0.782
A7.2S-10-H5	7000	0.2	10	210.04	0.791
A8.2S-10-H5	8000	0.2	10	187.15	0.977

MODEL DESIGNATION	DIA (mm)	λ	ϕ (DEG)	Pu (Kn)	% δ
A2.2S-10-H6	2000	0.2	10	1090.45	0.246
A3.2S-10-H6	3000	0.2	10	778.59	0.356
A4.2S-10-H6	4000	0.2	10	609.60	0.474
A5.2S-10-H6	5000	0.2	10	489.50	0.578
A6.2S-10-H6	6000	0.2	10	405.07	0.668
A7.2S-10-H6	7000	0.2	10	326.33	0.670
A8.2S-10-H6	8000	0.2	10	292.42	0.824

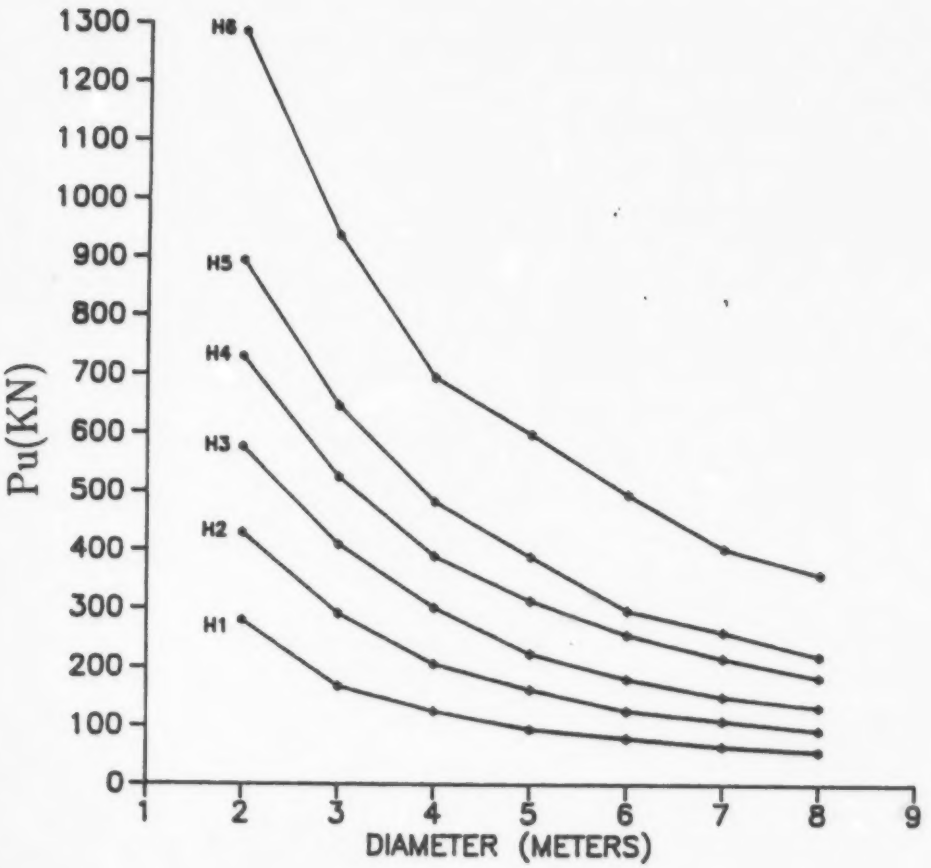

Figure 2.18: Splay Leg Arch under Sinusoidal Load with $\lambda = 0.2$ and $\phi = 15°$

MODEL DESIGNATION	DIA (mm)	λ	ϕ (DEG)	Pu (Kn)	% δ
A2.2S-15-H1	2000	0.2	15	279.09	0.524
A3.2S-15-H1	3000	0.2	15	166.99	0.504
A4.2S-15-H1	4000	0.2	15	124.86	0.705
A5.2S-15-H1	5000	0.2	15	94.57	0.850
A6.2S-15-H1	6000	0.2	15	78.57	1.121
A7.2S-15-H1	7000	0.2	15	64.81	1.319
A8.2S-15-H1	8000	0.2	15	56.44	1.497
A2.2S-15-H2	2000	0.2	15	428.56	0.398
A3.2S-15-H2	3000	0.2	15	290.13	0.571
A4.2S-15-H2	4000	0.2	15	205.02	0.605
A5.2S-15-H2	5000	0.2	15	161.37	0.777
A6.2S-15-H2	6000	0.2	15	125.13	0.878
A7.2S-15-H2	7000	0.2	15	108.64	1.112
A8.2S-15-H2	8000	0.2	15	92.59	1.265
A2.2S-15-H3	2000	0.2	15	575.38	0.329
A3.2S-15-H3	3000	0.2	15	408.52	0.561

Table 2.11: Effect of Sinusoidal Load Distribution on the Behaviour of Splay Leg Arch (A-Type)

MODEL DESIGNATION.	DIA (mm)	λ	ϕ (DEG)	Pu (Kn)	% δ
A4.2S-15-H3	4000	0.2	15	299.99	0.658
A5.2S-15-H3	5000	0.2	15	222.22	0.633
A6.2S-15-H3	6000	0.2	15	179.49	0.769
A7.2S-15-H3	7000	0.2	15	149.38	0.898
A8.2S-15-H3	8000	0.2	15	131.92	1.108
A2.2S-15-H4	2000	0.2	15	728.82	0.288
A3.2S-15-H4	3000	0.2	15	523.59	0.460
A4.2S-15-H4	4000	0.2	15	388.08	0.525
A5.2S-15-H4	5000	0.2	15	311.81	0.681
A6.2S-15-H4	6000	0.2	15	254.62	0.828
A7.2S-15-H4	7000	0.2	15	214.81	0.943
A8.2S-15-H4	8000	0.2	15	182.53	1.050
A2.2S-15-H5	2000	0.2	15	892.53	0.322
A3.2S-15-H5	3000	0.2	15	644.82	0.455
A4.2S-15-H5	4000	0.2	15	481.47	0.524
A5.2S-15-H5	5000	0.2	15	386.89	0.686
A6.2S-15-H5	6000	0.2	15	295.23	0.602
A7.2S-15-H5	7000	0.2	15	259.25	0.766
A8.2S-15-H5	8000	0.2	15	209.52	0.794

MODEL DESIGNATION.	DIA (mm)	λ	ϕ (DEG)	Pu (Kn)	% δ
A2.2S-15-H6	2000	0.2	15	1283.43	0.275
A3.2S-15-H6	3000	0.2	15	934.79	0.344
A4.2S-15-H6	4000	0.2	15	692.25	0.463
A5.2S-15-H6	5000	0.2	15	595.66	0.586
A6.2S-15-H6	6000	0.2	15	492.84	0.712
A7.2S-15-H6	7000	0.2	15	401.22	0.640
A8.2S-15-H6	8000	0.2	15	357.13	0.846

Chapter 3

Stress Analysis

3.1 Introduction

In order to achieve an economical design of a tunnel support, it is important that the roof pressure be estimated as accurately as possible so that while the support should be strong enough to sustain the anticipated pressure, it should also be as light as possible for handling, installation and economy purposes. It is for that reason that parametric studies were carried out in Chapter 2 to provide handy information on the load bearing capacity of different section sizes. In this Chapter, it is the objective to undertake two-dimensional stress analysis of the No. 2 Tunnel opening of the Donkin Morien project without the steel support with a view of gaining some insight into the ground response without a ring support, i.e stresses and deformation, thus providing a basis for deciding the need for ground support. The stress analyses to follow have been conducted by the finite element technique using the computer model MSAP2D.

3.2 Computer Software MSAP2D

A computer model, MSAP2D (Microcomputer Static Analysis Program for 2-Dimensional Problems),is a computer model that has been developed for use on personal computers equipped with mathematical coprocessor and hard disk (3). MSAP2D is a finite element program with two-dimensional, quadrilateral isoparametric elements. Each element has four corner nodes with two

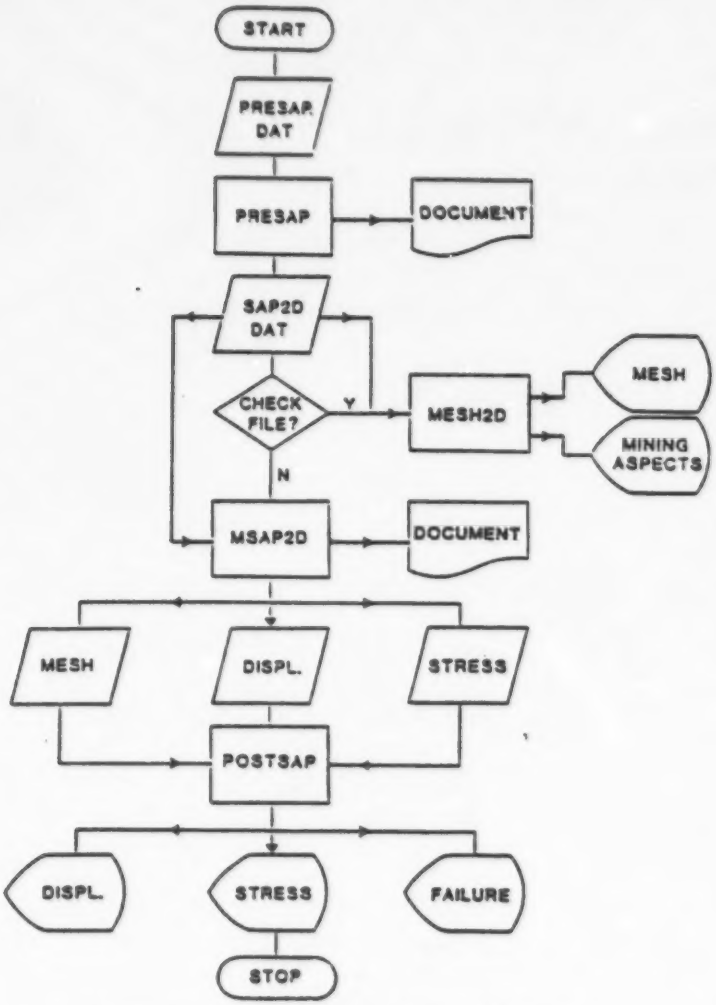

Figure 3.1: Flowchart of MSAP2D System

degrees of freedom per node making a total of eight degrees of freedom per element. Fig. 3.1 shows a flowchart of the basic structure of the MSAP2D system, which is composed of the following five modules, ZONE, PRESAP, MESH2D, MSAP2D and POSTSAP. The ZONE, PRESAP and MESH2D modules represent the pre-processor and the input interface of the system. The fourth module MSAP2D is the core system processor, whereas the fifth module, POSTSAP, is the post- processor

PRESAP basically generates the finite element mesh for the core program MSAP2D. It reads a simple datafile (which is checked by using the first module, ZONE) and generates the required datafile for the core program. With this, PRESAP also outputs a document file which gives general information

of the input data. The data for program PRESAP can be checked graphically by program ZONE; which displays the geometry of the model, its geology, intended mesh grading and boundary conditions. MESH2D is a graphic program for checking the output file from program PRESAP, which is also the input file for program MSAP2D. The basic purpose of MESH2D is to check visually the geometry of the structure (tunnel opening, ditch, syphon opening etc), generated mesh, boundary conditions, mining sequences and material types simulated.

MSAP2D is the main finite element program of the system. Displacements of the nodal points as well as stresses at prescribed locations are computed. The stress output locations include the centroid and the mid-points of the four sides of each element.

POSTSAP is a graphic program designed to interpret the output from MSAP2D. Nodal displacements are displayed in vectorial form. Major and minor principal stresses at the centroid of all elements are also plotted in vectorial form. Moreover, failure criteria have been incorporated into the program to allow parameter studies to be performed and to check the safety level of an excavation design. Another significant feature of MESH2D and POSTSAP is that they have the option to display the graphical representation on an enlarged scale with the node number and element number of the enlarged portion. The solution procedure is as follows

1. Prepare the datafile for the program PRESAP (e.g FILE.DAT) which identifies the problem layout, boundary conditions, material properties and loading conditions, as well as the required meshing of the domain. If needed,this file may be checked graphically using ZONE.

2. Using FILE.DAT, run PRESAP. This will generate the required datafile for the core program, FILE.SAP, as well as an information output for documentation purposes.

3. There is a further option of visual check of FILE.SAP using the MESH2D and if not required then just bypass this stage and run the core program MSAP2D.

4. MSAP2D, outputs three files (FILE.NDE, FILE.DIS, FILE.STS), which are subsequently used by the postprocessor. MSAP2D at this stage also generates a documentary file (FILE.DOC) for the user.

5. Finally with the help of the postprocessor three datafiles (generated by MSAP2D) are converted into graphical output. This enables checking of stresses, displacements and material safety levels. The latter is achieved by means of Mohr-Coulomb, Drucker- Prager or Hoek-Brown failure criterion.

3.3 Pre- and Post- Processors

3.3.1 PRESAP

The mesh generation scheme in PRESAP is based on the shape functions of the 8-node quadratic isoparametric elements to subdivide a quadrilateral zone into any number of subdivisions to create a finite element mesh. The zone is defined by 4 corner nodes, 4 side nodes and 4 sides which can be either straight or curved depending on the location of the side node. Fig 3.9 is one of the sections of No.2 Tunnel of Donkin Morien which is selected for analysis. The modelled domain is divided into 22 zones (zones are constructed according to the geology around the tunnel). Zones are 4 nodes, 5 nodes, 6 nodes and 8 nodes, depending on the location of the zone in the model. At the opening, more nodes are used to define the circular boundary. Similarly nodes 11, 47 and 16 are used to generate the mesh in this direction of the model. Fig. 3.12 shows both the layout and the geology of the chainage section. The actual finite element mesh generated by PRESAP which was graphically produced by MESH2D is shown in Fig, 3.10. This figure further demonstrates that with only 22 user-specified zones, it is possible to simulate 6 geological materials and generate a mesh of 540 elements. As can be seen from Fig. 3.10 the mesh around the opening is very fine, which makes it difficult to see the circular boundary of the opening and elements around it, so this portion is enlarged as shown in Fig. 3.11 to visually check before running the program.

3.3.2 POSTSAP

The numerical output of any practical problem solved by the finite element method is often tedious to examine by hand. A postprocessor routine, exploiting high resolution color graphics, which is capable of transforming such

outputs into graphical representation of displacement vectors and principal stresses is an essential component for any computer model to be efficient and easy to use. Another main function of POSTSAP is to evaluate the safety level of the material by calculating the stress at the element centroid and comparing it with the material strength. The stress is obtained from MSAP2D output while the strength of material is based on a failure criterion. Three failure criteria are considered in POSTSAP; the first two are Mohr-Coulomb and Drucker-Prager and their input parameters include the cohesion and the internal friction angle of material (C,ϕ). The third failure criterion considered is Hoek- Brown and the required parameters include the uniaxial compressive strength σ_c, and m and s parameters of the material.

Given the principal stresses (σ_1, σ_2 and σ_3) at a point, the quantities with subscripts "all" and "max" representing respectively the strength and the existing stress of the material can be calculated using any of the failure criteria. The equations used for the calculation are as follows.

1. Mohr-Coulomb:

   $\tau_{all} = c - [\frac{\sigma_1+\sigma_3}{2} - \frac{\sigma_1-\sigma_3}{2}\sin\phi]\tan\phi$

   $\tau_{max} = \frac{\sigma_1-\sigma_3}{2}\cos\phi$

2. Drucker-Prager:

   $K_{all} = \frac{6c\cos\phi}{\sqrt{3}(3-\sin\phi)}$

   $K_{max} = \frac{2\sin\phi}{\sqrt{3}(3-\sin\phi)}(\sigma_1+\sigma_2+\sigma_3)+\{\frac{1}{6}[(\sigma_1-\sigma_3)^2+(\sigma_2-\sigma_3)^2+(\sigma_3-\sigma_1)^2]\}^{1/2}$

3. Hoek-Brown:

   $\sigma_{all} = \sigma_3 + (m\sigma_c\sigma_3 + s\sigma_c^2)^{1/2}$

   $\sigma_{max} = \sigma_1$ (positive in compression)

The safety level of the material (S.L) can then be easily calculated by dividing the strength (or "all" quantity) by the stress (or "max" quantity). When this ratio is greater than 1.43 (stress $\not>$ 70% of strength), the material is considered to be "stable", and when it is less than 1.0, it is considered "unsafe". Otherwise, the stability is viewed as being "critical" ($1.0 < S.L \not< 1.43$).

As an example, let us consider again the previously mentioned example of tunnel section. Fig. 3.14 shows the pattern of principal stresses around the

tunnel opening. This is an output of MSAP2D and further converted into graphical representation by POSTSAP. Stresses are compressive and shown on an enlarged scale only around the tunnel opening (the critical section). similarly Fig. 3.13 shows the displacements of the nodal points on an enlarged scale.

Fig. 3.17 shows the safety level of the materials around the tunnel. Hoek-Brown method is used and its input parameters are shown on Fig.3.16. "FAILED", "CRITICAL", and "SAFE" sign conventions are also shown with the figure. No "FAILED" or "CRITICAL" patterns are observed which means materials are safe around the tunnel.

3.4 Model Simulation

In order to analyze the stresses and deformations around the tunnel opening, a model of tunnel section is taken as shown in Fig. 3.2 . The boundary of the modelled domain is taken at a distance 8 to 10 times the size of the opening.Due to symmetry, only half of the opening is taken into account. The tunnel is simulated by confining the outer boundary by rollers on the sides and hinges at the corner, then applying the in-situ stresses as initial stresses throughout the domain as well as gravity load as body forces in the vertical directions.

3.4.1 Input Stresses

Prior to excavating the No.2 Tunnel a program of in-situ stress determination was undertaken in May 1983. The in-situ stress measurement program was undertaken in 100 mm diameter borehole at chainage 964 in NO.3 Tunnel, by the method of overcoring using the CSIRO (Australian Council of Scientific and Industrial Research Organization(8)) hollow inclusion gauge and the USBM (United States Bureau of Mines) deformation gauge. The CSIRO gauge enables the determination of the three-dimensional stress field but the USBM gauge provides the stress on a plane normal to the axis of the borehole. From these experiments, the in-situ horizontal (Ph) to vertical stress (Pv) ratio (Ko) is found to be 2.5 . Thus the vertical stress is 4.9 MPa and horizontal stress is 12.5 MPa . The in-situ stress system is assumed to be acting in the plane of extensometer. As the No.2 Tunnel is in the same

vicinity, the same in-situ stresses are assumed for it.

3.4.2 Selection of Chainages

When the tunnel was excavated it encountered different types of rocks at different gradients. Initially, the tunnel is at a grade of -20 % for the first 875 meters and then its grade decreased to -10 % .The tunnel is completely in the Portal sandstone in the first 1300 meters. At chainage 925 where tunnel starts changing its grade, it is considered as critical section, so a stress/displacement analysis of the section was deemed necessary at this chainage. From 1300 meters onwards the tunnel is on -1.07 % grade. At chainage 1420 meter the tunnel is partially in Portal sandstone and partially in siltstone. Chainage 1420 was also selected as one of the chainages for analysis. Chainage 1831 was also selected because the tunnel encountered McRury seam (a kind of a coal seam) not a hardrock and local failure could be anticipated. All the way, tunnel passes through different rocks including different types of coal seams like Phalen seam, Backpit seam, Bouthiller seam and finally at chainage 3522 tunnel reached the Harbour seam (the coal seam for which tunnel was excavated). Keeping the geology in consideration, the following chainages were selected for stress/displacement analysis,

- Chainage 925 meter
- Chainage 1420 meter
- Chainage 1831 meter
- Chainage 2263 meter
- Chainage 2433 meter
- Chainage 2996 meter
- Chainage 3522 meter
- Chainage 3385 meter.

3.5 Results

3.5.1 Stress Analysis

When an underground excavation is made, the stresses which previously existed in that area are disturbed, and new stresses are induced in the rocks around the opening in the closed vicinity. The virgin stresses are due to the weight of the overlying strata and the geological history of the rock masses. The disturbances in these stresses sometimes cause so enormous stresses that they exceed the strength of the rock and result in the failure of the rocks adjacent to the excavation boundary. Failure could be a gradual closure of excavation or roof falls etc. This type of failure means that stresses are basically compressive stresses and are excessive near the opening as compared to a distance away from the centre of the opening.

The stress analysis of No. 2 Tunnel of Donkin Morien was done by using MSAP2D and the results are displayed in Figures. The figures graphically show the stresses around the tunnel opening. These stresses are primarily compressive and their concentration is in the adjacent rocks of the opening. In some of the cases as in Fig. 3.56 tensile stresses are also observed near the boundary. This is mainly because of the mechanical properties of these rocks (Mechanical properties are given in Table 1.2). For example tensile stresses are observed near the boundary of the tunnel section at chainage 3522 (Fig. 3.56). The reason is that the tunnel intercepted to the Harbour Coal Seam and the mechanical properties of this rock show that it is not a hard rock. Any excavation in this type of rocks could have some tensile stresses, in addition to the compressive stresses, and roof falling could result due to rock fracturation.

3.5.2 Displacements

When a tunnel is excavated, the existing in-situ stresses are disturbed and new stresses are developed. But the rocks around the opening regain the equilibrium and the opening remain stable. "This regain of equilibrium" is accompanied by displacements of the rocks around the opening. The principal interest in the study of displacement of the No.2 tunnel of Donkin Morien are:

1. To study the response of the rock strata to the excavation of the tunnel.

2. To provide a means of determining the zone of active movement adjacent to the excavation boundary and the stability condition of the tunnel.

Because of the difference in the tunnel grade and the general dip of the rock strata through which the Tunnel No. 2 was driven, different rock types were encountered along the length of the tunnel. The displacement results obtained at different sections of the tunnel are different with each other and within the section. This difference is in accordance with the rock types. If the tunnel is driven in one type of rock then the displacements are more at the shoulder than at the base and the crown which is because of the in-situ stresses. But if the tunnel is in different types of rocks then displacement pattern will vary according to the rocks around the opening. For example the study of the displacement pattern of chainage 925 (Fig.3.13) shows that the displacement of nodal points are more between A and B than between B and C which is attributed to the mechanical properties of these rocks (Fig. 3.12 shows the geology around the opening). Similarly the displacement pattern of the section at chainage 925 is different from section at chainage 3522. This further proves that the stability of the tunnel depends on the rocks in which it is excavated.

In short, the displacement profile around the opening appears with what is normally observed in practice i.e excessive displacements near the opening and floor heave. However the calculated displacements are smaller then could be anticipated. This is to be expected since the modelling is based on linear elasticity. The maximum displacement is observed at the shoulder and this may be attributed to the high in-situ horizontal stress.

3.5.3 Material Safety Level

In MSAP2D, three failure criterion are available for the material safety level. These are Mohr-Coulomb, Drucker-Prager and Hoek-Brown (explained earlier). Using the Hoek-Brown failure criterion the safety levels of the ground around the opening are calculated. The parameters required for this criterion are: uniaxial compressive strength and m & s values which are available from Donkin Morien Project.

Figures 3.18 show the graphical representation of the resulting material safety levels. From these figures the following conclusions can be drawn:

1. The rocks around the opening are primarily in 'safe' condition.

2. All those sections of the No.2 Tunnel which did not encounter any type of coal seam are observed safe.

3. Wherever the tunnel encountered the coal seam, a 'critical' zone is observed at that specific location of that section. This is due to the poor mechanical properties of the coal seam.

4. The 'critical' safety levels are predominantly observed at the location where the weak rocks (coal seam) intersected with the tunnel opening.

5. The safety levels of rocks which are in 'critical' condition occur only near the opening boundary and are in 'safe' condition away from the opening.

6. It should be noted that if a potential failure region is detected a redistribution of stresses will occur and a non-linear solution technique will be required. However, the observed 'failure' zones are localized i.e near the tunnel opening, and hence the results are deemed to be useful to a large extent.

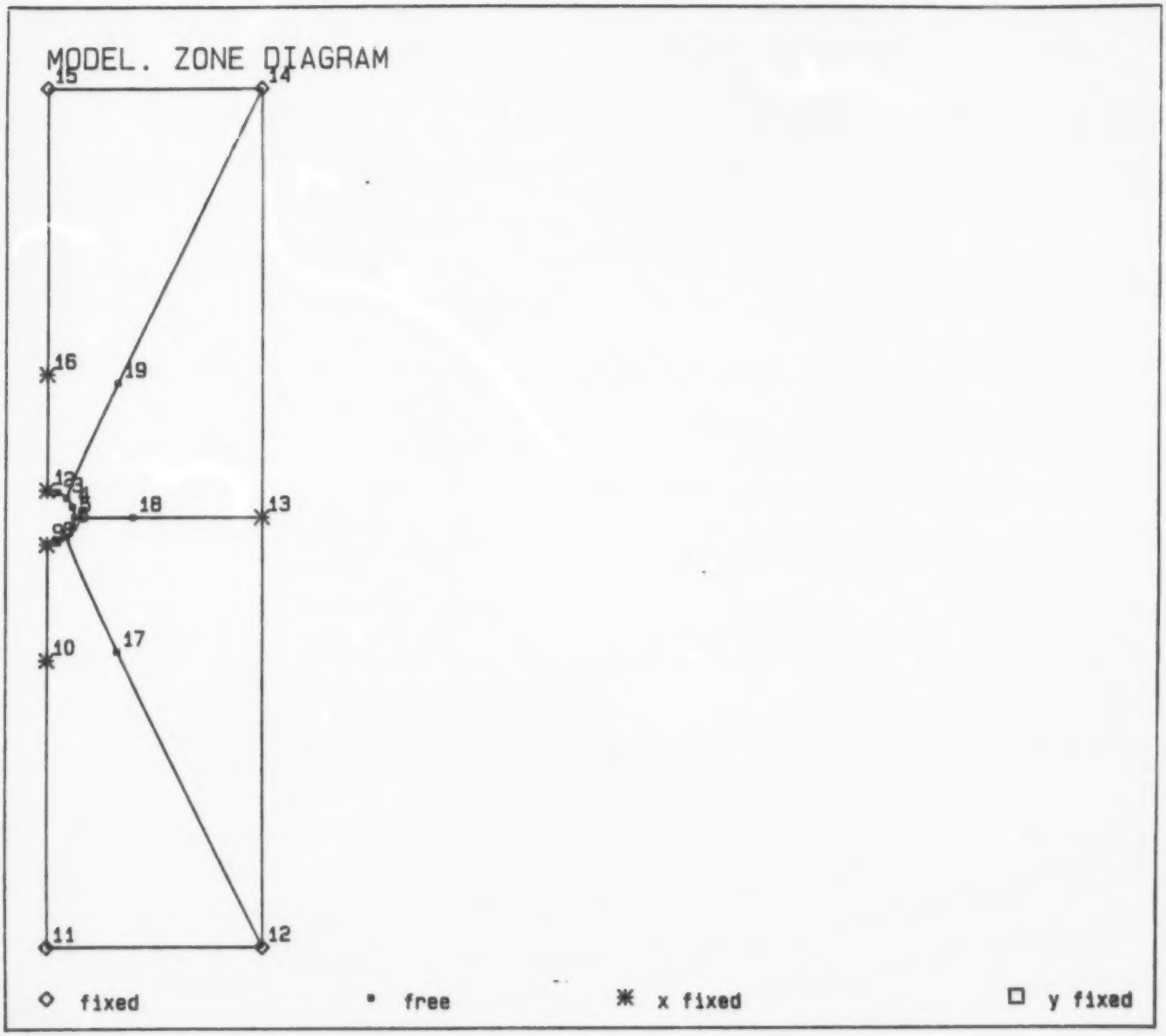

Figure 3.2: No.2 Tunnel, Model Diagram User-Specified Nodes

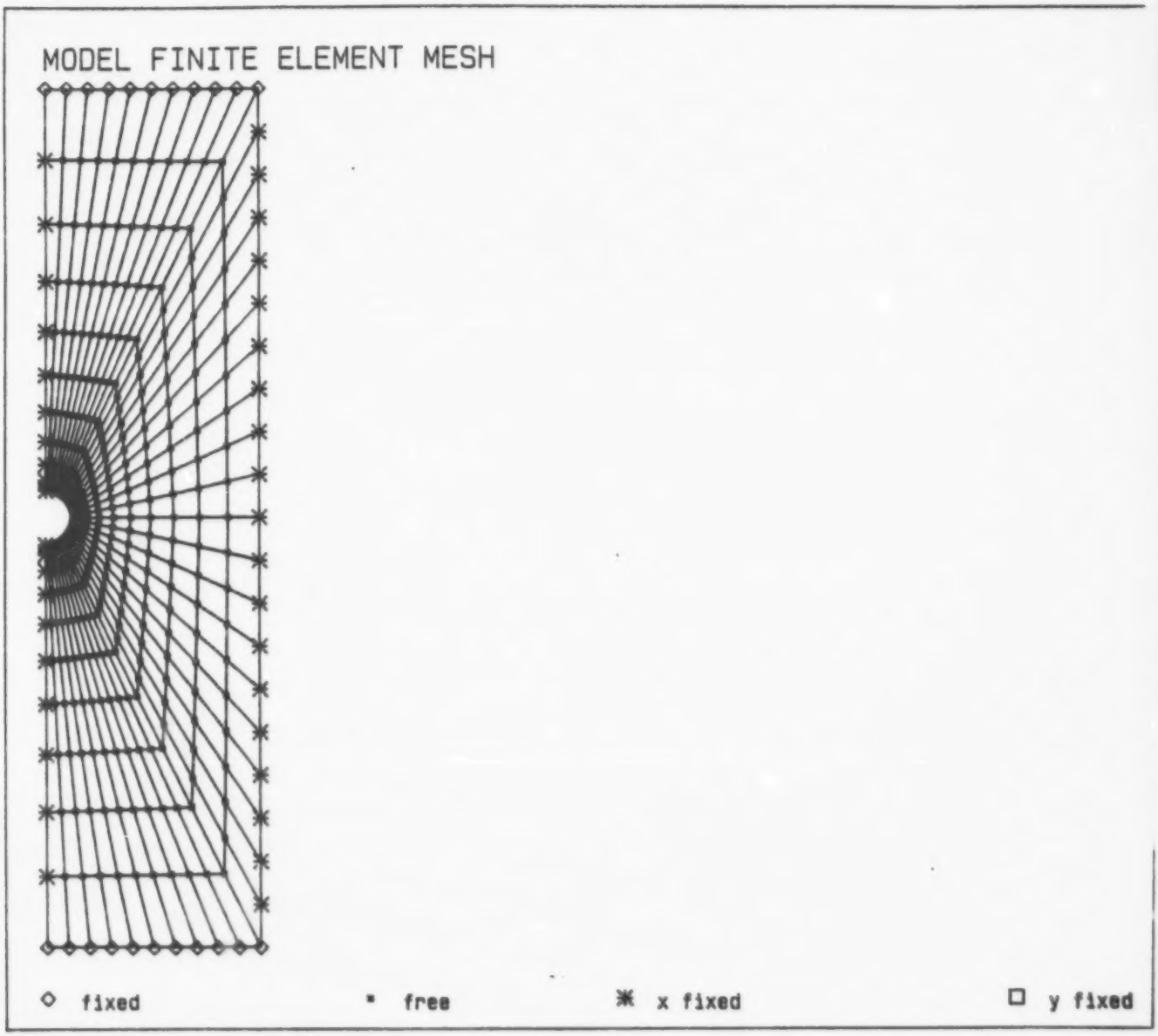

Figure 3.3: No.2 Tunnel, Model Diagram. Finite Element Mesh around the Tunnel Opening

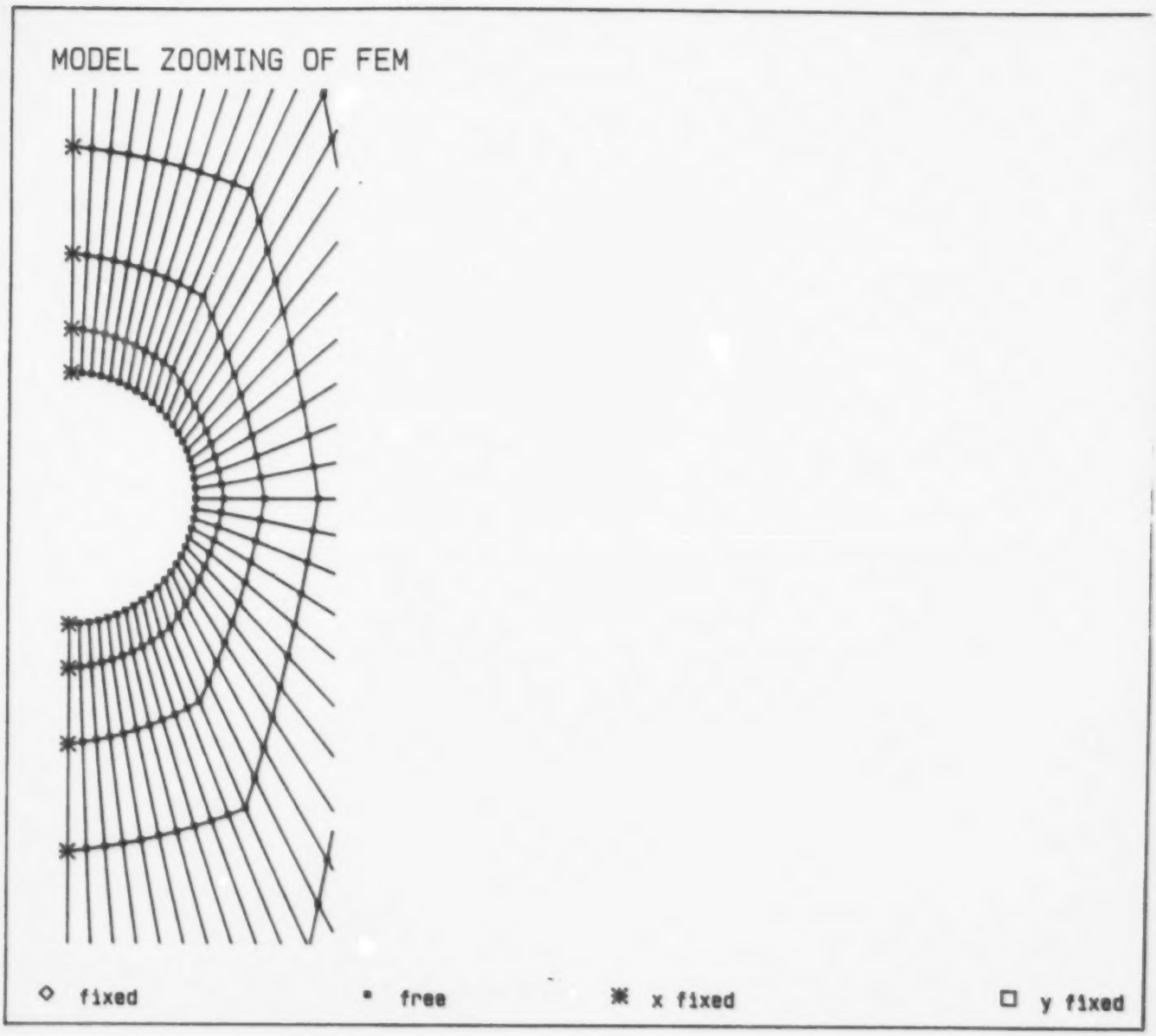

Figure 3.4: No.2 Tunnel, Model Diagram. Zooming of Finite Element Mesh around the Opening

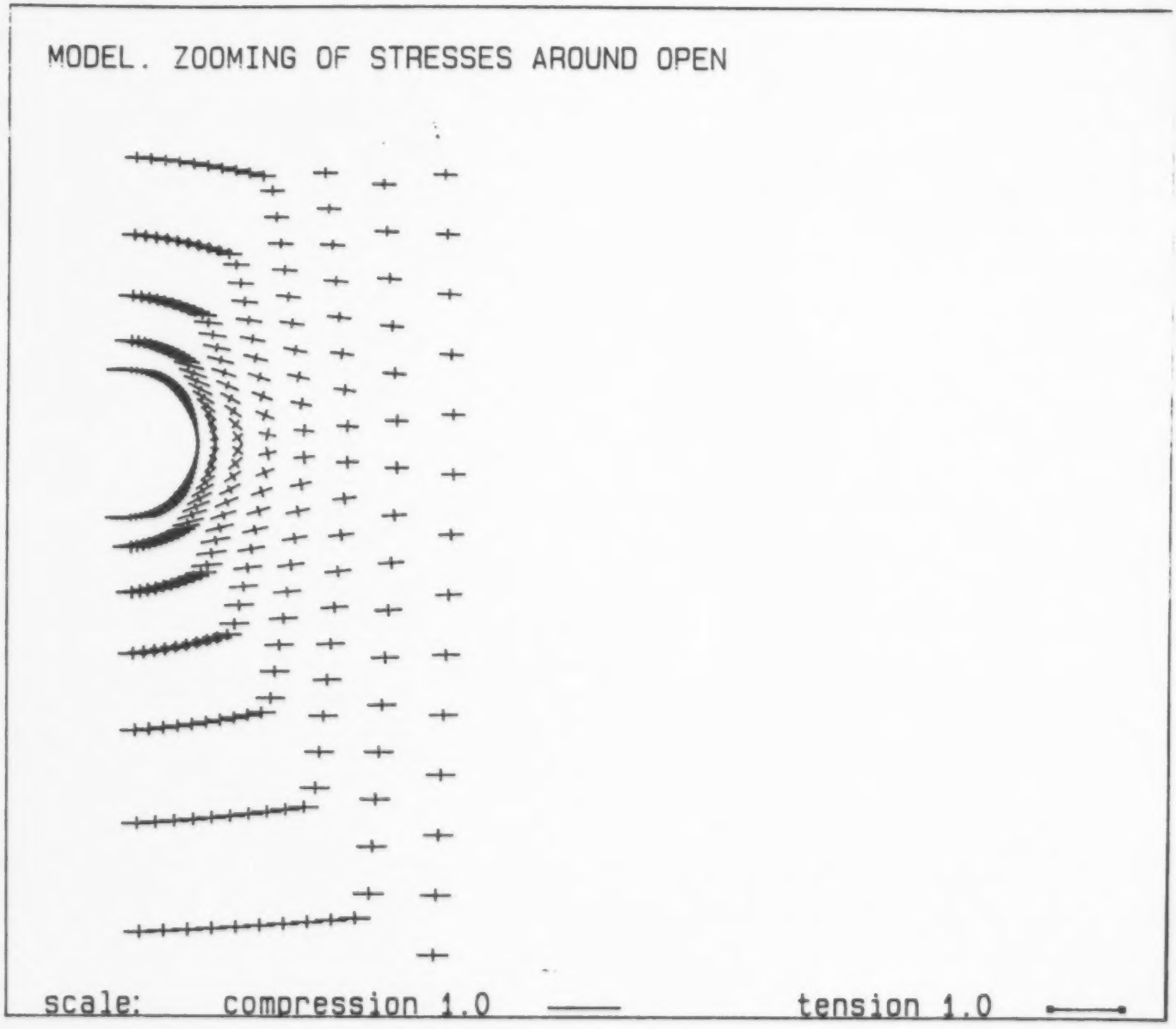

Figure 3.5: No.2 Tunnel, Model Diagram. Stress Pattern around the Opening

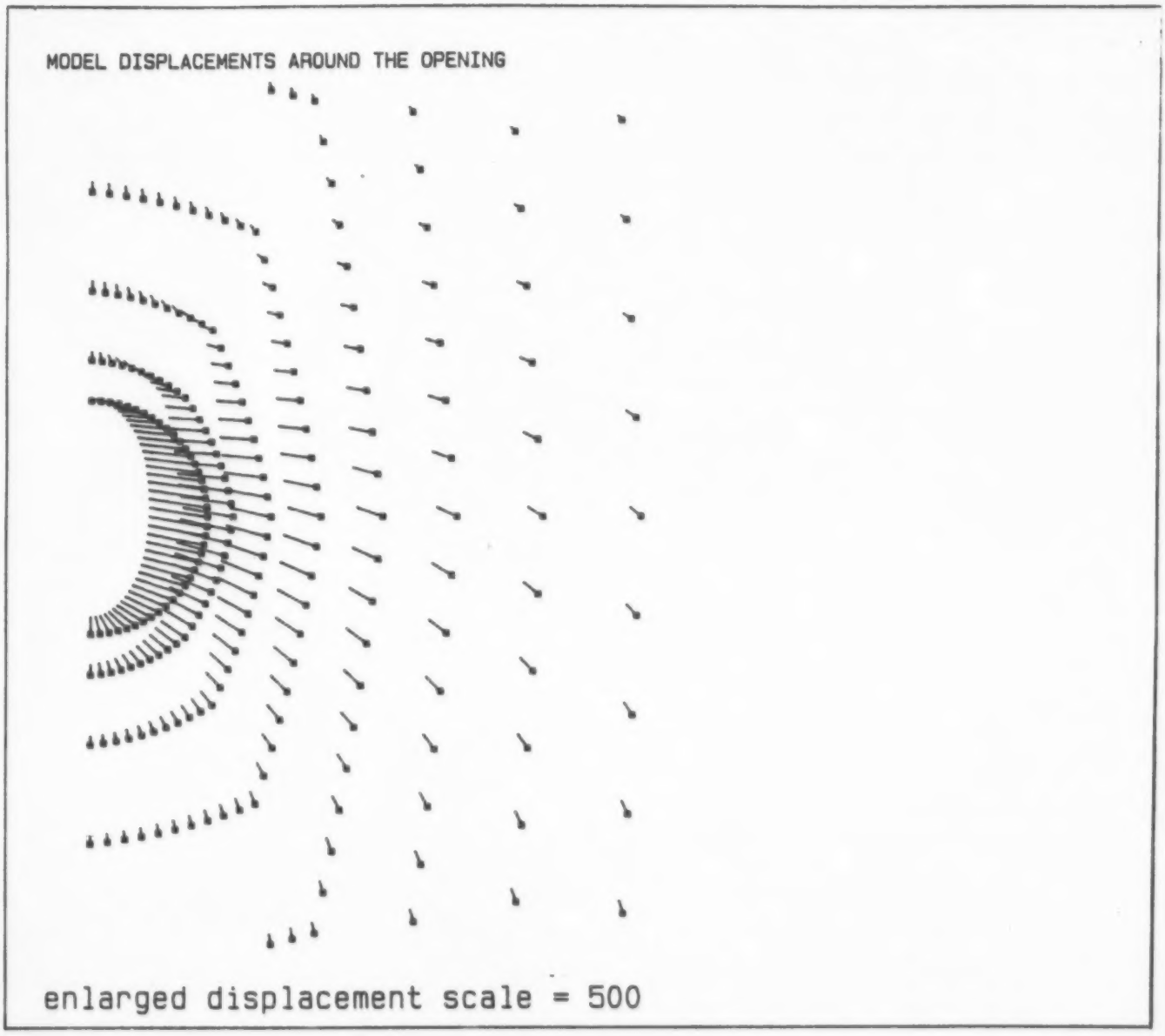

Figure 3.6: No.2 Tunnel, Model Diagram. Displacements of Nodal Points around the Opening

FAILURE CRITERIA	COEFFICIENTS		
	first	second	third
1.Mohr_Coulomb	C	Angle	
2.Drucker_Prager	C	Angle	
3.Hoek and Brown	M	S	Sigma C

TOTAL NO. OF MATERIAL TYPES = 1

MATERIAL NO.	FAIL. CRITERIA	COEFFICIENTS		
1	3	5	0.14	53

Figure 3.7: No.2 Tunnel, Model Diagram. Parameters of the Failure Criteria

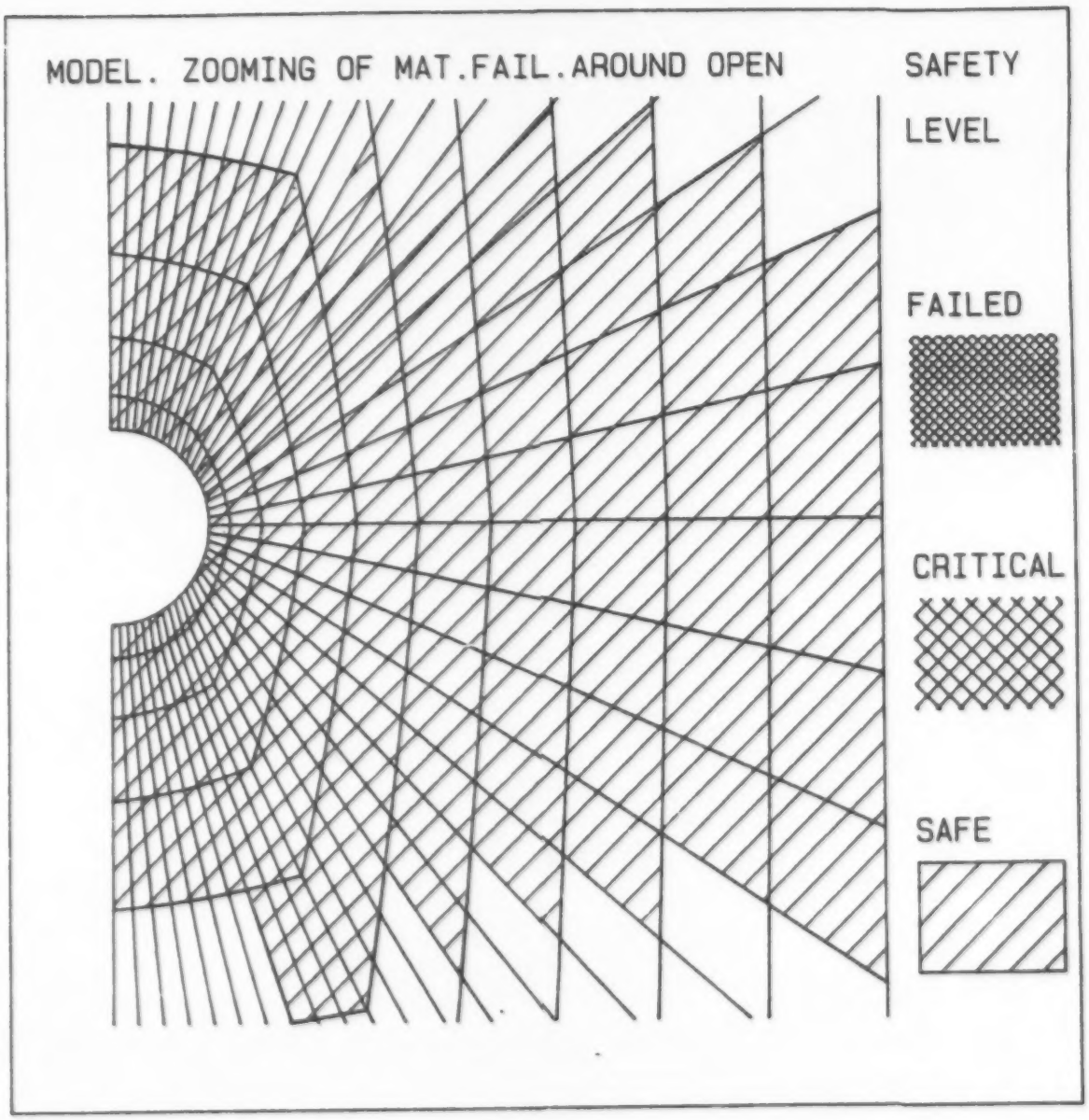

Figure 3.8: No.2 Tunnel, Model Diagram. Zooming of Material Failure Pattern

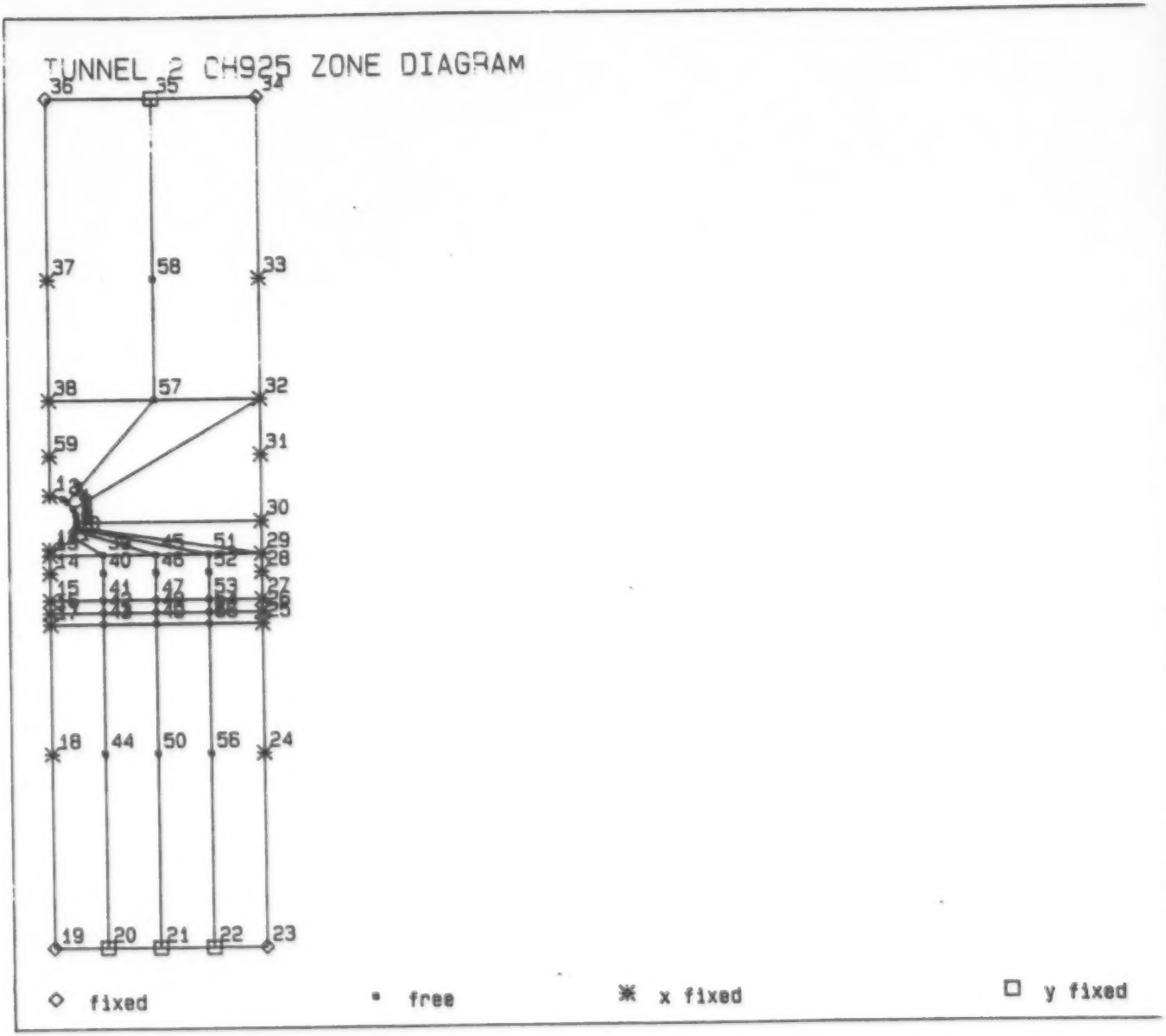

Figure 3.9: No.2 Tunnel, CH925 User-Specified Finite Element Diagram

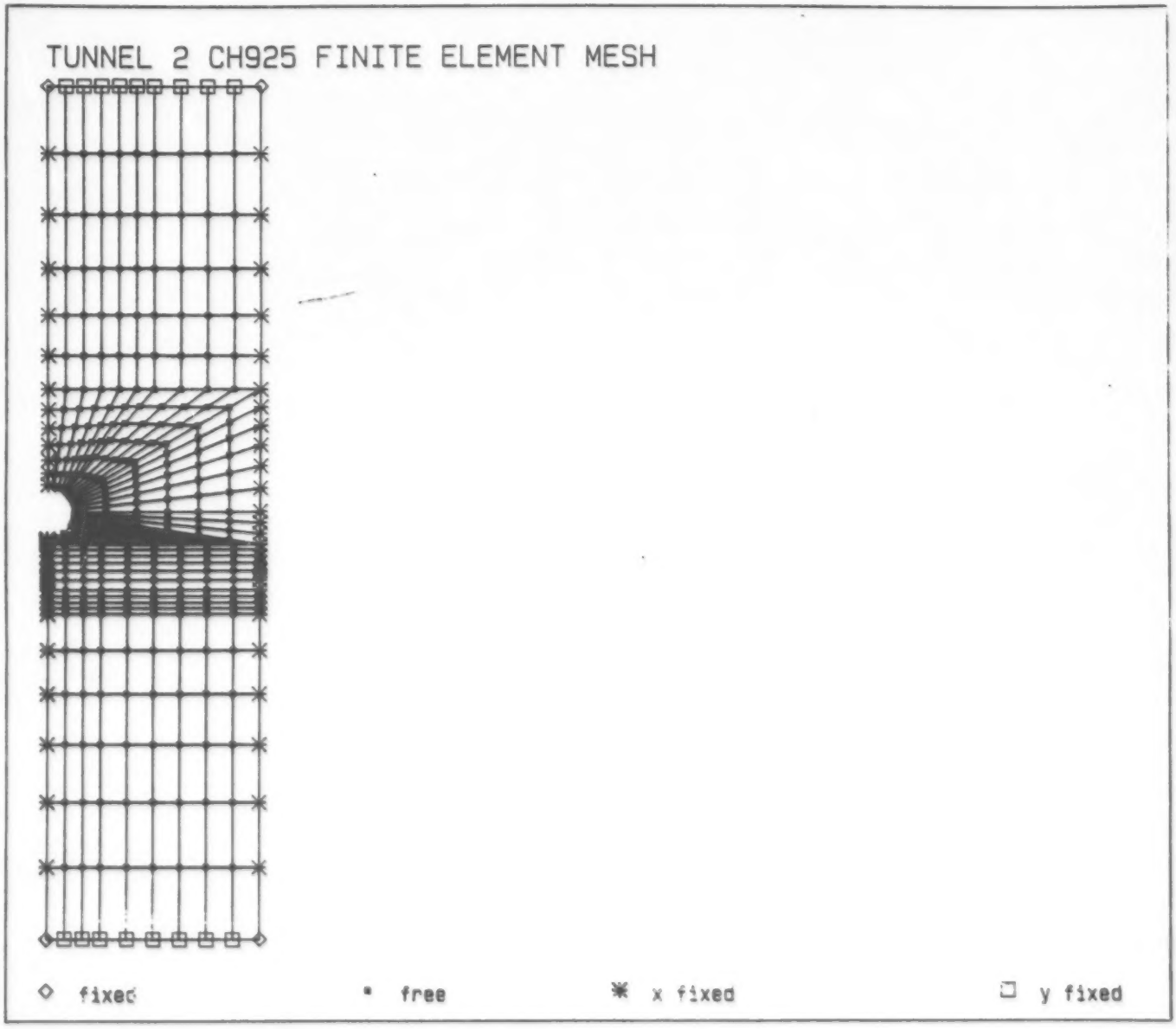

Figure 3.10: No.2 Tunnel, CH925. Finite Element Mesh

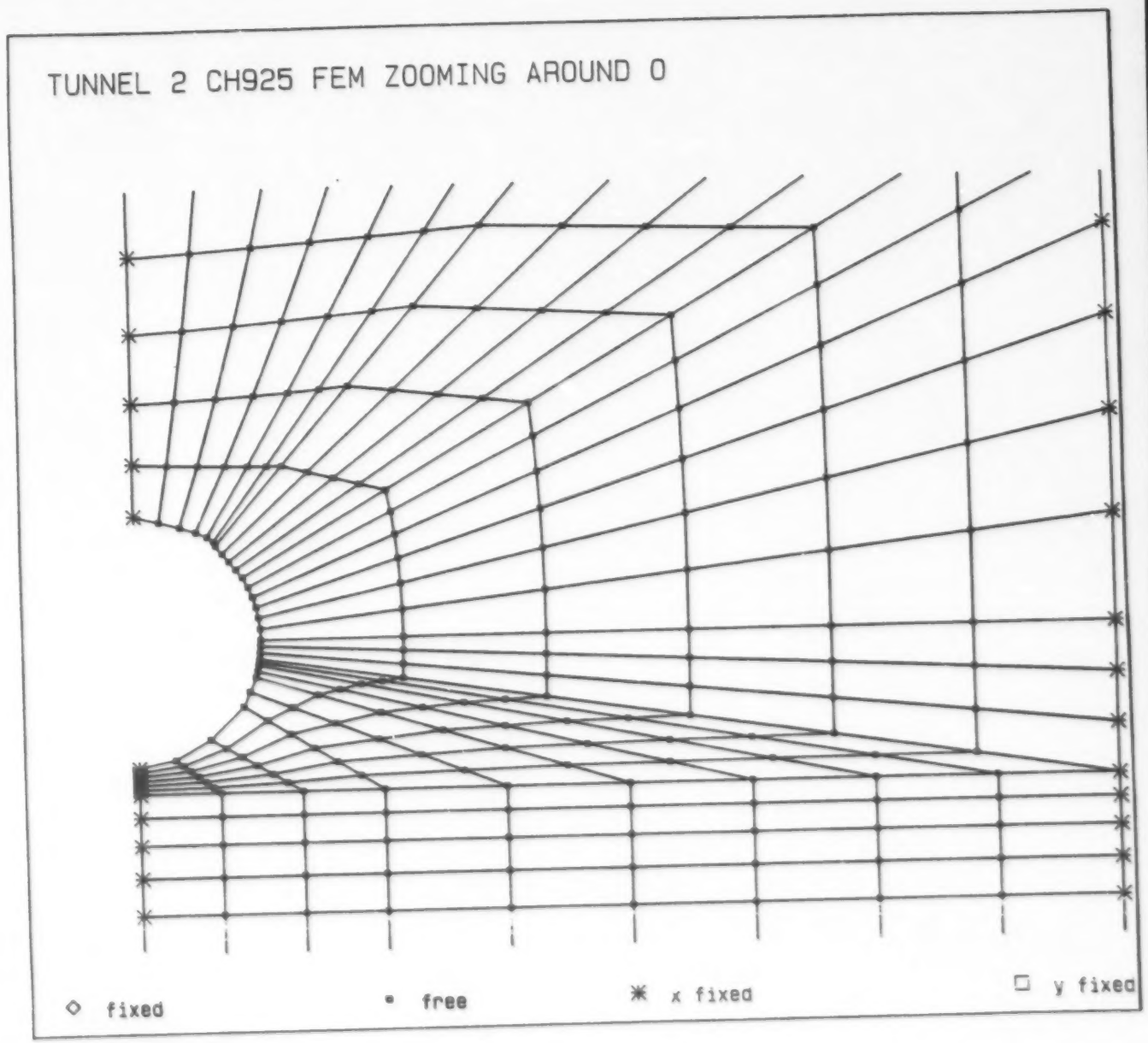

Figure 3.11: No.2 Tunnel, CH925. Zooming of Mesh around the Opening

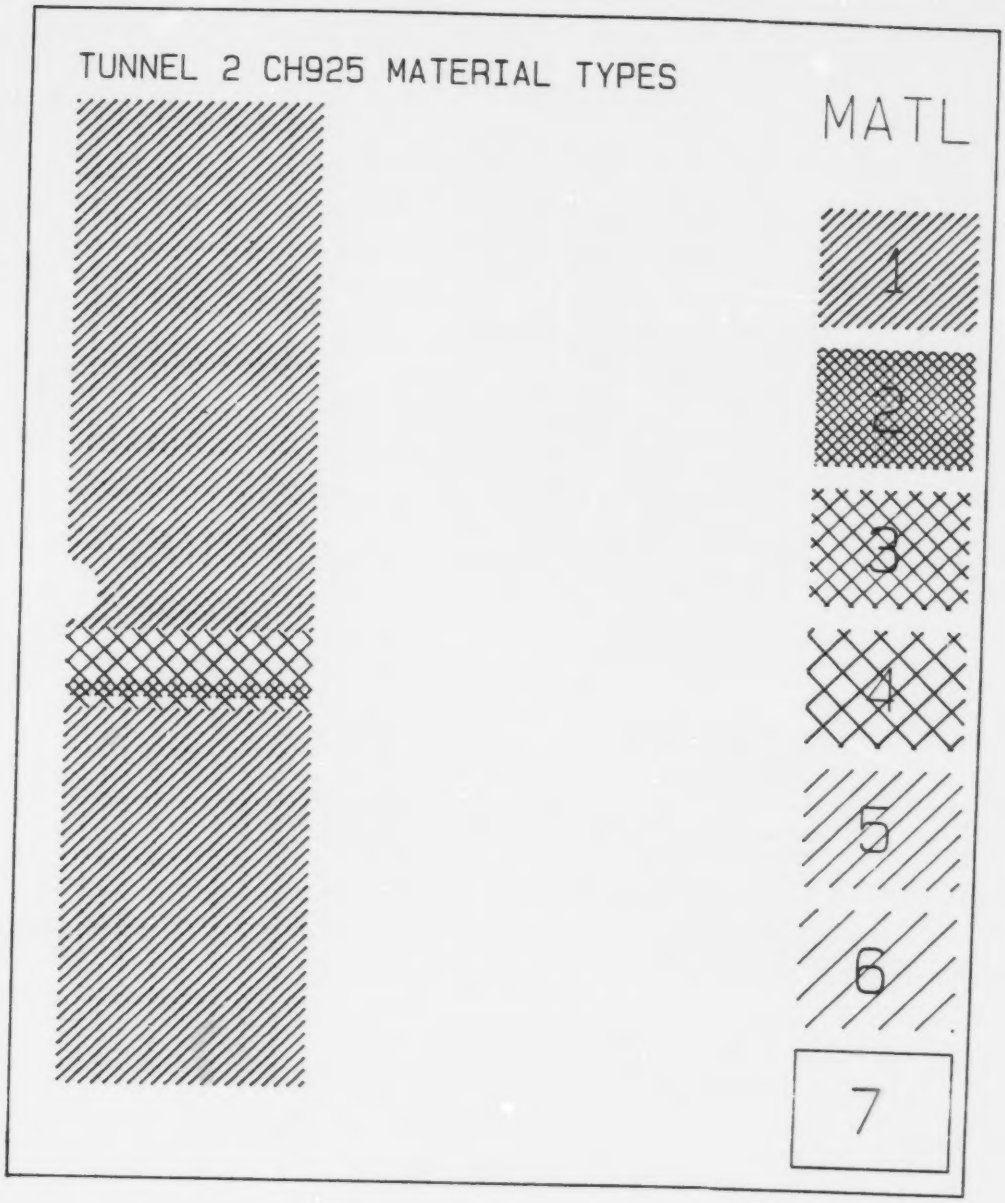

Figure 3.12: No.2 Tunnel, CH925. Material Pattern around the Opening

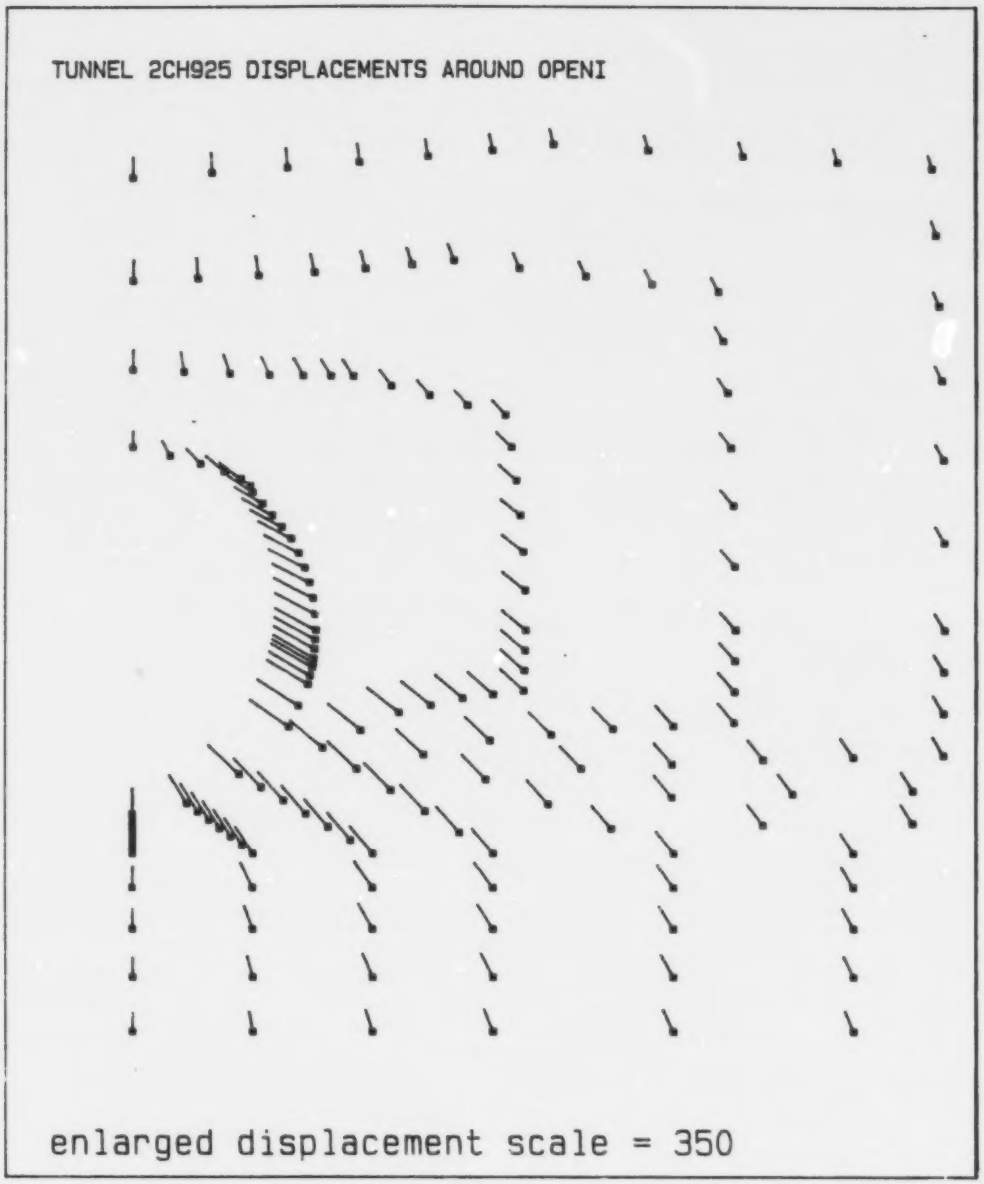

Figure 3.13: No.2 Tunnel, CH925. Zooming of Nodal Point Displacements around the Opening

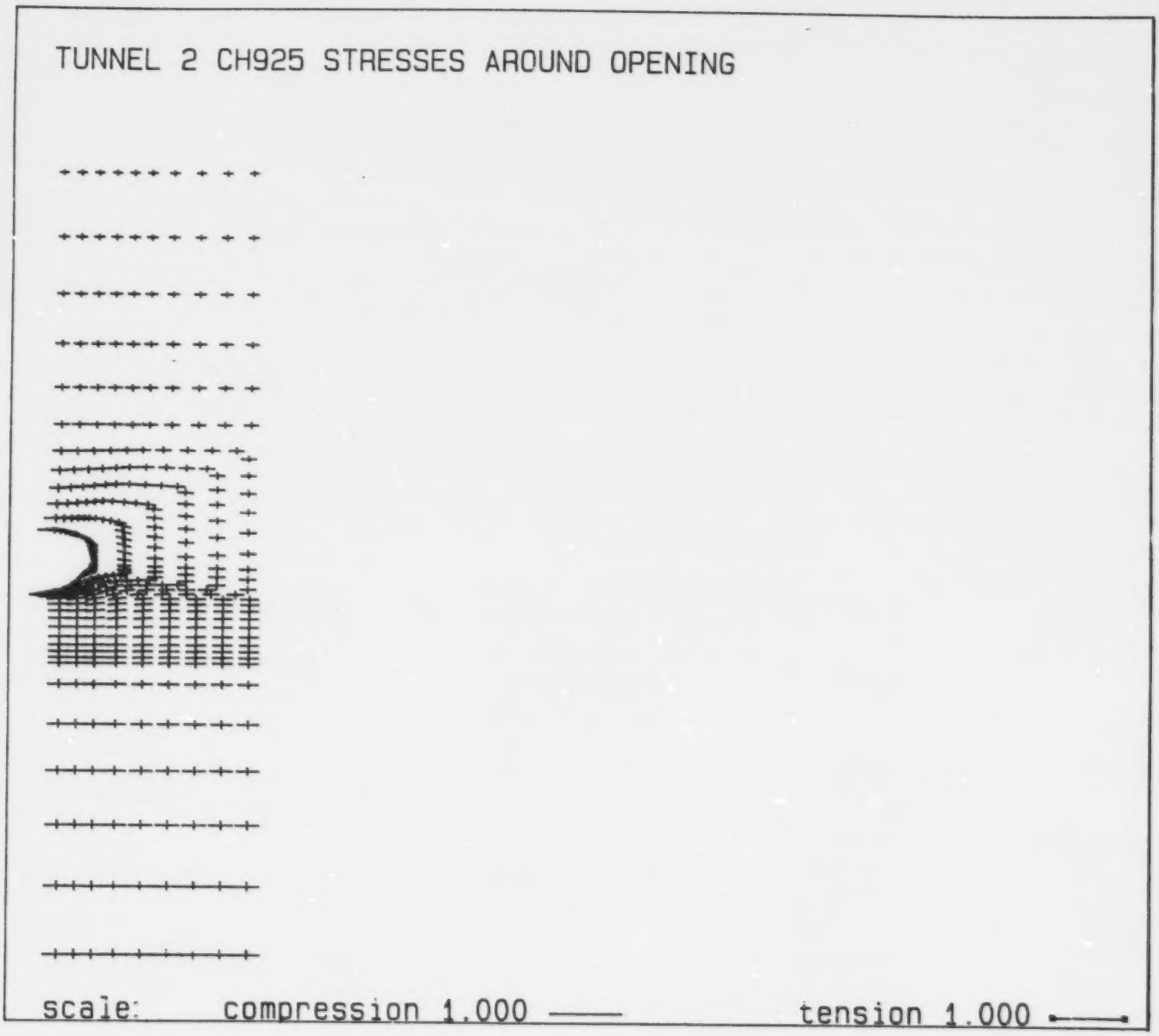

Figure 3.14: No.2 Tunnel, CH925. Stress Pattern around the Opening

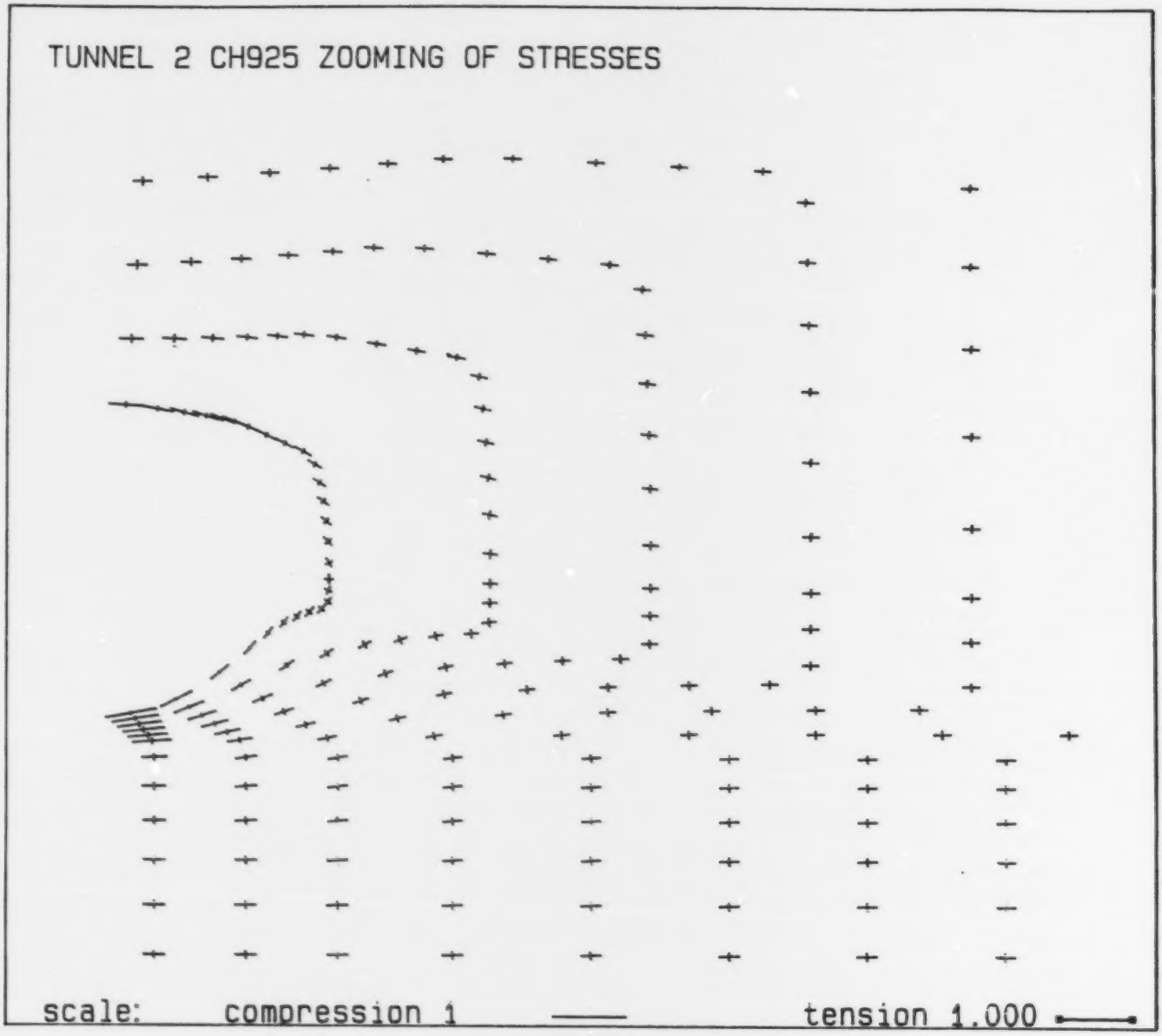

Figure 3.15: No.2 Tunnel, CH925. Zooming of Stresses around the Opening

FAILURE CRITERIA	COEFFICIENTS		
	first	second	third
1.Mohr_Coulomb	C	Angle	
2.Drucker_Prager	C	Angle	
3.Hoek and Brown	M	S	Sigma C

TOTAL NO. OF MATERIAL TYPES = 3

MATERIAL NO.	FAIL. CRITERIA	COEFFICIENTS		
1	3	5	.1	92
2	3	5	.1	53
3	3	5	.1	36

Figure 3.16: No.2 Tunnel, CH925. Parameters of the Material Failure Criteria

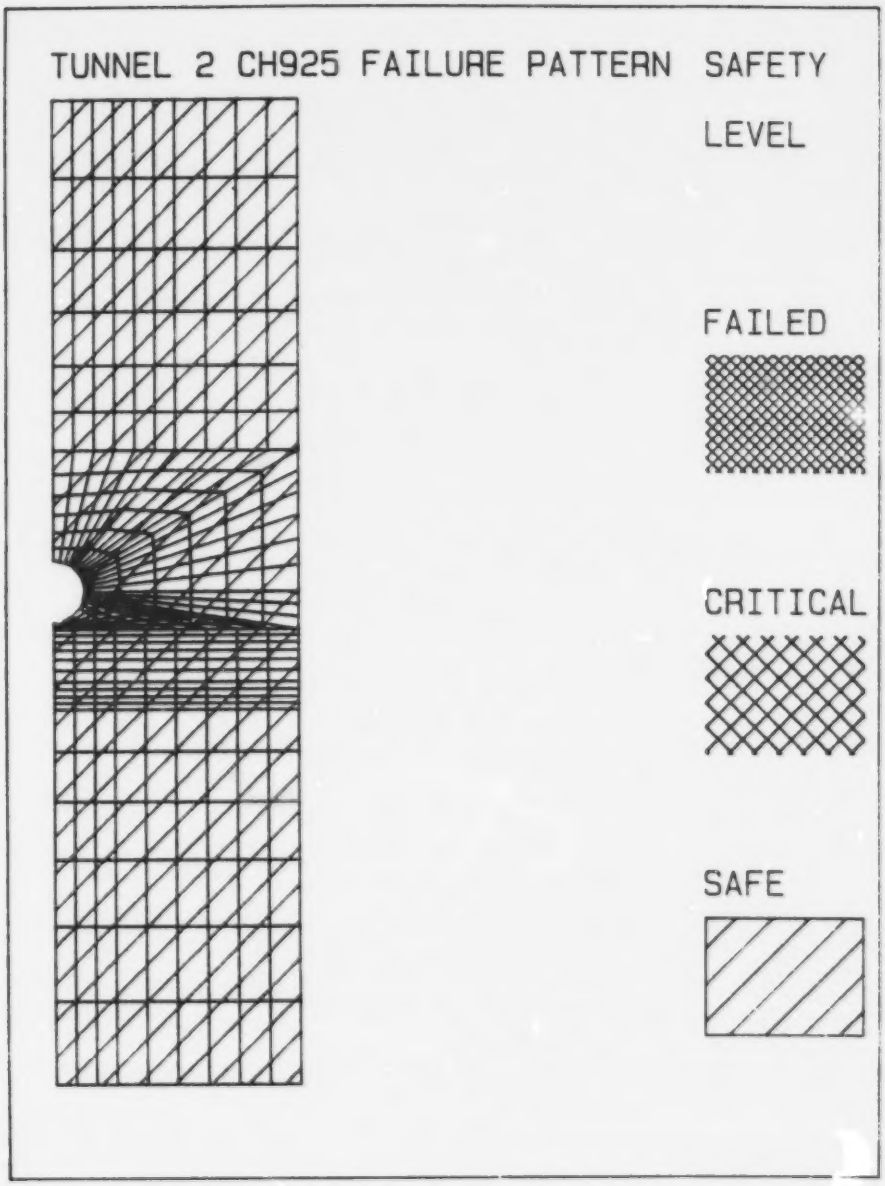

Figure 3.17: No.2 Tunnel, CH925. Failure Pattern around the Opening

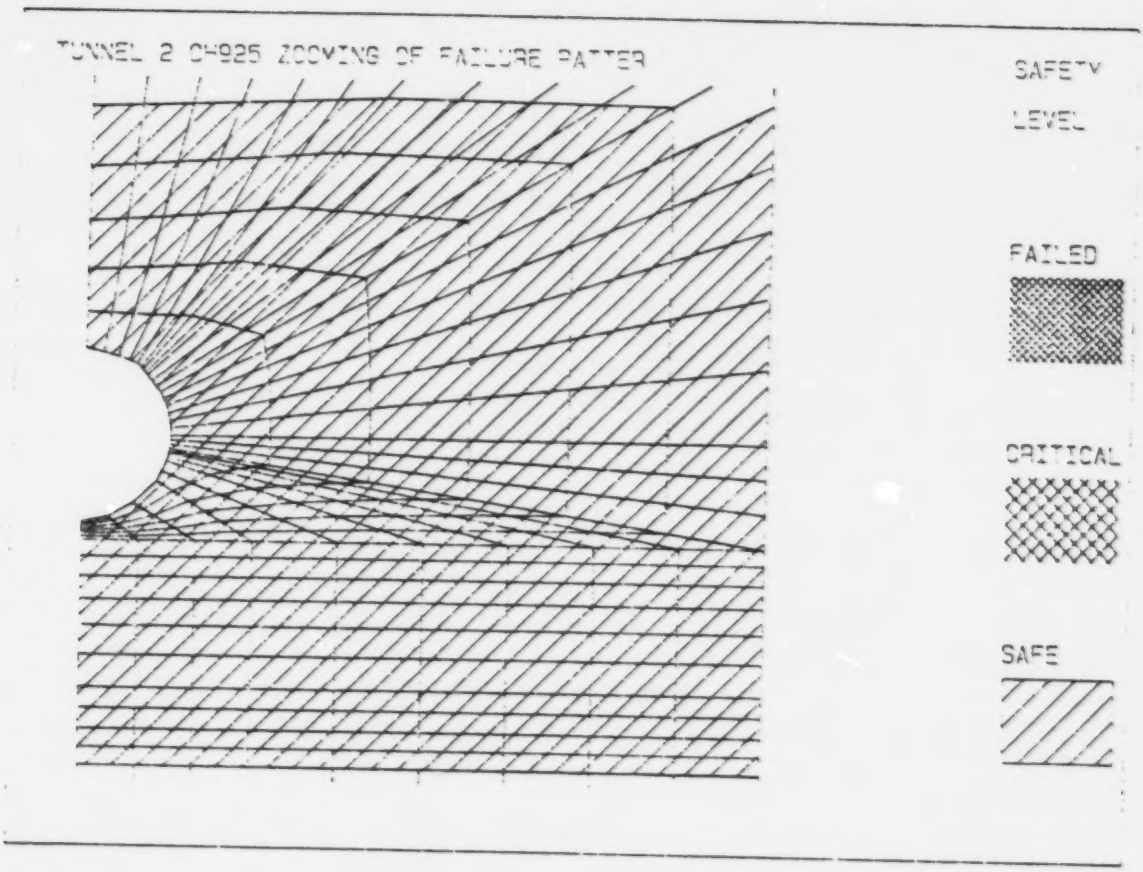

Figure 3.18: No.2 Tunnel, CH925. Zooming of Failure Pattern

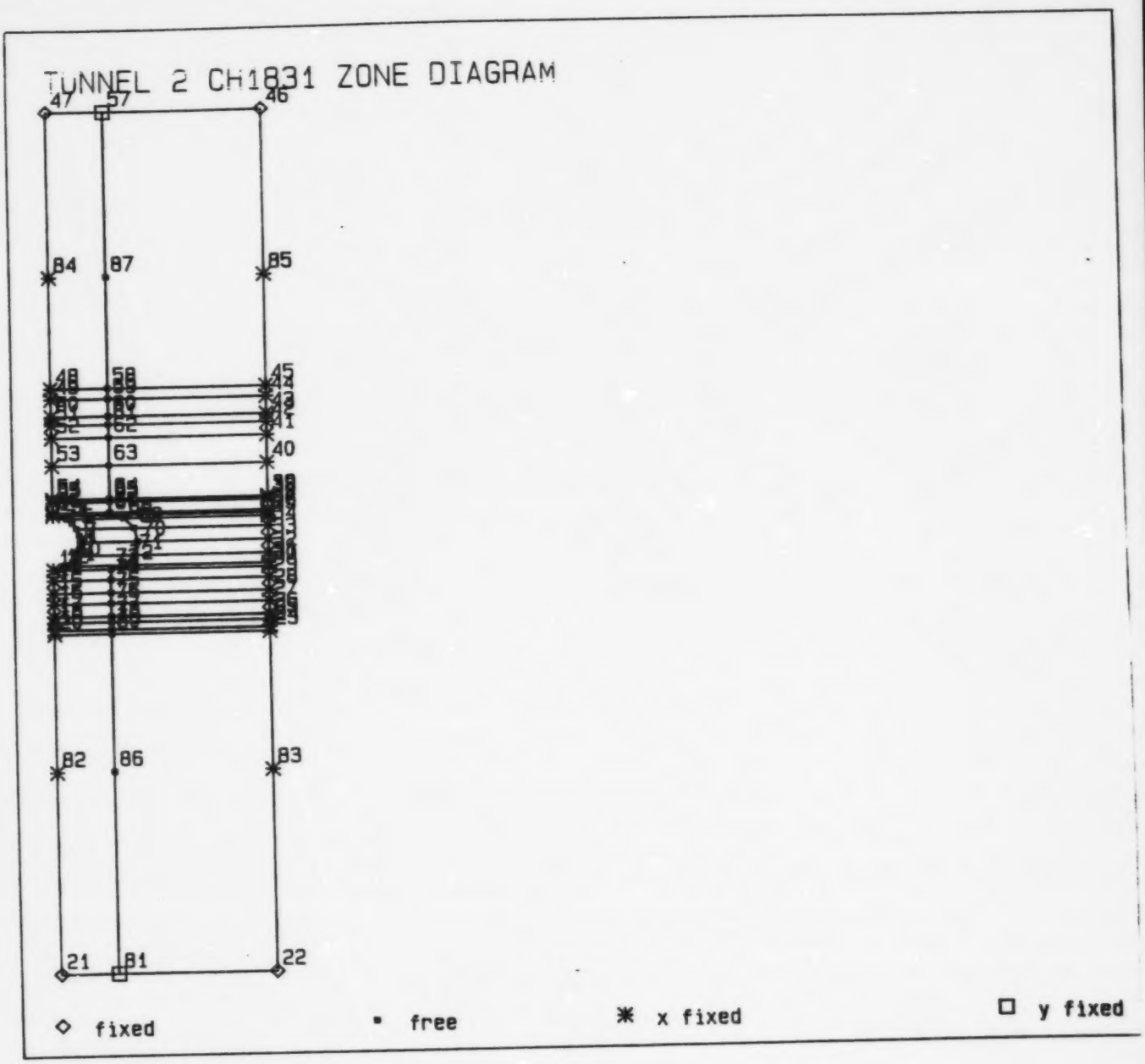

Figure 3.19: No.2 Tunnel, CH1831. User Specified Finite Element Diagram with Node Numbers

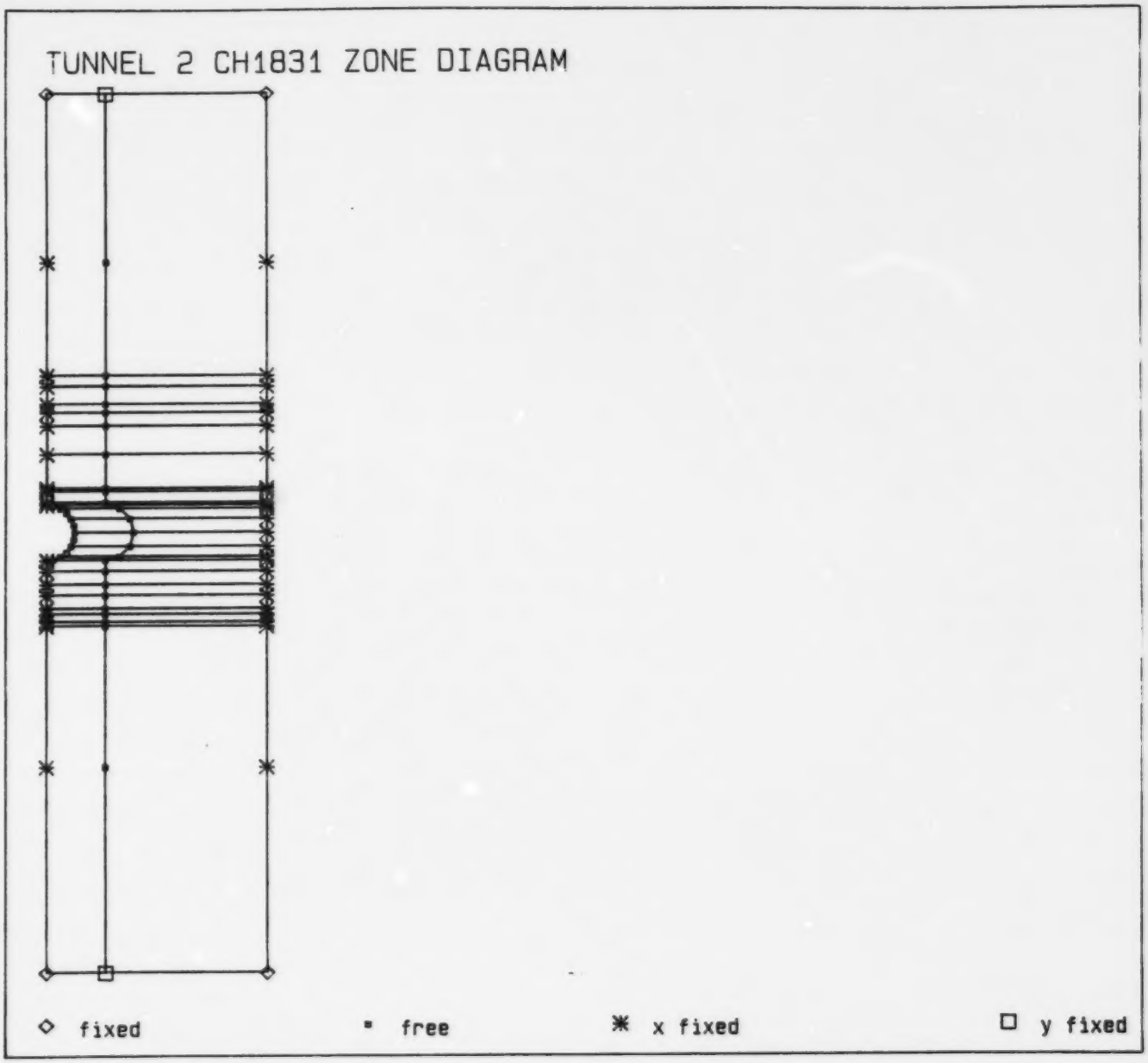

Figure 3.20: No.2 Tunnel, CH1831. User Specified Finite Element Diagram without Node Numbers

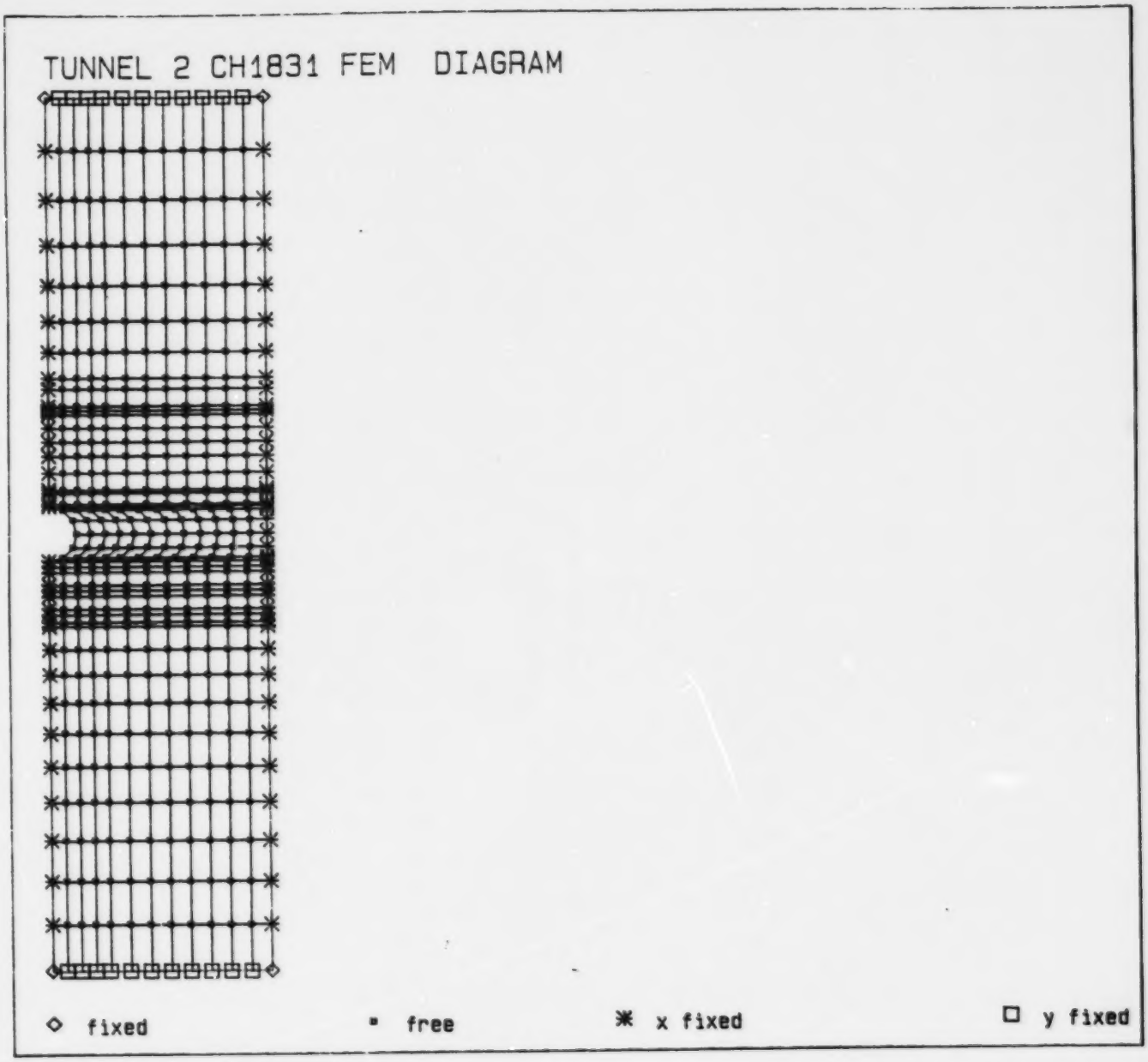

Figure 3.21: No.2 Tunnel, CH1831. Finite Element Mesh

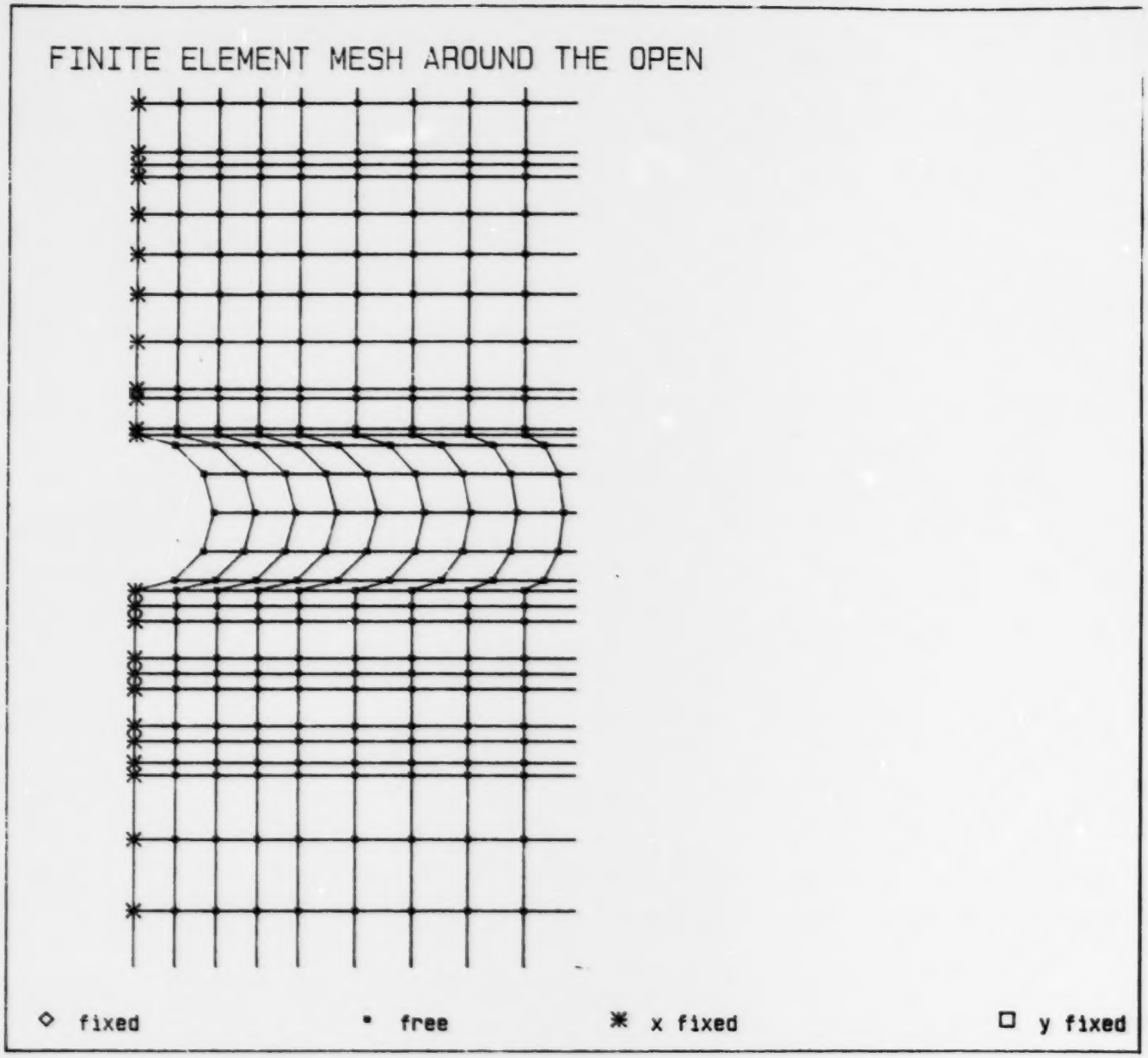

Figure 3.22: No.2 Tunnel, CH1831. Zooming of Mesh around the Opening

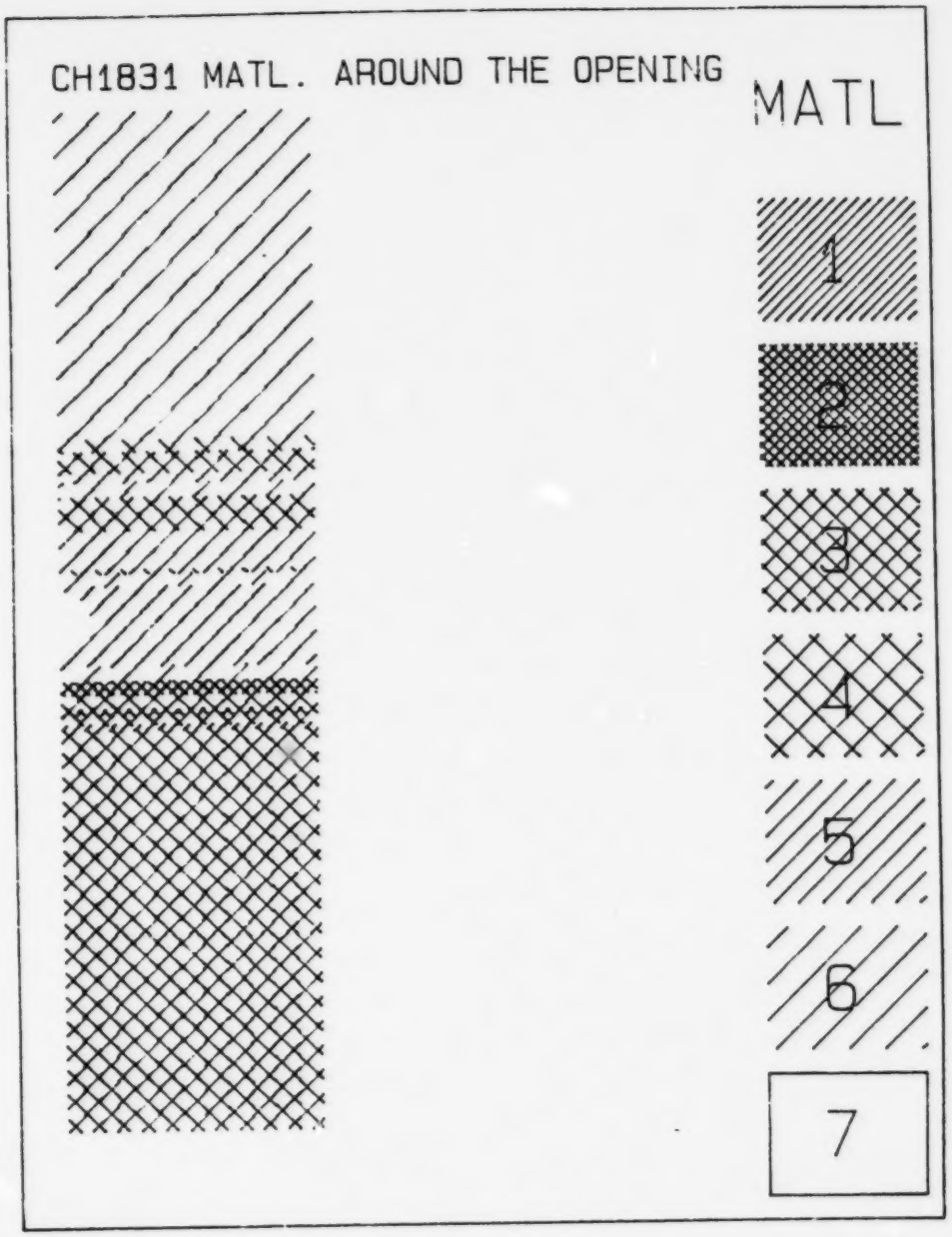

Figure 3.23: No.2 Tunnel, CH1831. Material Pattern around the Opening

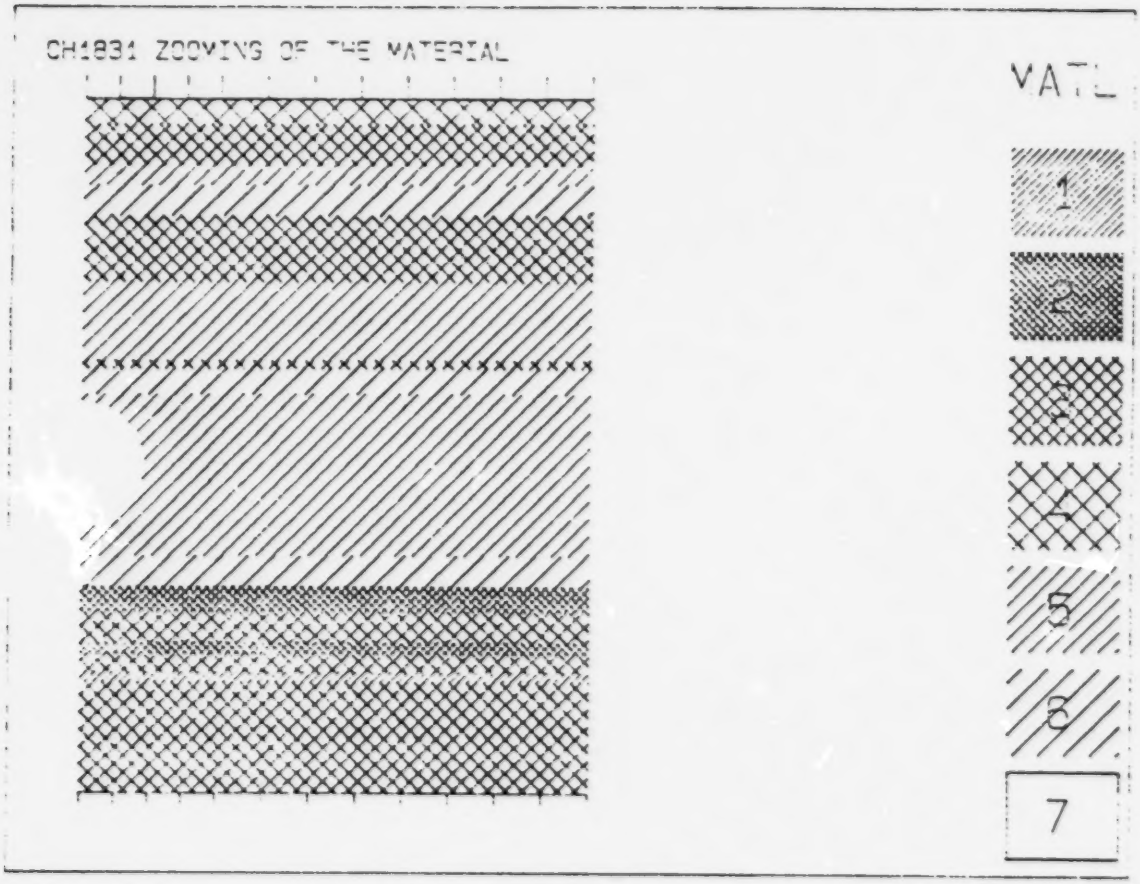

Figure 3.24: No.2 Tunnel, CH1831. Zooming of Material around the Opening

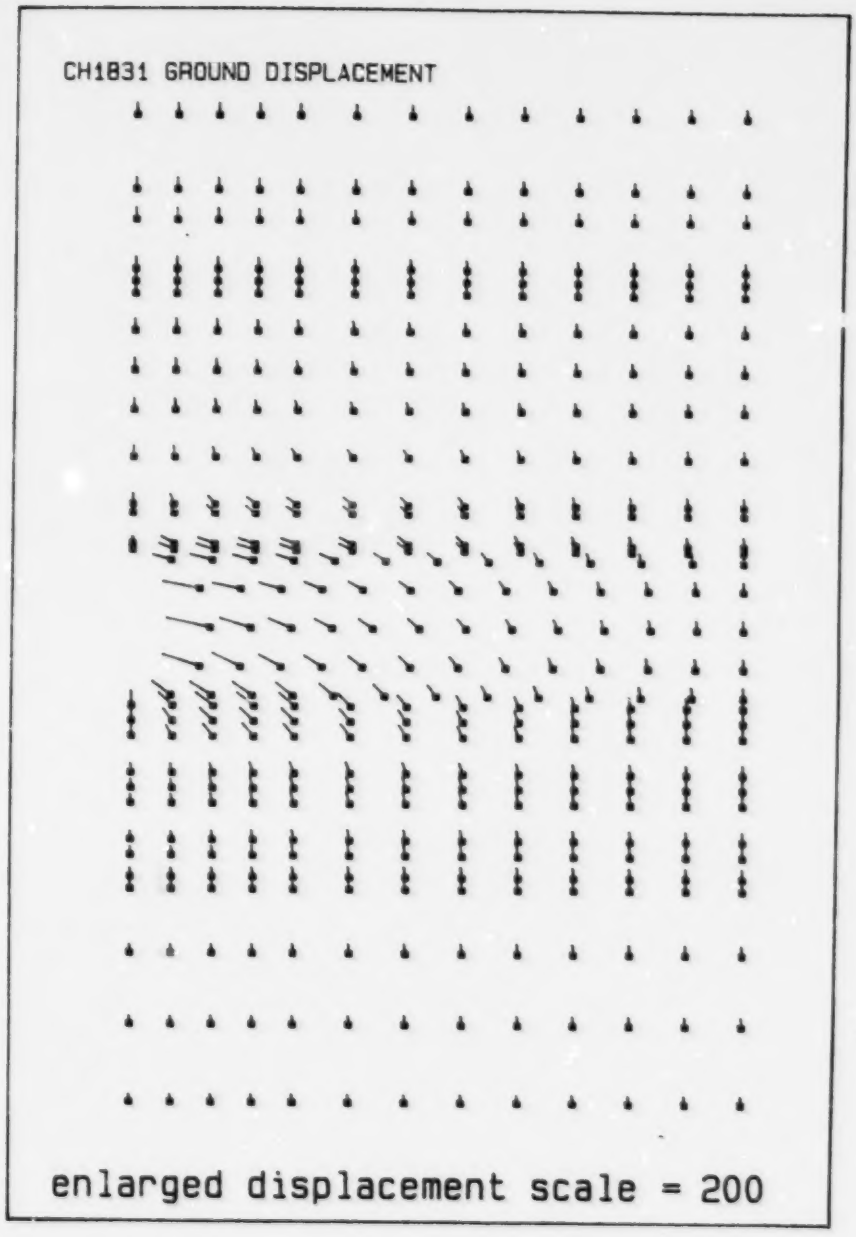

Figure 3.25: No.2 Tunnel, CH1831. Ground Displacement around the Opening

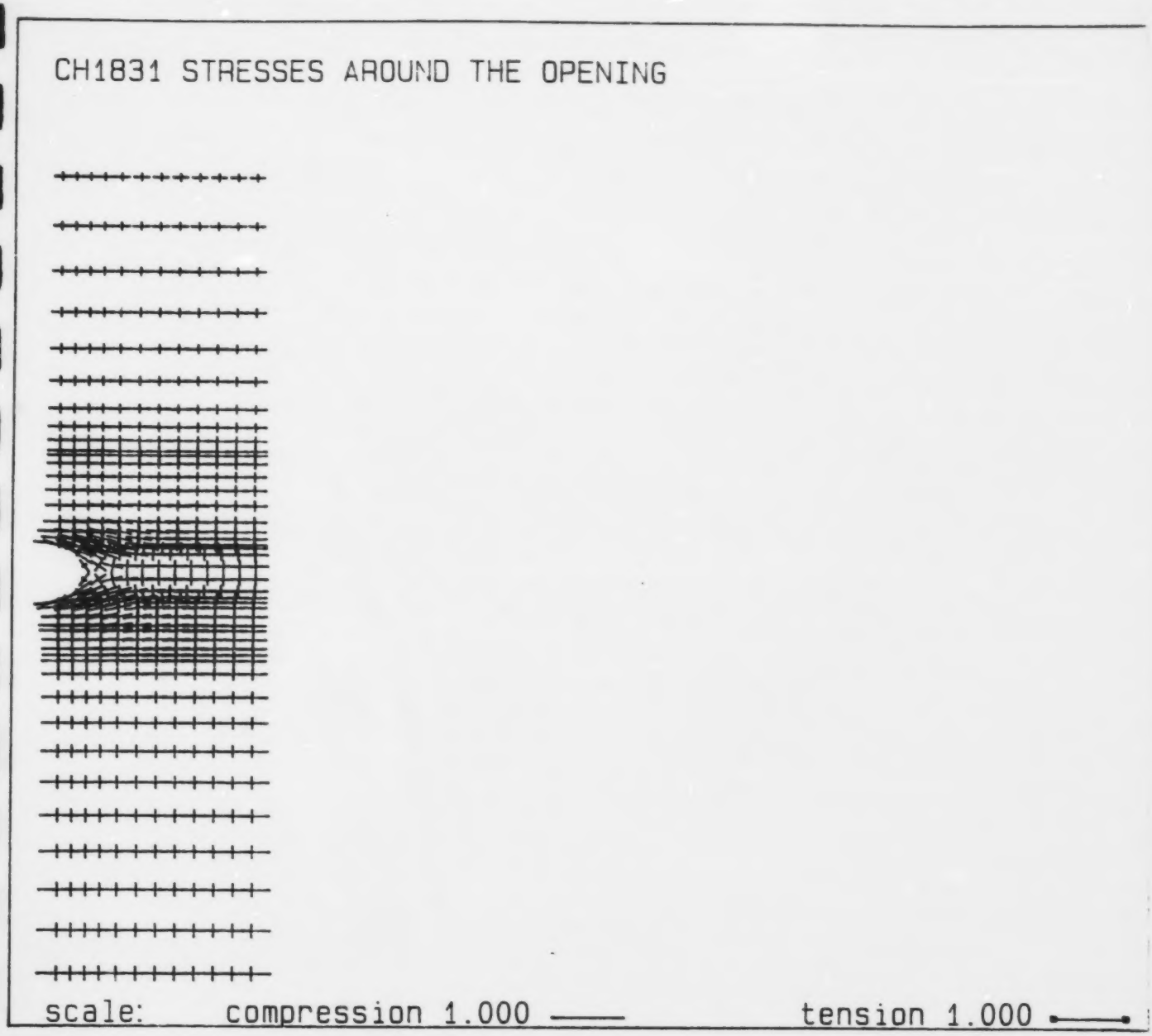

Figure 3.26: No.2 Tunnel, CH1831. Stress Pattern

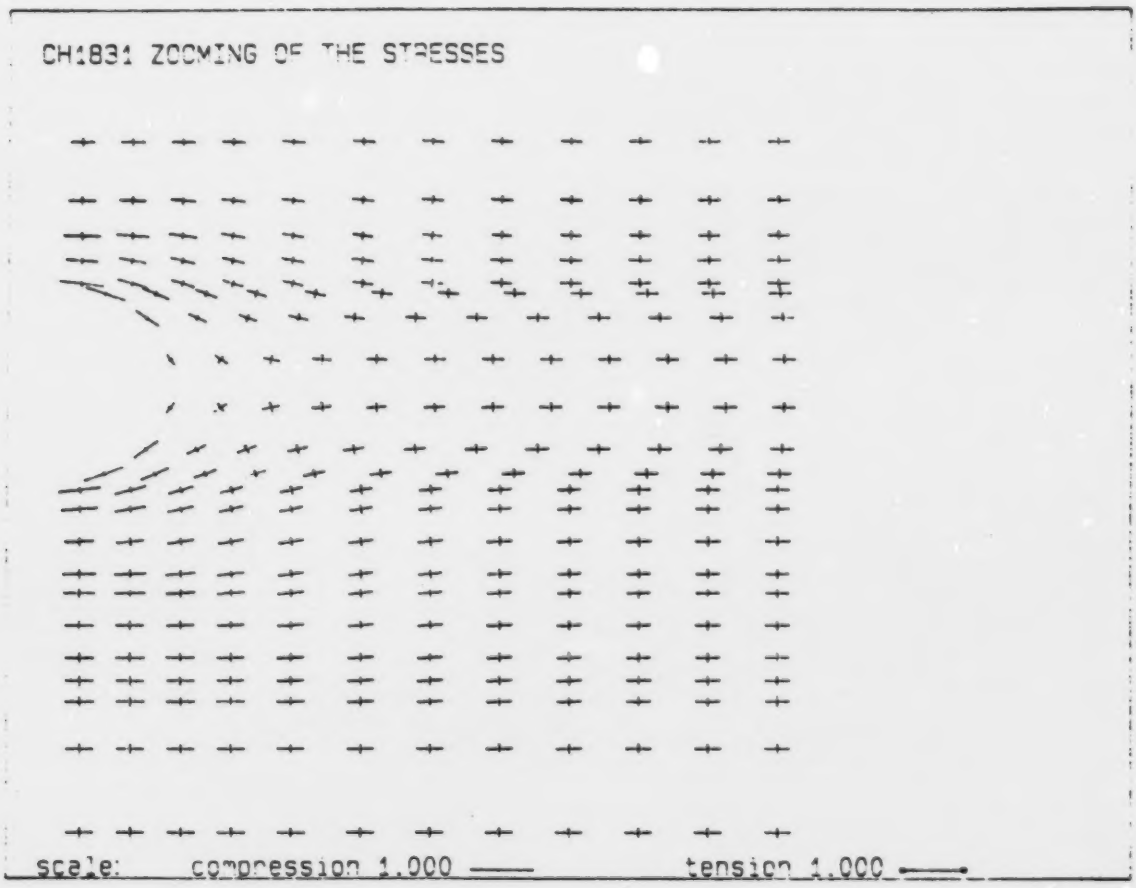

Figure 3.27: No.2 Tunnel, CH1831. Zooming of Stress Pattern around the Opening

FAILURE CRITERIA	COEFFICIENTS		
	first	second	third
1.Mohr_Coulomb	C	Angle	
2.Drucker_Prager	C	Angle	
3.Hoek and Brown	M	S	Sigma C

TOTAL NO. OF MATERIAL TYPES = 6

MATERIAL NO.	FAIL. CRITERIA	COEFFICIENTS		
1	3	5	0.1	92
2	3	5	0.1	121
3	3	5	0.1	53
4	3	5	0.1	36
5	3	5	0.1	36
6	3	5	0.65	16.6

Figure 3.28: No.2 Tunnel, CH1831. Parameters of Material Failure Criteria

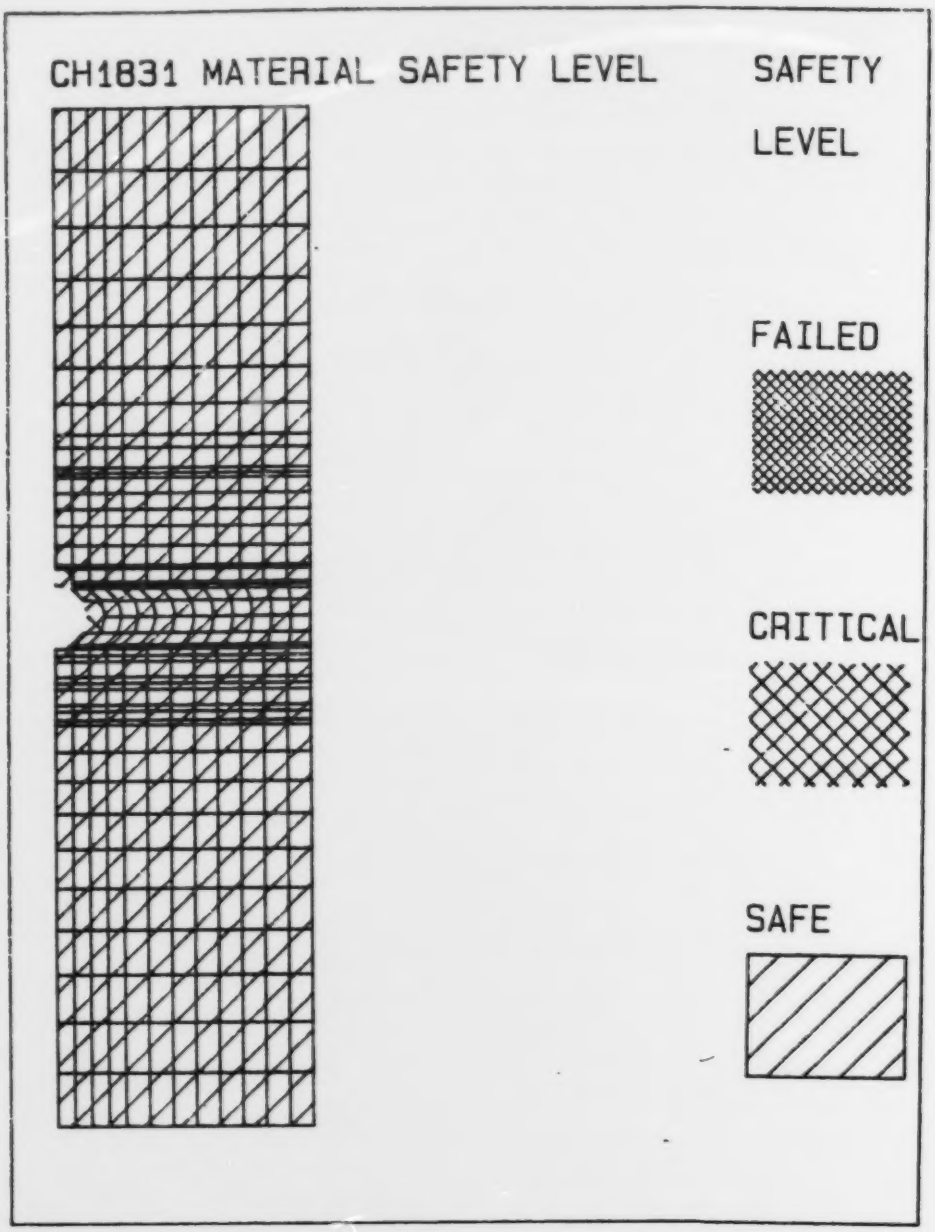

Figure 3.29: No.2 Tunnel, CH1831. Material Safety Level around the Opening

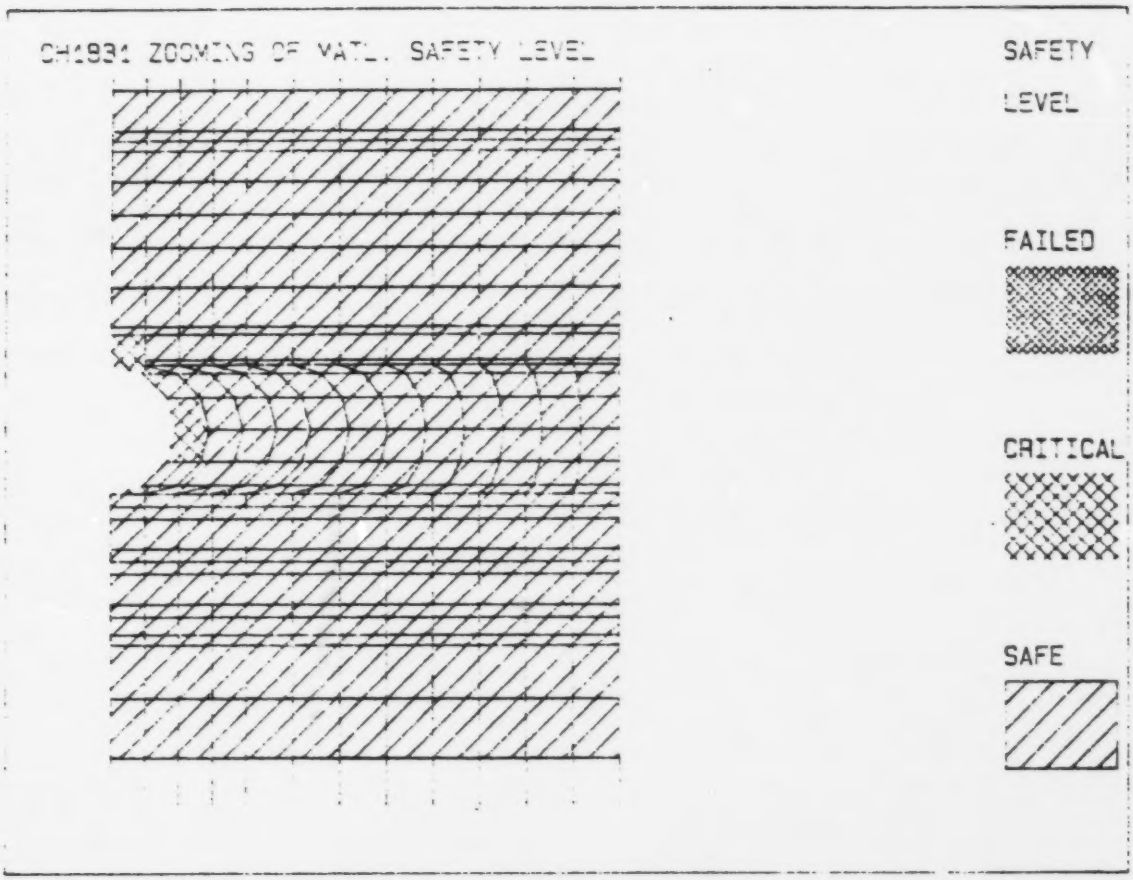

Figure 3.30: No.2 Tunnel, CH1831. Zooming of Material Safety Level

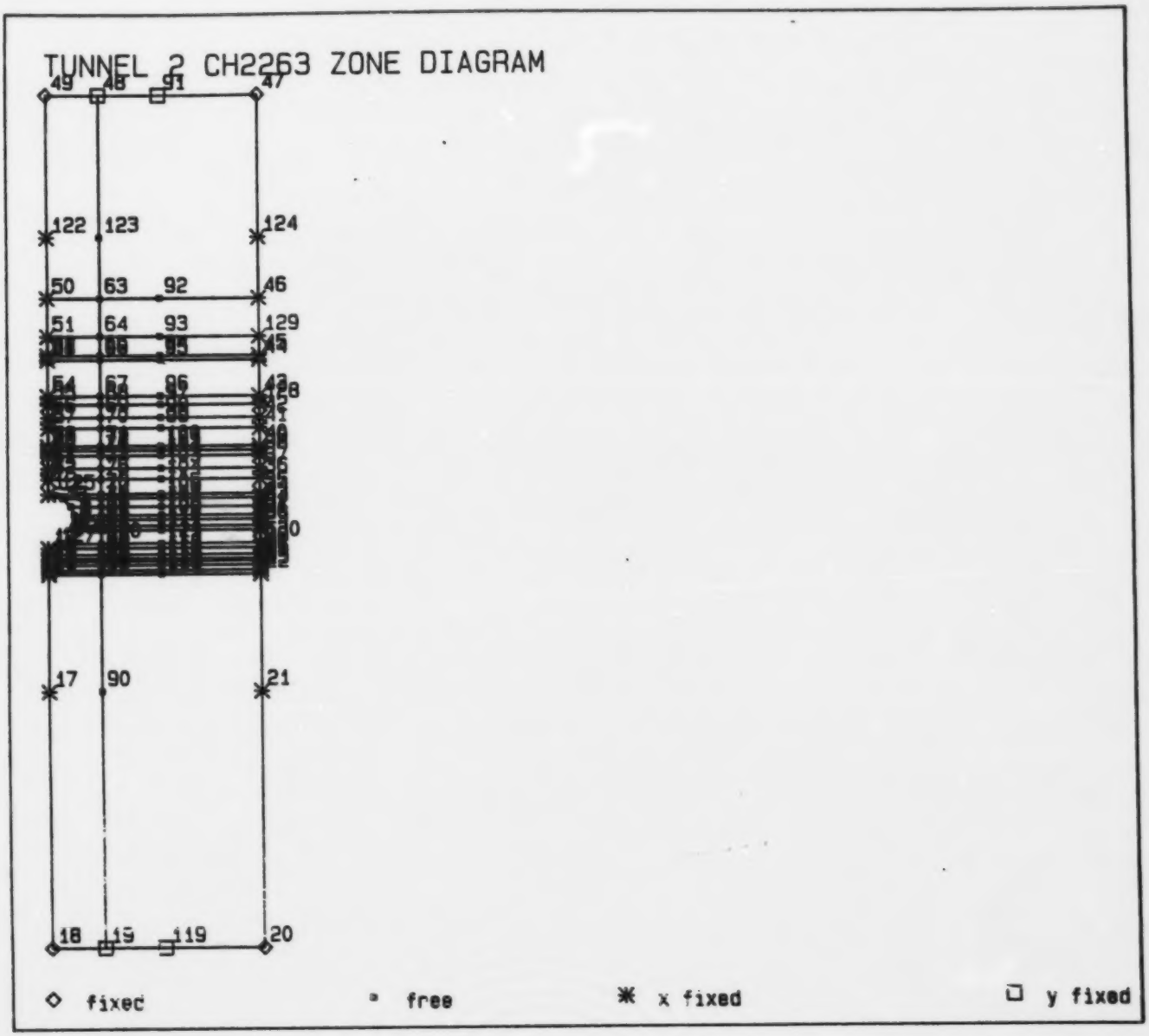

Figure 3.31: No.2 Tunnel, CH2263. User Specified Finite Element Diagram with Node Numbers

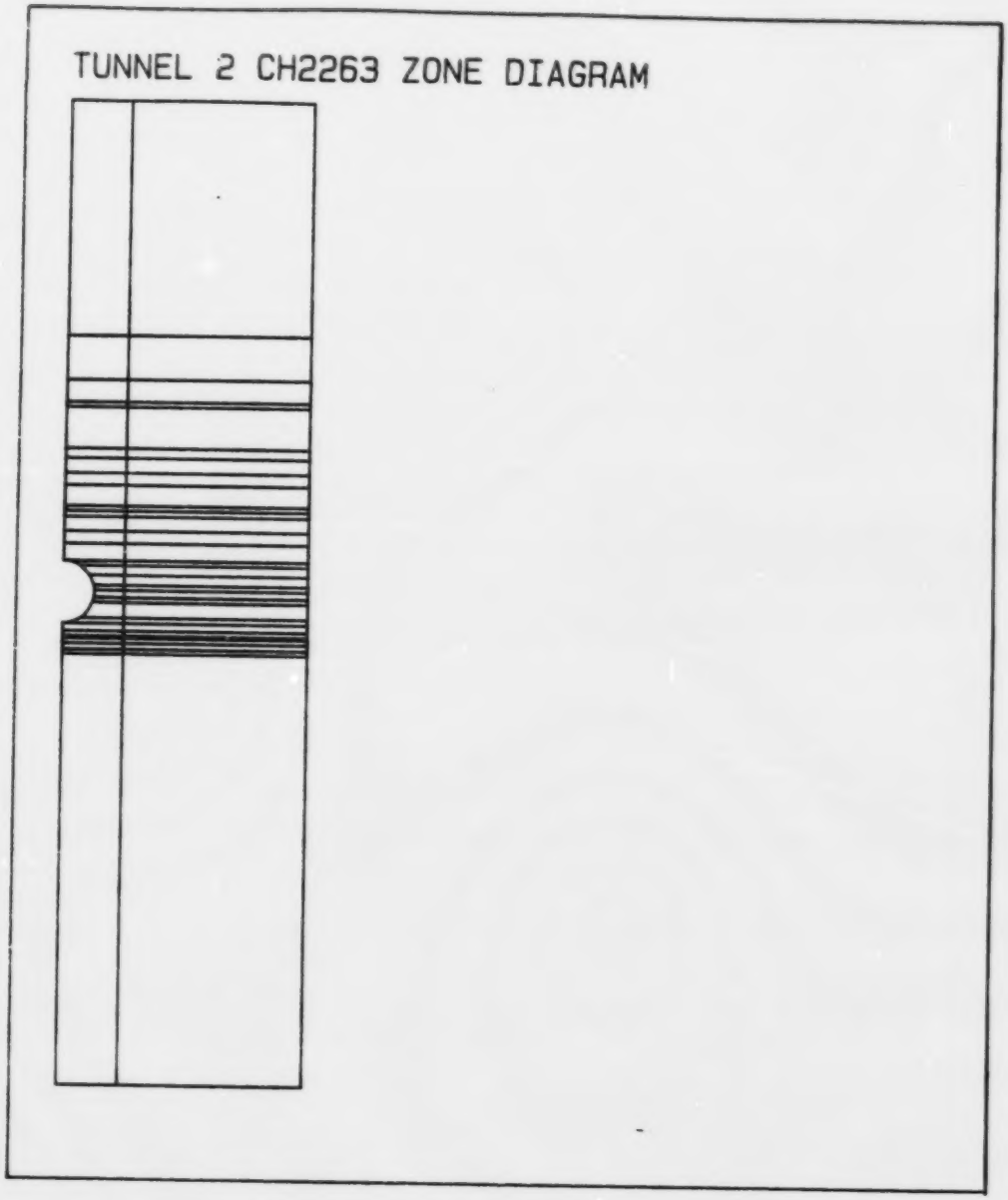

Figure 3.32: No.2 Tunnel, CH2263. User Specified Finite Element Diagram without Node Numbers

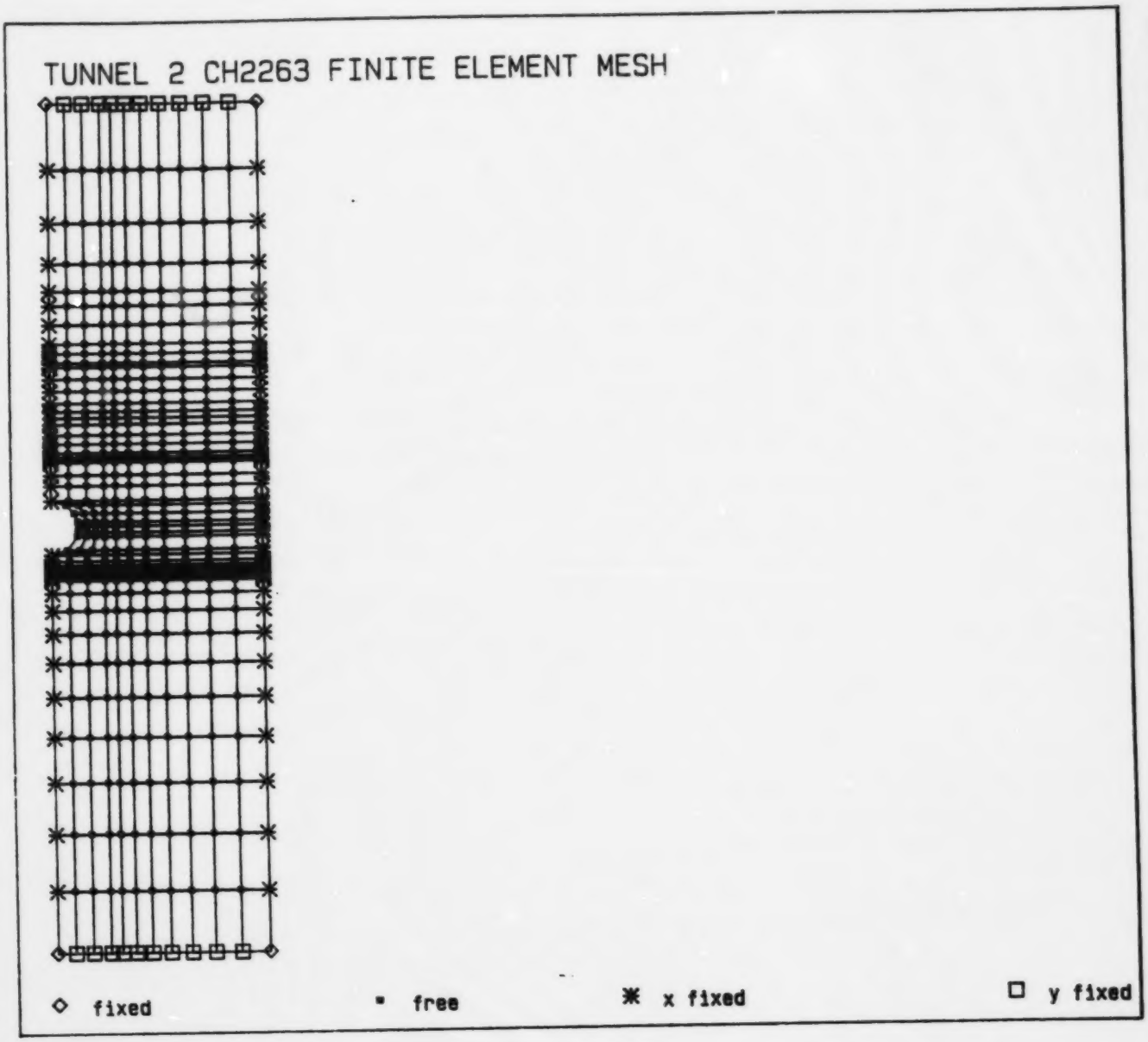

Figure 3.33: No.2 Tunnel, CH2263. Finite Element Mesh

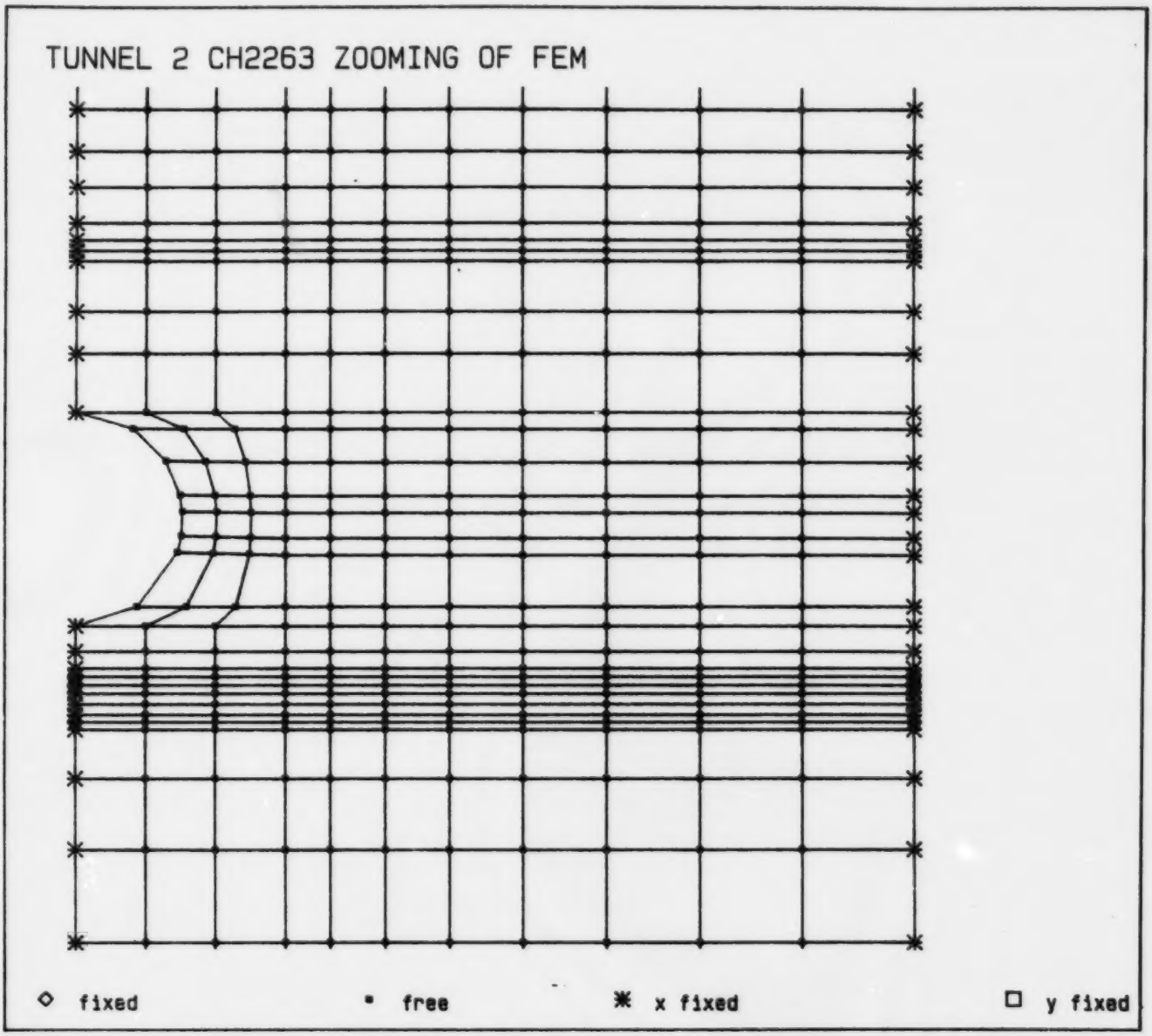

Figure 3.34: No.2 Tunnel, CH2263. Zooming of Mesh around the Opening

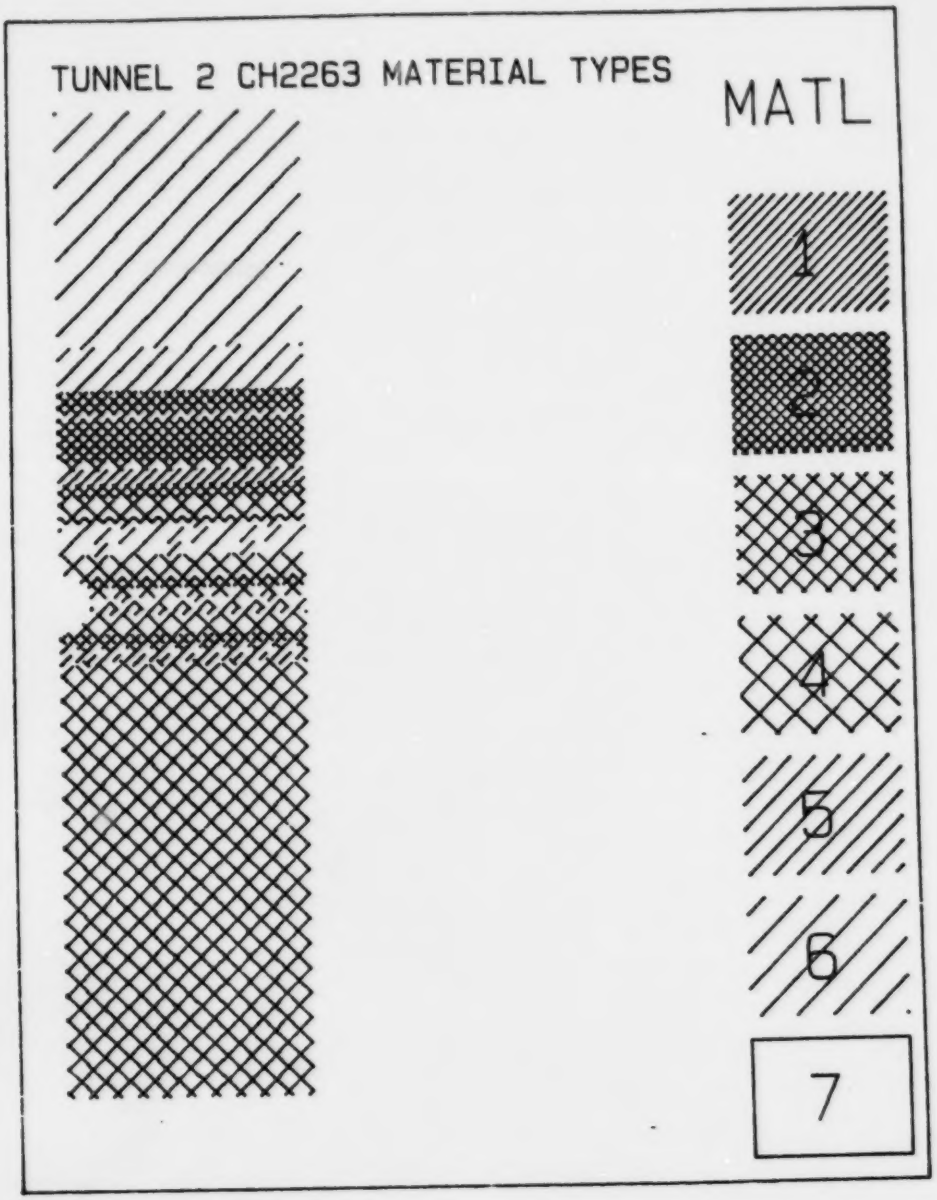

Figure 3.35: No.2 Tunnel, CH2263. Material Pattern around the Opening

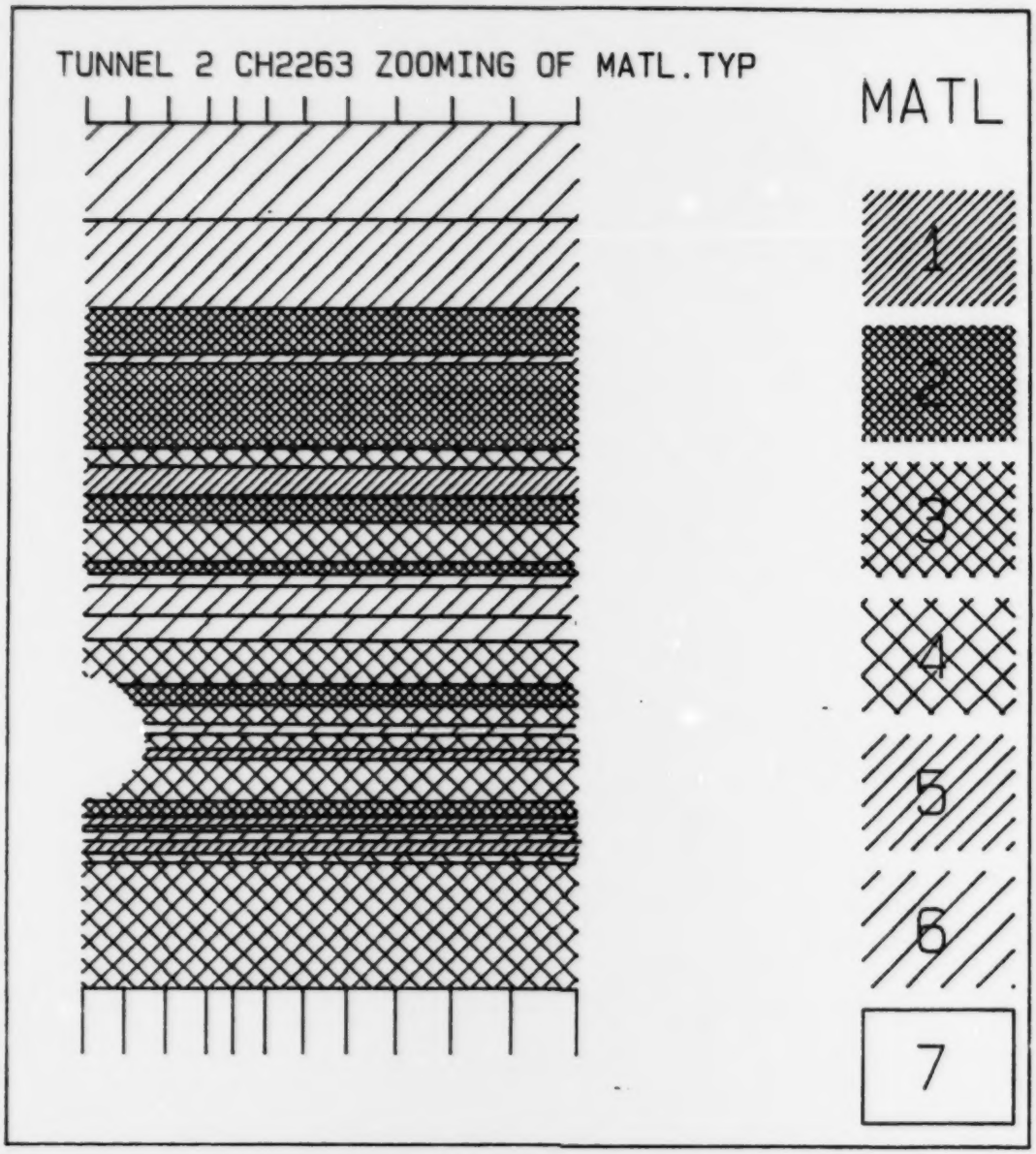

Figure 3.36: No.2 Tunnel, CH2263. Zooming of Material around the Opening

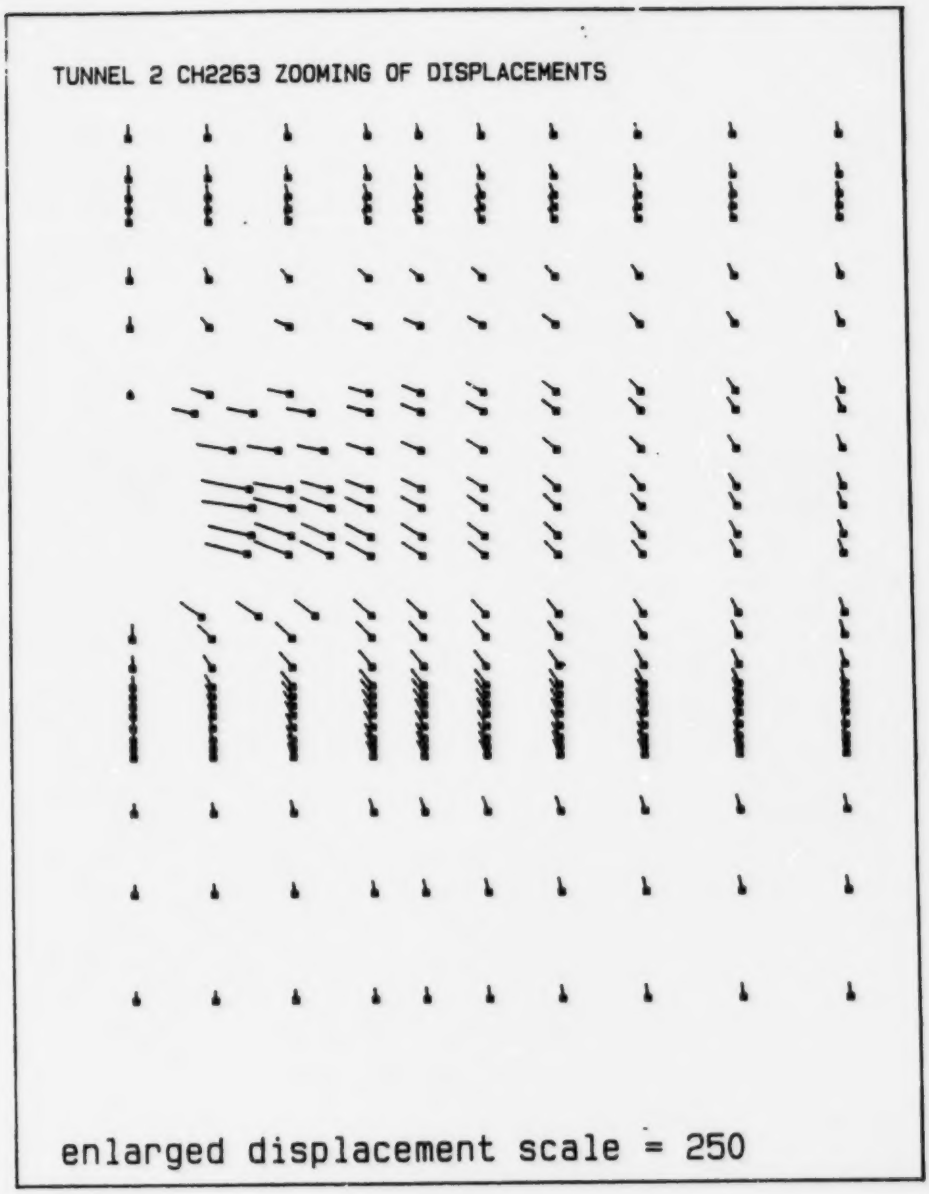

Figure 3.37: No.2 Tunnel, CH2263. Ground Displacement around the Opening

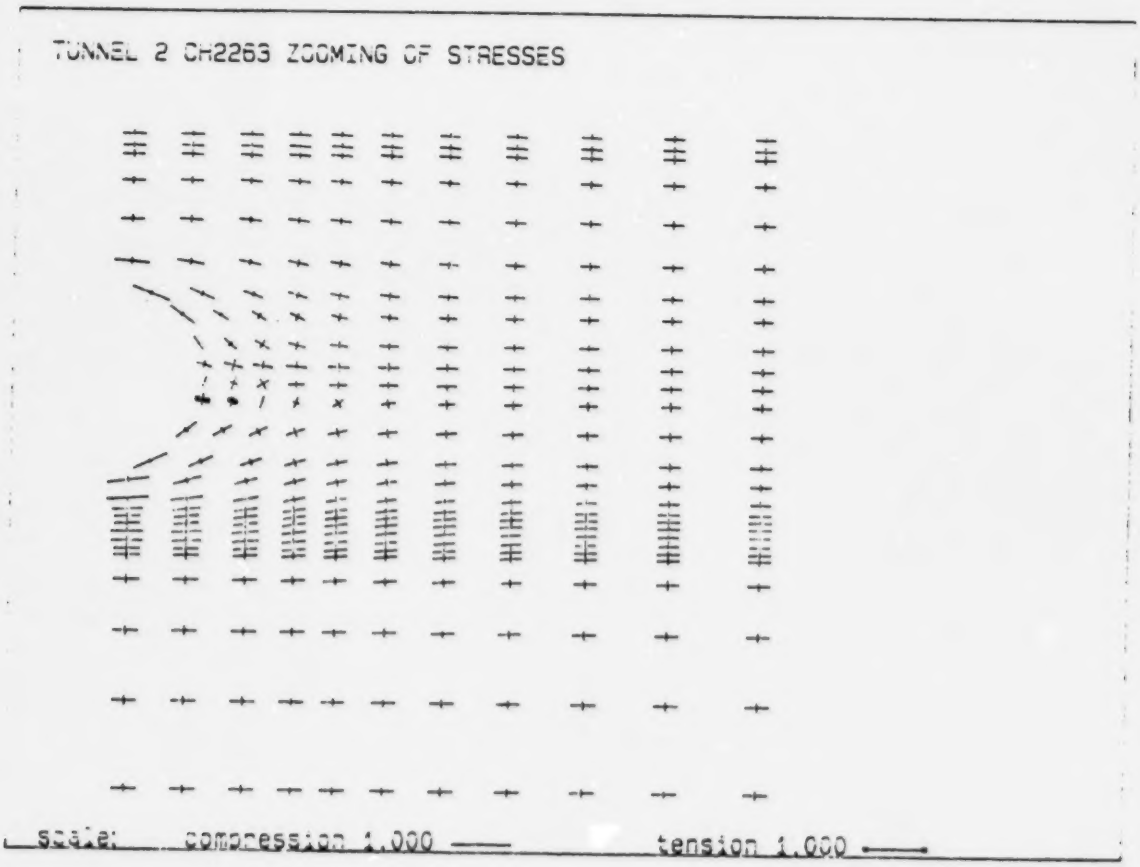

Figure 3.38: No.2 Tunnel, CH2263. Zooming of Stress Pattern around the Opening

FAILURE CRITERIA	COEFFICIENTS		
	first	second	third
1.Mohr_Coulomb	C	Angle	
2.Drucker_Prager	C	Angle	
3.Hoek and Brown	M	S	Sigma C

TOTAL NO. OF MATERIAL TYPES = 6

MATERIAL NO.	FAIL. CRITERIA	COEFFICIENTS		
1	3	5	0.1	92
2	3	5	0.1	121
3	3	5	0.1	53
4	3	5	0.1	36
5	3	5	0.1	36
6	3	5	0.65	16.6

Figure 3.39: No.2 Tunnel, CH2263. Parameters of Material Failure Criteria

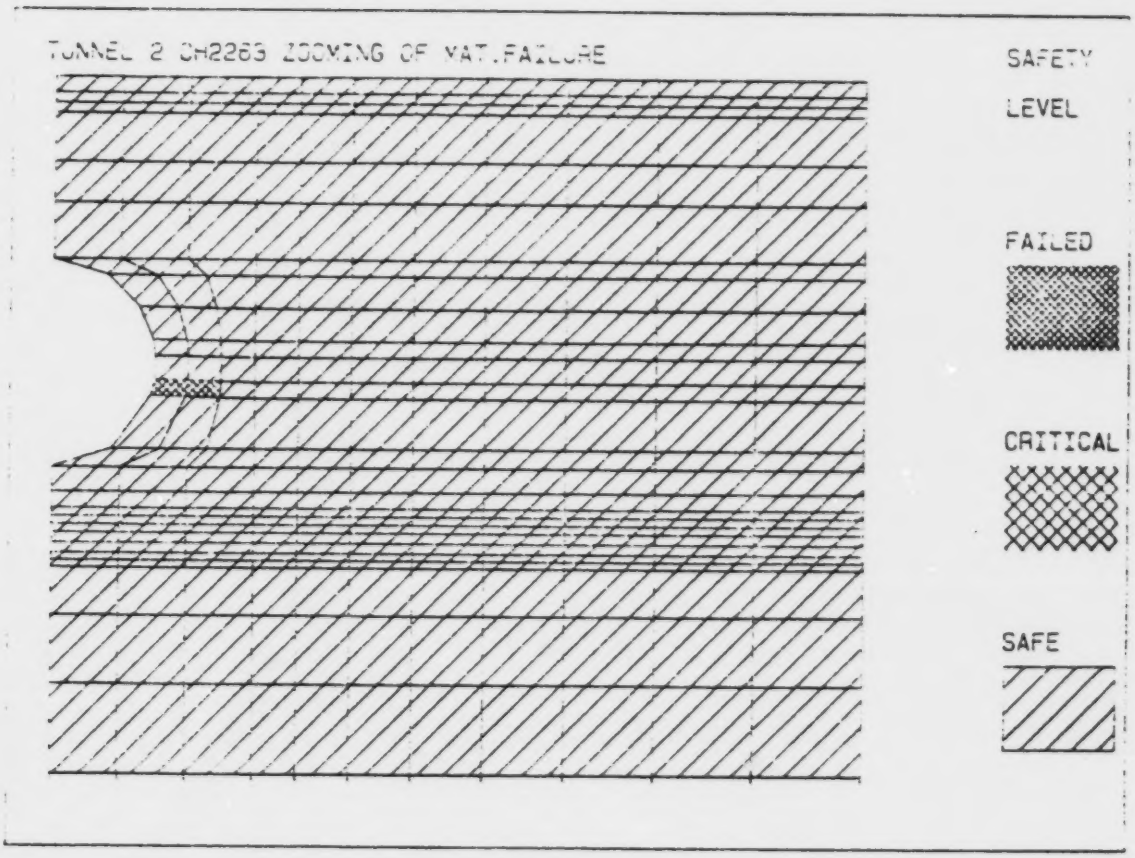

Figure 3.40: No.2 Tunnel, CH2263. Zooming of Material Safety Level

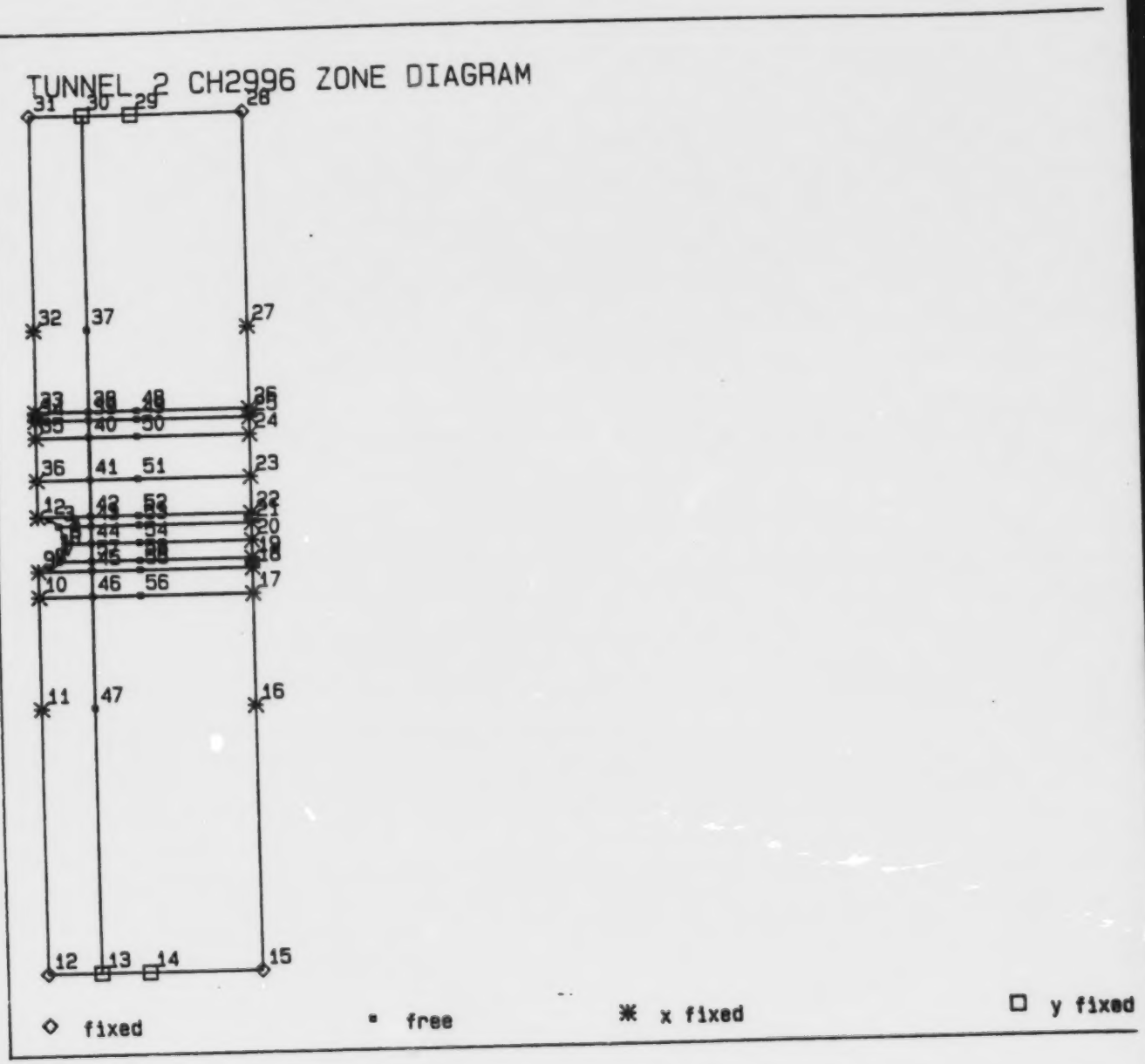

Figure 3.41: No.2 Tunnel, CH2996. User Specified Finite Element Diagram with Node Numbers

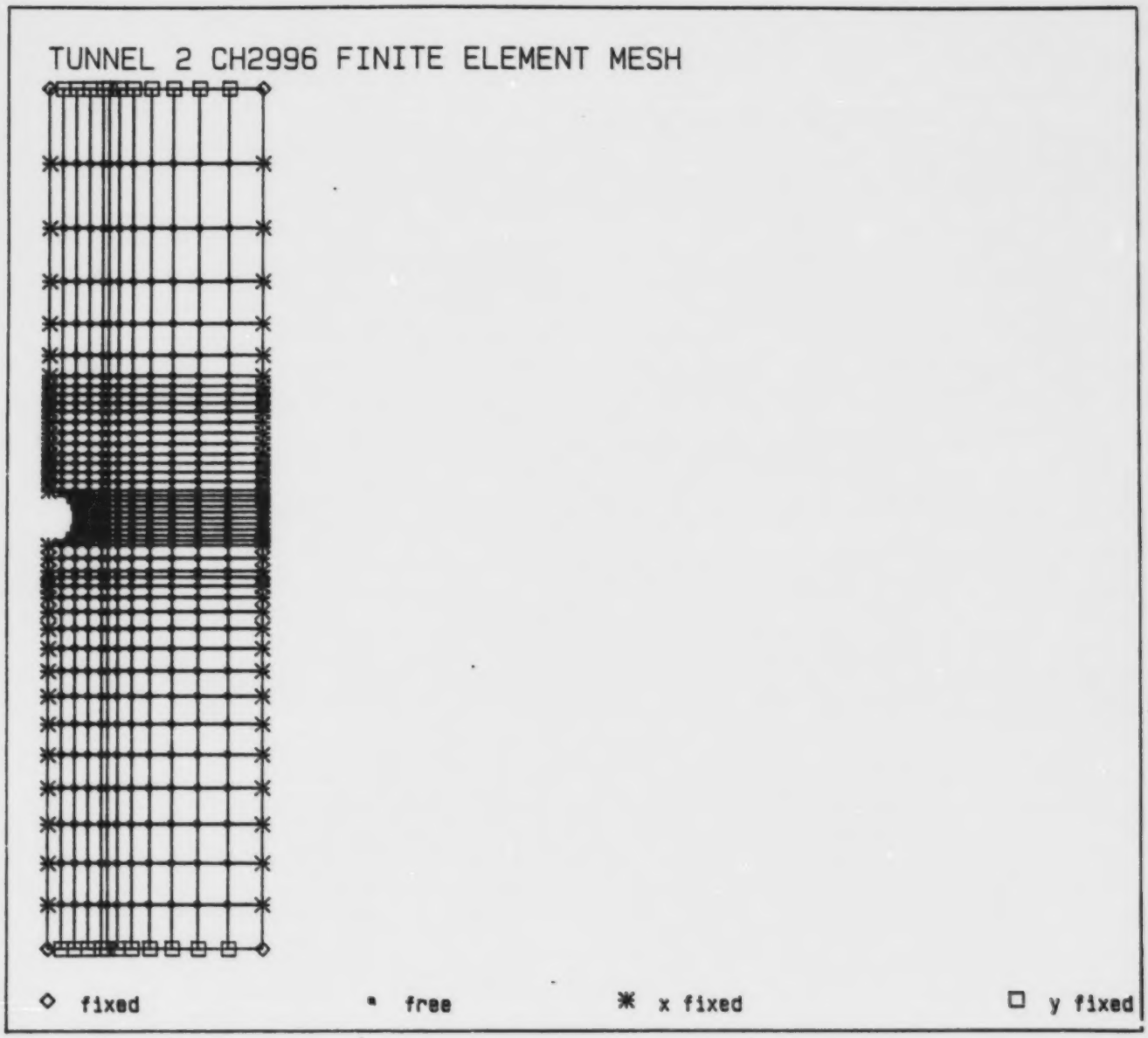

Figure 3.42: No.2 Tunnel, CH2996. Finite Element Mesh

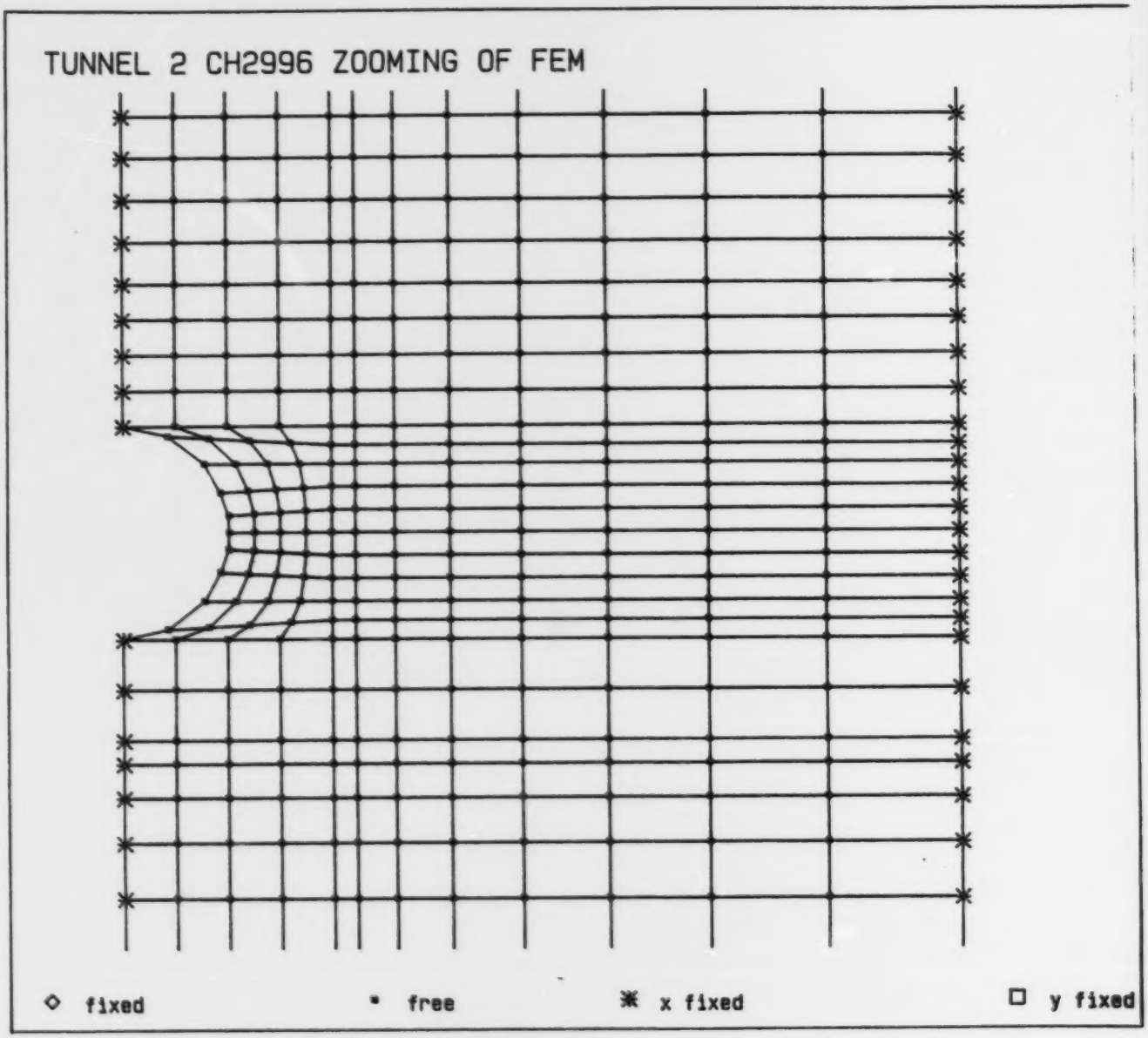

Figure 3.43: No.2 Tunnel, CH2996. Zooming of Mesh around the Opening

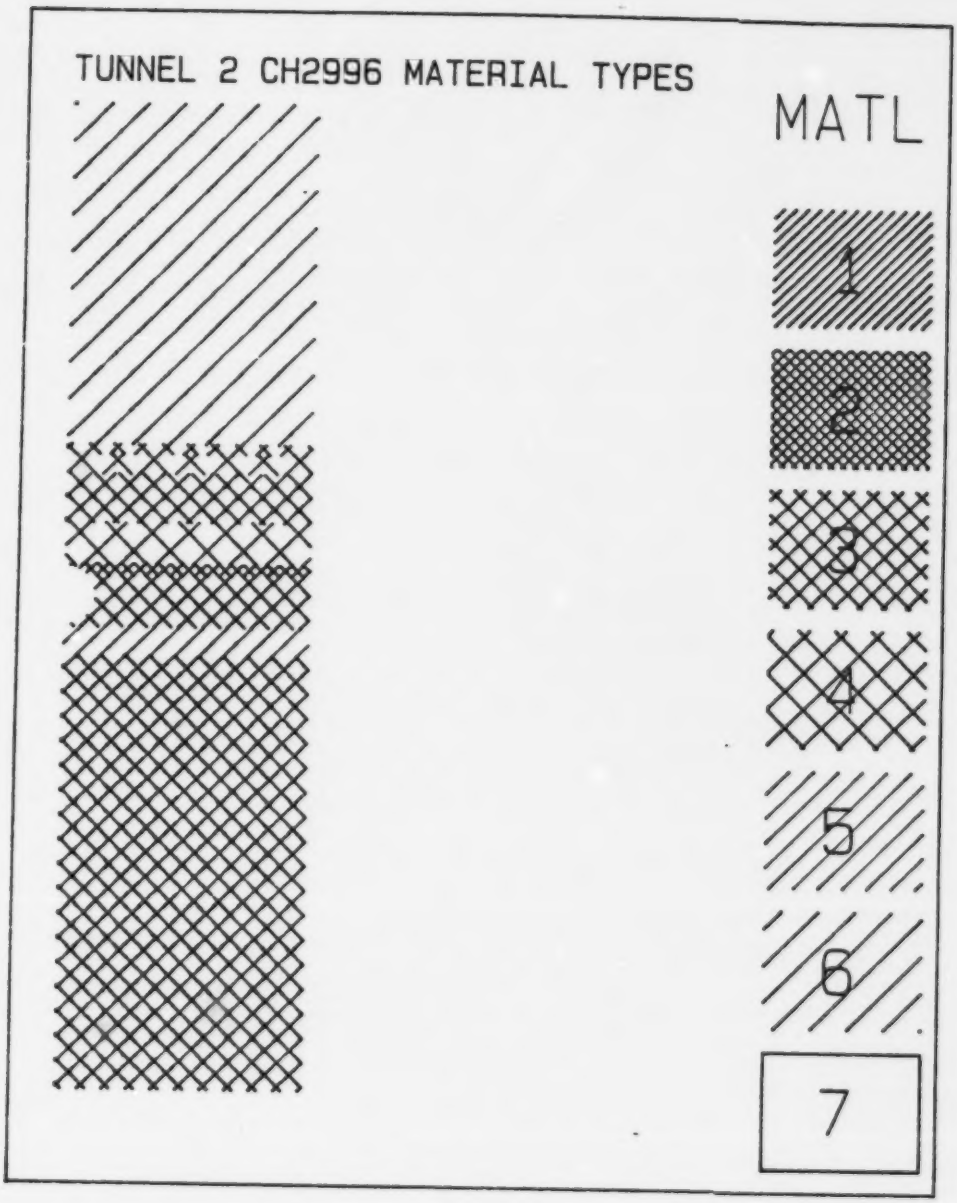

Figure 3.44: No.2 Tunnel, CH2996. Material Pattern around the Opening

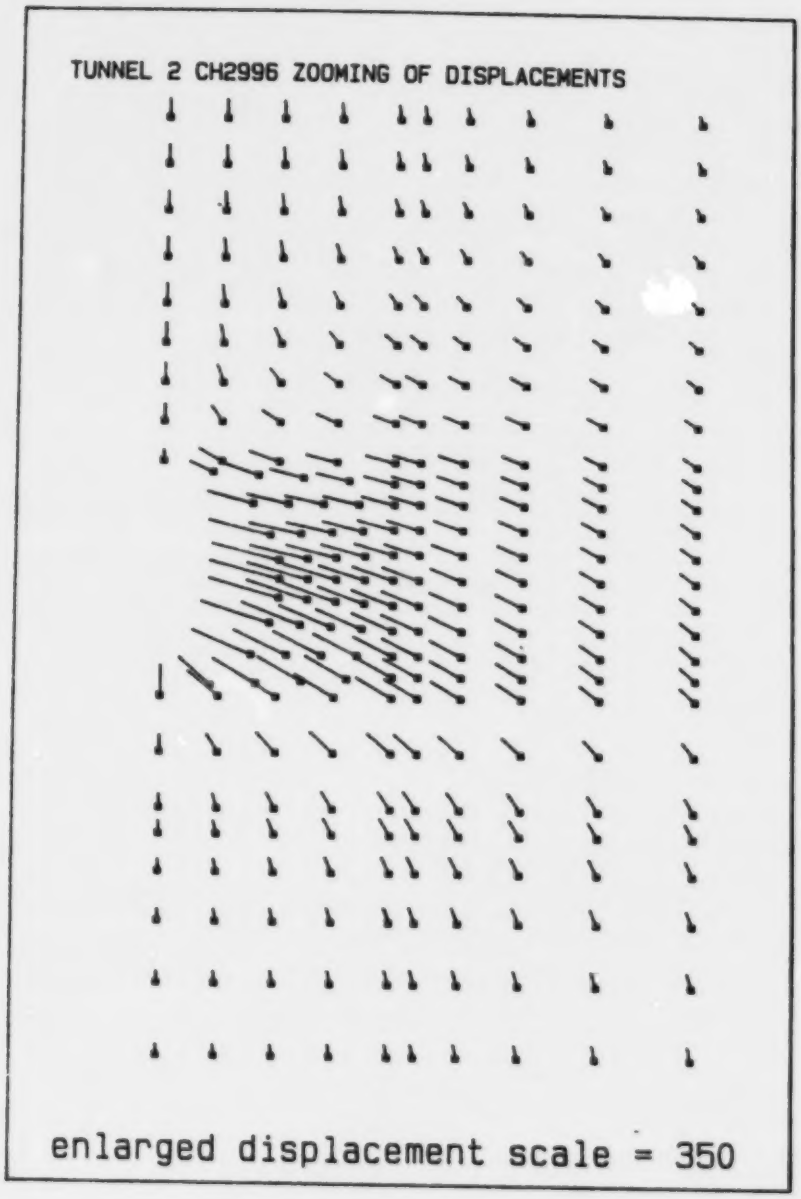

Figure 3.45: No.2 Tunnel, CH2996. Ground Displacement around the Opening

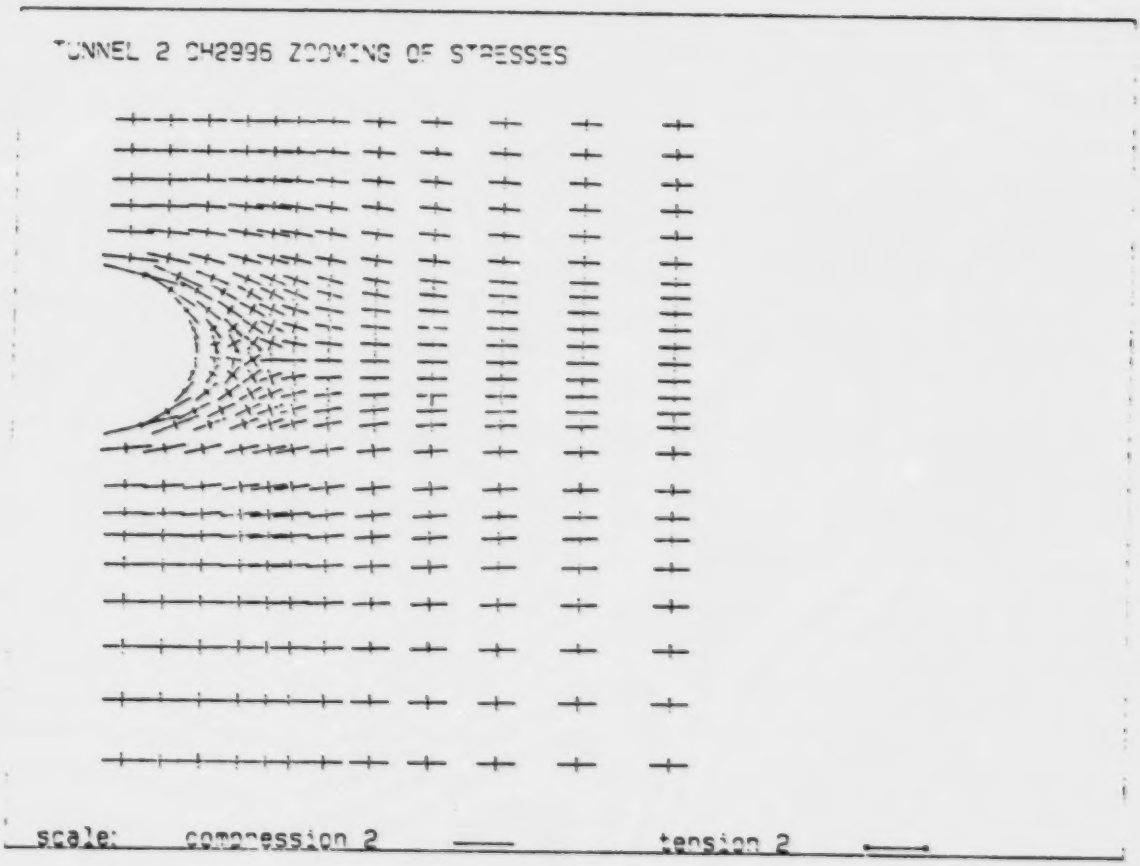

Figure 3.46: No.2 Tunnel, CH2996. Zooming of Stress Pattern around the Opening

FAILURE CRITERIA	COEFFICIENTS		
	first	second	third
1.Mohr_Coulomb	C	Angle	
2.Drucker_Prager	C	Angle	
3.Hoek and Brown	M	S	Sigma C

TOTAL NO. OF MATERIAL TYPES = 6

MATERIAL NO.	FAIL. CRITERIA	COEFFICIENTS		
1	3	5	0.1	92
2	3	5	0.1	121
3	3	5	0.1	53
4	3	5	0.1	36
5	3	5	0.1	36
6	3	5	0.65	16.6

Figure 3.47: No.2 Tunnel, CH2996. Parameters of Material Failure Criteria

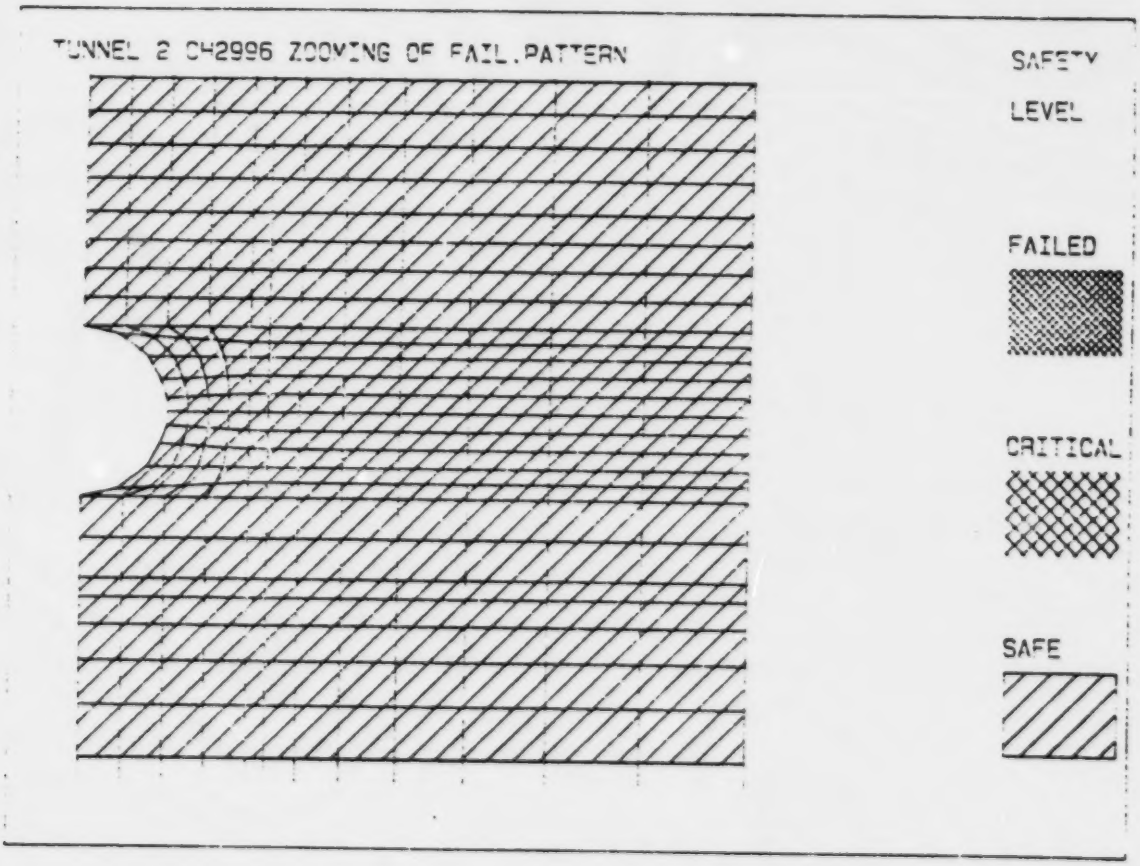

Figure 3.48: No.2 Tunnel, CH2996. Zooming of Material Safety Level

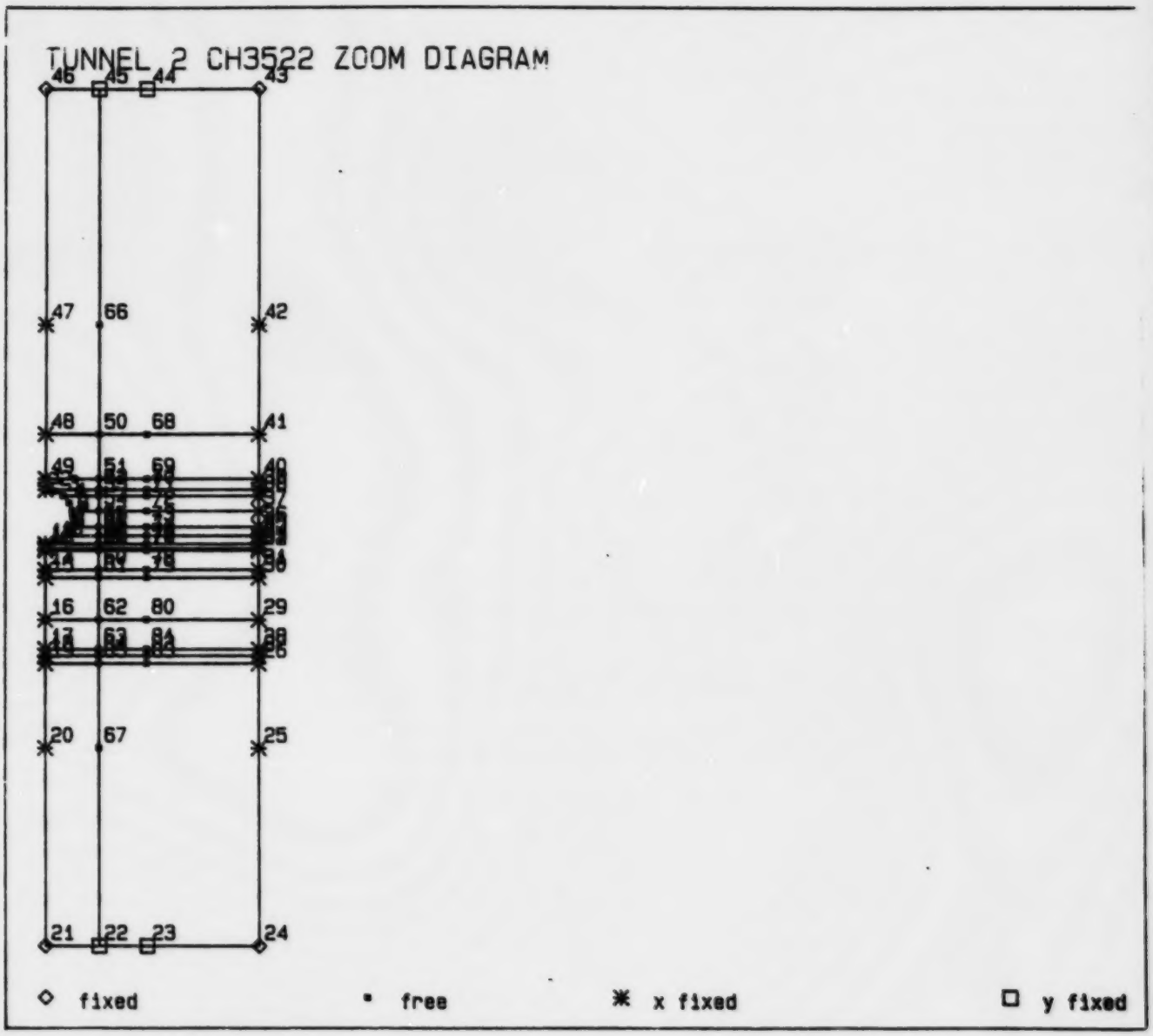

Figure 3.49: No.2 Tunnel, CH3522. User Specified Finite Element Diagram with Node Numbers

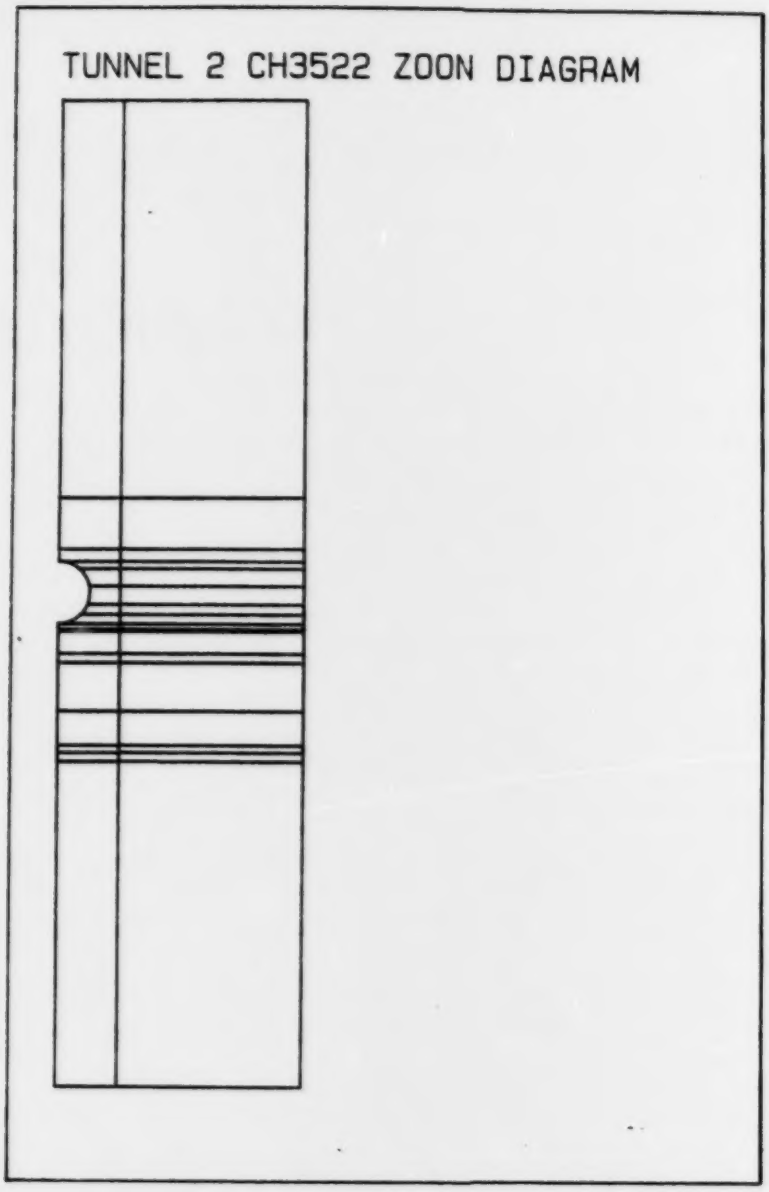

Figure 3.50: No.2 Tunnel, CH3522. User Specified Finite Element Diagram without Node Numbers

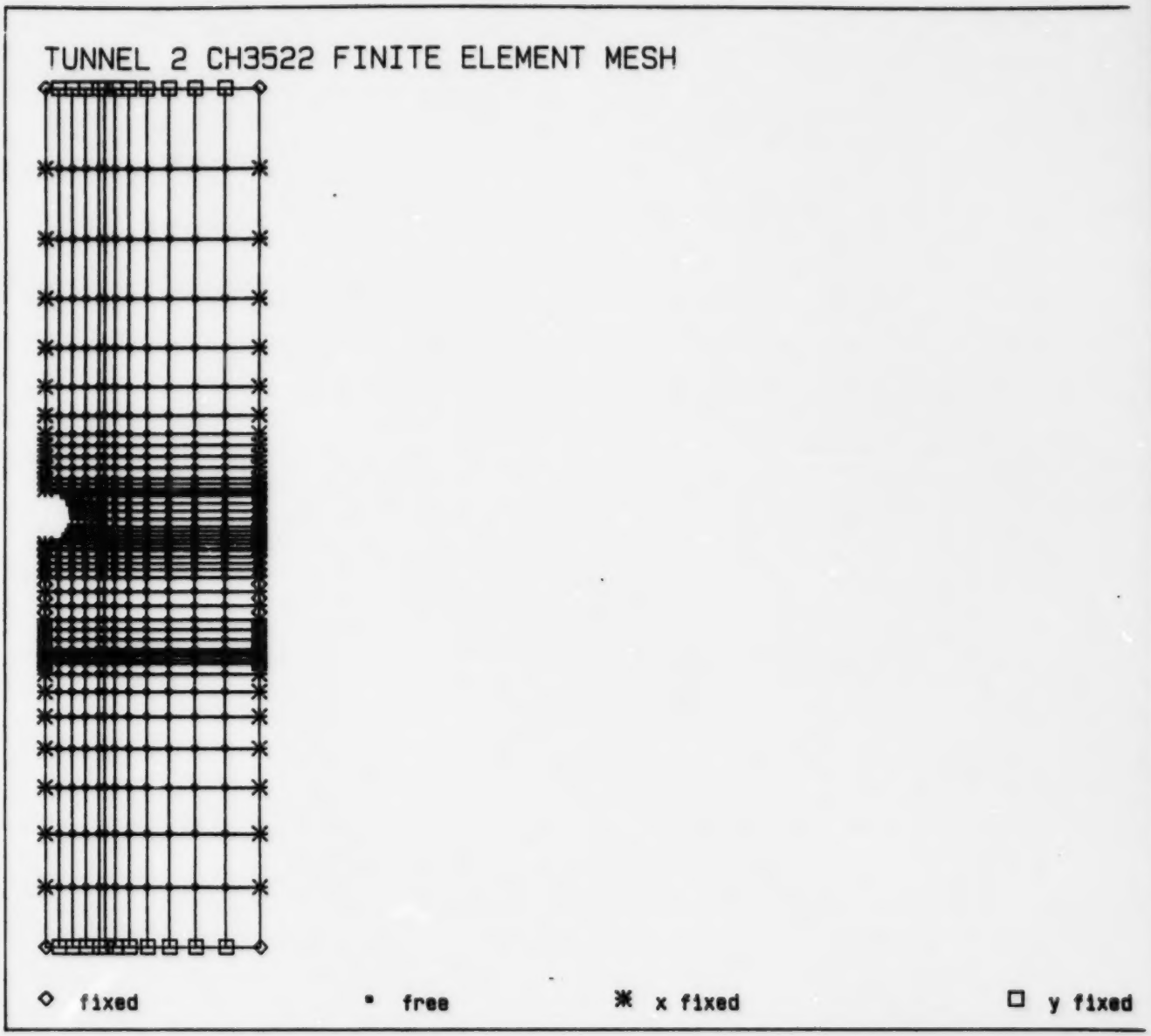

Figure 3.51: No.2 Tunnel, CH3522. Finite Element Mesh

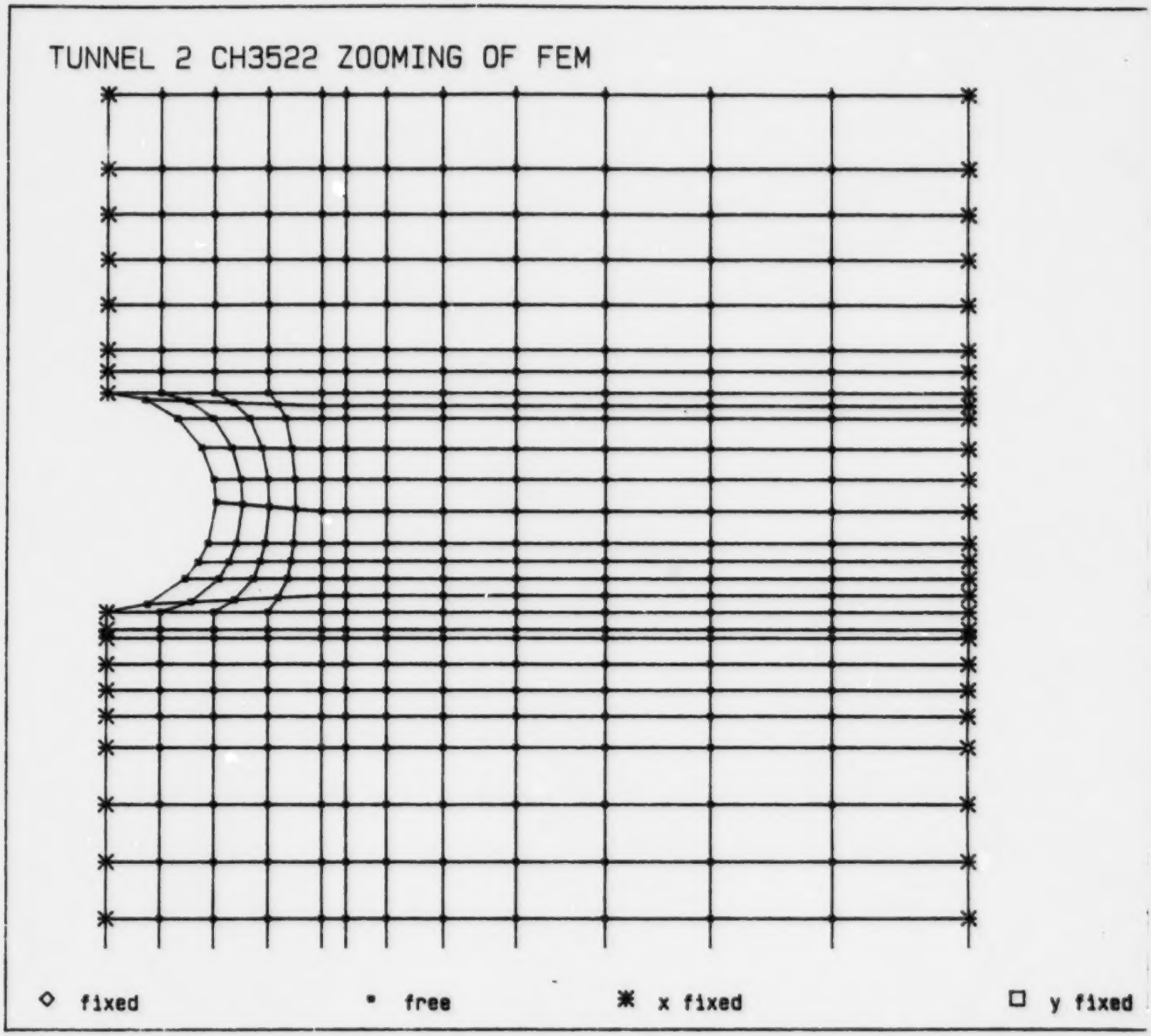

Figure 3.52: No.2 Tunnel, CH3522. Zooming of Mesh around the Opening

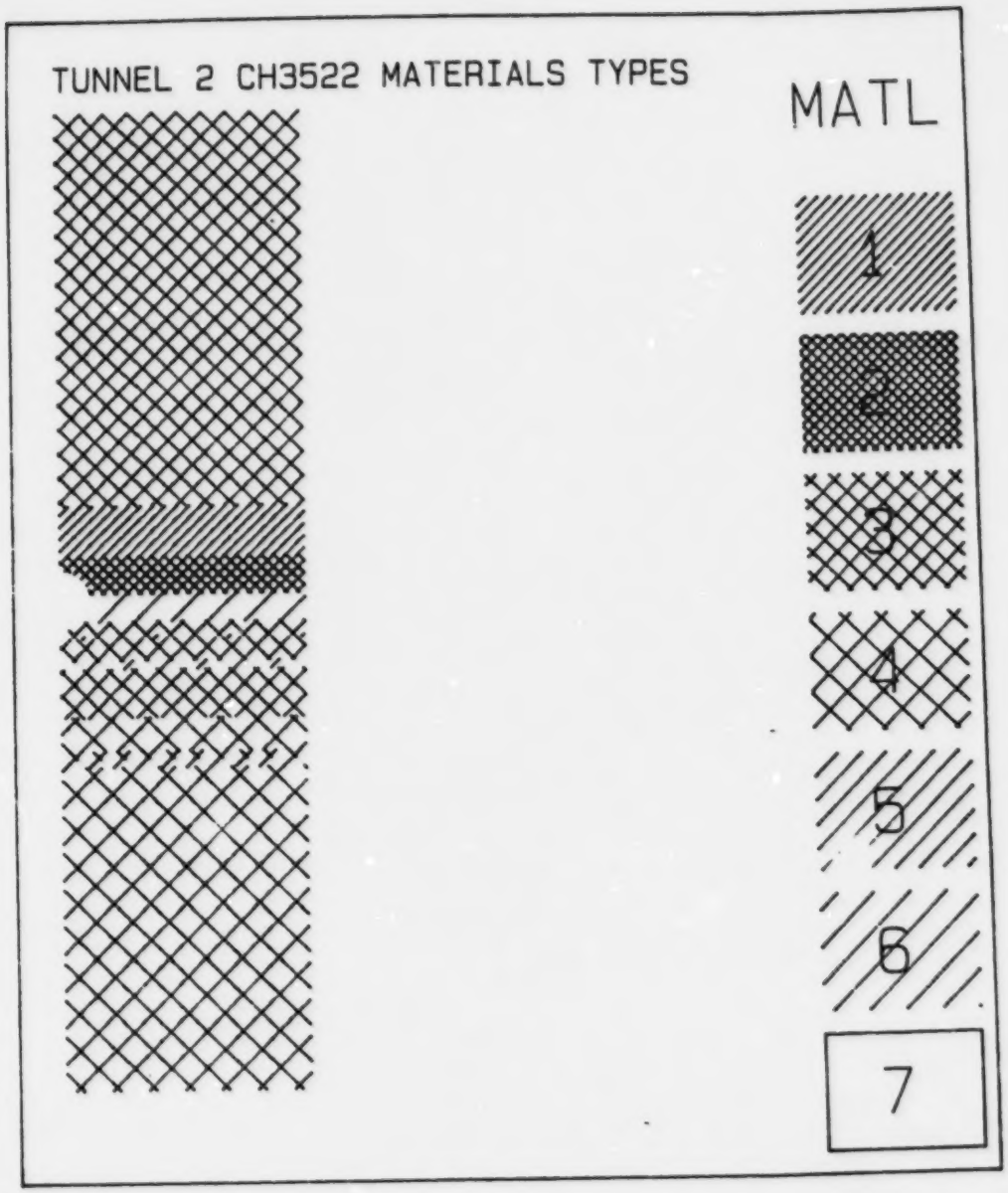

Figure 3.53: No.2 Tunnel, CH3522. Material Pattern around the Opening

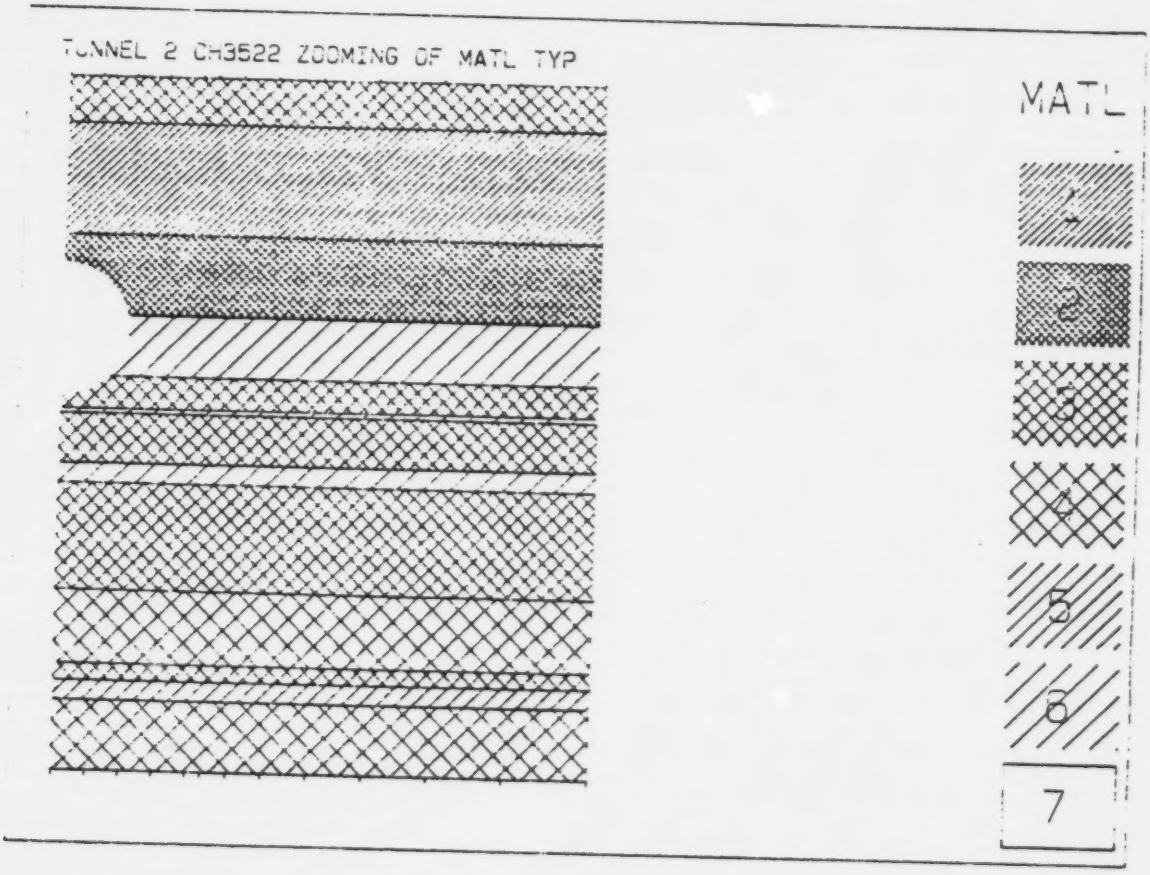

Figure 3.54: No.2 Tunnel, CH3522. Zooming of Material around the Opening

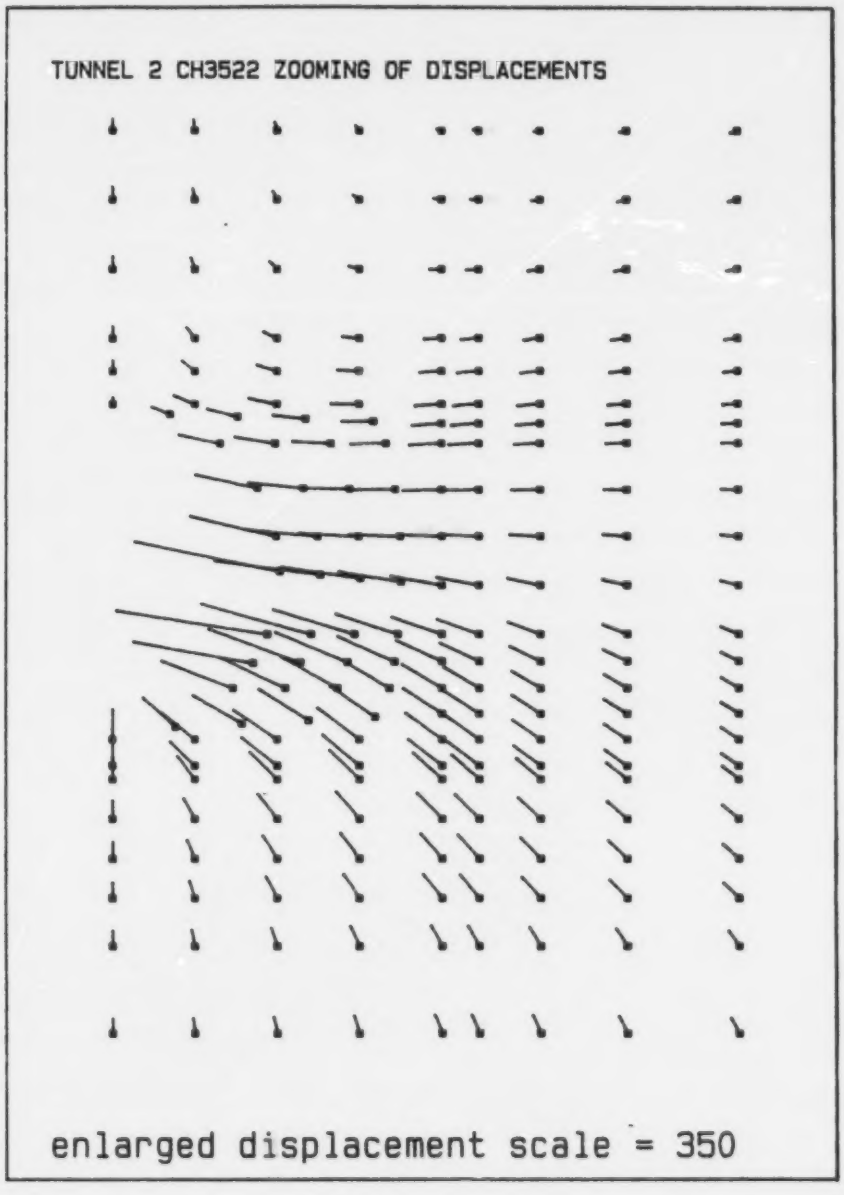

Figure 3.55: No.2 Tunnel, CH3522. Ground Displacement around the Opening

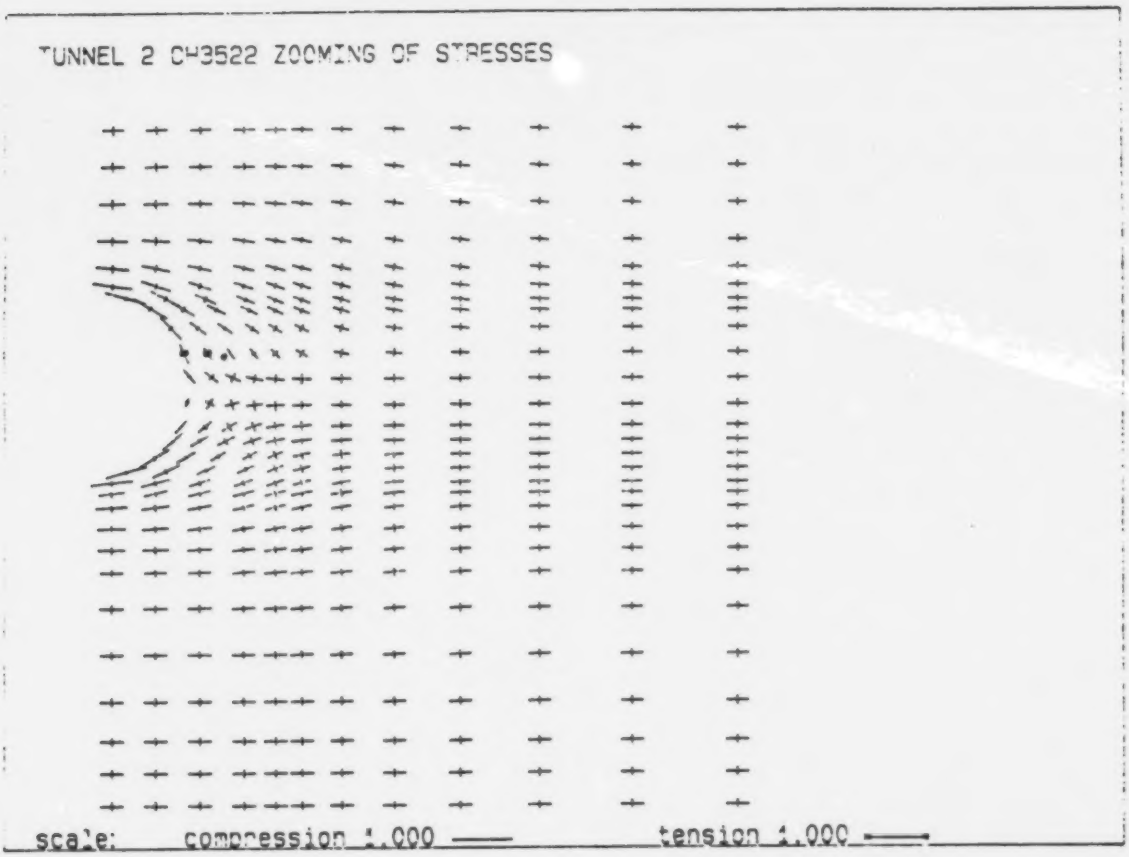

Figure 3.56: No.2 Tunnel, CH3522. Zooming of Stress Pattern around the Opening

FAILURE CRITERIA	COEFFICIENTS		
	first	second	third
1.Mohr_Coulomb	C	Angle	
2.Drucker_Prager	C	Angle	
3.Hoek and Brown	M	S	Sigma C

TOTAL NO. OF MATERIAL TYPES = 6

MATERIAL NO.	FAIL. CRITERIA	COEFFICIENTS		
1	3	5	0.1	92
2	3	5	0.1	121
3	3	5	0.1	53
4	3	5	0.1	36
5	3	5	0.1	36
6	3	5	0.65	16.6

Figure 3.57: No.2 Tunnel, CH3522. Parameters of Material Failure Criteria

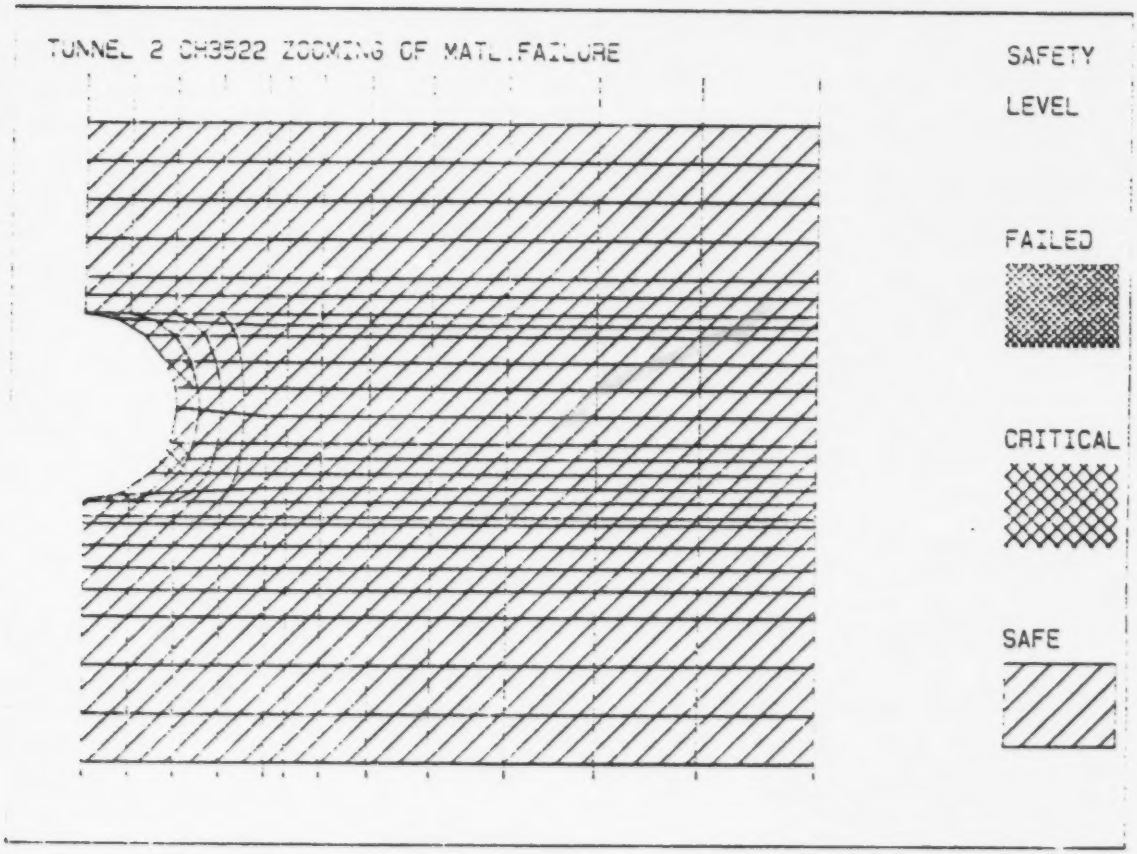

Figure 3.58: No.2 Tunnel, CH3522. Zooming of Material Safety Level

Chapter 4

Geotechnical Assessment of the No.2 Tunnel

4.1 Rock-Support Interaction

The primary aim in the design of underground excavation support system is to help the rockmass support itself.

Upon excavation of underground opening, a redistribution of the pre-existing stresses (virgin stresses) takes place, and to attain stability, a new equilibrium condition is developed within the rockmass. This process can cause straining of the rockmass with varying degree of fracture and deformation, depending on the type and magnitude of the original stress field and rock strength properties. This usually produces closure of the mining excavation. If the induced stresses are within the elastic, then the displacement of opening excavation is likely to be very small. However if the stresses are high enough to cause fracturing of rock, then these can ultimately become the reason of closure of the tunnel opening. This fractured zone is also termed as "yield zone". Beyond this zone, the rock is largely unaffected by the stress redistribution process and the portion remain in the elastic zone. The attainment of maximum load bearing capacity of the rock and the tunnel support can be based upon the analysis of the rock-support interaction.

Immediately after the excavation of the tunnel, the ground around the tunnel will not collapse because the radial deformation is limited by the proximity of the tunnel face which provides a significant amount of restraint.

However, as the tunnel face is advanced, and its supporting effect is reduced, the wall, roof and floor will deform further into the excavation opening. As the deformation proceeds, a greater proportion of the inherent rock strength is mobilized and more stress is redistributed around the opening. If time-dependency effects are neglected, the process of stress redistribution is deemed to be completed when the closure of the tunnel surface is halted and equilibrium is restored to the system.

In the case of strong and competent rock- mass, the stress distribution may be accomplished with sufficient self-supporting strength being generated by the rock itself, in such a case no additional support is required and the tunnel experiences little deformation. However, when considering weaker incompetent rocks, especially the coal measure strata, stress redistribution will almost certainly cause excessive deformation and failure of the tunnel walls. Equilibrium can only be achieved at the expense of large, and usually unacceptable levels of radial displacement.

In fact, the effect of gravity loading of tunnel walls by detached roof blocks is to give the rock a rising characteristic curve as shown by curve KLMN on Fig. 4.1 . The result of that "loosening pressure" is to ensure that equilibrium is only attainable through the use of additional support because the maximum rock strength (point M on Fig. 4.1) is insufficient to halt closure. The installation of support lining provides a means for confining the rock mass and thus reinforces its strength and "self-supporting" capacity.

Some degree of rock displacement almost invariably occurs prior to installation of the tunnel lining. This is represented by the off-set 'OA' on the displacement axis. The cure 'AB' represents the initial portion of the support characteristic curve.

4.2 Rationale for Calculating Safety Margins

The factor of safety is obtained by comparing the load exerted on the arches (8,9) (Fig. 5.2) and the ultimate load which is calculated by using S4. Load measurement techniques used in the Donkin Morien Project were not very satisfactory. The axial stresses in the arches were measured by means of pressure cells placed at the butt joints at the spring line.(Fig.5.3) The axial

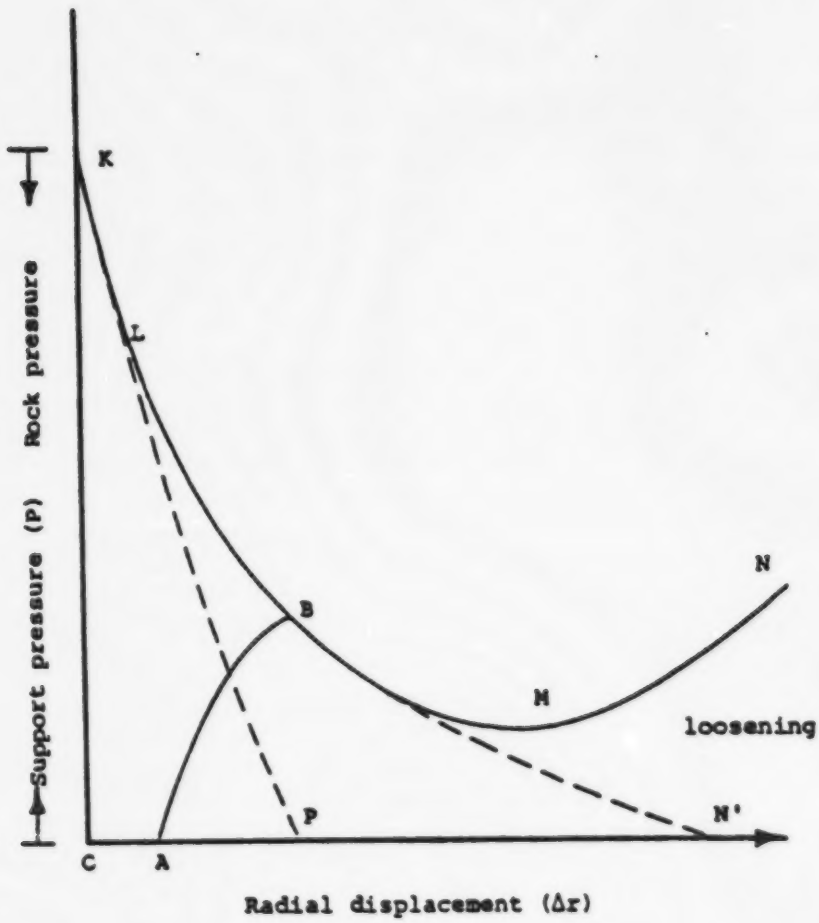

Figure 4.1: Rock-Support Interaction Diagram

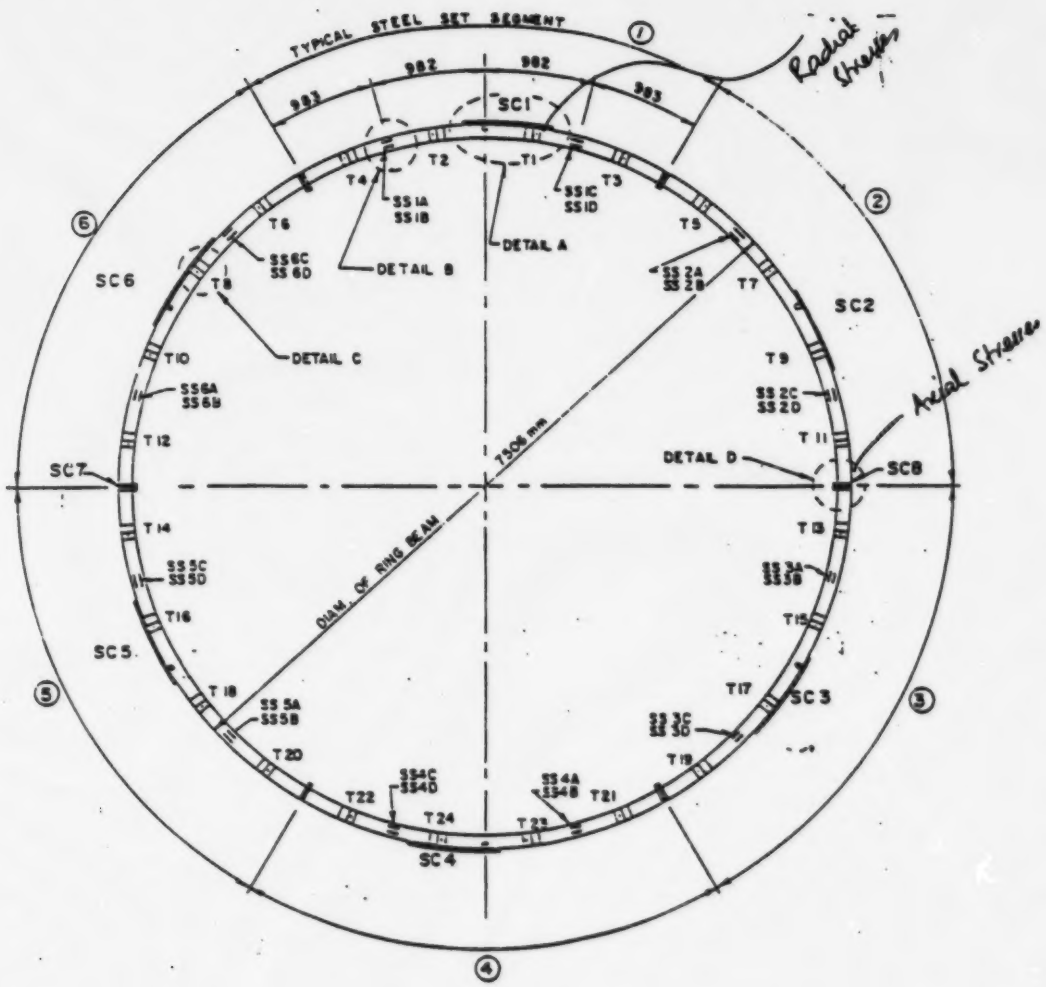

Figure 4.2: Typical Layout of Instrumentation on Steel Set

stresses were measured over a 150 mm × 150 mm area. This pressure is then multiplied by a factor of 8.15 (ratio of area of end plate to the cross sectional area of the beam section) to obtain the corresponding stress in the beam section.

Similarly radial pressure (stresses) measured by the curved pressure cells at the rock/arch interface.(Fig. 5.4) The pressures, reported in the report were very low except at chainage 3353 meters. In general, the rock-arch contact at the crown was not very uniform, because of the fracturing (spalling) of the rock in the immediate vicinity of the crown.

The axial stresses and the corresponding factor of safety is given in Table 4.1, and radial stresses and respective factor of safety is in Table 4.2. Generally the factor of safety is well within the range of geomechanical acceptance. The tables show that supports are not designed economically as the factor of safety is very high. The explanation of very high factor of safety (above 25) on some of the loald cells was either due to improper installation/use of load measuring cells or because of very small deformation of tunnel opening. As was shown in Chapter 3, the displacement of the crown of the tunnel opening was very small, therefore the crown was not under high pressure/load which resulted in a very high factor of safety. In case of radial stresses, the factor of safety ranges between 2 and 5.

4.3 Discussions

The circular arches which were provided in the Donkin Morien Tunnel appear to be very stable. From the analysis, the following results can be generalized:

1. Measured strains appears to be well within the elastic range
2. As previously explained, the load measurement techniques used in the Donkin Morien Project are not satisfactory, they record the local stress at the location of installation only and hence do not represent the force exerted on the complete support.
3. Generally, it can be said that the existing support system is structurally sound.
4. The design of the tunnel supports of Donkin Morien Project could have been made more economical had a thorough analysis of the rock-

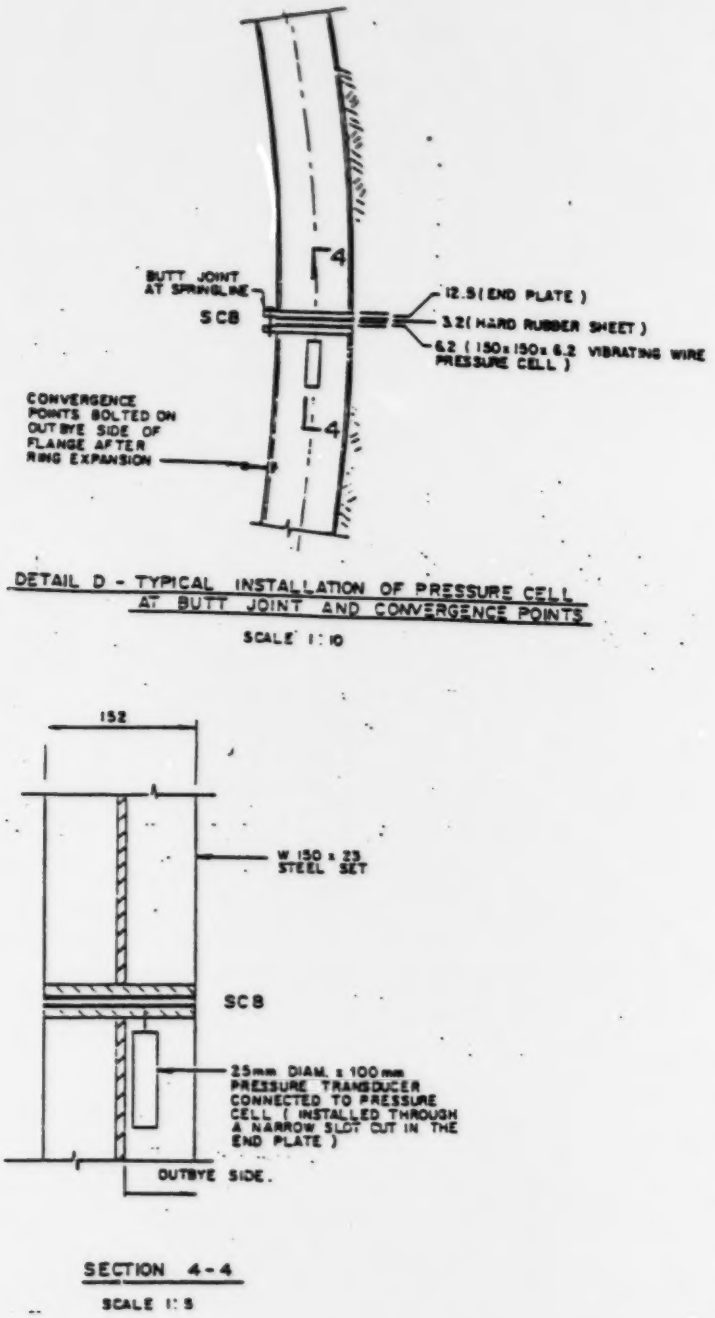
BUTT JOINT AT SPRINGLINE
SCB
12.5 (END PLATE)
3.2 (HARD RUBBER SHEET)
6.2 (150 x 150 x 6.2 VIBRATING WIRE PRESSURE CELL)
CONVERGENCE POINTS BOLTED ON OUTBYE SIDE OF FLANGE AFTER RING EXPANSION
4
4
DETAIL D - TYPICAL INSTALLATION OF PRESSURE CELL AT BUTT JOINT AND CONVERGENCE POINTS
SCALE 1:10
152
W 150 x 23 STEEL SET
SCB
25mm DIAM. x 100mm PRESSURE TRANSDUCER CONNECTED TO PRESSURE CELL (INSTALLED THROUGH A NARROW SLOT CUT IN THE END PLATE)
OUTBYE SIDE.
SECTION 4-4
SCALE 1:5

Figure 4.3: Pressure Cell (to Measure Axial Stresses)

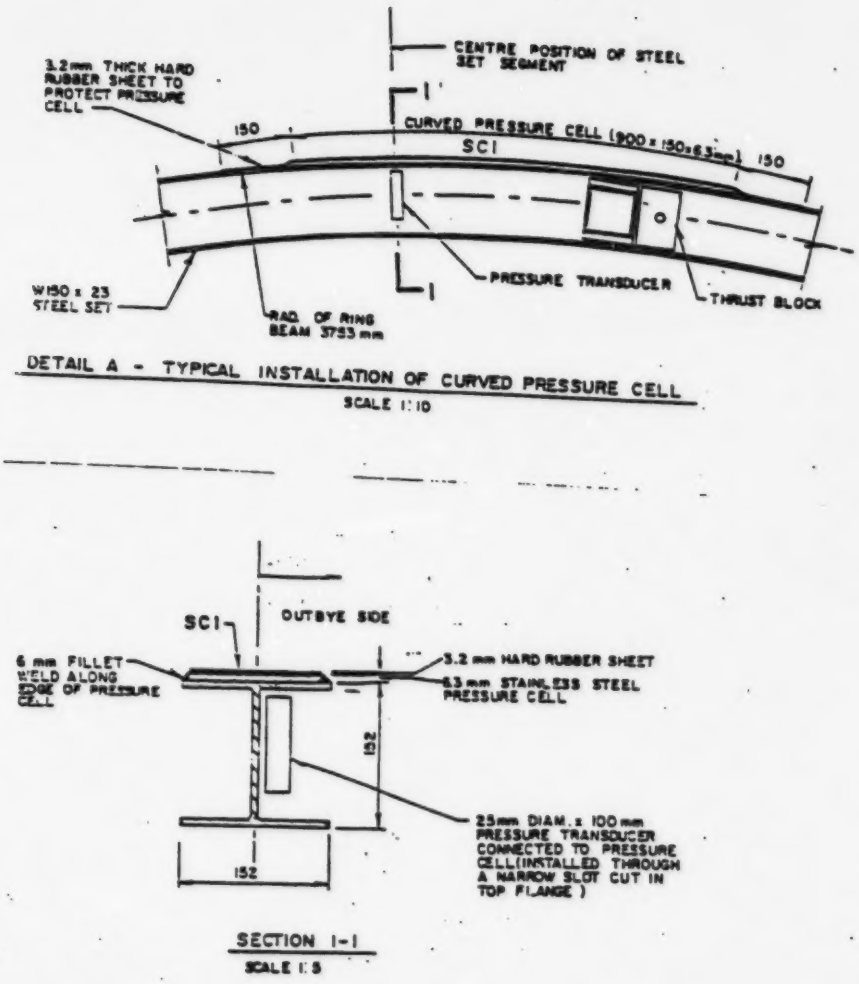
CENTRE POSITION OF STEEL SET SEGMENT
3.2mm THICK HARD RUBBER SHEET TO PROTECT PRESSURE CELL
150
CURVED PRESSURE CELL (900 x 150 x 6.3mm)
150
SC1
PRESSURE TRANSDUCER
THRUST BLOCK
W150 x 23 STEEL SET
RAD. OF RING BEAM 3753 mm
DETAIL A - TYPICAL INSTALLATION OF CURVED PRESSURE CELL
SCALE 1:10
SC1
OUTBYE SIDE
6 mm FILLET WELD ALONG EDGE OF PRESSURE CELL
3.2 mm HARD RUBBER SHEET
6.3 mm STAINLESS STEEL PRESSURE CELL
152
25mm DIAM. x 100 mm PRESSURE TRANSDUCER CONNECTED TO PRESSURE CELL (INSTALLED THROUGH A NARROW SLOT CUT IN TOP FLANGE)
152
SECTION 1-1
SCALE 1:5

Figure 4.4: Pressure Cell (to Measure Radial Pressure)

CHAINAGE		SC7	SC8
925	MEASURED STRESSES MPA **	0.82	7.58
	F.O.S *	243	26.0
1423	MEASURED STRESSES MPA	79.14	59.74
	F.O.S	2.53	3.35
1831	MEASURED STRESSES MPA	-	62.27
	F.O.S	-	3.21
3353	MEASURED STRESSES MPA	79.32	104.55
	F.O.S	2.52	1.92

Table 4.1: Comparison of Measured and Computed Axial Stresses

Notes: * The factor of Safety (F.O.S) calculations are based on a axial stress of 200 MPa computed from Program S4.

** Using strains gauges in the web of the steel arch.

CHAINAGE		SC1	SC2	SC3	SC4	SC5	SC6
925	MEASURED STRESSES KPA **	-	-	440	40	-	160
	F.O.S *	-	-	2.27	25	-	6.25
1423	MEASURED STRESSES KPA	40	400	380	280	580	170
	F.O.S	25	2.5	2.63	3.57	1.72	5.88
1831	MEASURED STRESSES KPA	110	240	300	470	230	280
	F.O.S	9.09	4.17	3.33	2.13	4.35	3.57
3353	MEASURED STRESSES KPA	470	190	250	820	230	360
	F.O.S	2.13	5.26	4.0	1.22	4.35	2.78

Table 4.2: Comparison of Measured and Computed Radial Pressure

Notes: ⋆ The factor of Safety (F.O.S) calculations are based on a radial pressure of 1000 KPa computed from Program S4.

⋆⋆ Using load cells

support interaction been undertaken using the analytical procedure mentioned in Chapter 3 and Chapter 4.

5. The stability of the underground opening largely depends upon the rock properties around the opening e.g harder rocks will give more stability.

6. Tunnel deformation was not significant at distances 3 meters or more from the tunnel opening.

7. Tunnel deformation depends on the in-situ stresses. If horizontal stresses are more than the vertical stresses, then the floor heave and crown displacements would be very small, where as large displacement could be anticipated at shoulders of the circular opening. On the contrary, if vertical stresses are dominating then floor and crown would displace more than the shoulders.

8. Spacing of arches largely depend on the geology around the tunnel. But in the Donkin-Morien Project the spacing of the arches was kept constant as 1 meter throughout the length irrespective of the of the different kinds of the rocks. The spacing was decreased in the weak rocks like coal seam, but never increased in the hard rocks. On the basis of the analyses done in Chapter 3, the spacing in the hard rocks could have been increased.

Chapter 5

Conclusions

5.1 Summary

Parametric studies of the steel arches have been undertaken by using Finite Element Computer Program S4(steel set support system). The Following are the conclusions;

1. Program S4 reasonably analysed all types of steel arches .
2. It accounts for both material and geometric nonlinearties.
3. All types of loads are simulated effectively i.e concentrated (point load) load, uniformly distributed load, sinusoidal load, and arches under pressure.
4. Program S4 simulates the following types of arches: semi-circular arches, circular arches, straight-leg arches and splay legged arches.
5. Ultimate load is found by using Newton-Raphson method and results are in good agreement with different other methods.

The No.2 Underground Tunnel of the Donkin-Morien Project of Sydney, Nova Scotia, has been analyzed by using finite element computer program MSAP2D. Conclusions are:

1. MSAP2D is a user friendly tool for 2-D linear finite element analyses.

2. Program MSAP2D calculates the displacement around the opening and checks the material safety levels by using different failure criteria.

3. Stresses around the opening could also be found by MSAP2D.

4. Geology (different types of rocks) around the tunnel opening is reasonably simulated by Finite Element Analysis.

5. In-situ stresses (reported in Donkin Morien Project) have been used for analyses.

6. Different cross-sections of tunnel are modelled (cross-sections are taken those chainages which were considered critical in the Donkin Morien Project) and their results are discussed in the previous chapter. Displacements and material safety level are critical near the opening.

In the Donkin Morien Project, axial stresses and radial pressure were measured by using strain gauges and pressure cells respectively. This approach is classical, however the results are not very satisfactory. The method used gives the stresses in MPa at the point of the installation only, and it does not represent the complete load on the arch.

The calculated factor of safety is very high, which indicates that the design of arches are not very economical.

5.2 Further Research

1. In order to analyse underground excavation, a complete 3-D non-linear Finite Element package is necessary. A further development and improvement of MSAP2D is essential in this regard.

2. Program MSAP2D does not have an option of the time- dependency, which is important in the underground excavation.

3. Program S4 should have capabilities of analyzing 3-D tunnel junction, effect of blocking on arches and should take load other than the ultimate load.

4. Both program MSAP2D and S4 should work interactively so that displacements obtained in MSAP2D could be applied on arches and their behaviour could be assessed.

5. Program S4 should then have the capabilities of simulating the rock-support interaction.

References

1. Mitri, H.S., Hassani, F.P. Nonlinear finite element analysis of mine roadways arch support systems. Comp. Struc., 29, No.3 pp 355-364 (1988)

2. Chau, K. S., Mitri, H.S., Hassani, F.P., Scoble, M.J., A finite element computer model for stress analysis of underground openings. Computer Applications in the Mineral Industry. Quebec 7-9 March 1988 pp 256-263

3. Hassani, F.P., Mitri, H.S. and Aston, T. Numerical modelling of tunnel steel supports. Third International Conference on Computing in Civil Engineering. 10-12 August 1988 Vancouver, B.C., Canada. pp 251-260.

4. Hoek, E., Brown, E.T., Underground Excavation in Rock, Institution of Mining and Metallurgy, London, (1980).

5. Obert, Leonard., Duvall, W.I., Rock Mechanics and the Design of Structures in Rock. John Wiley & Sons, Inc. 1967.

6. Brady, B.H.G., Brown, E.T., Rock Mechanics for Underground Mining London George Allen & Unwin 1985.

7. Mitri, H.S. and Hassani, F.P., Load Bearing Capacity of Steel Arch Support Systems. 91st AGM-C.I.M., Quebec City, April 30-May 4,1989

8. Measurement and Analysis of Rock Deformation and Support System response in the Drill and Blast and Bored Access Driviges at the Donkin-Morien Project (UP-G198),. Prepared by Golder Associates. Volume I, June 1985

9. Measurement and Analysis of Rock Deformation and Support System response in the Drill and Blast and Bored Access Driviges at the Donkin-Morien Project (UP-G198),. Prepared by Golder Associates. Volume II, June 1985

10. Measurement and Analysis of Rock Deformation and Support System response in the Drill and Blast and Bored Access Driviges at the Donkin-Morien Project (UP-G198),. Prepared by Golder Associates. Volume III, June 1985

11. Measurement and Analysis of Rock Deformation and Support System response in the Drill and Blast and Bored Access Driviges at the Donkin-Morien Project (UP-G198),. Prepared by Golder Associates. Volume IV, June 1985

12. Brown, A., Campbell, S.G., A Comparison of Arches of Different construction under single point loading. National Coal Board Central Engineering Establishment, Report No. LT 651, (1965).

13. Paul, S.L., Siess, C.P., and Gaylord, E.H., Large scale tests of tunnel supports. Proceedings of Rapid Excavations and Tunneling Conference, San Francisco, Vol. 2, (CH. 91) pp.1395-1417, (1974)

14. Cunliffe, H., Johnston, A.G., Roadway supports with special references to Yielding arches. Transactions of the Inst. Mining Engineers, Vol. 117, pp.804-818, (1957)

15. Round, C., Lewis, S., Drift, R., New techniques. The Mining Engineer, Vol. 141, pp. 17-24, (1981).

16. Jukes, S.G., Hassani, F.P, and Whittaker, B.N., Characteristics of steel arch support systems for the mine roadways, Part I, Modelling Theory, Instrumentation and Preliminary Results. Mining Science and Technology, Vol. 1, pp. 43-58, (1983)

17. Underground Roadway Supports. British Steel Corporation. BSC Sections. Cleveland, British.

Appendix A

Input Data of Program MSAP2D

```
CHAINAGE 3522 OF TUNNEL NO.2 (CIRCULAR OPENING)
83 34  17  2  1  0
7  4  2  2  2  2  2  2  1  1  3  1  3  3  2  2  8
4  8
1    1  0.0      3.815
2    0  1.305    3.585
3    0  2.452    2.922
4    0  3.304    1.9075
5    0  3.732    0.793
6    0  3.815    0.0
7    0  3.537   -1.429
8    0  3.20    -2.078
9    0  2.744   -2.650
10   0  1.429   -3.537
11   1  0.0     -3.815
12   1  0.0     -4.415
13   1  0.0     -4.715
14   1  0.0     -7.415
15   1  0.0     -8.50
16   1  0.0     -14.415
17   1  0.0     -18.515
18   1  0.0     -19.415
19   1  0.0     -20.50
20   1  0.0     -32.35
21   3  0.0     -60.0
22   2  7.5     -60.0
23   2  14.25   -60.0
24   3  30.0    -60.0
25   1  30.0    -32.35
26   1  30.0    -20.50
27   1  30.0    -19.415
28   1  30.0    -18.515
29   1  30.0    -14.415
30   1  30.0    -8.50
31   1  30.0    -7.415
32   1  30.0    -4.715
33   1  30.0    -4.415
34   1  30.0    -3.815
35   1  30.0    -2.650
36   1  30.0    -1.429
37   1  30.0     0.793
38   1  30.0     2.922
39   1  30.0     3.815
40   1  30.0     5.315
41   1  30.0     11.615
42   1  30.0     27.0
43   3  30.0     60.0
44   2  14.25    60.0
45   2  7.5      60.0
46   3  0.0      60.0
47   1  0.0      27.0
48   1  0.0      11.615
49   1  0.0      5.315
```

```
50   0   7.5      11.615
51   0   7.5      5.315
52   0   7.5      3.815
53   0   7.5      2.922
54   0   7.5      0.793
55   0   7.5     -1.429
56   0   7.5     -2.650
57   0   7.5     -3.815
58   0   7.5     -4.415
59   0   7.5     -4.715
60   0   7.5     -7.415
61   0   7.5     -8.50
62   0   7.5     -14.415
63   0   7.5     -18.515
64   0   7.5     -19.415
65   0   7.5     -20.50
66   0   7.5      27.0
67   0   7.5     -32.35
68   0   14.25    11.615
69   0   14.25    5.315
70   0   14.25    3.815
71   0   14.25    2.922
72   0   14.25    0.793
73   0   14.25   -1.429
74   0   14.25   -2.650
75   0   14.25   -3.815
76   0   14.25   -4.415
77   0   14.25   -4.715
78   0   14.25   -7.415
79   0   14.25   -8.50
80   0   14.25   -14.415
81   0   14.25   -18.515
82   0   14.25   -19.415
83   0   14.25   -20.50
1    46   48   50   45   47    0   66    0   3   2   0
2    48   49   51   50    0    0    0    0   1   2   0
3    49   1    52   51    0    0    0    0   2   2   0
4    1    3    53   52    2    0    0    0   2   2   0
5    3    5    54   53    4    0    0    0   2   2   0
6    5    7    55   54    6    0    0    0   6   2   0
7    7    9    56   55    8    0    0    0   6   2   0
8    9    11   57   56   10    0    0    0   3   2   0
9    11   12   58   57    0    0    0    0   3   2   0
10   12   13   59   58    0    0    0    0   6   2   0
11   13   14   60   59    0    0    0    0   3   2   0
12   14   15   61   60    0    0    0    0   6   2   0
13   15   16   62   61    0    0    0    0   3   2   0
14   16   17   63   62    0    0    0    0   4   2   0
15   17   18   64   63    0    0    0    0   3   2   0
16   18   19   65   64    0    0    0    0   5   2   0
17   19   21   22   65   20    0   67    0   4   2   0
18   45   50   41   43   66   68   42   44   3   2   0
19   50   51   40   41    0   69    0   68   1   2   0
20   51   52   39   40    0   70    0   69   2   2   0
21   52   53   38   39    0   71    0   70   2   2   0
22   53   54   37   38    0   72    0   71   2   2   0
23   54   55   36   37    0   73    0   72   6   2   0
24   55   56   35   36    0   74    0   73   6   2   0
25   56   57   34   35    0   75    0   74   3   2   0
26   57   58   33   34    0   76    0   75   3   2   0
27   58   59   32   33    0   77    0   76   6   2   0
28   59   60   31   32    0   78    0   77   3   2   0
29   60   61   30   31    0   79    0   78   6   2   0
30   61   62   29   30    0   80    0   79   3   2   0
31   62   63   28   29    0   81    0   80   4   2   0
32   63   64   27   28    0   82    0   81   3   2   0
```

```
33  64  65  26  27  0   83  0   82  5  2  0
34  65  22  24  26  67  23  25  83  4  2  0
0  1  1  1  1  0  1  0  1.0  6  1  1.0  1
 1    0.022       1
      24000.0     0.25
 2    0.022       1
      17600.0     0.25
 3    0.0261      1
      11000.0     0.25
 4    0.0216      1
      9000.0      0.25
 5    0.0216      1
      5400.0      0.25
 6    0.015       1
      3450.0      0.1
   -11.91 0.0658  -4.763 0.0263  -1.667 0.00921  0.0
 0.0  0.0  1.0  0.0 -1.0
```

Appendix B

Input and Output Data of Program S4

Input data of a circular arch under sinusoidal load.

```
C2S-H2
   1       3
  25      24
   5       2       1
2000.0000     2000.0000      180.0000
   1      89.0000       9.9000       69.2000       9.5000
   0       0
 100       0
      200.0000              .8155              .2680              .4300
   1
END OF RUN
   0       0
```

****

Output data for a circular arch under sinusoidal load.

```
**********                PROGRAM  STEEL2D                **********
**********     NONLINEAR ANALYSIS OF PLANAR STEEL STRUCTURES    **********
                                  BY
**********                     H.S. MITRI                    **********
**********                  MCGILL UNIVERSITY                **********
**********                MONTREAL, QUEBEC, 1986             **********
*****************************************************************************



2S-H2
  PROBLEM NUMBER           1
  EXECUTION MODE           3
  TOTAL NODES        =    25
  TOTAL ELEMENTS     =    24

  STRUCTURE TYPE     =CIRCLE
  LOAD TYPE          =SINUSOIDAL LOAD
  NUMBER OF SECTIONS=     1

  GEOMETRY OF THE STRUCTURE

  DIAMETER    = 2000.0000
  HEIGHT      = 2000.0000
  SPLAY ANGLE=  180.0000
  *************************      NODAL POINT DATA      *************************

  NODE          X           Y          U     V     THETA
    1         .0000    1000.0000      0     1     0
    2       130.5262    991.4449      1     1     1
    3       258.8191    965.9258      1     1     1
    4       382.6834    923.8795      1     1     1
    5       500.0000    866.0254      1     1     1
    6       608.7614    793.3533      1     1     1
    7       707.1068    707.1068      1     1     1
```

8	793.3534	608.7614	1	1	1
9	866.0254	500.0000	1	1	1
10	923.8795	382.6834	1	1	1
11	965.9258	258.8190	1	1	1
12	991.4449	130.5262	1	1	1
13	1000.0000	.0000	1	1	1
14	991.4449	-130.5262	1	1	1
15	965.9258	-258.8191	1	1	1
16	923.8795	-382.6835	1	1	1
17	866.0254	-500.0001	1	1	1
18	793.3533	-608.7615	1	1	1
19	707.1067	-707.1068	1	1	1
20	608.7614	-793.3534	1	1	1
21	499.9999	-866.0254	1	1	1
22	382.6834	-923.8796	1	1	1
23	258.8190	-965.9258	1	1	1
24	130.5261	-991.4449	1	1	1
25	-.0001	-1000.0000	0	0	0

********** MEMBER DATA **********

NO	ELEMENT NODES		IT	IS	IF	FLANGE WIDTH	FLANGE THICKNESS	WEB DEPTH	WEB THICKNESS
1	1	2	2	1	1	89.000	9.900	69.200	9.500
2	2	3	2	1	1	89.000	9.900	69.200	9.500
3	3	4	2	1	1	89.000	9.900	69.200	9.500
4	4	5	2	1	1	89.000	9.900	69.200	9.500
5	5	6	2	1	1	89.000	9.900	69.200	9.500
6	6	7	2	1	1	89.000	9.900	69.200	9.500
7	7	8	2	1	1	89.000	9.900	69.200	9.500
8	8	9	2	1	1	89.000	9.900	69.200	9.500
9	9	10	2	1	1	89.000	9.900	69.200	9.500
10	10	11	2	1	1	89.000	9.900	69.200	9.500
11	11	12	2	1	1	89.000	9.900	69.200	9.500
12	12	13	2	1	1	89.000	9.900	69.200	9.500
13	13	14	2	1	1	89.000	9.900	69.200	9.500
14	14	15	2	1	1	89.000	9.900	69.200	9.500
15	15	16	2	1	1	89.000	9.900	69.200	9.500
16	16	17	2	1	1	89.000	9.900	69.200	9.500
17	17	18	2	1	1	89.000	9.900	69.200	9.500
18	18	19	2	1	1	89.000	9.900	69.200	9.500
19	19	20	2	1	1	89.000	9.900	69.200	9.500
20	20	21	2	1	1	89.000	9.900	69.200	9.500
21	21	22	2	1	1	89.000	9.900	69.200	9.500
22	22	23	2	1	1	89.000	9.900	69.200	9.500
23	23	24	2	1	1	89.000	9.900	69.200	9.500
24	24	25	2	1	1	89.000	9.900	69.200	9.500

********** INITIAL LOAD DATA **********

NO. OF NODES OF PROPORTIONAL LOAD = 0
NO. OF NODES OF CONSTANT LOAD = 0

PERCENT OF CRONW LENGTH = 100
NO. OF ELEMENTS OF CONSTANT LOAD = 0

ELEMENT LOAD DATA

ELEMENT	WXG	WYGFIXED END FORCES			
1	.0000	-.9957			
-.9888E-15	.6512E+02	.1417E+04	-.9888E-15	.6512E+02	-.1417E+04
2	.0000	-.9787			
-.3808E-15	.6401E+02	.1369E+04	-.3808E-15	.6401E+02	-.1369E+04
3	.0000	-.9449			
-.5187E-15	.6180E+02	.1276E+04	-.5187E-15	.6180E+02	-.1276E+04
4	.0000	-.8950			

```
 .2139E-14    .5853E+02    .1144E+04    .2139E-14    .5853E+02   -.1144E+04
  5      .0000     -.8297
 .1561E-16    .5426E+02    .9836E+03    .1561E-16    .5426E+02   -.9836E+03
  6      .0000     -.7502
-.1828E-14    .4907E+02    .8043E+03   -.1828E-14    .4907E+02   -.8043E+03
  7      .0000     -.6579
-.2418E-14    .4303E+02    .6185E+03   -.2418E-14    .4303E+02   -.6185E+03
  8      .0000     -.5544
 .1551E-14    .3626E+02    .4392E+03    .1551E-14    .3626E+02   -.4392E+03
  9      .0000     -.4413
-.2645E-15    .2887E+02    .2783E+03   -.2645E-15    .2887E+02   -.2783E+03
 10      .0000     -.3208
-.1123E-15    .2098E+02    .1470E+03   -.1123E-15    .2098E+02   -.1470E+03
 11      .0000     -.1947
-.2036E-15    .1273E+02    .5415E+02   -.2036E-15    .1273E+02   -.5415E+02
 12      .0000     -.0653
-.2895E-16    .4268E+01    .6086E+01   -.2895E-16    .4268E+01   -.6086E+01
   ************************     MATERIAL PROPERTIES     **********************
     MODULUS OF ELASTICITY =   200.000       TANGENT MODULUS        =      .816
     YIELD STRESS          =      .268       ULTIMATE STRESS        =      .430
     YIELD-TO-ULT ST RATIO =      .623

   ********************************************************************************

   NO. OF EQUATIONS =   70
   MATRIX SIZE      =  340
   MAX COL HEIGHT   =    6


   ELASTIC LIMIT STRESSES OF EL NO. 1
   .0281     .0250     .0219     .0003    -.0213    -.0244    -.0275
   .0277     .0247     .0216     .0003    -.0211    -.0241    -.0272
   .0274     .0244     .0214     .0003    -.0208    -.0238    -.0269

   ELASTIC LIMIT STRESSES OF EL NO. 2
   .0269     .0239     .0210     .0002    -.0206    -.0236    -.0266
   .0259     .0230     .0202     .0002    -.0198    -.0227    -.0256
   .0249     .0222     .0194     .0002    -.0191    -.0218    -.0246

   ELASTIC LIMIT STRESSES OF EL NO. 3
   .0240     .0213     .0186     .0000    -.0186    -.0213    -.0240
   .0224     .0199     .0174     .0000    -.0174    -.0199    -.0224
   .0208     .0185     .0162     .0000    -.0162    -.0185    -.0208

   ELASTIC LIMIT STRESSES OF EL NO. 4
   .0194     .0173     .0151    -.0003    -.0156    -.0178    -.0200
   .0174     .0154     .0134    -.0003    -.0140    -.0159    -.0179
   .0153     .0135     .0118    -.0003    -.0123    -.0141    -.0158

   ELASTIC LIMIT STRESSES OF EL NO. 5
   .0136     .0120     .0105    -.0006    -.0116    -.0132    -.0148
   .0112     .0099     .0086    -.0006    -.0097    -.0110    -.0123
   .0087     .0077     .0067    -.0006    -.0078    -.0088    -.0099

   ELASTIC LIMIT STRESSES OF EL NO. 6
   .0069     .0060     .0051    -.0009    -.0070    -.0079    -.0087
   .0042     .0036     .0031    -.0009    -.0049    -.0055    -.0061
   .0016     .0013     .0010    -.0009    -.0029    -.0031    -.0034

   ELASTIC LIMIT STRESSES OF EL NO. 7
  -.0004    -.0005    -.0006    -.0013    -.0020    -.0021    -.0022
  -.0031    -.0029    -.0027    -.0013     .0001     .0003     .0005
  -.0058    -.0053    -.0048    -.0013     .0022     .0027     .0032

   ELASTIC LIMIT STRESSES OF EL NO. 8
```

-.0077	-.0070	-.0064	-.0017	.0031	.0037	.0044
-.0103	-.0093	-.0084	-.0017	.0051	.0060	.0070
-.0129	-.0116	-.0104	-.0017	.0071	.0083	.0096

ELASTIC LIMIT STRESSES OF EL NO. 9

-.0147	-.0132	-.0118	-.0020	.0079	.0093	.0107
-.0170	-.0153	-.0136	-.0020	.0097	.0113	.0130
-.0193	-.0174	-.0154	-.0020	.0115	.0134	.0153

ELASTIC LIMIT STRESSES OF EL NO.10

-.0208	-.0187	-.0167	-.0023	.0122	.0142	.0163
-.0227	-.0204	-.0182	-.0023	.0136	.0159	.0182
-.0246	-.0221	-.0196	-.0023	.0151	.0176	.0201

ELASTIC LIMIT STRESSES OF EL NO.11

-.0258	-.0232	-.0206	-.0025	.0157	.0183	.0209
-.0272	-.0244	-.0217	-.0025	.0168	.0195	.0222
-.0286	-.0257	-.0228	-.0025	.0178	.0207	.0236

ELASTIC LIMIT STRESSES OF EL NO.12

-.0293	-.0263	-.0234	-.0026	.0182	.0212	.0242
-.0301	-.0271	-.0240	-.0026	.0188	.0219	.0250
-.0309	-.0278	-.0246	-.0026	.0195	.0226	.0258

ELASTIC LIMIT STRESSES OF EL NO.13

-.0313	-.0281	-.0249	-.0026	.0196	.0228	.0260
-.0315	-.0283	-.0250	-.0026	.0198	.0230	.0262
-.0317	-.0284	-.0252	-.0026	.0199	.0232	.0264

ELASTIC LIMIT STRESSES OF EL NO.14

-.0316	-.0284	-.0251	-.0026	.0199	.0231	.0263
-.0311	-.0280	-.0248	-.0026	.0196	.0227	.0259
-.0307	-.0276	-.0245	-.0026	.0192	.0223	.0255

ELASTIC LIMIT STRESSES OF EL NO.15

-.0302	-.0272	-.0241	-.0026	.0189	.0220	.0251
-.0292	-.0262	-.0233	-.0026	.0181	.0211	.0241
-.0282	-.0253	-.0225	-.0026	.0173	.0202	.0230

ELASTIC LIMIT STRESSES OF EL NO.16

-.0273	-.0245	-.0218	-.0025	.0168	.0196	.0223
-.0256	-.0231	-.0205	-.0025	.0155	.0181	.0207
-.0240	-.0216	-.0192	-.0025	.0143	.0167	.0191

ELASTIC LIMIT STRESSES OF EL NO.17

-.0228	-.0205	-.0182	-.0023	.0135	.0158	.0181
-.0206	-.0185	-.0165	-.0023	.0118	.0139	.0159
-.0184	-.0166	-.0148	-.0023	.0101	.0119	.0137

ELASTIC LIMIT STRESSES OF EL NO.18

-.0167	-.0151	-.0135	-.0022	.0092	.0108	.0124
-.0140	-.0127	-.0114	-.0022	.0071	.0084	.0097
-.0113	-.0103	-.0093	-.0022	.0049	.0060	.0070

ELASTIC LIMIT STRESSES OF EL NO.19

-.0093	-.0085	-.0077	-.0019	.0038	.0046	.0055
-.0061	-.0057	-.0052	-.0019	.0013	.0018	.0023
-.0029	-.0028	-.0027	-.0019	-.0012	-.0011	-.0010

ELASTIC LIMIT STRESSES OF EL NO.20

-.0007	-.0008	-.0009	-.0017	-.0025	-.0026	-.0027
.0030	.0024	.0019	-.0017	-.0053	-.0058	-.0063
.0066	.0057	.0048	-.0017	-.0081	-.0091	-.0100

ELASTIC LIMIT STRESSES OF EL NO.21

.0091	.0079	.0068	-.0014	-.0096	-.0108	-.0119

```
.0131     .0115     .0099     -.0014    -.0127    -.0143    -.0159
.0171     .0151     .0130     -.0014    -.0158    -.0179    -.0199

ELASTIC LIMIT STRESSES OF EL NO.22
.0198     .0175     .0152     -.0011    -.0174    -.0197    -.0220
.0241     .0213     .0185     -.0011    -.0207    -.0235    -.0263
.0284     .0251     .0219     -.0011    -.0241    -.0274    -.0306

ELASTIC LIMIT STRESSES OF EL NO.23
.0313     .0277     .0242     -.0008    -.0257    -.0293    -.0329
.0358     .0318     .0277     -.0008    -.0293    -.0333    -.0374
.0404     .0358     .0312     -.0008    -.0328    -.0374    -.0419

ELASTIC LIMIT STRESSES OF EL NO.24
.0434     .0385     .0336     -.0004    -.0345    -.0394    -.0443
.0480     .0426     .0372     -.0004    -.0381    -.0435    -.0489
.0527     .0468     .0409     -.0004    -.0418    -.0477    -.0536

**********      ELASTIC LIMIT SOLUTION      **********

SCALING FACTOR    =      .0064


ELASTIC LIMIT LOADS

NODE        FX          FY          MX


NODAL DISPLACEMENTS

NODE          U           V          RX

    1     .00000E+00    -.24336E+01     .00000E+00
    2     .19090E-02    -.24071E+01     .40353E-03
    3     .17223E-01    -.23307E+01     .78164E-03
    4     .57209E-01    -.22129E+01     .11105E-02
    5     .12918E+00    -.20666E+01     .13695E-02
    6     .23522E+00    -.19072E+01     .15422E-02
    7     .37176E+00    -.17506E+01     .16177E-02
    8     .52983E+00    -.16108E+01     .15912E-02
    9     .69627E+00    -.14983E+01     .14640E-02
   10     .85538E+00    -.14184E+01     .12437E-02
   11     .99109E+00    -.13708E+01     .94318E-03
   12     .10891E+01    -.13497E+01     .58005E-03
   13     .11386E+01    -.13447E+01     .17520E-03
   14     .11340E+01    -.13427E+01    -.24856E-03
   15     .10753E+01    -.13293E+01    -.66781E-03
   16     .96853E+00    -.12913E+01    -.10592E-02
   17     .82440E+00    -.12184E+01    -.13998E-02
   18     .65768E+00    -.11051E+01    -.16676E-02
   19     .48518E+00    -.95200E+00    -.18419E-02
   20     .32374E+00    -.76599E+00    -.19035E-02
   21     .18798E+00    -.56082E+00    -.18351E-02
   22     .88074E-01    -.35616E+00    -.16217E-02
   23     .27796E-01    -.17633E+00    -.12508E-02
   24     .28816E-02    -.48452E-01    -.71259E-03
   25     .00000E+00     .00000E+00     .00000E+00
REQUIRED DYNAMIC STORAGE          =      1927
N O N L I N E A R   A N A L Y S I S
```

NEWTON RAPHSON METHOD

LOAD INCREMENT NO. 1 INCR= 1.000

AFTER 2 ITERATIONS, ERROR = .00184

AFTER 3 ITERATIONS, ERROR = .00004

SOLUTION FOR LOAD INCREMENT 1 AFTER 3ITERATIONS TOLERENCE .37362E

CURRENT LOAD FACTOR = 2.00000 X INITIAL YIELD

NODAL DISPLACEMENTS

NODE	U	V	R
1	.00000E+00	-.49015E+01	.00000E+00
2	.38206E-02	-.48484E+01	.81053E-03
3	.34488E-01	-.46949E+01	.15702E-02
4	.11460E+00	-.44581E+01	.22315E-02
5	.25887E+00	-.41638E+01	.27527E-02
6	.47159E+00	-.38431E+01	.31009E-02
7	.74569E+00	-.35277E+01	.32541E-02
8	.10633E+01	-.32460E+01	.32021E-02
9	.13979E+01	-.30190E+01	.29473E-02
10	.17181E+01	-.28577E+01	.25046E-02
11	.19913E+01	-.27615E+01	.18999E-02
12	.21886E+01	-.27188E+01	.11685E-02
13	.22884E+01	-.27089E+01	.35270E-03
14	.22790E+01	-.27048E+01	-.50138E-03
15	.21608E+01	-.26777E+01	-.13463E-02
16	.19456E+01	-.26009E+01	-.21347E-02
17	.16553E+01	-.24537E+01	-.28204E-02
18	.13198E+01	-.22251E+01	-.33589E-02
19	.97298E+00	-.19161E+01	-.37084E-02
20	.64872E+00	-.15410E+01	-.38306E-02
21	.37635E+00	-.11277E+01	-.36911E-02
22	.17617E+00	-.71584E+00	-.32603E-02
23	.55536E-01	-.35425E+00	-.25134E-02
24	.57416E-02	-.97296E-01	-.14311E-02
25	.00000E+00	.00000E+00	.00000E+00

LOAD INCREMENT NO. 2 INCR= 1.000

AFTER 2 ITERATIONS, ERROR = .00048

SOLUTION FOR LOAD INCREMENT 2 AFTER 2ITERATIONS TOLERENCE .48420E

CURRENT LOAD FACTOR = 3.00000 X INITIAL YIELD

NODAL DISPLACEMENTS

NODE	U	V	R
1	.00000E+00	-.73759E+01	.00000E+00

2	.57111E-02	-.72961E+01	.12169E-02
3	.51570E-01	-.70656E+01	.23577E-02
4	.17141E+00	-.67099E+01	.33507E-02
5	.38730E+00	-.62677E+01	.41335E-02
6	.70581E+00	-.57854E+01	.46569E-02
7	.11164E+01	-.53109E+01	.48873E-02
8	.15925E+01	-.48868E+01	.48096E-02
9	.20945E+01	-.45448E+01	.44271E-02
10	.25750E+01	-.43016E+01	.37622E-02
11	.29852E+01	-.41565E+01	.28536E-02
12	.32815E+01	-.40921E+01	.17546E-02
13	.34312E+01	-.40771E+01	.52852E-03
14	.34169E+01	-.40710E+01	-.75511E-03
15	.32391E+01	-.40301E+01	-.20249E-02
16	.29155E+01	-.39142E+01	-.32097E-02
17	.24795E+01	-.36922E+01	-.42398E-02
18	.19759E+01	-.33475E+01	-.50485E-02
19	.14557E+01	-.28818E+01	-.55730E-02
20	.96989E+00	-.23171E+01	-.57558E-02
21	.56222E+00	-.16951E+01	-.55454E-02
22	.26294E+00	-.10756E+01	-.48974E-02
23	.82802E-01	-.53211E+00	-.37749E-02
24	.85385E-02	-.14611E+00	-.21492E-02
25	.00000E+00	.00000E+00	.00000E+00

LOAD INCREMENT NO. 3 INCR= 1.000

AFTER 2 ITERATIONS, ERROR = .00051

SOLUTION FOR LOAD INCREMENT 3 AFTER 2ITERATIONS TOLERENCE .50681E

CURRENT LOAD FACTOR = 4.00000 X INITIAL YIELD

NODAL DISPLACEMENTS

NODE	U	V	R
1	.00000E+00	-.98780E+01	.00000E+00
2	.76012E-02	-.97714E+01	.16259E-02
3	.68656E-01	-.94634E+01	.31503E-02
4	.22825E+00	-.89879E+01	.44776E-02
5	.51591E+00	-.83965E+01	.55246E-02
6	.94055E+00	-.77511E+01	.62252E-02
7	.14883E+01	-.71157E+01	.65345E-02
8	.21239E+01	-.65474E+01	.64317E-02
9	.27944E+01	-.60888E+01	.59213E-02
10	.34366E+01	-.57625E+01	.50325E-02
11	.39851E+01	-.55677E+01	.38173E-02
12	.43813E+01	-.54812E+01	.23467E-02
13	.45814E+01	-.54610E+01	.70582E-03
14	.45622E+01	-.54528E+01	-.10123E-02
15	.43240E+01	-.53980E+01	-.27118E-02
16	.38909E+01	-.52424E+01	-.42972E-02
17	.33076E+01	-.49443E+01	-.56751E-02
18	.26344E+01	-.44818E+01	-.67560E-02
19	.19396E+01	-.38573E+01	-.74562E-02
20	.12914E+01	-.31003E+01	-.76988E-02
21	.74798E+00	-.22672E+01	-.74155E-02
22	.34951E+00	-.14381E+01	-.65472E-02
23	.10995E+00	-.71118E+00	-.50453E-02
24	.11313E-01	-.19522E+00	-.28717E-02
25	.00000E+00	.00000E+00	.00000E+00

LOAD INCREMENT NO. 4 INCR= 1.000

AFTER 2 ITERATIONS, ERROR = .00054

SOLUTION FOR LOAD INCREMENT 4 AFTER 2ITERATIONS TOLERENCE .53885E

CURRENT LOAD FACTOR = 5.00000 X INITIAL YIELD

NODAL DISPLACEMENTS

NODE	U	V	R
1	.00000E+00	-.12402E+02	.00000E+00
2	.94869E-02	-.12268E+02	.20367E-02
3	.85710E-01	-.11882E+02	.39464E-02
4	.28502E+00	-.11287E+02	.56098E-02
5	.64442E+00	-.10545E+02	.69226E-02
6	.11752E+01	-.97354E+01	.78019E-02
7	.18604E+01	-.89378E+01	.81911E-02
8	.26559E+01	-.82239E+01	.80637E-02
9	.34957E+01	-.76475E+01	.74250E-02
10	.43004E+01	-.72371E+01	.63114E-02
11	.49880E+01	-.69919E+01	.47877E-02
12	.54849E+01	-.68830E+01	.29429E-02
13	.57357E+01	-.68576E+01	.88396E-03
14	.57114E+01	-.68474E+01	-.12721E-02
15	.54123E+01	-.67784E+01	-.34047E-02
16	.48688E+01	-.65825E+01	-.53937E-02
17	.41372E+01	-.62074E+01	-.71217E-02
18	.32935E+01	-.56256E+01	-.84764E-02
19	.24235E+01	-.48404E+01	-.93527E-02
20	.16124E+01	-.38893E+01	-.96548E-02
21	.93320E+00	-.28433E+01	-.92972E-02
22	.43569E+00	-.18029E+01	-.82066E-02
23	.13692E+00	-.89137E+00	-.63226E-02
24	.14031E-01	-.24467E+00	-.35984E-02
25	.00000E+00	.00000E+00	.00000E+00

***** ELEMENT NO. 24 *****

POINT	X-CRD	Y-CRD	STRESS	STRAIN
1	.1127	-.5000	.21971E+00	.10985E-02
2	.1127	-.3333	.19509E+00	.97544E-03
3	.1127	-.1667	.17047E+00	.85233E-03
4	.1127	.0000	-.16333E-02	-.81664E-05
5	.1127	.1667	-.17373E+00	-.86867E-03
6	.1127	.3333	-.19835E+00	-.99177E-03
7	.1127	.5000	-.22298E+00	-.11149E-02
8	.5000	-.5000	.24244E+00	.12122E-02
9	.5000	-.3333	.21520E+00	.10760E-02
10	.5000	-.1667	.18797E+00	.93985E-03
11	.5000	.0000	-.23982E-02	-.11991E-04
12	.5000	.1667	-.19277E+00	-.96383E-03
13	.5000	.3333	-.22000E+00	-.11000E-02
14	.5000	.5000	-.24724E+00	-.12362E-02
15	.8873	-.5000	.26555E+00	.13277E-02
16	.8873	-.3333	.23570E+00	.11785E-02
17	.8873	-.1667	.20585E+00	.10293E-02
18	.8873	.0000	-.27843E-02	-.13921E-04
19	.8873	.1667	-.21142E+00	-.10571E-02
20	.8873	.3333	-.24127E+00	-.12063E-02

```
   21   .8873    .5000 -.26801E+00       -.13556E-02

LOAD INCREMENT NO.  5  INCR= 1.000

AFTER     2 ITERATIONS, ERROR =      .02342

AFTER     3 ITERATIONS, ERROR =      .01449

AFTER     4 ITERATIONS, ERROR =      .00004

SOLUTION FOR LOAD INCREMENT  5 AFTER  4ITERATIONS      TOLERENCE      .36911E


CURRENT LOAD FACTOR =       6.00000 X  INITIAL YIELD

NODAL DISPLACEMENTS

NODE         U               V               R

   1      .00000E+00     -.15455E+02      .00000E+00
   2      .11595E-01     -.15292E+02      .24841E-02
   3      .10431E+00     -.14821E+02      .48147E-02
   4      .34680E+00     -.14094E+02      .68477E-02
   5      .78441E+00     -.13187E+02      .84563E-02
   6      .14315E+01     -.12197E+02      .95394E-02
   7      .22681E+01     -.11219E+02      .10028E-01
   8      .32411E+01     -.10343E+02      .98875E-02
   9      .42706E+01     -.96339E+01      .91236E-02
  10      .52600E+01     -.91274E+01      .77784E-02
  11      .61089E+01     -.88237E+01      .59293E-02
  12      .67266E+01     -.86880E+01      .36833E-02
  13      .70448E+01     -.86563E+01      .11692E-02
  14      .70263E+01     -.86446E+01     -.14713E-02
  15      .66707E+01     -.85624E+01     -.40918E-02
  16      .60138E+01     -.83249E+01     -.65465E-02
  17      .51237E+01     -.78670E+01     -.86929E-02
  18      .40925E+01     -.71533E+01     -.10395E-01
  19      .30250E+01     -.61858E+01     -.11525E-01
  20      .20254E+01     -.50082E+01     -.11967E-01
  21      .11834E+01     -.37047E+01     -.11618E-01
  22      .56104E+00     -.23956E+01     -.10391E-01
  23      .18107E+00     -.12285E+01     -.82111E-02
  24      .18628E-01     -.36681E+00     -.50239E-02
  25      .00000E+00      .00000E+00      .00000E+00
***** ELEMENT NO.    24  *****

POINT      X-CRD  Y-CRD     STRESS        STRAIN

    1     .1127  -.5000   .24310E+00       .12155E-02
    2     .1127  -.3333   .21548E+00       .10774E-02
    3     .1127  -.1667   .18785E+00       .93925E-03
    4     .1127    .0000 -.52535E-02      -.26268E-04
    5     .1127    .1667 -.19836E+00      -.99179E-03
    6     .1127    .3333 -.22598E+00      -.11299E-02
    7     .1127    .5000 -.25361E+00      -.12680E-02
    8     .5000  -.5000   .26827E+00       .16759E-02
    9     .5000  -.3333   .26812E+00       .14858E-02
   10     .5000  -.1667   .25913E+00       .12957E-02
   11     .5000    .0000 -.66452E-02      -.33226E-04
   12     .5000    .1667 -.26802E+00      -.13621E-02
   13     .5000    .3333 -.26817E+00      -.15522E-02
   14     .5000    .5000 -.26833E+00      -.17424E-02
   15     .8873  -.5000   .26865E+00       .21388E-02
```

16	.8873	-.3333	.26845E+00	.18967E-02
17	.8873	-.1667	.26826E+00	.16546E-02
18	.8873	.0000	-.75381E-02	-.37691E-04
19	.8873	.1667	-.26832E+00	-.17300E-02
20	.8873	.3333	-.26852E+00	-.19721E-02
21	.8873	.5000	-.26871E+00	-.22142E-02

LOAD INCREMENT NO. 6 INCR= .600

AFTER 2 ITERATIONS, ERROR = .04760

AFTER 3 ITERATIONS, ERROR = .00052

SOLUTION FOR LOAD INCREMENT 6 AFTER 3ITERATIONS TOLERENCE .51685E

CURRENT LOAD FACTOR = 6.60000 X INITIAL YIELD

NODAL DISPLACEMENTS

NODE	U	V	R
1	.00000E+00	-.19194E+02	.00000E+00
2	.13693E-01	-.19005E+02	.28794E-02
3	.12118E+00	-.18459E+02	.55854E-02
4	.40216E+00	-.17615E+02	.79543E-02
5	.90995E+00	-.16561E+02	.98423E-02
6	.16627E+01	-.15405E+02	.11133E-01
7	.26392E+01	-.14261E+02	.11746E-01
8	.37801E+01	-.13231E+02	.11640E-01
9	.49949E+01	-.12392E+02	.10815E-01
10	.61725E+01	-.11787E+02	.93154E-02
11	.71965E+01	-.11420E+02	.72236E-02
12	.79600E+01	-.11253E+02	.46557E-02
13	.83802E+01	-.11213E+02	.17528E-02
14	.84097E+01	-.11203E+02	-.13287E-02
15	.80423E+01	-.11118E+02	-.44267E-02
16	.73138E+01	-.10854E+02	-.73785E-02
17	.62983E+01	-.10330E+02	-.10025E-01
18	.50988E+01	-.94974E+01	-.12212E-01
19	.38349E+01	-.83477E+01	-.13796E-01
20	.26286E+01	-.69200E+01	-.14646E-01
21	.15879E+01	-.52996E+01	-.14645E-01
22	.79231E+00	-.36135E+01	-.13692E-01
23	.27932E+00	-.20216E+01	-.11701E-01
24	.34729E-01	-.70332E+00	-.86088E-02
25	.00000E+00	.00000E+00	.00000E+00

***** ELEMENT NO. 24 *****

POINT	X-CRD	Y-CRD	STRESS	STRAIN
1	.1127	-.5000	.23773E+00	.11887E-02
2	.1127	-.3333	.21050E+00	.10525E-02
3	.1127	-.1667	.18327E+00	.91635E-03
4	.1127	.0000	-.70813E-02	-.35406E-04
5	.1127	.1667	-.19743E+00	-.98716E-03
6	.1127	.3333	-.22466E+00	-.11233E-02
7	.1127	.5000	-.25190E+00	-.12595E-02
8	.5000	-.5000	.26925E+00	.28745E-02
9	.5000	-.3333	.26899E+00	.25487E-02
10	.5000	-.1667	.26872E+00	.22229E-02
11	.5000	.0000	-.10847E-01	-.54234E-04
12	.5000	.1667	-.26881E+00	-.23314E-02

13	.5000	.3333	-.26907E+00	-.26572E-02
14	.5000	.5000	-.26934E+00	-.29829E-02
15	.8873	-.5000	.27063E+00	.45599E-02
16	.8873	-.3333	.27021E+00	.40445E-02
17	.8873	-.1667	.26979E+00	.35291E-02
18	.8873	.0000	-.14685E-01	-.73426E-04
19	.8873	.1667	-.26990E+00	-.36760E-02
20	.8873	.3333	-.27033E+00	-.41914E-02
21	.8873	.5000	-.27075E+00	-.47068E-02

LOAD INCREMENT NO. 7 INCR= .200

AFTER 2 ITERATIONS, ERROR = .00083

SOLUTION FOR LOAD INCREMENT 7 AFTER 2ITERATIONS TOLERENCE .83340E

CURRENT LOAD FACTOR = 6.80000 X INITIAL YIELD

NODAL DISPLACEMENTS

NODE	U	V	R
1	.00000E+00	-.20453E+02	.00000E+00
2	.14392E-01	-.20256E+02	.30115E-02
3	.12679E+00	-.19685E+02	.58428E-02
4	.42058E+00	-.18801E+02	.83239E-02
5	.95174E+00	-.17697E+02	.10305E-01
6	.17396E+01	-.16487E+02	.11666E-01
7	.27627E+01	-.15287E+02	.12320E-01
8	.39597E+01	-.14205E+02	.12225E-01
9	.52362E+01	-.13322E+02	.11380E-01
10	.64767E+01	-.12685E+02	.98291E-02
11	.75592E+01	-.12297E+02	.76565E-02
12	.83714E+01	-.12119E+02	.49812E-02
13	.88258E+01	-.12076E+02	.19485E-02
14	.88714E+01	-.12067E+02	-.12805E-02
15	.85001E+01	-.11980E+02	-.45384E-02
16	.77478E+01	-.11707E+02	-.76568E-02
17	.66903E+01	-.11162E+02	-.10471E-01
18	.54344E+01	-.10289E+02	-.12821E-01
19	.41048E+01	-.90780E+01	-.14559E-01
20	.28293E+01	-.75660E+01	-.15548E-01
21	.17222E+01	-.58386E+01	-.15664E-01
22	.86874E+00	-.40253E+01	-.14804E-01
23	.31152E+00	-.22898E+01	-.12880E-01
24	.39907E-01	-.81712E+00	-.98212E-02
25	.00000E+00	.00000E+00	.00000E+00

***** ELEMENT NO. 24 *****

POINT	X-CRD	Y-CRD	STRESS	STRAIN
1	.1127	-.5000	.23637E+00	.11818E-02
2	.1127	-.3333	.20927E+00	.10463E-02
3	.1127	-.1667	.18217E+00	.91083E-03
4	.1127	.0000	-.72771E-02	-.36385E-04
5	.1127	.1667	-.19672E+00	-.98360E-03
6	.1127	.3333	-.22382E+00	-.11191E-02
7	.1127	.5000	-.25092E+00	-.12546E-02
8	.5000	-.5000	.26958E+00	.32812E-02
9	.5000	-.3333	.26928E+00	.29095E-02
10	.5000	-.1667	.26898E+00	.25378E-02
11	.5000	.0000	-.12002E-01	-.60009E-04

12	.5000	.1667	-.26907E+00	-.26579E-02
13	.5000	.3333	-.26938E+00	-.30295E-02
14	.5000	.5000	-.26968E+00	-.34012E-02
15	.8873	-.5000	.27129E+00	.53785E-02
16	.8873	-.3333	.27080E+00	.47707E-02
17	.8873	-.1667	.27030E+00	.41629E-02
18	.8873	.0000	-.17113E-01	-.85564E-04
19	.8873	.1667	-.27044E+00	-.43340E-02
20	.8873	.3333	-.27094E+00	-.49418E-02
21	.8873	.5000	-.27143E+00	-.55496E-02

LOAD INCREMENT NO. 8 INCR= .200

AFTER 2 ITERATIONS, ERROR = .00082

SOLUTION FOR LOAD INCREMENT 8 AFTER 2ITERATIONS TOLERENCE .82182E

CURRENT LOAD FACTOR = 7.00000 X INITIAL YIELD

NODAL DISPLACEMENTS

NODE	U	V	R
1	.00000E+00	-.21729E+02	.00000E+00
2	.15098E-01	-.21523E+02	.31448E-02
3	.13245E+00	-.20926E+02	.61026E-02
4	.43914E+00	-.20003E+02	.86972E-02
5	.99385E+00	-.18850E+02	.10773E-01
6	.18173E+01	-.17584E+02	.12204E-01
7	.28874E+01	-.16327E+02	.12900E-01
8	.41409E+01	-.15193E+02	.12817E-01
9	.54799E+01	-.14266E+02	.11952E-01
10	.67840E+01	-.13595E+02	.10349E-01
11	.79257E+01	-.13186E+02	.80949E-02
12	.87873E+01	-.12997E+02	.53108E-02
13	.92763E+01	-.12951E+02	.21464E-02
14	.93382E+01	-.12943E+02	-.12323E-02
15	.89628E+01	-.12855E+02	-.46523E-02
16	.81862E+01	-.12573E+02	-.79398E-02
17	.70861E+01	-.12005E+02	-.10924E-01
18	.57730E+01	-.11092E+02	-.13440E-01
19	.43767E+01	-.98182E+01	-.15333E-01
20	.30312E+01	-.82206E+01	-.16461E-01
21	.18569E+01	-.63847E+01	-.16697E-01
22	.94517E+00	-.44424E+01	-.15932E-01
23	.34349E+00	-.25614E+01	-.14073E-01
24	.44892E-01	-.93233E+00	-.11049E-01
25	.00000E+00	.00000E+00	.00000E+00

***** ELEMENT NO. 24 *****

POINT	X-CRD	Y-CRD	STRESS	STRAIN
1	.1127	-.5000	.23508E+00	.11754E-02
2	.1127	-.3333	.20810E+00	.10405E-02
3	.1127	-.1667	.18113E+00	.90566E-03
4	.1127	.0000	-.74008E-02	-.37004E-04
5	.1127	.1667	-.19593E+00	-.97966E-03
6	.1127	.3333	-.22290E+00	-.11145E-02
7	.1127	.5000	-.24988E+00	-.12494E-02
8	.5000	-.5000	.26992E+00	.36927E-02
9	.5000	-.3333	.26958E+00	.32746E-02
10	.5000	-.1667	.26924E+00	.28565E-02

```
   11    .5000    .0000 -.13203E-01       -.66013E-04
   12    .5000    .1667 -.26934E+00       -.29885E-02
   13    .5000    .3333 -.26969E+00       -.34066E-02
   14    .5000    .5000 -.27003E+00       -.38247E-02
   15    .8873   -.5000  .27197E+00        .62060E-02
   16    .8873   -.3333  .27140E+00        .55047E-02
   17    .8873   -.1667  .27082E+00        .48033E-02
   18    .8873    .0000 -.19790E-01       -.98950E-04
   19    .8873    .1667 -.27099E+00       -.50012E-02
   20    .8873    .3333 -.27156E+00       -.57026E-02
   21    .8873    .5000 -.27213E+00       -.64039E-02

LOAD INCREMENT NO.  9  INCR=  .200

AFTER    2 ITERATIONS, ERROR =      .00086

SOLUTION FOR LOAD INCREMENT  9 AFTER  2ITERATIONS     TOLERENCE     .85850E


CURRENT LOAD FACTOR =      7.20000 X  INITIAL YIELD

NODAL DISPLACEMENTS

NODE        U               V               R

   1     .00000E+00     -.23011E+02      .00000E+00
   2     .15803E-01     -.22796E+02      .32782E-02
   3     .13811E+00     -.22174E+02      .63629E-02
   4     .45770E+00     -.21211E+02      .90710E-02
   5     .10360E+01     -.20008E+02      .11241E-01
   6     .18949E+01     -.18686E+02      .12743E-01
   7     .30121E+01     -.17373E+02      .13482E-01
   8     .43223E+01     -.16186E+02      .13410E-01
   9     .57238E+01     -.15215E+02      .12525E-01
  10     .70916E+01     -.14510E+02      .10871E-01
  11     .82926E+01     -.14079E+02      .85342E-02
  12     .92036E+01     -.13880E+02      .56410E-02
  13     .97273E+01     -.13831E+02      .23444E-02
  14     .98054E+01     -.13824E+02     -.11844E-02
  15     .94259E+01     -.13734E+02     -.47673E-02
  16     .86248E+01     -.13443E+02     -.82246E-02
  17     .74819E+01     -.12853E+02     -.11379E-01
  18     .61113E+01     -.11898E+02     -.14061E-01
  19     .46482E+01     -.10562E+02     -.16110E-01
  20     .32325E+01     -.88784E+01     -.17379E-01
  21     .19910E+01     -.69334E+01     -.17734E-01
  22     .10209E+01     -.48614E+01     -.17064E-01
  23     .37495E+00     -.28341E+01     -.15271E-01
  24     .49630E-01     -.10480E+01     -.12281E-01
  25     .00000E+00      .00000E+00      .00000E+00
***** ELEMENT NO.    24  *****

POINT     X-CRD  Y-CRD    STRESS       STRAIN

    1    .1127  -.5000  .23384E+00        .11692E-02
    2    .1127  -.3333  .20700E+00        .10350E-02
    3    .1127  -.1667  .18016E+00        .90079E-03
    4    .1127    .0000 -.74636E-02       -.37318E-04
    5    .1127    .1667 -.19509E+00       -.97543E-03
    6    .1127    .3333 -.22193E+00       -.11096E-02
    7    .1127    .5000 -.24877E+00       -.12438E-02
    8    .5000  -.5000  .27026E+00        .41056E-02
    9    .5000  -.3333  .26988E+00        .36409E-02
```

10	.5000	-.1667	.26950E+00	.31761E-02
11	.5000	.0000	-.14454E-01	-.72270E-04
12	.5000	.1667	-.26962E+00	-.33207E-02
13	.5000	.3333	-.26999E+00	-.37854E-02
14	.5000	.5000	-.27037E+00	-.42502E-02
15	.8873	-.5000	.27264E+00	.70357E-02
16	.8873	-.3333	.27200E+00	.62404E-02
17	.8873	-.1667	.27135E+00	.54452E-02
18	.8873	.0000	-.22713E-01	-.11357E-03
19	.8873	.1667	-.27153E+00	-.56723E-02
20	.8873	.3333	-.27218E+00	-.64676E-02
21	.8873	.5000	-.27283E+00	-.72628E-02

LOAD INCREMENT NO. 10 INCR= .200

AFTER 2 ITERATIONS, ERROR = .00201

AFTER 3 ITERATIONS, ERROR = .00051

SOLUTION FOR LOAD INCREMENT 10 AFTER 3ITERATIONS TOLERENCE .53808E

CURRENT LOAD FACTOR = 7.40000 X INITIAL YIELD

NODAL DISPLACEMENTS

NODE	U	V	R
1	.00000E+00	-.24338E+02	.00000E+00
2	.16525E-01	-.24114E+02	.34150E-02
3	.14389E+00	-.23466E+02	.66296E-02
4	.47669E+00	-.22463E+02	.94546E-02
5	.10791E+01	-.21208E+02	.11722E-01
6	.19744E+01	-.19829E+02	.13297E-01
7	.31401E+01	-.18457E+02	.14081E-01
8	.45086E+01	-.17216E+02	.14023E-01
9	.59748E+01	-.16199E+02	.13119E-01
10	.74086E+01	-.15460E+02	.11412E-01
11	.86714E+01	-.15006E+02	.89926E-02
12	.96341E+01	-.14795E+02	.59881E-02
13	.10194E+02	-.14744E+02	.25564E-02
14	.10290E+02	-.14737E+02	-.11311E-02
15	.99063E+01	-.14646E+02	-.48925E-02
16	.90790E+01	-.14345E+02	-.85268E-02
17	.78909E+01	-.13731E+02	-.11857E-01
18	.64602E+01	-.12733E+02	-.14710E-01
19	.49276E+01	-.11332E+02	-.16918E-01
20	.34392E+01	-.95586E+01	-.18330E-01
21	.21282E+01	-.75005E+01	-.18808E-01
22	.10982E+01	-.52941E+01	-.18234E-01
23	.40678E+00	-.31158E+01	-.16508E-01
24	.54264E-01	-.11674E+01	-.13552E-01
25	.00000E+00	.00000E+00	.00000E+00

***** ELEMENT NO. 13 *****

POINT	X-CRD	Y-CRD	STRESS	STRAIN
1	.1127	-.5000	-.26579E+00	-.13289E-02
2	.1127	-.3333	-.23839E+00	-.11919E-02
3	.1127	-.1667	-.21099E+00	-.10549E-02
4	.1127	.0000	-.19462E-01	-.97311E-04
5	.1127	.1667	.17206E+00	.86031E-03
6	.1127	.3333	.19946E+00	.99731E-03

7	.1127	.5000	.22686E+00	.11343E-02
8	.5000	-.5000	-.26801E+00	-.13539E-02
9	.5000	-.3333	-.24288E+00	-.12144E-02
10	.5000	-.1667	-.21497E+00	-.10749E-02
11	.5000	.0000	-.19893E-01	-.99467E-04
12	.5000	.1667	.17518E+00	.87592E-03
13	.5000	.3333	.20309E+00	.10155E-02
14	.5000	.5000	.23100E+00	.11550E-02
15	.8873	-.5000	-.26803E+00	-.13768E-02
16	.8873	-.3333	-.24694E+00	-.12347E-02
17	.8873	-.1667	-.21852E+00	-.10926E-02
18	.8873	.0000	-.19891E-01	-.99457E-04
19	.8873	.1667	.17874E+00	.89369E-03
20	.8873	.3333	.20716E+00	.10358E-02
21	.8873	.5000	.23557E+00	.11779E-02

***** ELEMENT NO. 14 *****

POINT	X-CRD	Y-CRD	STRESS	STRAIN
1	.1127	-.5000	-.26804E+00	-.13891E-02
2	.1127	-.3333	-.24926E+00	-.12463E-02
3	.1127	-.1667	-.22070E+00	-.11035E-02
4	.1127	.0000	-.21048E-01	-.10524E-03
5	.1127	.1667	.17860E+00	.89301E-03
6	.1127	.3333	.20717E+00	.10358E-02
7	.1127	.5000	.23573E+00	.11786E-02
8	.5000	-.5000	-.26803E+00	-.13813E-02
9	.5000	-.3333	-.24779E+00	-.12389E-02
10	.5000	-.1667	-.21932E+00	-.10966E-02
11	.5000	.0000	-.20327E-01	-.10164E-03
12	.5000	.1667	.17866E+00	.89332E-03
13	.5000	.3333	.20713E+00	.10357E-02
14	.5000	.5000	.23560E+00	.11780E-02
15	.8873	-.5000	-.26803E+00	-.13712E-02
16	.8873	-.3333	-.24586E+00	-.12293E-02
17	.8873	-.1667	-.21749E+00	-.10874E-02
18	.8873	.0000	-.19156E-01	-.95779E-04
19	.8873	.1667	.17918E+00	.89588E-03
20	.8873	.3333	.20755E+00	.10378E-02
21	.8873	.5000	.23593E+00	.11796E-02

***** ELEMENT NO. 15 *****

POINT	X-CRD	Y-CRD	STRESS	STRAIN
1	.1127	-.5000	-.26803E+00	-.13735E-02
2	.1127	-.3333	-.24654E+00	-.12327E-02
3	.1127	-.1667	-.21838E+00	-.10919E-02
4	.1127	.0000	-.21549E-01	-.10774E-03
5	.1127	.1667	.17528E+00	.87642E-03
6	.1127	.3333	.20344E+00	.10172E-02
7	.1127	.5000	.23160E+00	.11580E-02
8	.5000	-.5000	-.26698E+00	-.13349E-02
9	.5000	-.3333	-.23948E+00	-.11974E-02
10	.5000	-.1667	-.21197E+00	-.10599E-02
11	.5000	.0000	-.19707E-01	-.98534E-04
12	.5000	.1667	.17256E+00	.86279E-03
13	.5000	.3333	.20006E+00	.10003E-02
14	.5000	.5000	.22757E+00	.11378E-02
15	.8873	-.5000	-.25889E+00	-.12944E-02
16	.8873	-.3333	-.23204E+00	-.11602E-02
17	.8873	-.1667	-.20519E+00	-.10259E-02
18	.8873	.0000	-.17490E-01	-.87448E-04
19	.8873	.1667	.17021E+00	.85103E-03
20	.8873	.3333	.19706E+00	.98529E-03
21	.8873	.5000	.22391E+00	.11196E-02

***** ELEMENT NO. 24 *****

POINT	X-CRD	Y-CRD	STRESS	STRAIN
1	.1127	-.5000	.23271E+00	.11636E-02
2	.1127	-.3333	.20600E+00	.10300E-02
3	.1127	-.1667	.17929E+00	.89645E-03
4	.1127	.0000	-.74249E-02	-.37124E-04
5	.1127	.1667	-.19414E+00	-.97070E-03
6	.1127	.3333	-.22085E+00	-.11043E-02
7	.1127	.5000	-.24756E+00	-.12378E-02
8	.5000	-.5000	.27060E+00	.45317E-02
9	.5000	-.3333	.27018E+00	.40189E-02
10	.5000	-.1667	.26977E+00	.35060E-02
11	.5000	.0000	-.15753E-01	-.78764E-04
12	.5000	.1667	-.26989E+00	-.36636E-02
13	.5000	.3333	-.27031E+00	-.41764E-02
14	.5000	.5000	-.27073E+00	-.46893E-02
15	.8873	-.5000	.27334E+00	.78906E-02
16	.8873	-.3333	.27261E+00	.69985E-02
17	.8873	-.1667	.27189E+00	.61063E-02
18	.8873	.0000	-.25934E-01	-.12967E-03
19	.8873	.1667	-.27210E+00	-.63657E-02
20	.8873	.3333	-.27283E+00	-.72578E-02
21	.8873	.5000	-.27355E+00	-.81500E-02

LOAD INCREMENT NO. 11 INCR= .200

AFTER 2 ITERATIONS, ERROR = .00200

AFTER 3 ITERATIONS, ERROR = .00060

SOLUTION FOR LOAD INCREMENT 11 AFTER 3ITERATIONS TOLERENCE .60016E

CURRENT LOAD FACTOR = 7.60000 X INITIAL YIELD

NODAL DISPLACEMENTS

NODE	U	V	R
1	.00000E+00	-.25670E+02	.00000E+00
2	.17243E-01	-.25437E+02	.35515E-02
3	.14965E+00	-.24763E+02	.68958E-02
4	.49560E+00	-.23719E+02	.98373E-02
5	.11220E+01	-.22413E+02	.12203E-01
6	.20537E+01	-.20976E+02	.13850E-01
7	.32676E+01	-.19547E+02	.14680E-01
8	.46944E+01	-.18251E+02	.14636E-01
9	.62252E+01	-.17188E+02	.13713E-01
10	.77252E+01	-.16414E+02	.11956E-01
11	.90501E+01	-.15937E+02	.94558E-02
12	.10065E+02	-.15715E+02	.63428E-02
13	.10664E+02	-.15660E+02	.27770E-02
14	.10778E+02	-.15654E+02	-.10778E-02
15	.10389E+02	-.15561E+02	-.50222E-02
16	.95343E+01	-.15250E+02	-.88424E-02
17	.82996E+01	-.14610E+02	-.12346E-01
18	.68080E+01	-.13569E+02	-.15366E-01
19	.52055E+01	-.12102E+02	-.17731E-01
20	.36441E+01	-.10239E+02	-.19283E-01
21	.22639E+01	-.80672E+01	-.19882E-01
22	.11742E+01	-.57264E+01	-.19402E-01
23	.43783E+00	-.33969E+01	-.17743E-01

24	.58585E-01	-.12866E+01	-.14822E-01
25	.00000E+00	.00000E+00	.00000E+00

***** ELEMENT NO. 12 *****

POINT	X-CRD	Y-CRD	STRESS	STRAIN
1	.1127	-.5000	-.25097E+00	-.12548E-02
2	.1127	-.3333	-.22507E+00	-.11253E-02
3	.1127	-.1667	-.19917E+00	-.99587E-03
4	.1127	.0000	-.18170E-01	-.90849E-04
5	.1127	.1667	.16284E+00	.81418E-03
6	.1127	.3333	.18873E+00	.94365E-03
7	.1127	.5000	.21463E+00	.10731E-02
8	.5000	-.5000	-.26230E+00	-.13115E-02
9	.5000	-.3333	-.23532E+00	-.11766E-02
10	.5000	-.1667	-.20833E+00	-.10417E-02
11	.5000	.0000	-.19691E-01	-.98453E-04
12	.5000	.1667	.16895E+00	.84474E-03
13	.5000	.3333	.19594E+00	.97968E-03
14	.5000	.5000	.22292E+00	.11146E-02
15	.8873	-.5000	-.26802E+00	-.13665E-02
16	.8873	-.3333	-.24521E+00	-.12261E-02
17	.8873	-.1667	-.21713E+00	-.10857E-02
18	.8873	.0000	-.20858E-01	-.10429E-03
19	.8873	.1667	.17542E+00	.87708E-03
20	.8873	.3333	.20350E+00	.10175E-02
21	.8873	.5000	.23158E+00	.11579E-02

***** ELEMENT NO. 13 *****

POINT	X-CRD	Y-CRD	STRESS	STRAIN
1	.1127	-.5000	-.26804E+00	-.13890E-02
2	.1127	-.3333	-.24920E+00	-.12460E-02
3	.1127	-.1667	-.22059E+00	-.11030E-02
4	.1127	.0000	-.20669E-01	-.10335E-03
5	.1127	.1667	.17926E+00	.89628E-03
6	.1127	.3333	.20786E+00	.10393E-02
7	.1127	.5000	.23646E+00	.11823E-02
8	.5000	-.5000	-.26806E+00	-.14173E-02
9	.5000	-.3333	-.25428E+00	-.12714E-02
10	.5000	-.1667	-.22510E+00	-.11255E-02
11	.5000	.0000	-.21171E-01	-.10586E-03
12	.5000	.1667	.18276E+00	.91380E-03
13	.5000	.3333	.21194E+00	.10597E-02
14	.5000	.5000	.24111E+00	.12056E-02
15	.8873	-.5000	-.26808E+00	-.14432E-02
16	.8873	-.3333	-.25889E+00	-.12944E-02
17	.8873	-.1667	-.22914E+00	-.11457E-02
18	.8873	.0000	-.21203E-01	-.10601E-03
19	.8873	.1667	.18674E+00	.93368E-03
20	.8873	.3333	.21648E+00	.10824E-02
21	.8873	.5000	.24623E+00	.12312E-02

***** ELEMENT NO. 14 *****

POINT	X-CRD	Y-CRD	STRESS	STRAIN
1	.1127	-.5000	-.26810E+00	-.14571E-02
2	.1127	-.3333	-.26151E+00	-.13076E-02
3	.1127	-.1667	-.23160E+00	-.11580E-02
4	.1127	.0000	-.22495E-01	-.11248E-03
5	.1127	.1667	.18661E+00	.93303E-03
6	.1127	.3333	.21652E+00	.10826E-02
7	.1127	.5000	.24644E+00	.12322E-02
8	.5000	-.5000	-.26809E+00	-.14506E-02
9	.5000	-.3333	-.26026E+00	-.13013E-02
10	.5000	-.1667	-.23041E+00	-.11520E-02

11	.5000	.0000	-.21742E-01	-.10871E-03
12	.5000	.1667	.18692E+00	.93462E-03
13	.5000	.3333	.21678E+00	.10839E-02
14	.5000	.5000	.24663E+00	.12332E-02
15	.8873	-.5000	-.26808E+00	-.14415E-02
16	.8873	-.3333	-.25852E+00	-.12926E-02
17	.8873	-.1667	-.22873E+00	-.11436E-02
18	.8873	.0000	-.20494E-01	-.10247E-03
19	.8873	.1667	.18774E+00	.93869E-03
20	.8873	.3333	.21753E+00	.10876E-02
21	.8873	.5000	.24732E+00	.12366E-02

***** ELEMENT NO. 15 *****

POINT	X-CRD	Y-CRD	STRESS	STRAIN
1	.1127	-.5000	-.26809E+00	-.14456E-02
2	.1127	-.3333	-.25952E+00	-.12976E-02
3	.1127	-.1667	-.22991E+00	-.11495E-02
4	.1127	.0000	-.22945E-01	-.11473E-03
5	.1127	.1667	.18402E+00	.92008E-03
6	.1127	.3333	.21363E+00	.10681E-02
7	.1127	.5000	.24323E+00	.12162E-02
8	.5000	-.5000	-.26805E+00	-.14044E-02
9	.5000	-.3333	-.25197E+00	-.12598E-02
10	.5000	-.1667	-.22306E+00	-.11153E-02
11	.5000	.0000	-.20956E-01	-.10478E-03
12	.5000	.1667	.18114E+00	.90572E-03
13	.5000	.3333	.21006E+00	.10503E-02
14	.5000	.5000	.23897E+00	.11949E-02
15	.8873	-.5000	-.26802E+00	-.13611E-02
16	.8873	-.3333	-.24401E+00	-.12201E-02
17	.8873	-.1667	-.21579E+00	-.10790E-02
18	.8873	.0000	-.18555E-01	-.92773E-04
19	.8873	.1667	.17868E+00	.89342E-03
20	.8873	.3333	.20690E+00	.10345E-02
21	.8873	.5000	.23512E+00	.11756E-02

***** ELEMENT NO. 16 *****

POINT	X-CRD	Y-CRD	STRESS	STRAIN
1	.1127	-.5000	-.26801E+00	-.13574E-02
2	.1127	-.3333	-.24379E+00	-.12190E-02
3	.1127	-.1667	-.21610E+00	-.10805E-02
4	.1127	.0000	-.22574E-01	-.11287E-03
5	.1127	.1667	.17096E+00	.85478E-03
6	.1127	.3333	.19864E+00	.99321E-03
7	.1127	.5000	.22633E+00	.11316E-02
8	.5000	-.5000	-.25801E+00	-.12900E-02
9	.5000	-.3333	-.23149E+00	-.11574E-02
10	.5000	-.1667	-.20497E+00	-.10249E-02
11	.5000	.0000	-.19630E-01	-.98152E-04
12	.5000	.1667	.16571E+00	.82857E-03
13	.5000	.3333	.19223E+00	.96115E-03
14	.5000	.5000	.21874E+00	.10937E-02
15	.8873	-.5000	-.24428E+00	-.12214E-02
16	.8873	-.3333	-.21893E+00	-.10947E-02
17	.8873	-.1667	-.19359E+00	-.96795E-03
18	.8873	.0000	-.16432E-01	-.82158E-04
19	.8873	.1667	.16073E+00	.80363E-03
20	.8873	.3333	.18607E+00	.93036E-03
21	.8873	.5000	.21142E+00	.10571E-02

***** ELEMENT NO. 24 *****

POINT	X-CRD	Y-CRD	STRESS	STRAIN
1	.1127	-.5000	.23163E+00	.11581E-02

2	.1127	-.3333	.20505E+00	.10252E-02
3	.1127	-.1667	.17846E+00	.89231E-03
4	.1127	.0000	-.73526E-02	-.36763E-04
5	.1127	.1667	-.19317E+00	-.96583E-03
6	.1127	.3333	-.21975E+00	-.10983E-02
7	.1127	.5000	-.24633E+00	-.12317E-02
8	.5000	-.5000	.27095E+00	.49566E-02
9	.5000	-.3333	.27049E+00	.43958E-02
10	.5000	-.1667	.27003E+00	.38349E-02
11	.5000	.0000	-.17129E-01	-.85645E-04
12	.5000	.1667	-.27017E+00	-.40062E-02
13	.5000	.3333	-.27063E+00	-.45671E-02
14	.5000	.5000	-.27109E+00	-.51279E-02
15	.8873	-.5000	.27404E+00	.87425E-02
16	.8873	-.3333	.27323E+00	.77537E-02
17	.8873	-.1667	.27242E+00	.67648E-02
18	.8873	.0000	-.29429E-01	-.14715E-03
19	.8873	.1667	-.27266E+00	-.70591E-02
20	.8873	.3333	-.27347E+00	-.80480E-02
21	.8873	.5000	-.27428E+00	-.90368E-02

LOAD INCREMENT NO. 12 INCR= .200

AFTER 2 ITERATIONS, ERROR = .01176

AFTER 3 ITERATIONS, ERROR = .00083

SOLUTION FOR LOAD INCREMENT 12 AFTER 3ITERATIONS TOLERENCE .83210E

CURRENT LOAD FACTOR = 7.80000 X INITIAL YIELD

NODAL DISPLACEMENTS

NODE	U	V	R
1	.00000E+00	-.27083E+02	.00000E+00
2	.17984E-01	-.26841E+02	.36930E-02
3	.15560E+00	-.26140E+02	.71721E-02
4	.51519E+00	-.25054E+02	.10235E-01
5	.11666E+01	-.23694E+02	.12703E-01
6	.21360E+01	-.22198E+02	.14429E-01
7	.34004E+01	-.20707E+02	.15307E-01
8	.48883E+01	-.19354E+02	.15282E-01
9	.64875E+01	-.18243E+02	.14345E-01
10	.80581E+01	-.17431E+02	.12541E-01
11	.94502E+01	-.16930E+02	.99622E-02
12	.10524E+02	-.16695E+02	.67431E-02
13	.11166E+02	-.16636E+02	.30400E-02
14	.11303E+02	-.16630E+02	-.98870E-03
15	.10910E+02	-.16533E+02	-.51903E-02
16	.10022E+02	-.16208E+02	-.92123E-02
17	.87341E+01	-.15541E+02	-.12894E-01
18	.71753E+01	-.14451E+02	-.16081E-01
19	.54972E+01	-.12912E+02	-.18603E-01
20	.38583E+01	-.10953E+02	-.20296E-01
21	.24050E+01	-.86615E+01	-.21014E-01
22	.12528E+01	-.61792E+01	-.20630E-01
23	.46961E+00	-.36912E+01	-.19037E-01
24	.62810E-01	-.14112E+01	-.16149E-01
25	.00000E+00	.00000E+00	.00000E+00

***** ELEMENT NO. 12 *****

POINT	X-CRD	Y-CRD	STRESS	STRAIN
1	.1127	-.5000	-.25985E+00	-.12993E-02
2	.1127	-.3333	-.23304E+00	-.11652E-02
3	.1127	-.1667	-.20623E+00	-.10312E-02
4	.1127	.0000	-.18830E-01	-.94149E-04
5	.1127	.1667	.16857E+00	.84286E-03
6	.1127	.3333	.19538E+00	.97691E-03
7	.1127	.5000	.22219E+00	.11110E-02
8	.5000	-.5000	-.26802E+00	-.13623E-02
9	.5000	-.3333	-.24444E+00	-.12222E-02
10	.5000	-.1667	-.21641E+00	-.10821E-02
11	.5000	.0000	-.20508E-01	-.10254E-03
12	.5000	.1667	.17540E+00	.87698E-03
13	.5000	.3333	.20342E+00	.10171E-02
14	.5000	.5000	.23145E+00	.11572E-02
15	.8873	-.5000	-.26807E+00	-.14235E-02
16	.8873	-.3333	-.25546E+00	-.12773E-02
17	.8873	-.1667	-.22622E+00	-.11311E-02
18	.8873	.0000	-.21812E-01	-.10906E-03
19	.8873	.1667	.18259E+00	.91297E-03
20	.8873	.3333	.21184E+00	.10592E-02
21	.8873	.5000	.24108E+00	.12054E-02

***** ELEMENT NO. 13 *****

POINT	X-CRD	Y-CRD	STRESS	STRAIN
1	.1127	-.5000	-.26809E+00	-.14495E-02
2	.1127	-.3333	-.26013E+00	-.13007E-02
3	.1127	-.1667	-.23036E+00	-.11518E-02
4	.1127	.0000	-.22230E-01	-.11115E-03
5	.1127	.1667	.18590E+00	.92949E-03
6	.1127	.3333	.21567E+00	.10784E-02
7	.1127	.5000	.24545E+00	.12272E-02
8	.5000	-.5000	-.26812E+00	-.14847E-02
9	.5000	-.3333	-.26644E+00	-.13322E-02
10	.5000	-.1667	-.23595E+00	-.11797E-02
11	.5000	.0000	-.22820E-01	-.11410E-03
12	.5000	.1667	.19031E+00	.95154E-03
13	.5000	.3333	.22080E+00	.11040E-02
14	.5000	.5000	.25129E+00	.12564E-02
15	.8873	-.5000	-.26814E+00	-.15172E-02
16	.8873	-.3333	-.26802E+00	-.13612E-02
17	.8873	-.1667	-.24103E+00	-.12051E-02
18	.8873	.0000	-.22901E-01	-.11450E-03
19	.8873	.1667	.19523E+00	.97614E-03
20	.8873	.3333	.22643E+00	.11322E-02
21	.8873	.5000	.25764E+00	.12882E-02

***** ELEMENT NO. 14 *****

POINT	X-CRD	Y-CRD	STRESS	STRAIN
1	.1127	-.5000	-.26819E+00	-.15721E-02
2	.1127	-.3333	-.26806E+00	-.14126E-02
3	.1127	-.1667	-.25060E+00	-.12530E-02
4	.1127	.0000	-.27547E-01	-.13773E-03
5	.1127	.1667	.19551E+00	.97754E-03
6	.1127	.3333	.22742E+00	.11371E-02
7	.1127	.5000	.25933E+00	.12966E-02
8	.5000	-.5000	-.26818E+00	-.15631E-02
9	.5000	-.3333	-.26805E+00	-.14041E-02
10	.5000	-.1667	-.24903E+00	-.12451E-02
11	.5000	.0000	-.26750E-01	-.13375E-03
12	.5000	.1667	.19553E+00	.97764E-03
13	.5000	.3333	.22733E+00	.11366E-02
14	.5000	.5000	.25913E+00	.12956E-02

15	.8873	-.5000	-.26817E+00	-.15514E-02
16	.8873	-.3333	-.26804E+00	-.13929E-02
17	.8873	-.1667	-.24690E+00	-.12345E-02
18	.8873	.0000	-.25396E-01	-.12698E-03
19	.8873	.1667	.19611E+00	.98054E-03
20	.8873	.3333	.22780E+00	.11390E-02
21	.8873	.5000	.25949E+00	.12974E-02

***** ELEMENT NO. 15 *****

POINT	X-CRD	Y-CRD	STRESS	STRAIN
1	.1127	-.5000	-.26816E+00	-.15312E-02
2	.1127	-.3333	-.26803E+00	-.13748E-02
3	.1127	-.1667	-.24370E+00	-.12185E-02
4	.1127	.0000	-.25134E-01	-.12567E-03
5	.1127	.1667	.19343E+00	.96717E-03
6	.1127	.3333	.22470E+00	.11235E-02
7	.1127	.5000	.25597E+00	.12799E-02
8	.5000	-.5000	-.26812E+00	-.14831E-02
9	.5000	-.3333	-.26618E+00	-.13309E-02
10	.5000	-.1667	-.23574E+00	-.11787E-02
11	.5000	.0000	-.22967E-01	-.11484E-03
12	.5000	.1667	.18980E+00	.94902E-03
13	.5000	.3333	.22024E+00	.11012E-02
14	.5000	.5000	.25068E+00	.12534E-02
15	.8873	-.5000	-.26808E+00	-.14327E-02
16	.8873	-.3333	-.25694E+00	-.12847E-02
17	.8873	-.1667	-.22733E+00	-.11366E-02
18	.8873	.0000	-.20351E-01	-.10175E-03
19	.8873	.1667	.18662E+00	.93312E-03
20	.8873	.3333	.21623E+00	.10812E-02
21	.8873	.5000	.24585E+00	.12292E-02

***** ELEMENT NO. 16 *****

POINT	X-CRD	Y-CRD	STRESS	STRAIN
1	.1127	-.5000	-.26807E+00	-.14277E-02
2	.1127	-.3333	-.25642E+00	-.12821E-02
3	.1127	-.1667	-.22730E+00	-.11365E-02
4	.1127	.0000	-.23756E-01	-.11878E-03
5	.1127	.1667	.17978E+00	.89892E-03
6	.1127	.3333	.20890E+00	.10445E-02
7	.1127	.5000	.23802E+00	.11901E-02
8	.5000	-.5000	-.26801E+00	-.13554E-02
9	.5000	-.3333	-.24321E+00	-.12160E-02
10	.5000	-.1667	-.21534E+00	-.10767E-02
11	.5000	.0000	-.20541E-01	-.10271E-03
12	.5000	.1667	.17426E+00	.87129E-03
13	.5000	.3333	.20213E+00	.10106E-02
14	.5000	.5000	.22999E+00	.11500E-02
15	.8873	-.5000	-.25634E+00	-.12817E-02
16	.8873	-.3333	-.22972E+00	-.11486E-02
17	.8873	-.1667	-.20311E+00	-.10155E-02
18	.8873	.0000	-.17047E-01	-.85234E-04
19	.8873	.1667	.16901E+00	.84506E-03
20	.8873	.3333	.19563E+00	.97815E-03
21	.8873	.5000	.22225E+00	.11112E-02

***** ELEMENT NO. 24 *****

POINT	X-CRD	Y-CRD	STRESS	STRAIN
1	.1127	-.5000	.23066E+00	.11533E-02
2	.1127	-.3333	.20420E+00	.10210E-02
3	.1127	-.1667	.17775E+00	.88873E-03
4	.1127	.0000	-.71916E-02	-.35958E-04
5	.1127	.1667	-.19213E+00	-.96064E-03

6	.1127	.3333	-.21859E+00	-.10929E-02
7	.1127	.5000	-.24504E+00	-.12252E-02
8	.5000	-.5000	.27131E+00	.54009E-02
9	.5000	-.3333	.27081E+00	.47898E-02
10	.5000	-.1667	.27031E+00	.41787E-02
11	.5000	.0000	-.18604E-01	-.93021E-04
12	.5000	.1667	-.27047E+00	-.43647E-02
13	.5000	.3333	-.27097E+00	-.49758E-02
14	.5000	.5000	-.27146E+00	-.55869E-02
15	.8873	-.5000	.27476E+00	.96319E-02
16	.8873	-.3333	.27387E+00	.85420E-02
17	.8873	-.1667	.27298E+00	.74520E-02
18	.8873	.0000	-.33334E-01	-.16667E-03
19	.8873	.1667	-.27326E+00	-.77853E-02
20	.8873	.3333	-.27415E+00	-.88753E-02
21	.8873	.5000	-.27503E+00	-.99653E-02

LOAD INCREMENT NO. 13 INCR= .200

AFTER 2 ITERATIONS, ERROR = .06665

AFTER 3 ITERATIONS, ERROR = .00283

AFTER 4 ITERATIONS, ERROR = .00017

SOLUTION FOR LOAD INCREMENT 13 AFTER 4ITERATIONS TOLERENCE .17487E

CURRENT LOAD FACTOR = 8.00000 X INITIAL YIELD

NODAL DISPLACEMENTS

NODE	U	V	R
1	.00000E+00	-.28993E+02	.00000E+00
2	.18899E-01	-.28739E+02	.38673E-02
3	.16291E+00	-.28005E+02	.75129E-02
4	.53931E+00	-.26867E+02	.10729E-01
5	.12218E+01	-.25441E+02	.13329E-01
6	.22387E+01	-.23869E+02	.15162E-01
7	.35676E+01	-.22300E+02	.16118E-01
8	.51354E+01	-.20873E+02	.16137E-01
9	.68264E+01	-.19695E+02	.15209E-01
10	.84958E+01	-.18832E+02	.13380E-01
11	.99877E+01	-.18293E+02	.10742E-01
12	.11155E+02	-.18037E+02	.74330E-02
13	.11879E+02	-.17972E+02	.36018E-02
14	.12073E+02	-.17964E+02	-.71710E-03
15	.11676E+02	-.17850E+02	-.55772E-02
16	.10719E+02	-.17495E+02	-.99457E-02
17	.93351E+01	-.16777E+02	-.13814E-01
18	.76698E+01	-.15611E+02	-.17163E-01
19	.58814E+01	-.13968E+02	-.19838E-01
20	.41354E+01	-.11875E+02	-.21670E-01
21	.25848E+01	-.94229E+01	-.22506E-01
22	.13517E+01	-.67559E+01	-.22215E-01
23	.50897E+00	-.40644E+01	-.20686E-01
24	.67777E-01	-.15689E+01	-.17830E-01
25	.00000E+00	.00000E+00	.00000E+00

***** ELEMENT NO. 1 *****

POINT	X-CRD	Y-CRD	STRESS	STRAIN

1	.1127	-.5000	.26801E+00	.13501E-02
2	.1127	-.3333	.24041E+00	.12020E-02
3	.1127	-.1667	.21080E+00	.10540E-02
4	.1127	.0000	.38438E-02	.19219E-04
5	.1127	.1667	-.20311E+00	-.10156E-02
6	.1127	.3333	-.23272E+00	-.11636E-02
7	.1127	.5000	-.26233E+00	-.13116E-02
8	.5000	-.5000	.26736E+00	.13368E-02
9	.5000	-.3333	.23809E+00	.11904E-02
10	.5000	-.1667	.20882E+00	.10441E-02
11	.5000	.0000	.42259E-02	.21129E-04
12	.5000	.1667	-.20037E+00	-.10018E-02
13	.5000	.3333	-.22963E+00	-.11482E-02
14	.5000	.5000	-.25890E+00	-.12945E-02
15	.8873	-.5000	.26517E+00	.13258E-02
16	.8873	-.3333	.23624E+00	.11812E-02
17	.8873	-.1667	.20731E+00	.10365E-02
18	.8873	.0000	.50770E-02	.25385E-04
19	.8873	.1667	-.19715E+00	-.98576E-03
20	.8873	.3333	-.22608E+00	-.11304E-02
21	.8873	.5000	-.25501E+00	-.12751E-02

***** ELEMENT NO. 12 *****

POINT	X-CRD	Y-CRD	STRESS	STRAIN
1	.1127	-.5000	-.26772E+00	-.13405E-02
2	.1127	-.3333	-.24046E+00	-.12023E-02
3	.1127	-.1667	-.21281E+00	-.10640E-02
4	.1127	.0000	-.19541E-01	-.97704E-04
5	.1127	.1667	.17372E+00	.86862E-03
6	.1127	.3333	.20137E+00	.10069E-02
7	.1127	.5000	.22902E+00	.11451E-02
8	.5000	-.5000	-.26795E+00	-.14107E-02
9	.5000	-.3333	-.25314E+00	-.12657E-02
10	.5000	-.1667	-.22414E+00	-.11207E-02
11	.5000	.0000	-.21465E-01	-.10732E-03
12	.5000	.1667	.18121E+00	.90606E-03
13	.5000	.3333	.21021E+00	.10510E-02
14	.5000	.5000	.23920E+00	.11960E-02
15	.8873	-.5000	-.26800E+00	-.14789E-02
16	.8873	-.3333	-.26543E+00	-.13272E-02
17	.8873	-.1667	-.23509E+00	-.11754E-02
18	.8873	.0000	-.23001E-01	-.11501E-03
19	.8873	.1667	.18909E+00	.94543E-03
20	.8873	.3333	.21943E+00	.10971E-02
21	.8873	.5000	.24977E+00	.12489E-02

***** ELEMENT NO. 13 *****

POINT	X-CRD	Y-CRD	STRESS	STRAIN
1	.1127	-.5000	-.26818E+00	-.15665E-02
2	.1127	-.3333	-.26806E+00	-.14087E-02
3	.1127	-.1667	-.25016E+00	-.12508E-02
4	.1127	.0000	-.29488E-01	-.14744E-03
5	.1127	.1667	.19118E+00	.95592E-03
6	.1127	.3333	.22275E+00	.11138E-02
7	.1127	.5000	.25432E+00	.12716E-02
8	.5000	-.5000	-.26823E+00	-.16207E-02
9	.5000	-.3333	-.26810E+00	-.14573E-02
10	.5000	-.1667	-.25876E+00	-.12938E-02
11	.5000	.0000	-.30280E-01	-.15140E-03
12	.5000	.1667	.19820E+00	.99102E-03
13	.5000	.3333	.23089E+00	.11545E-02
14	.5000	.5000	.26358E+00	.13179E-02
15	.8873	-.5000	-.26827E+00	-.16720E-02
16	.8873	-.3333	-.26813E+00	-.15030E-02

17	.8873	-.1667	-.26679E+00	-.13340E-02
18	.8873	.0000	-.30498E-01	-.15249E-03
19	.8873	.1667	.20580E+00	.10290E-02
20	.8873	.3333	.23960E+00	.11980E-02
21	.8873	.5000	.26802E+00	.13670E-02

***** ELEMENT NO. 14 *****

POINT	X-CRD	Y-CRD	STRESS	STRAIN
1	.1127	-.5000	-.26847E+00	-.19131E-02
2	.1127	-.3333	-.26832E+00	-.17286E-02
3	.1127	-.1667	-.26817E+00	-.15442E-02
4	.1127	.0000	-.50983E-01	-.25492E-03
5	.1127	.1667	.20687E+00	.10344E-02
6	.1127	.3333	.24376E+00	.12188E-02
7	.1127	.5000	.26805E+00	.14033E-02
8	.5000	-.5000	-.26846E+00	-.19039E-02
9	.5000	-.3333	-.26831E+00	-.17200E-02
10	.5000	-.1667	-.26816E+00	-.15360E-02
11	.5000	.0000	-.50098E-01	-.25049E-03
12	.5000	.1667	.20701E+00	.10351E-02
13	.5000	.3333	.24380E+00	.12190E-02
14	.5000	.5000	.26805E+00	.14029E-02
15	.8873	-.5000	-.26845E+00	-.18910E-02
16	.8873	-.3333	-.26830E+00	-.17076E-02
17	.8873	-.1667	-.26815E+00	-.15242E-02
18	.8873	.0000	-.48471E-01	-.24235E-03
19	.8873	.1667	.20790E+00	.10395E-02
20	.8873	.3333	.24457E+00	.12229E-02
21	.8873	.5000	.26805E+00	.14062E-02

***** ELEMENT NO. 15 *****

POINT	X-CRD	Y-CRD	STRESS	STRAIN
1	.1127	-.5000	-.26831E+00	-.17178E-02
2	.1127	-.3333	-.26817E+00	-.15459E-02
3	.1127	-.1667	-.26803E+00	-.13739E-02
4	.1127	.0000	-.34454E-01	-.17227E-03
5	.1127	.1667	.20588E+00	.10294E-02
6	.1127	.3333	.24026E+00	.12013E-02
7	.1127	.5000	.26803E+00	.13732E-02
8	.5000	-.5000	-.26825E+00	-.16458E-02
9	.5000	-.3333	-.26811E+00	-.14804E-02
10	.5000	-.1667	-.26303E+00	-.13151E-02
11	.5000	.0000	-.31916E-01	-.15958E-03
12	.5000	.1667	.19919E+00	.99597E-03
13	.5000	.3333	.23226E+00	.11613E-02
14	.5000	.5000	.26532E+00	.13266E-02
15	.8873	-.5000	-.26819E+00	-.15713E-02
16	.8873	-.3333	-.26806E+00	-.14126E-02
17	.8873	-.1667	-.25077E+00	-.12538E-02
18	.8873	.0000	-.28885E-01	-.14442E-03
19	.8873	.1667	.19300E+00	.96499E-03
20	.8873	.3333	.22474E+00	.11237E-02
21	.8873	.5000	.25649E+00	.12824E-02

***** ELEMENT NO. 16 *****

POINT	X-CRD	Y-CRD	STRESS	STRAIN
1	.1127	-.5000	-.26814E+00	-.15058E-02
2	.1127	-.3333	-.26801E+00	-.13525E-02
3	.1127	-.1667	-.23985E+00	-.11992E-02
4	.1127	.0000	-.25588E-01	-.12794E-03
5	.1127	.1667	.18867E+00	.94336E-03
6	.1127	.3333	.21933E+00	.10966E-02
7	.1127	.5000	.24998E+00	.12499E-02

8	.5000	-.5000	-.26807E+00	-.14257E-02
9	.5000	-.3333	-.25587E+00	-.12793E-02
10	.5000	-.1667	-.22659E+00	-.11330E-02
11	.5000	.0000	-.21967E-01	-.10983E-03
12	.5000	.1667	.18266E+00	.91330E-03
13	.5000	.3333	.21193E+00	.10597E-02
14	.5000	.5000	.24121E+00	.12060E-02
15	.8873	-.5000	-.26800E+00	-.13442E-02
16	.8873	-.3333	-.24094E+00	-.12047E-02
17	.8873	-.1667	-.21304E+00	-.10652E-02
18	.8873	.0000	-.18049E-01	-.90246E-04
19	.8873	.1667	.17694E+00	.88471E-03
20	.8873	.3333	.20484E+00	.10242E-02
21	.8873	.5000	.23273E+00	.11637E-02

***** ELEMENT NO. 24 *****

POINT	X-CRD	Y-CRD	STRESS	STRAIN
1	.1127	-.5000	.23013E+00	.11507E-02
2	.1127	-.3333	.20378E+00	.10189E-02
3	.1127	-.1667	.17743E+00	.88714E-03
4	.1127	.0000	-.67766E-02	-.33883E-04
5	.1127	.1667	-.19098E+00	-.95491E-03
6	.1127	.3333	-.21733E+00	-.10867E-02
7	.1127	.5000	-.24369E+00	-.12184E-02
8	.5000	-.5000	.27177E+00	.59636E-02
9	.5000	-.3333	.27122E+00	.52889E-02
10	.5000	-.1667	.27067E+00	.46141E-02
11	.5000	.0000	-.20442E-01	-.10221E-03
12	.5000	.1667	-.27084E+00	-.48186E-02
13	.5000	.3333	-.27139E+00	-.54933E-02
14	.5000	.5000	-.27194E+00	-.61680E-02
15	.8873	-.5000	.27568E+00	.10754E-01
16	.8873	-.3333	.27468E+00	.95366E-02
17	.8873	-.1667	.27369E+00	.83189E-02
18	.8873	.0000	-.38557E-01	-.19278E-03
19	.8873	.1667	-.27401E+00	-.87045E-02
20	.8873	.3333	-.27500E+00	-.99222E-02
21	.8873	.5000	-.27599E+00	-.11140E-01

LOAD INCREMENT NO. 14 INCR= .200

AFTER 2 ITERATIONS, ERROR = .10250

AFTER 3 ITERATIONS, ERROR = .00666

AFTER 4 ITERATIONS, ERROR = .00466

AFTER 5 ITERATIONS, ERROR = .00010

SOLUTION FOR LOAD INCREMENT 14 AFTER 5ITERATIONS TOLERENCE .10467E

CURRENT LOAD FACTOR = 8.20000 X INITIAL YIELD

NODAL DISPLACEMENTS

NODE	U	V	R
1	.00000E+00	-.32008E+02	.00000E+00
2	.20639E-01	-.31737E+02	.41411E-02
3	.17433E+00	-.30952E+02	.80194E-02
4	.57532E+00	-.29738E+02	.11449E-01

5	.13028E+01	-.28214E+02	.14241E-01
6	.23891E+01	-.26532E+02	.16239E-01
7	.38131E+01	-.24847E+02	.17327E-01
8	.55011E+01	-.23307E+02	.17441E-01
9	.73342E+01	-.22027E+02	.16570E-01
10	.91621E+01	-.21079E+02	.14758E-01
11	.10822E+02	-.20479E+02	.12098E-01
12	.12160E+02	-.20185E+02	.87301E-02
13	.13046E+02	-.20106E+02	.47807E-02
14	.13355E+02	-.20090E+02	-.18321E-03
15	.12962E+02	-.19948E+02	-.61477E-02
16	.11883E+02	-.19524E+02	-.11463E-01
17	.10309E+02	-.18702E+02	-.15562E-01
18	.84495E+01	-.17397E+02	-.19072E-01
19	.64731E+01	-.15574E+02	-.21894E-01
20	.45534E+01	-.13265E+02	-.23859E-01
21	.28513E+01	-.10560E+02	-.24808E-01
22	.14957E+01	-.76115E+01	-.24606E-01
23	.56511E+00	-.46153E+01	-.23136E-01
24	.74297E-01	-.18008E+01	-.20308E-01
25	.00000E+00	.00000E+00	.00000E+00

***** ELEMENT NO. 1 *****

POINT	X-CRD	Y-CRD	STRESS	STRAIN
1	.1127	-.5000	.26809E+00	.14513E-02
2	.1127	-.3333	.25850E+00	.12925E-02
3	.1127	-.1667	.22674E+00	.11337E-02
4	.1127	.0000	.47432E-02	.23716E-04
5	.1127	.1667	-.21726E+00	-.10863E-02
6	.1127	.3333	-.24902E+00	-.12451E-02
7	.1127	.5000	-.26805E+00	-.14039E-02
8	.5000	-.5000	.26808E+00	.14347E-02
9	.5000	-.3333	.25560E+00	.12780E-02
10	.5000	-.1667	.22426E+00	.11213E-02
11	.5000	.0000	.51800E-02	.25900E-04
12	.5000	.1667	-.21390E+00	-.10695E-02
13	.5000	.3333	-.24524E+00	-.12262E-02
14	.5000	.5000	-.26803E+00	-.13829E-02
15	.8873	-.5000	.26807E+00	.14208E-02
16	.8873	-.3333	.25323E+00	.12661E-02
17	.8873	-.1667	.22230E+00	.11115E-02
18	.8873	.0000	.61505E-02	.30752E-04
19	.8873	.1667	-.21000E+00	-.10500E-02
20	.8873	.3333	-.24093E+00	-.12046E-02
21	.8873	.5000	-.26802E+00	-.13593E-02

***** ELEMENT NO. 2 *****

POINT	X-CRD	Y-CRD	STRESS	STRAIN
1	.1127	-.5000	.26803E+00	.13774E-02
2	.1127	-.3333	.24508E+00	.12254E-02
3	.1127	-.1667	.21467E+00	.10733E-02
4	.1127	.0000	.21333E-02	.10667E-04
5	.1127	.1667	-.21040E+00	-.10520E-02
6	.1127	.3333	-.24081E+00	-.12040E-02
7	.1127	.5000	-.26801E+00	-.13561E-02
8	.5000	-.5000	.26774E+00	.13387E-02
9	.5000	-.3333	.23839E+00	.11919E-02
10	.5000	-.1667	.20903E+00	.10452E-02
11	.5000	.0000	.38644E-02	.19322E-04
12	.5000	.1667	-.20130E+00	-.10065E-02
13	.5000	.3333	-.23066E+00	-.11533E-02
14	.5000	.5000	-.26001E+00	-.13000E-02
15	.8873	-.5000	.26040E+00	.13020E-02
16	.8873	-.3333	.23210E+00	.11605E-02

17	.8873	-.1667	.20380E+00	.10190E-02
18	.8873	.0000	.60024E-02	.30012E-04
19	.8873	.1667	-.19180E+00	-.95900E-03
20	.8873	.3333	-.22010E+00	-.11005E-02
21	.8873	.5000	-.24840E+00	-.12420E-02

***** ELEMENT NO. 12 *****

POINT	X-CRD	Y-CRD	STRESS	STRAIN
1	.1127	-.5000	-.26795E+00	-.13736E-02
2	.1127	-.3333	-.24648E+00	-.12324E-02
3	.1127	-.1667	-.21823E+00	-.10912E-02
4	.1127	.0000	-.20785E-01	-.10393E-03
5	.1127	.1667	.17666E+00	.88330E-03
6	.1127	.3333	.20491E+00	.10245E-02
7	.1127	.5000	.23316E+00	.11658E-02
8	.5000	-.5000	-.26800E+00	-.14593E-02
9	.5000	-.3333	-.26196E+00	-.13098E-02
10	.5000	-.1667	-.23207E+00	-.11604E-02
11	.5000	.0000	-.23141E-01	-.11570E-03
12	.5000	.1667	.18579E+00	.92896E-03
13	.5000	.3333	.21568E+00	.10784E-02
14	.5000	.5000	.24557E+00	.12279E-02
15	.8873	-.5000	-.26805E+00	-.15430E-02
16	.8873	-.3333	-.26804E+00	-.13854E-02
17	.8873	-.1667	-.24554E+00	-.12277E-02
18	.8873	.0000	-.25121E-01	-.12560E-03
19	.8873	.1667	.19530E+00	.97649E-03
20	.8873	.3333	.22683E+00	.11342E-02
21	.8873	.5000	.25837E+00	.12918E-02

***** ELEMENT NO. 13 *****

POINT	X-CRD	Y-CRD	STRESS	STRAIN
1	.1127	-.5000	-.26843E+00	-.18734E-02
2	.1127	-.3333	-.26829E+00	-.16947E-02
3	.1127	-.1667	-.26814E+00	-.15159E-02
4	.1127	.0000	-.53356E-01	-.26678E-03
5	.1127	.1667	.19648E+00	.98238E-03
6	.1127	.3333	.23222E+00	.11611E-02
7	.1127	.5000	.26796E+00	.13398E-02
8	.5000	-.5000	-.26851E+00	-.19620E-02
9	.5000	-.3333	-.26835E+00	-.17741E-02
10	.5000	-.1667	-.26820E+00	-.15863E-02
11	.5000	.0000	-.54650E-01	-.27325E-03
12	.5000	.1667	.20796E+00	.10398E-02
13	.5000	.3333	.24553E+00	.12276E-02
14	.5000	.5000	.26806E+00	.14155E-02
15	.8873	-.5000	-.26858E+00	-.20469E-02
16	.8873	-.3333	-.26842E+00	-.18500E-02
17	.8873	-.1667	-.26826E+00	-.16530E-02
18	.8873	.0000	-.55214E-01	-.27607E-03
19	.8873	.1667	.22017E+00	.11008E-02
20	.8873	.3333	.25956E+00	.12978E-02
21	.8873	.5000	.26813E+00	.14948E-02

***** ELEMENT NO. 14 *****

POINT	X-CRD	Y-CRD	STRESS	STRAIN
1	.1127	-.5000	-.26806E+00	-.24993E-02
2	.1127	-.3333	-.26806E+00	-.22738E-02
3	.1127	-.1667	-.26805E+00	-.20484E-02
4	.1127	.0000	-.94548E-01	-.47274E-03
5	.1127	.1667	.22059E+00	.11029E-02
6	.1127	.3333	.26567E+00	.13284E-02
7	.1127	.5000	.26789E+00	.15538E-02

8	.5000	-.5000	-.26806E+00	-.24970E-02
9	.5000	-.3333	-.26806E+00	-.22713E-02
10	.5000	-.1667	-.26805E+00	-.20456E-02
11	.5000	.0000	-.93581E-01	-.46790E-03
12	.5000	.1667	.22196E+00	.11098E-02
13	.5000	.3333	.26710E+00	.13355E-02
14	.5000	.5000	.26802E+00	.15612E-02
15	.8873	-.5000	-.26807E+00	-.24891E-02
16	.8873	-.3333	-.26806E+00	-.22631E-02
17	.8873	-.1667	-.26806E+00	-.20371E-02
18	.8873	.0000	-.91479E-01	-.45739E-03
19	.8873	.1667	.22446E+00	.11223E-02
20	.8873	.3333	.26801E+00	.13483E-02
21	.8873	.5000	.26802E+00	.15743E-02

***** ELEMENT NO. 15 *****

POINT	X-CRD	Y-CRD	STRESS	STRAIN
1	.1127	-.5000	-.26874E+00	-.22501E-02
2	.1127	-.3333	-.26857E+00	-.20397E-02
3	.1127	-.1667	-.26840E+00	-.18293E-02
4	.1127	.0000	-.71703E-01	-.35852E-03
5	.1127	.1667	.22244E+00	.11122E-02
6	.1127	.3333	.26453E+00	.13226E-02
7	.1127	.5000	.26816E+00	.15330E-02
8	.5000	-.5000	-.26866E+00	-.21496E-02
9	.5000	-.3333	-.26850E+00	-.19484E-02
10	.5000	-.1667	-.26833E+00	-.17473E-02
11	.5000	.0000	-.68239E-01	-.34119E-03
12	.5000	.1667	.21298E+00	.10649E-02
13	.5000	.3333	.25321E+00	.12661E-02
14	.5000	.5000	.26810E+00	.14672E-02
15	.8873	-.5000	-.26858E+00	-.20456E-02
16	.8873	-.3333	-.26842E+00	-.18537E-02
17	.8873	-.1667	-.26826E+00	-.16618E-02
18	.8873	.0000	-.64062E-01	-.32031E-03
19	.8873	.1667	.20423E+00	.10211E-02
20	.8873	.3333	.24261E+00	.12130E-02
21	.8873	.5000	.26805E+00	.14050E-02

***** ELEMENT NO. 16 *****

POINT	X-CRD	Y-CRD	STRESS	STRAIN
1	.1127	-.5000	-.26824E+00	-.16289E-02
2	.1127	-.3333	-.26810E+00	-.14645E-02
3	.1127	-.1667	-.26003E+00	-.13002E-02
4	.1127	.0000	-.30271E-01	-.15136E-03
5	.1127	.1667	.19949E+00	.99744E-03
6	.1127	.3333	.23236E+00	.11618E-02
7	.1127	.5000	.26523E+00	.13261E-02
8	.5000	-.5000	-.26815E+00	-.15236E-02
9	.5000	-.3333	-.26802E+00	-.13685E-02
10	.5000	-.1667	-.24269E+00	-.12134E-02
11	.5000	.0000	-.25882E-01	-.12941E-03
12	.5000	.1667	.19092E+00	.95461E-03
13	.5000	.3333	.22194E+00	.11097E-02
14	.5000	.5000	.25295E+00	.12648E-02
15	.8873	-.5000	-.26806E+00	-.14170E-02
16	.8873	-.3333	-.25424E+00	-.12712E-02
17	.8873	-.1667	-.22508E+00	-.11254E-02
18	.8873	.0000	-.21234E-01	-.10617E-03
19	.8873	.1667	.18261E+00	.91307E-03
20	.8873	.3333	.21178E+00	.10589E-02
21	.8873	.5000	.24094E+00	.12047E-02

***** ELEMENT NO. 17 *****

POINT	X-CRD	Y-CRD	STRESS	STRAIN
1	.1127	-.5000	-.26805E+00	-.14028E-02
2	.1127	-.3333	-.25219E+00	-.12609E-02
3	.1127	-.1667	-.22382E+00	-.11191E-02
4	.1127	.0000	-.25533E-01	-.12766E-03
5	.1127	.1667	.17275E+00	.86377E-03
6	.1127	.3333	.20112E+00	.10056E-02
7	.1127	.5000	.22949E+00	.11474E-02
8	.5000	-.5000	-.25945E+00	-.12972E-02
9	.5000	-.3333	-.23288E+00	-.11644E-02
10	.5000	-.1667	-.20631E+00	-.10316E-02
11	.5000	.0000	-.20604E-01	-.10302E-03
12	.5000	.1667	.16510E+00	.82552E-03
13	.5000	.3333	.19167E+00	.95836E-03
14	.5000	.5000	.21824E+00	.10912E-02
15	.8873	-.5000	-.23829E+00	-.11914E-02
16	.8873	-.3333	-.21352E+00	-.10676E-02
17	.8873	-.1667	-.18875E+00	-.94376E-03
18	.8873	.0000	-.15622E-01	-.78111E-04
19	.8873	.1667	.15751E+00	.78754E-03
20	.8873	.3333	.18228E+00	.91138E-03
21	.8873	.5000	.20704E+00	.10352E-02

***** ELEMENT NO. 24 *****

POINT	X-CRD	Y-CRD	STRESS	STRAIN
1	.1127	-.5000	.23067E+00	.11533E-02
2	.1127	-.3333	.20437E+00	.10219E-02
3	.1127	-.1667	.17807E+00	.89037E-03
4	.1127	.0000	-.57280E-02	-.28640E-04
5	.1127	.1667	-.18953E+00	-.94766E-03
6	.1127	.3333	-.21583E+00	-.10791E-02
7	.1127	.5000	-.24212E+00	-.12106E-02
8	.5000	-.5000	.27245E+00	.67930E-02
9	.5000	-.3333	.27182E+00	.60245E-02
10	.5000	-.1667	.27119E+00	.52561E-02
11	.5000	.0000	-.23113E-01	-.11557E-03
12	.5000	.1667	-.27138E+00	-.54872E-02
13	.5000	.3333	-.27201E+00	-.62557E-02
14	.5000	.5000	-.27264E+00	-.70241E-02
15	.8873	-.5000	.27702E+00	.12401E-01
16	.8873	-.3333	.27587E+00	.10995E-01
17	.8873	-.1667	.27473E+00	.95897E-02
18	.8873	.0000	-.46894E-01	-.23447E-03
19	.8873	.1667	-.27511E+00	-.10059E-01
20	.8873	.3333	-.27626E+00	-.11464E-01
21	.8873	.5000	-.27740E+00	-.12870E-01

LOAD INCREMENT NO. 15 INCR= .200

AFTER 2 ITERATIONS, ERROR = .14160

AFTER 3 ITERATIONS, ERROR = .15968

AFTER 4 ITERATIONS, ERROR = 2.25588

SOLUTION IS DIVERGING- PLASTIC INSTABILITY
TOLERENCE = .22559E+01

1 ********** S U M M A R Y O F R E S U L T S

LOAD INCR	LOAD LEVEL	NOMINAL SLOPE

-1	.00	.00000E+00
0	1.00	.24537E+00
1	2.00	.24209E+00
2	3.00	.24175E+00
3	4.00	.23923E+00
4	5.00	.23734E+00
5	6.00	.19147E+00
6	6.60	.87066E-01
7	6.80	.86337E-01
8	7.00	.85015E-01
9	7.20	.84619E-01
10	7.40	.81655E-01
11	7.60	.81396E-01
12	7.80	.76623E-01
13	8.00	.56421E-01
14	8.20	.35581E-01
15	.00	.00000E+00